METAL-ATOM MEDIATED CHEMICAL TRANSFORMATIONS: The reaction of Group 13 metal atoms with arenes

BY

HADI FERGANI

A Thesis

Submitted to the Department of Chemistry and Biochemistry in Partial Fulfillment

of the Requirements for the Degree of Master of Science in Chemistry

Laurentian University

Sudbury, Ontario

© Copyright by Hadi Fergani 1999

National Library of Canada
Acquisitions and Bibliographic Services
395 Wellington Street
Ottawa ON K1A 0N4
Canada

Bibliothèque nationale du Canada
Acquisitions et services bibliographiques
395, rue Wellington
Ottawa ON K1A 0N4
Canada

Your file Votre référence

Our file Notre référence

The author has granted a non-exclusive licence allowing the National Library of Canada to reproduce, loan, distribute or sell copies of this thesis in microform, paper or electronic formats.

The author retains ownership of the copyright in this thesis. Neither the thesis nor substantial extracts from it may be printed or otherwise reproduced without the author's permission.

L'auteur a accordé une licence non exclusive permettant à la Bibliothèque nationale du Canada de reproduire, prêter, distribuer ou vendre des copies de cette thèse sous la forme de microfiche/film, de reproduction sur papier ou sur format électronique.

L'auteur conserve la propriété du droit d'auteur qui protège cette thèse. Ni la thèse ni des extraits substantiels de celle-ci ne doivent être imprimés ou autrement reproduits sans son autorisation.

0-612-46480-6

Canada

ABSTRACT

Group 13 metal atoms (Al, Ga, In and/or Tl) were reacted with benzene, toluene, trifluorotoluene, *p* -bromotoluene and chlorobenzene at 77 K in a specialized metal atom reactor known as a 'rotating cryostat'. The products resulting from the hydrolysis or deuterolysis of the organometallic compounds formed in the metal atom reaction were studied by gas chromatography-mass spectrometry.

The only product detected in the hydrolysis of the Al- and Ga-benzene reaction mixtures was 1,4-cyclohexadiene. Addition of deuterium oxide to the Al-benzene reaction mixture resulted in the formation of 1,4-cyclohexadiene-3,6-*d* $_2$. Incorporation of deuterium at positions 3 and 6 supports Howard and co-workers interpretation of the EPR data, (Chenier, J.H.B.; Howard, J.A.; Tse, J.S.; Mile, B. *J. Am. Chem. Soc.* **1985**, 107, 7290.) i.e., that Al atoms add cheleotropically to benzene to form an η^2 complex in which the Al lies along the C_{6v} axis of the benzene ring.

When an electron donating group is found on the benzene ring, as is the case with toluene, Al and Ga atoms also mediate the reduction of the aromatic ring resulting in the formation of 1-methyl-1,4-cyclohexadiene.

An interesting result was obtained when the group 13 metal atoms were reacted with trifluorotoluene, where trifluoromethyl is an electron withdrawing group. More specifically, there are at least nine compounds formed in both the reaction of Al atoms and Ga atoms with trifluorotoluene. The mass spectral data for these compounds are consistent with the formation of four different isomers of trifluoromethylcyclohexadiene (differing

only in the position of the double bonds with respect to the substituent), two isomers of difluoromethylcyclohexadiene, toluene, difluorotoluene and monofluorotoluene. This result showed that electron withdrawing groups, like CF_3, make the benzene ring susceptible to reduction by Al and Ga atoms. It also showed that Al and Ga atoms can insert into one, two or three of the C-F bonds of the substituent to form difluorotoluene, monofluorotoluene and toluene respectively. Indium and thallium atoms were less effective. In the case of indium atoms, reaction with trifluorotoluene resulted in the formation of one trifluoromethylcyclohexadiene isomer, toluene and difluorotoluene whereas no products were detected in the case of thallium. The reactivity displayed by the group 13 metal atoms (Al, Ga > In >> Tl) is similar to that reported for reactions involving H_2O, aromatic alkenes and methyl bromide as substrates.

Reduction products were not obtained when Al atoms were reacted with chlorobenzene and bromotoluene. In the case of chlorobenzene Al atoms inserted into the C-Cl bond. Deuterolysis of the reaction mixture resulted in the formation of deuterated benzene, C_6H_5D and 1,1'-biphenyl. Hydrolysis of the reaction mixture of Al atoms with bromotoluene resulted in the formation of toluene (Al inserted in the C-Br bond) and bromobenzene (Al atoms inserted in the C-CH_3 bond).

To gain some insights into the structures of the compounds formed, a number of quantum-mechanical electronic (ab initio) analyses were performed. Firstly, as a benchmark, we repeated McKee's work (McKee, M.L. *J. Phys. Chem.* **1991**, 95, 7247.) using the Gaussian 92 Program. Our calculations confirmed that there are two Al-benzene complexes, one with C_{2v} symmetry and the other with C_{6v} symmetry. The theoretical analysis shows that in the C_{2v} complex, the benzene ring distorts producing nonequivalent C atoms. The highest spin density (0.449) was found for the C1 and C4 atoms. These

results indicate H^+ would be drawn to C1 and C4 atoms preferentially resulting in the formation of 1,4-cyclohexadiene. The theoretical study was extended to include interaction between toluene and an Al atom. Two conformers were studied. The conformers were found to be similar in energy. From the spin density results, H^+ attack on the Al-toluene complex would most likely occur at the C2 or C3 atoms.

Finally, a preliminary study of the alkylation reaction of the Al-benzene complex was initiated. Reaction of Al atoms with benzene in the presence of methyl iodide produced a methyl radical. This radical reacts with benzene to form the toluene compound.

ACKNOWLEDGMENTS

I would like to sincerely thank my supervisor Dr. Helen Joly for her support, and helpful suggestions throughout my M.Sc. studies. Her patience and guidance is greatly appreciated.

I would also like to thank my co-supervisor Dr. Gustavo Arteca for his valuable assistance, kindness and critical review of the theoretical section of this thesis. Special thanks is also extended to Dr. Ken Westaway for his valuable suggestions in reading the thesis.

Finally, I am grateful to all of the Chemistry Department staff for their help and support throughout my studies at Laurentian University. I wish to extend a special thank you to Leslie Mantle, Maria Kepes and Dan Wunderlich for their assistance and support throughout my research.

TABLE OF CONTENTS

LIST OF FIGURES

LIST OF TABLES

LIST OF SCHEMES

1. INTRODUCTION

1.1 Organometallic Chemistry:

Organometallic chemistry is the study of the properties of compounds which contain metal-carbon bonds with the exceptions of metal cyanides, carbides and carbonyls. Organometallic compounds have been known for well over a hundred years. The earliest known organometallic compounds were the alkyls of zinc, mercury and arsenic, and $K[Pt(C_2H_4)Cl_3]$, a compound referred to as Zeise's salt. The study of organometallic compounds has proven to be important in furthering chemical theory and practice. The properties of ethylzinc iodide[1] and diethylzinc[2] led Frankland to introduce the concept of valency (combining power) and the term organometallic in 1853. The discovery of organomagnesium halides[3] (Grignard reagents) in 1900 provided the intermediates for a wide range of organic syntheses. In the 1940s, organosilicon halides, which are intermediates in silicon manufacture, were prepared from silicon and organic halides.[4] Also, the study of aluminum alkyls has led to their use as catalysts for the large scale polymerization and oligomerization of olefins.[5,6] In 1951, the chance synthesis of ferrocene,[7,8] $(\eta\text{-}C_5H_5)_2Fe$, and the determination of its structure in the following year, opened up a new area of organometallic research and contributed greatly to our understanding of chemical bonding. Now a days, organotransition metal complexes are used as reagents for specific organic synthesis and are also used as intermediates in many catalytic processes, such as the conversion of carbon monoxide, hydrogen, alkenes and other small molecules into useful organic chemicals.[9,10]

As this thesis is concerned with the formation of Group 13 organometallic compounds by a high energy process, the introduction will cover the following topics: (a)

the properties of organometallic compounds, (b) their stability to heat, oxidation and hydrolysis, (c) the kinetic and thermodynamic factors which affect their chemistry, (d) the work done up to date on group 13 (Al, Ga, In and Tl) organometallic compounds, (e) the development and use of high energy processes in organometallic chemistry and (f) some of the theoretical methods used to study the chemistry of organometallic reactions.

1.1.1 Properties of Organometallic Compounds:

Most organometallic compounds resemble organic rather than inorganic compounds in their physical properties. Many exist at ordinary temperatures as low melting crystals, liquids or gases, Table 1.1. Commonly they are soluble in weakly polar organic solvents such as toluene, ethers or dichloromethane. Their chemical properties vary widely and their thermal stability depends on their chemical composition. For example, tetramethylsilane (Me_4Si) is unchanged after many days at 500°C, whereas tetramethyltitanium decomposes rapidly at room temperature. Similarly there are wide differences in their kinetic stability to oxidation, some (e.g. Me_4Si, Me_2Hg, $(\eta\text{-}C_5H_5)_2Fe$) are not attacked at room temperature by the oxygen in air, whereas others (e.g. Me_3B, Me_2Zn, $(\eta\text{-}C_5H_5)_2Co$) are spontaneously inflammable.[9,10]

Table 1.1. Mean metal-carbon bond dissociation enthalpies (D(M-Me), kJ mol^{-1}) and boiling points (°C, 1 atm) for compounds Me_nM. (Taken from reference 9, page 6).

Me_nM	D* (kJ mol^{-1})	Boiling Point (°C)	Me_nM	D (kJ mol^{-1})	Boiling Point (°C)
Me_2Be	-	220**	Me_4C	367	10
Me_2Mg	-	involatile	Me_4Si	320	27
Me_2Zn	186	44	Me_4Ge	258	43
Me_2Cd	149	106	Me_4Sn	226	77
Me_2Hg	130	93	Me_4Pb	161	110
Me_3B	373.9	-22	Me_3N	312	3
Me_3Al	283	126	Me_3P	286	40
Me_3Ga	256	56	Me_3As	238	52
Me_3In	170	136	Me_3Sb	224	79
Me_3Tl	-	147***	Me_3Bi	151	110

* The dissociation energies quoted have an experimental error of ca. ± 5 kJ mol^{-1}.

** Extrapolated sublimation temperature.

*** Extrapolated boiling point.

1.1.2 The Stability of Organometallic Compounds:

Many organometallic compounds are readily oxidized in air but may be stored for a long period under an inert atmosphere. Very reactive species, such as silaethene, $Me_2Si{=}CHMe$, which in most cases would have only a transient existence, can be generated in solid inert-gas matrices at very low temperatures (4-20 K). Under these conditions, the individual molecules are trapped in isolation from each other, so that they can be studied spectroscopically. Above 45 K, diffusion through the solid matrix is sufficiently rapid for dimerization to occur. The environment is therefore critical in

determining whether or not a compound can be isolated or studied. Kinetic factors such as the effect of temperature, pressure or the concentration of reactants will also influence the suitability of an organometallic compound for study.[9,10]

1.1.2.1 Thermal stability:

The standard heats of formation (ΔHf°) of a number of organometallic compounds are presented in Table 1.2.[9] The ΔHf° of a compound gives a measure of its thermodynamic stability, i.e., compounds with large, negative ΔHf° are stable.

Table 1.2. Enthalpies of formation of some organometallic compounds. (Taken from reference 9, page 10).

Compound*	ΔHf° (kJ mol^{-1})	Compound	ΔHf° (kJ mol^{-1})
EtLi (c)	-59	Me_4Ge (g)	-71
MeMgI (ether)	-288	Me_4Sn (g)	-19
Me_2Zn (g)	50	Me_4Pb (g)	136
Me_2Cd (g)	106	Me_3P (g)	-101
Me_2Hg (g)	94	Me_3As (g)	13
Me_3B (g)	-123	Me_3Sb (g)	32
Me_3Al (g)	-81	Me_3Bi (g)	194
Me_3Ga (g)	-42	Ph_3P (c)	218
Me_3In (g)	173	Ph_3Bi (c)	601
Me_4Si (g)	-245	$(C_6Me_6)Cr(CO)_3$ (c)	-671

* (g) denotes gaseous state; (c) denotes crystalline state.

For instance, Me_4Si and Me_3B with a ΔHf° of -245 and -123 kJ mol^{-1}, respectively, are thermodynamically stable at room temperature with respect to decomposition to their constituent elements whereas Me_2Hg, Me_3In and Me_4Pb with a ΔHf° of 94, 173 and 136 kJ mol^{-1}, respectively, are unstable and easily undergo decomposition, equation 1.1,

$$R_nM \longrightarrow \text{Metal} + \text{Hydrocarbons} \qquad 1.1$$

i.e. they are endothermic compounds.[9] For example, the decomposition of tetramethyllead to lead and ethane is thermodynamically favoured ($\Delta H_{Rx} = -306$ kJ mol^{-1}), equation 1.2.

$$Me_4Pb_{(g)} \longrightarrow Pb_{(s)} + 2\,C_2H_{6(g)} \qquad 1.2$$

In Figure 1.1, the mean metal-carbon (M-C) bond dissociation enthalpies for Me_3M (where M = B, N, P, Al, etc.) are plotted as a function of the ΔHf° of the metal in the gas phase. The stability of the Me_nM compounds, reflected in the M-C bond enthalpies, is dependent on the binding energies of the elements in their standard states. Therefore from this analysis, the low ΔHf° of Me_3B (Table 1.2) is largely due to the high binding energy of B in the standard state (298 K and 1 atm).

The decomposition of the isolable, yet thermodynamically unstable compounds, may be kinetically controlled. In order for decomposition to proceed, the activation energy for the rate determining step of the process must be low. There are two possible mechanisms by which decomposition of the organometallic compounds can occur. The first involves the homolytic rupture of the M—C bond to form radicals in the slow step of the reaction. For example, the pyrolysis of tetramethyllead in a flow system at low pressure yields $(CH_3)_3Pb^\bullet$ and methyl radicals, equation 1.3.[11] In this case,

$$Pb(CH_3)_4 \xrightarrow[\text{step}]{\text{slow}} (CH_3)_3Pb^\bullet + CH_3^\bullet \longrightarrow \text{products} \qquad 1.3$$

the activation energy depends on the strength of the metal-carbon bond.

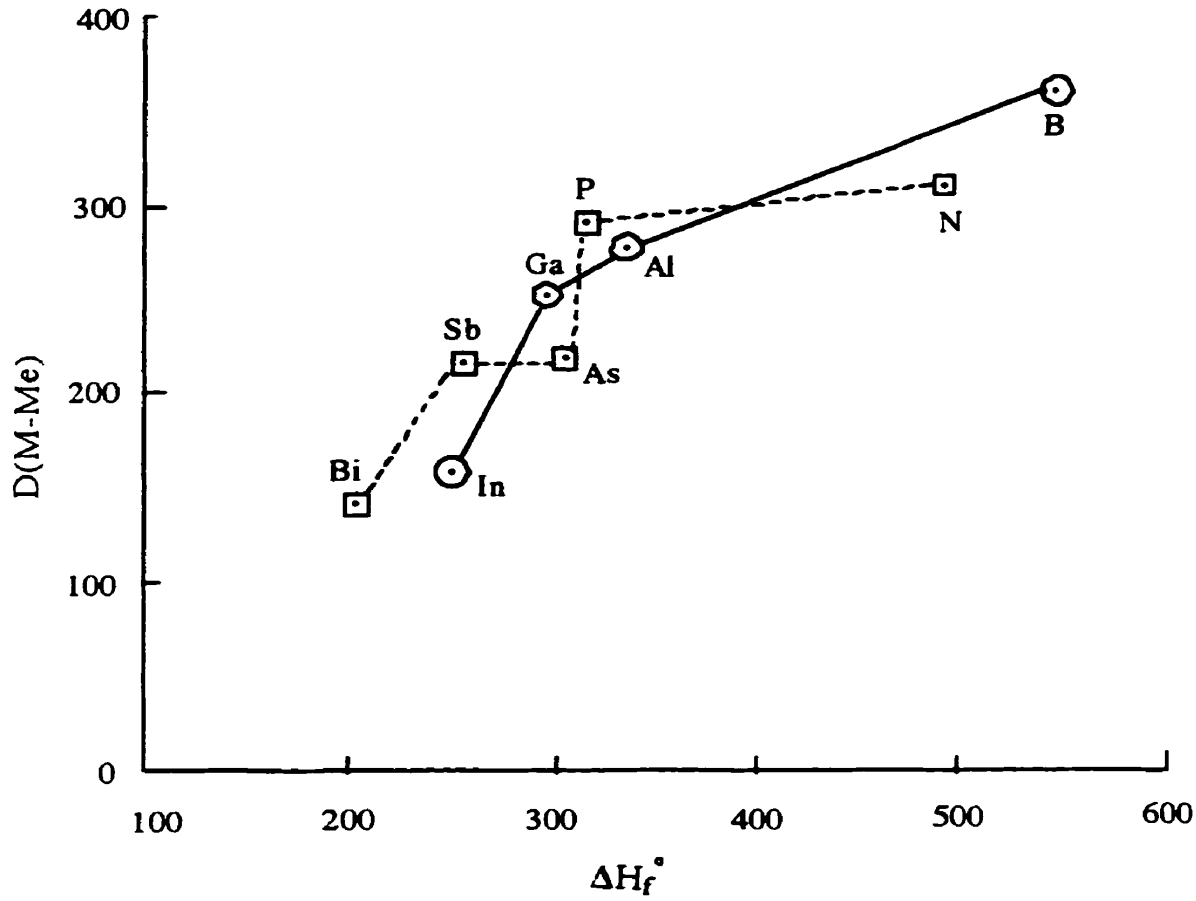

Figure 1.1. A plot of the mean M-C bond dissociation enthalpies (D(M-Me), kJ mol^{-1}) of Me_3M (where M = B, N, P, Al, etc.) versus the standard enthalpies of formation (ΔH_f°, kJ mol^{-1}) of M. (Taken from reference 9, page 10.)

The second mechanism involves β or α-hydrogen transfer. β-hydrogen transfer is common in main group chemistry as a pathway for decomposition of alkyl derivatives. Scheme 1.1 shows the mechanism of a β-hydrogen transfer where an alkyl metal complex eliminates ethene on heating, leaving a metal hydride. For example, triethylaluminum,

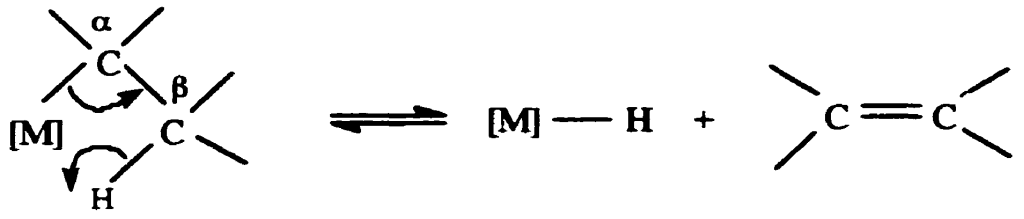

Scheme 1.1. β-Hydrogen transfer.

undergoes β-hydrogen transfer (β-elimination) resulting in the formation of diethylalumina hydride and ethene, equation 1.4.

$$Al(CH_2CH_3)_3 \rightleftharpoons (CH_3CH_2)_2AlH + CH_2=CH_2 \qquad 1.4$$

The metal hydride can react with ethene under pressure to regenerate the ethyl complex, indicating that the reaction is reversible. The equilibrium involving β-hydrogen transfer has been observed directly by proton NMR spectroscopy. For the elimination to proceed, a vacant coordination site at the metal centre is required. For a complex which has only a 16-electron configuration (coordinatively unsaturated) the transfer is easy, but for 18-electron compounds the site has to be provided by dissociation or by change of the hapto number of a ligand, η^n, (number of ligand atoms coordinated to the metal). For unsaturated hydrocarbon ligands the maximum hapto number is equal to the number of carbon atoms in the unsaturated system (for example benzene has a hapto number of 6, η^6).

If the metal alkyl does not possess a β-hydrogen atom this pathway is suppressed. Other mechanisms such as α-hydrogen transfer, may then take place. The product of the initial step of the α-hydrogen transfer mechanism is an alkylidene hydride, $[M]H(=CH_2)$,

scheme 1.2. In all known cases, the alkylidene hydride intermediate is unstable and undergoes decomposition. If there are other alkyl groups (R) in the molecule, a hydrocarbon (RH) can be lost as a result of an intramolecular process. Intermolecular loss of RH is also a possibility.[9] For example, in the case of penta-(2,2-dimethylpropyl) tantalum,

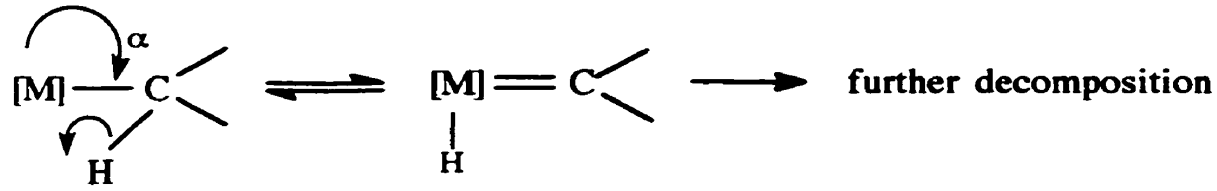

Scheme 1.2. α-Hydrogen Transfer

it has been proposed that a α-hydrogen transfer (α-elimination) results in the formation of an alkylidene hydride.[9] In a subsequent step, the unstable hydride decomposes and 2,2-dimethylpropane is produced in the process, equation 1.5.

$$(Me_3CCH_2)_5\,Ta \rightleftharpoons (Me_3CCH_2)_4\,\underset{\displaystyle H}{Ta}=CHCMe_3 \qquad 1.5$$

$$\downarrow$$

$$(Me_3CCH_2)_3\,Ta = CHCMe_3 + CMe_4$$

1.1.2.2 Stability to oxidation:

The vast majority of organometallic compounds, with the exception of Me_2Hg and derivatives of group 14 elements, are sensitive to oxygen and must be handled under an inert atmosphere.[9, 10] Both thermodynamic and kinetic factors control the stability of the organometallic compounds to oxidation. All organometallic compounds are thermodynamically unstable to oxidation due to the large negative free energies of formation of metal oxide, carbon dioxide (ΔG_f° = -394 kJ) and water (ΔG_f° = -242 kJ). For example, zinc diethyl is converted to a mixture of zinc oxide, water and carbon dioxide when exposed to oxygen, equation 1.6.

$$Zn\,(C_2H_5)_2 \xrightarrow{7.5\,O_2} ZnO_2 + 5\,H_2O + 4\,CO_2 \qquad 1.6$$

The heat of combustion of this reaction is -1920 kJ mol^{-1}.

Many organometallic compounds are kinetically unstable to oxidation at or below room temperature. Kinetic instability to oxidation is a result of the presence of empty low-lying orbitals, e.g. 5p in Me_3In, or of a non-bonding pair of electrons, as is the case for Me_3Sb.

1.1.2.3 Stability to hydrolysis:

The hydrolysis of an organometallic compound often involves nucleophilic attack by water and is facilitated by the presence of empty low-lying orbitals on the metal atom.[11] The organic derivatives of the elements of Group 1 and 2 and of Zn, Cd, Al, Ga and In are readily hydrolyzed. The rate of hydrolysis is dependent on the polarity of the M—C bond. Compounds with a relatively polar M—C bond, like Me_3Al, are subject to rapid attack by water, whereas Me_3B is unaffected by water at room temperature.[9] Organolanthanides are extremely susceptible to hydrolysis because of the polar character of the bond, the large

size of the central atom and the presence of many low-lying empty orbitals; factors which aid coordination of a nucleophile.[10]

The alkyls and aryls of Group 14 and 15 elements are kinetically inert to hydrolysis. In these compounds the metal atom is surrounded by filled shells of eight electrons and as a result, nucleophilic attack is no longer favoured.[10] The majority of the neutral organic derivatives of the transition elements are also inert to hydrolysis.

1.1.2.4 General features relating to stability:

The M-C bond of organometallic compounds is weak compared to M-nitrogen, M-oxygen and M-halogen bonds. This bond weakness is reflected in the uses that organometallics find in synthesis. All organic compounds are thermodynamically unstable to oxidation and exist in the presence of air only because no suitable low energy oxidation mechanism is available.[9] The kinetic stability of organic compounds, for example alkanes, is due to the full use of the four valence orbitals (sp^3) in carbon, leading to the common maximum coordination number (CN) of four. Another reason for the kinetic stability of organic compounds is the high energy of empty antibonding orbitals into which electrons could be donated in the case of nucleophilic attack. Expansion of the coordination number above four commonly occurs in compounds of silicon and of other main group elements of the second and later periods. Their kinetic stability increases when strongly electronegative groups such as halogen atoms are attached to the metal atom (e.g. SiF_6^{2-}). Thus kinetic stability of organometallic compounds may be associated with a closed shell of electrons around the metal atom. A number of stable organometallic compounds have coordination numbers greater than four, for example Me_4Li_4 with a CN of 7 and $(Me_3Al)_2$ with a CN of 5. The stability of compounds such as $(Me_3Al)_2$ has been explained in terms of the interaction of three center molecular orbitals to form 2 electron, 3 center (2e, 3c) bonds. More specifically, if the valence orbitals of Al are sp^3 hybridized, two of the hybrids can

form the terminal Al-CH_3 bonds, scheme 1.3**a**. Two of the three valence electrons of each Al form the electron pair bonds. The remaining sp^3 hybrids are directed in the Al_2C_2 plane and are well placed to interact with the C (sp^3) orbitals of the bridging methyl groups. Each of these 3 center bonding molecular orbitals contains 2 electrons, one from Al and one from a bridging methyl group.

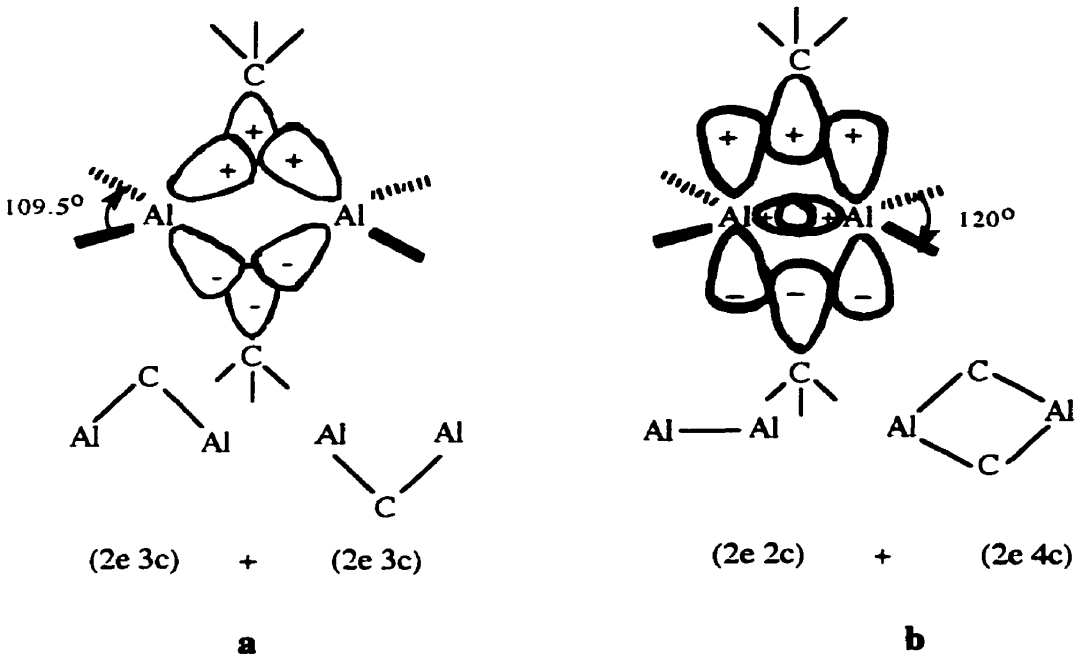

Scheme 1.3. Alternative descriptions of bridge bonding in $(Me_3Al)_2$. Bonding combinations only are shown. (**a**) Model 1: sp^3 hybridization of Al orbitals. (**b**) Model 2: sp^2 hybridization of Al orbitals. Taken from reference 11, page 79.

Alternatively, the bonding could arise from the interaction of the 3p orbitals of two Al atoms with the sp^3-hybridized carbon atom of the methyl group, scheme 1.3**b**. In this model the valence orbitals of Al are sp^2 hybridized. Two of the sp^2-hybrid orbitals interact with sp^3-hybrid orbitals of the C atoms of terminal methyl groups. The third sp^2 orbital of Al overlaps with that of the second Al to form a 2-electron 2-center (2e, 2c) bond. As stated earlier, the 3p orbitals of Al interact with the sp^3-hybridized C of the bridging methyl group forming a 2-electron 4-center (2e, 4c) bond.

The latter model which involves direct Al-Al interaction is consistent with the relatively short Al-Al bond distances observed for these dimers (ca. 2.60 Å). However, the bonding of most dimeric organoaluminum compounds can be explained in terms of a compromise between model 1 and model 2.

For compounds of the transition elements, empty valence shell ns, np or (n-1)d orbitals are often available and this can decrease their kinetic stability. This accounts for the ready thermal decomposition of many binary alkyls by α- or β-hydrogen transfer. A closed shell for transition elements consists of 18 electrons i.e. ns^2, np^6, $(n-1)d^{10}$. These additional electrons can be supplied by a spectator ligand such as cyclopentadienyl, which themselves are not readily displaced. Whereas WMe_6 decomposes below room temperature, sometimes explosively, $(\eta\text{-}C_5H_5)_2WMe_2$ can be sublimed without decomposition at 120°C/10^{-3}mm. In the former compound, the tungsten atom has a configuration of only 12 electrons, whereas in the latter the closed shell of 18 electrons is attained. Transition metal atoms are like atoms of Group 1 and 2 elements, inherently electron deficient, and this electron deficiency must be satisfied if thermally stable organometallic compounds are to be formed.[9,11]

1.1.3 High-Energy Processes in Organometallic Chemistry:

Thermodynamic and kinetic factors influence the course of chemical reactions and the stability of compounds. Chemists seeking to achieve particular goals are always manipulating these factors using chemical or physical means. The use of high energy processes to produce organometallic compounds is a good example of how physical means can be applied to get around the thermodynamic and kinetic limitations of conventional organometallic chemistry. Conventional processes occur between -100-250°C and do not involve the injection of forms of energy other than thermal or the addition of very short-lived reagents such as atoms or radicals. High energy processes are those in which the energy input is not thermal, i.e. the energy comes from either the absorption of light, ultrasonic cavitation or the addition of unstable gaseous species, produced by external energetic processes.

One of the first uses of a high energy process in organometallic chemistry was the work by Paneth and Hofeditz[12] and Rice et al.[13] on the reaction of metal mirrors with free alkyl radicals. Alkyl radicals, formed by thermal decomposition of a zinc or lead alkyl in a flowing gas stream, were reacted with metal films to give new organometallic compounds.

High energy processes can be divided into two classes. In the first class of high energy processes, energy is applied to reactants *in situ* to excite molecules to high translational, vibrational or electronic states so that the excited molecules can undergo immediate intra- or inter-molecular reactions. Such processes include photochemistry, radiolysis, shock wave studies, sonication and some discharge reactions. The second class of high energy processes involves the reaction of high energy species such as free atoms, radicals, carbene-like molecules or ions (formed in the gas phase by a chemical, thermal, photo-chemical or discharge processes) with other molecules in the gas or condensed phase.

Gaseous metal atoms can be taken as representative of the class of endothermic species which are formed and subsequently reacted with substrates to form organometallic compounds, e.g. the reaction of Al atoms and benzene at liquid helium temperature (~ 4 K).[14] Aluminum atoms were produced, using high temperatures (~ 1050 °C) and reacted with an organic substrate (benzene) to form the organometallic complex AlC_6H_6.

Gaseous metal atoms have heats of formation of about 300-800 kJ mol^{-1}, and in chemical synthesis this value varies depending on thermodynamic (enthalpies and entropies) factors. A reaction of M + L (where M is a metal atom and L is a ligand molecule) will be exothermic if the M—L bond dissociation energy is positive. The exothermicity of a reaction where the M and L are in the gaseous state, equation 1.12, will be greater than that for a reaction where the M is in the solid state, equation 1.13, by an amount proportional to the heat of atomization of the metal, Figure 1.2.

$$M_{(gas)} + nL_{(gas)} \longrightarrow MLn_{(solid)} \qquad 1.12$$

$$M_{(solid)} + nL_{(gas)} \longrightarrow ML_{n\,(solid)} \qquad 1.13$$

Direct reaction between ligands and solid metals are not often successful because the kinetics and sometimes the thermodynamics of the process are unfavourable. However, a reductive process, also considered a high energy process, equation 1.14, has been used to successfully produce ML_n as in the case of gaseous metal atom synthesis described above.[15] The reductive process requires that a metal halide, MX_m, be treated with an electropositive metal, M', in the presence of a ligand, L, equation 1.14.

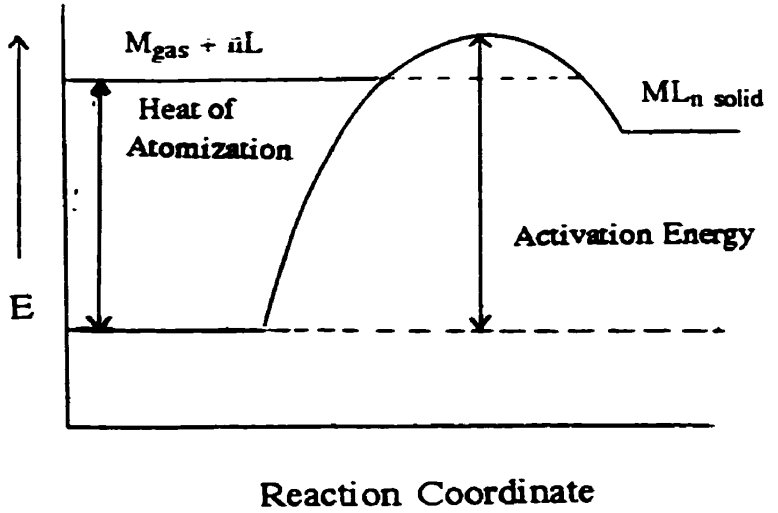

Figure 1.2. Reaction coordinate diagram of the ML_n reaction.

$$MX_m + nL + mM' \longrightarrow ML_n + mM'X \qquad 1.14$$

This reaction will be exothermic even if the product ML_n is endothermic because M'X is much more stable than MX_m. Thermodynamically, reductive routes can achieve almost as much as can be achieved using the reaction of metal atoms and ligands. However, in practice, atom-ligand reactions have such low activation energies that they will occur at lower temperatures than most reductive reactions, enhancing the chances of isolating unstable products, and reducing unwanted side reactions. Atom reactions have therefore proven to be more successful than reductive reactions in a number of cases.

1.1.3.1 Metal atom chemistry:

The reaction of organic and inorganic substrates at a metal surface, either in a catalytic way or in an oxidation addition reaction with consumption of the metal, represents an extremely important area of chemistry. Chemists are continually trying to increase the

reactivity of metals in order to allow reactions to be carried out under milder conditions, to improve yields and save energy, or to extend the reaction to less reactive substrates. In recent years, several new approaches to this problem have been reported. One method was to generate metal powders by the reduction of the metal salt with an alkali metal in a hydrocarbon solvent.[15,16] Another approach, which has been studied in this thesis, is the one that has evolved from Skell's carbon vapor reactor, namely the metal atom or metal vaporization technique.[17]

Metal atoms (vapours) are among the most easily produced high-temperature species, and their synthetic chemistry is interesting and useful. Most studies of high-temperature species have been carried out at low temperature (e.g. 77 K) because slow reaction rates allow intermediate reactive species to be observed spectroscopically. In addition, since most high-temperature species must be generated in a vacuum system, low vapour pressure is maintained in the system by immediately condensing all incoming intermediates. Vapourization is carried out under high vacuum, so that the metal atoms can pass by collision-free paths from a hot zone where they are formed to a liquid nitrogen cooled surface a few centimeters away.[17,18,19]

The co-condensation of metal vapour and the vapour of an organic compound on a very cold surface results in the formation of organometallic compounds. As indicated above, the success of the method is dependent upon the heat of atomization of the metal and that the vapourization is carried out under high vacuum (pressure $<10^{-5}$ Torr). When a metal is vapourized, atoms are formed which are very endothermic with respect to the solid metal. The atoms are likely to be more chemically reactive than the solid metal both for thermodynamic and kinetic reasons. The essence of the cryogenic method is to separate the generation of the metal atoms from the reaction site so that the organics are not pyrolysed by the furnace.

1.1.3.2 Metal atom reactor (Rotating Cryostat):

The first metal atom reactor (carbon vapour reactor) was devised by Skell and collaborators[17,20] to study the reactions of carbon species with organic compounds at 77 K. Carbon was vaporized using carbon arc electrodes in a vacuum chamber. The resulting carbon vapour was codeposited with organic substrates on the liquid nitrogen cooled walls of the reactor. Timms used techniques similar to those of Skell and Wescott to vapourize metals.[21] In 1975, a new metal atom reactor in which metals were vaporized using resistive heating was designed.[22,23] The metal vapor, deposited on the inside walls of the reactor, was bombarded with the vapors of an organic substrate directed to the metal deposition site via a shower head.

A metal atom reactor, which operated on the same principle as a rotary evaporator, was subsequently devised by Timms and Mackenzie[24] and Benfield et al.[25]. In this type of reactor, metal vapour was generated with the aid of resistively heated electrodes mounted in the centre of the rotating flask. The substrate, dissolved in an inert solvent, was added to the rotating flask. The vapour pressure of the solvent was reduced by dipping the rotating flask in an appropriate low temperature bath. During operation the metal vapour was sprayed upwards onto the thin cold film of solution covering the walls of the rotating flask.

The restriction of reactions to single, specific steps in systems that are wholly gaseous, liquid or solid gives experimental problems. However the use of a gas-solid system offers a greater chance of success because the reactive intermediates can be trapped on a solid surface where they can not migrate and react with one another, but where they can react with molecules colliding with the surface from the gas phase. On this basis, Thomas and Bennett[26] developed a reactor known as a "rotating cryostat" which has largely overcome the experimental problems of such a gas-solid system. The principle employed is that of a conveyor belt. The reactants are continuously frozen on the surface

of the belt which is held at a low temperature (77 K) and then subjected sequentially to bombardment by a series of molecular reactants. Because the subsequent intermediates are also frozen on the surface they can not migrate and react with each other but they may react with further bombarding molecules from the gas phase. In practice, the belt is replaced by the surface of a rotating drum so that the process starts again after each complete revolution. Bennett and Thomas[27] developed this technique to provide both a general method for preparing specific free radicals and radical anions and also a method for studying single-step reactions between specific free radicals and selected molecular reactants. Because the reactions occur at low temperature (usually 77 K) subtle effects of molecular structure on reactivity are enhanced and more easily observed. The technique has been applied to metal-atom reactions by Howard et al.[28]

The rotating cryostat consists of a liquid nitrogen filled stainless steel drum, which spins about a vertical axis at high speed within an evacuated outer vessel, Figure 1.3. A hydrocarbon, R, is introduced via jet A which is fitted through a porthole in the outer reaction vessel. The hydrocarbon freezes to form a solid layer as it hits the rotating drum. Metal vapour produced by resistive heating effuses through a second porthole (B) and is deposited on top of the hydrocarbon layer producing the organometallic layer. The metal-hydrocarbon ratio is controlled by controlling the deposition rate of both reactants. During the next revolution the metal-hydrocarbon layer is covered by a fresh layer of hydrocarbon sheltering the bulk deposit from further reactions. With time, a deposit is built up in which the radicals are sandwiched between layers of excess hydrocarbon.

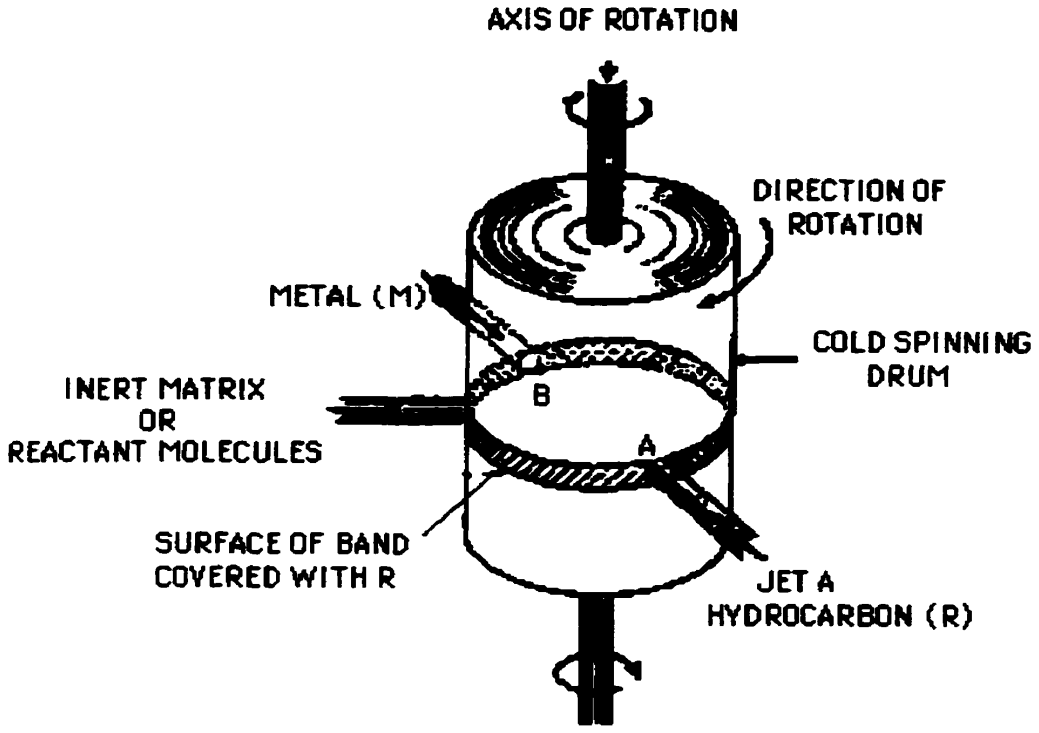

Figure 1.3. Liquid-nitrogen filled drum in the rotating cryostat.[27]

Independent matrices are sometimes used because excess hydrocarbon is not always the most suitable material in which to trap the organometallic intermediates formed. This material is admitted through a third jet which is placed before the jet through which the hydrocarbon flows, Figure 1.4, and forms the bulk of the deposit. The ratio of the hydrocarbon to metal is controlled so that most of the hydrocarbon is converted into radicals. The characteristics of a good matrix is inertness to radical attack, transparency to ultraviolet or infrared light and improved resolution of electron spin resonance (ESR) spectra. Compounds that have been useful as matrices are water and benzene (inert towards radical attack), and camphane and adamantane (improved resolution of ESR spectra).

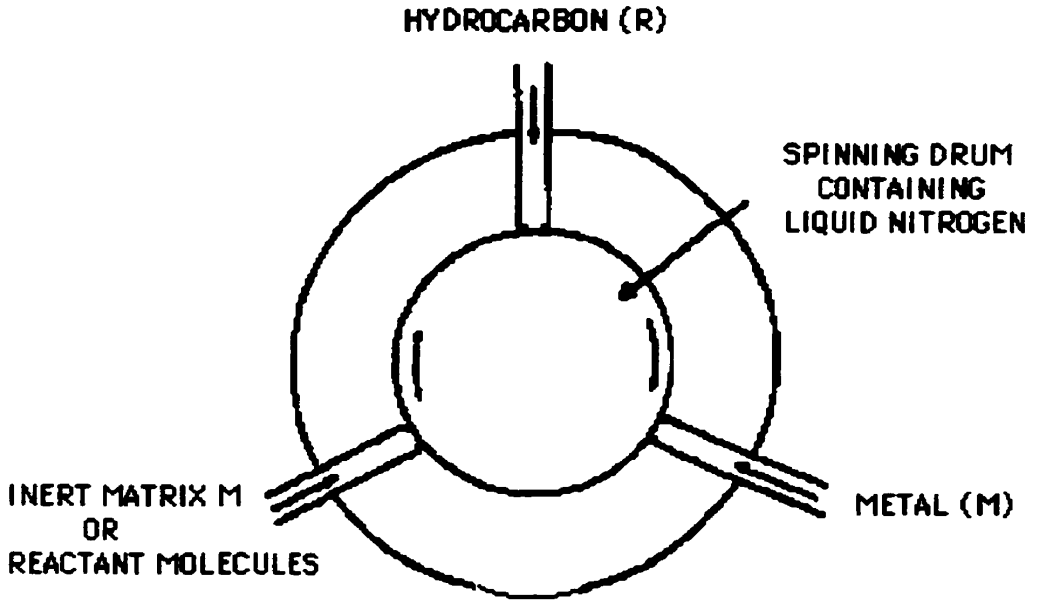

Figure 1.4. Arrangement of jets for independent matrix deposition.[27]

The rotating cryostat is also a unique metal-atom reactor because it allows the study of the reactivity of the organometallic intermediates. Once the organometallic intermediates have been covered up by the next layer of matrix they are trapped and no longer accessible to other reactants. However, between the point at which they are formed and that at which they are covered up they lie exposed on the surface of the deposit and may undergo reaction with another reactant which can be brought in through a fourth jet. Further reactants may be admitted through additional jets to permit a sequence of single step reactions to occur.

1.1.4 Organometallic Compounds Of Group 13 Elements:

1.1.4.1 Organoaluminum compounds:

In 1859, Hallwachs and Schafarik[29] showed that alkylaluminum iodides resulted when alkyl iodides were reacted with Al, equation 1.7.

$$2\,Al + 3\,RI \longrightarrow R_2AlI + RAlI_2 \qquad 1.7$$

Considerable interest in the chemistry of organoaluminum compounds has been generated in the past 50 years. Compared with the organometallics of groups 1 and 2, aluminum organyls are easily added to alkenes and alkynes. The regio- and stereoselectivity of these carbaluminations (addition of Al-C bonds to alkenes and alkynes), as well as of the related hydroaluminations (addition of Al-H bonds to alkenes and alkynes) using R_2AlH, are an additional asset. Aluminum organyls may gradually replace lithium- and magnesium organyls due to:

(a) the development of cost efficient processes for the production of certain aluminum alkyls from aluminum, hydrogen and olefins which are suitable for industrial operation,

(b) the discovery that aluminum alkyls react with olefins to form dimerization products, paraffin polymers or various 1-alkenes which are important to detergent manufacture.

(c) the development of olefin polymerization catalysts from aluminum alkyls and some transition metal compounds.

(d) the discovery that aluminum alkyls are precursors for the preparation of alkyls of other elements.

Alkylaluminum compounds are produced on a large scale, industrially. In 1975 about 20,000 tons were produced worldwide for sale and a further 90,000 tons were used as intermediates in the manufacture of linear alcohols and 1-alkenes.[9]

Alkylaluminum compounds are generally prepared by the addition of Al—H to an alkene. The aluminum surface must first be activated by grinding the metal with Et_3Al (where Et is CH_3CH_2) in order to remove surface oxides. Ziegler[30] proposed that Al metal takes up hydrogen in the presence of Et_3Al and the resulting Al-H bond adds to the olefin. With reactive alkenes such as ethene, the process is usually carried out in two stages at 150°C, using preformed trialkylaluminum:

$$2\,Al + 3\,H_2 + 4\,Et_3Al \xrightarrow{150^\circ C} 6\,Et_2Al\,H \xrightarrow{6C_2H_4} 6Et_3Al \qquad 1.8$$

With less reactive, bulky alkenes such as 2-methyl-1-propene, a single step reaction takes place at 110-160°C:

$$2\,Al + 3\,H_2 + 6\,Me_2C{=}CH_2 \xrightarrow{110\text{-}160^\circ C} 2\,(Me_2CHCH_2)_3\,Al \qquad 1.9$$

From a commercial point of view, the most important reactions of organoaluminum compounds are (1), the insertion of alkene into an aluminum—carbon bond, equation 1.10, and (2), the displacement of one alkene by another known as transalkylation, equation 1.11.

$$Al\text{-}R + H_2C{=}CH_2 \longrightarrow AlCH_2CH_2R \xrightarrow{H_2C=CH_2} Al\,(CH_2CH_2)_2R \xrightarrow{\text{etc.}} \qquad 1.10$$

$$AlCH_2CH_2R + H_2C{=}CHR' \longrightarrow AlCH_2CH_2R' + RCH{=}CH_2 \qquad 1.11$$

Insertion has been found to be very rapid with respect to transalkylation in the case of the reaction of ethene and organoaluminum compounds at low temperatures (90-120°C). The alkyl chains grow by the successive insertion of ethene. The multiple insertion of ethylene into the Al-C bond, discovered by Ziegler[30], has become known as the Aufbaureaktion (growth reaction). It is used to produce 1-alkenes and unbranched primary alcohols, scheme 1.4.

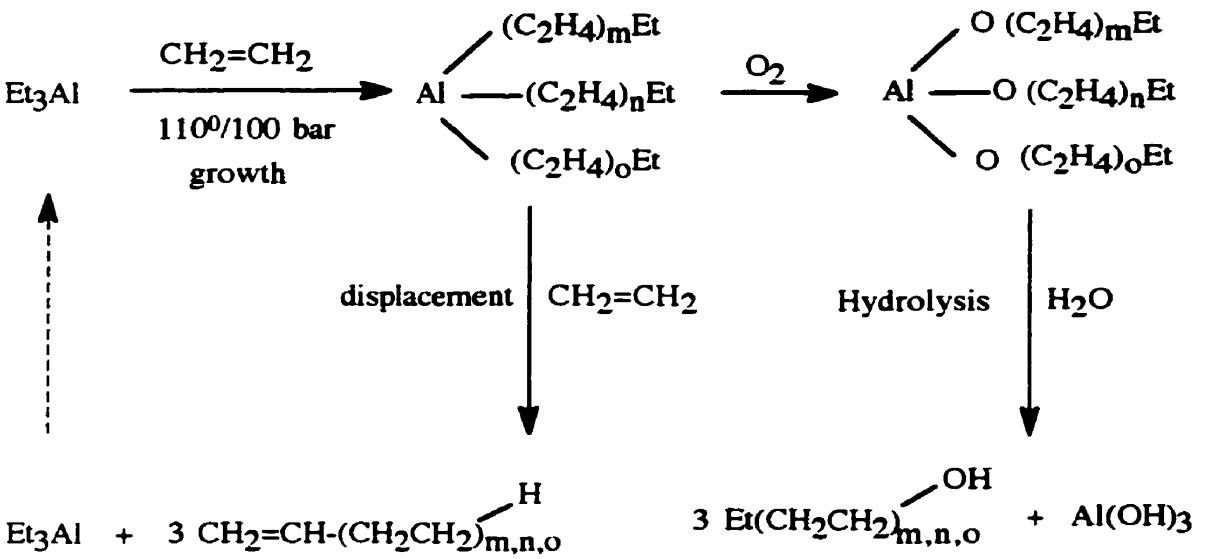

Scheme 1.4. The growth reaction (Taken from reference 11, page 77.)

The sequence of insertions can proceed up to chain lengths of about C_{200}. A limiting factor is the competition between the growth and displacement reactions. The mixture of

aluminum alkyls is converted into linear primary alcohols of chain lengths C_{12}—C_{16} (detergent alcohols) by controlled oxidation followed by hydrolysis. C_{12}—C_{16} alcohols are precursors to surfactants and biodegradable detergents such as alkyl sulfates and alkyl sulfonates ($ROSO_3H$).[11]

If instead of ethene, propene or another 1-alkene is used, only a single insertion into the Al-C bond takes place. An example is the catalytic dimerization of propene, followed by thermal elimination of methane, providing an industrial route to isoprene, scheme 1.5, which itself is subsequently polymerized by a transition metal aluminum alkyl catalyst to give polyisoprene, a synthetic route to produce rubber.[11]

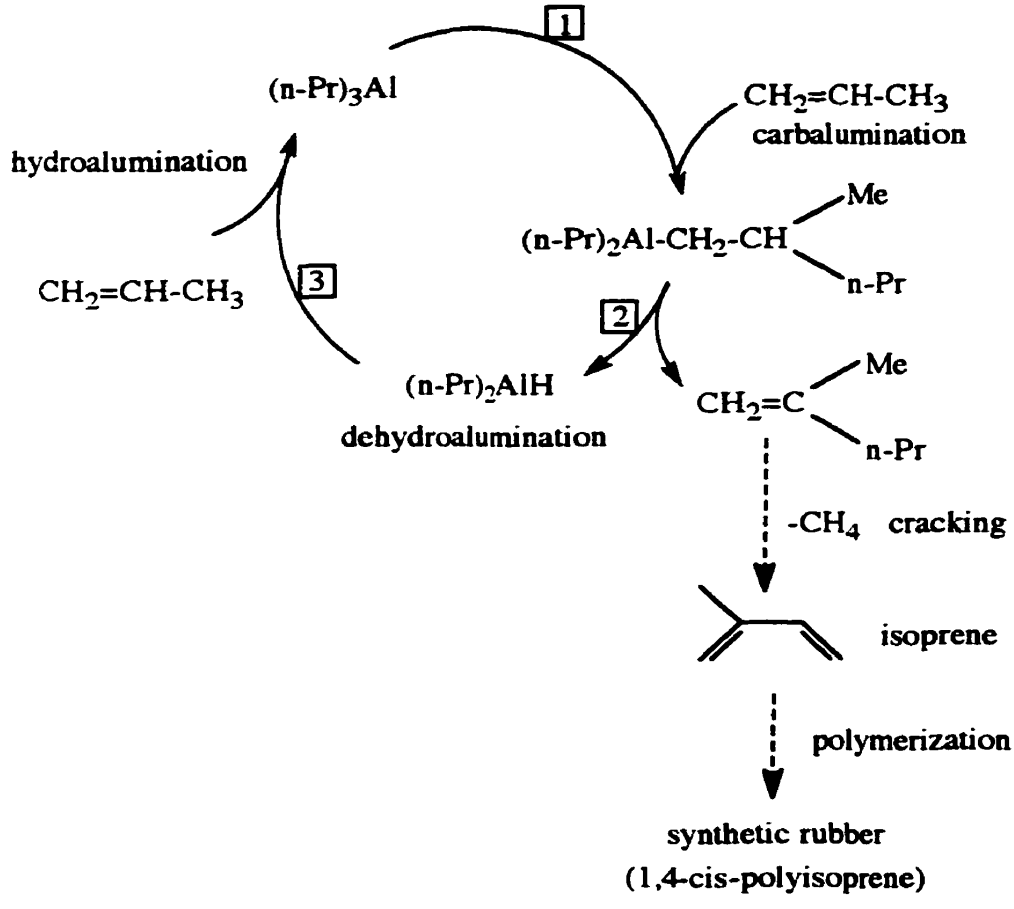

Scheme 1.5. Catalytic dimerization of propene (Taken from reference 11, page 77).

At about 180°C in the presence of excess ethene, alkene insertion and transalkylation take place at comparable rates. Under these conditions ethene is converted into a mixture of 1-alkenes, the alkyl aluminum acting as a catalyst.

1.1.4.2 Organo-gallium, -indium and -thallium compounds:

The organic chemistry of gallium, indium and thallium has not been studied as extensively as that of boron and aluminum; the elements are relatively scarce and costly. Organogallium and organoindium compounds serve as doping agents in the manufacture of semiconductors. Despite their high toxicity, organothallium compounds have found use in organic synthesis.

Gallium trialkyls (GaR_3) can be prepared by alkylating Ga with HgR_2 or by the action of RMgBr or AlR_3 on $GaCl_3$. They are low-melting, ionic, flammable liquids. The corresponding In and Tl compounds are similar but tend to have higher melting and boiling points. The gallium, indium and thallium trialkyls do not dimerize. The thermal stability of the trialkyl compounds as well as the chemical reactivity of the M—C bond decrease with increasing atomic weight of M. As in the case of R_3Al, alcohol can displace one of the alkyl groups of R_3Ga. Displacement of the first alkyl group from R_3Al by reaction with an alcohol, takes place more readily than that of the remaining alkyl groups and those that do remain are normally highly sensitive to air and moisture. Gallium, indium and thallium differ in that displacement of the second and third alkyl groups is much more difficult. Compounds such as Me_3GaOEt_2 or $(Me_2GaCN)_4$ are readily hydrolyzed, but the process stops at the dimethylgallium stage $(Me_2GaOH)_4$. This effect reaches a maximum with thallium, whose trialkyls are reactive and unstable, and the dialkyl compounds tend to be ionic (R_2Tl^+) and unreactive The triphenyls of Ga, In, and Tl are monomeric in solution but tend to associate into chain structures in the crystalline state as a result of weak intermolecular M···C interactions· $GaPh_3$ mp 166°C, $InPh_3$ mp 208°C, $TlPh_3$ mp 170°C.

For Ga and In compounds, the M—C bonds can be cleaved by HX, X_2, or MX_3 to give reactive halogen-bridged dimers $(R_2MX)_2$.[11]

A few organometallic compounds of Tl^I are known. TlC_5H_5 precipitates as air-stable yellow crystals when aqueous TlOH is shaken with cyclopentadiene. In the gas phase $Tl(\eta^5\text{-}C_5H_5)$ has C_{5v} symmetry, Figure 1.5, whereas in the crystalline phase there are zigzag chains of equispaced alternating C_5H_5 rings and Tl atoms. $In(\eta^5\text{-}C_5H_5)$ is less stable but has the same structure as the Tl compound in each phase.[11]

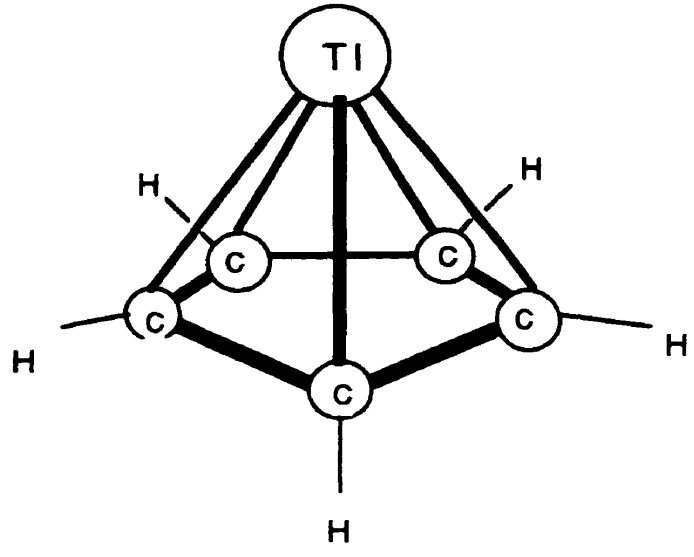

Figure 1.5. The C_{5v} structure of $Tl(\eta^5\text{-}C_5H_5)$ in the gas phase.

1.1.5 Group 13-Atom Reactions:

Reactions between vaporized metal atoms and organic or inorganic molecules condensed at cryogenic temperatures have been the subject of many recent studies. Group 13 metal atoms possess very high intrinsic chemical reactivity under low-temperature conditions.

1.1.5.1 Aluminum-atom reactions:

1.1.5.1.1 Aluminum-atom reactions with organic compounds:

(a) Alkene and alkyne reactions:

Skell and Wolf[31] demonstrated the formation of organoaluminum compounds when Al atoms were co-condensed with excess propene or propyne at liquid nitrogen temperature. Analysis of the deuterolysis products of the resulting organoaluminum compounds showed that the primary reaction between free Al atoms and alkene or alkyne molecules is an addition of one Al atom to the unsaturated bond. Propene did not give isolable products, but hydrolysis with D_2O to replace each C-Al bond with a C-D bond suggested the formation of the organoaluminum intermediate shown in Figure 1.6.[31]

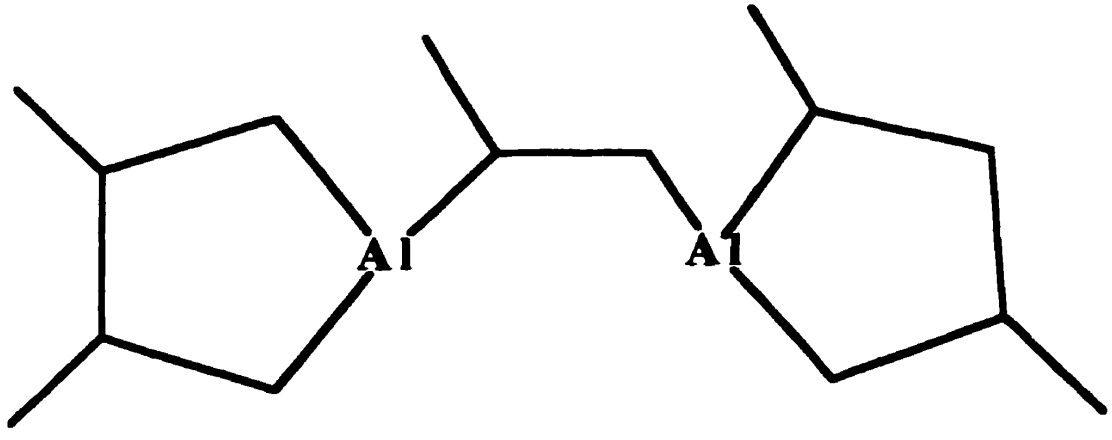

Figure 1.6. The organoaluminum intermediate.

The interaction of Al atoms with ethylene has been studied by two separate research groups. In 1975, Kasai and coworkers[32,33] studied the interaction of Al atoms with ethylene in rare gas matrices. The ESR spectral analyses suggested that the Al-ethylene complex has a π-coordinated structure, Figure 1.7.[32,34] More specifically, it was proposed that bonding involves electron donation from the ethylene π orbital into an empty Al orbital and counter electron flow from the Al into the ethylene π^* orbital. The unpaired electron on Al is located in the p orbital parallel to the ethylene π orbital, i.e., the complex has C_{2v} symmetry. The Al to ethylene bond is strong and has been estimated to be >77 kJ mol^{-1} in the gas phase.[35]

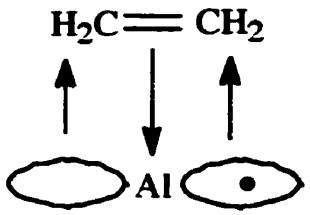

Figure 1.7. Structure of the Al-ethylene complex.

In a second study carried out by Howard et al.,[36] Al atoms were reacted with ethylene in an adamantane matrix at 77 K. These workers have suggested that Al adds to the double bond forming a fluxional intermediate which resembles aluminacyclopropane shown in Figure 1.8. The complex is fluxional in that the Al atom is thought to undergo a 1,2-shift. These workers have estimated the energy for the dissociation of the Al-ethylene bond to be between 95-145 kJ mol^{-1}.

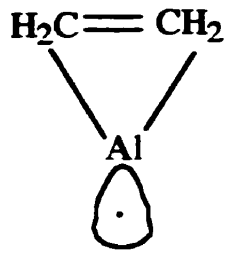

Figure 1.8. Structure of aluminacyclopropane.

Several high-level ab initio theoretical calculations of the Al-ethylene complex[37,38] predict the σ-bonded complex to be more stable than the π-bonded complex. Experimentally, the binding energy of the σ-bonded Al-ethylene complex has been determined to be greater than 67 kJ mol^{-1},[39] while the best theoretical estimate is about 50 kJ mol^{-1}.[40] These studies support the formation of a σ-bonded complex in reactions of Al atoms with ethylene. Al-C σ-bonds are well known in organoaluminum chemistry.[41,42]

(b) Butadiene reactions:

ESR studies of the reaction of ground state Al atoms with buta-1,3-diene[43] in adamantane at 77 K in a rotating cryostat have demonstrated the formation of two major paramagnetic products, a σ-bonded aluminacyclopentene, Figure 1.9**a**, and a π-complex, an aluminum-substituted allyl, Figure 1.9**b**.

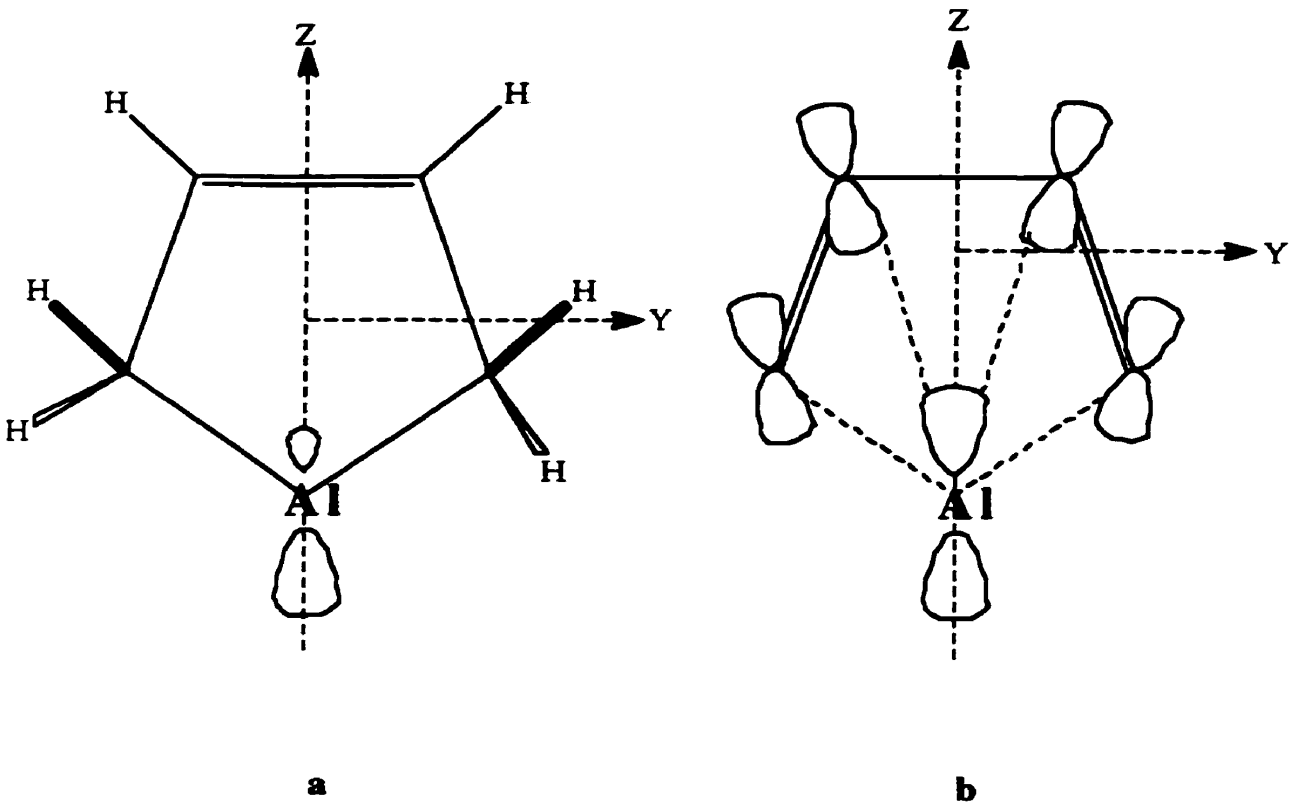

Figure 1.9. Structures of (**a**) the σ-complex and (**b**) the π-complex formed in the reaction of Al atoms and buta-1,3-diene.

(c) Benzene reactions:

ESR studies have also been carried out on the interaction of Al atoms with benzene in an adamantane matrix at 77 K. Kasai and McLeod[14] were the first to report the ESR spectrum of monobenzenealuminum from reaction of ground-state Al atoms ($3s^2 3p^1$) with benzene in a neon matrix at ca. 4 K. The spectrum revealed interaction with only two of the six equivalent protons of benzene with an unpaired spin population of ca. 0.2 in the 3p orbital of Al and ca. 0.4 on the ring. These authors suggested a structure, Figure 1.10, with Al complexed to one C=C unit by dative bonding of the semioccupied $3p_x$ orbital of

Al and two antibonding p_π orbitals on two ortho carbon atoms of benzene. Howard et al. studied the interaction of Al atoms with benzene in an adamantane matrix at 77 K.[44,45] The ESR spectrum recorded at 220 K suggested that the Al atom interacts with six equivalent hydrogen nuclei. The spectrum was highly dependent on temperature. Their results suggested that the Al atom added to the 1,4-positions of benzene, Figure 1.11, and had donated ca. 0.7 of its unpaired electron to benzene.

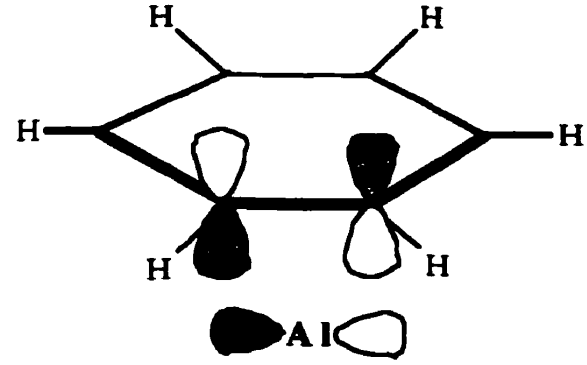

Figure 1.10. Structure of the π Al-benzene complex.

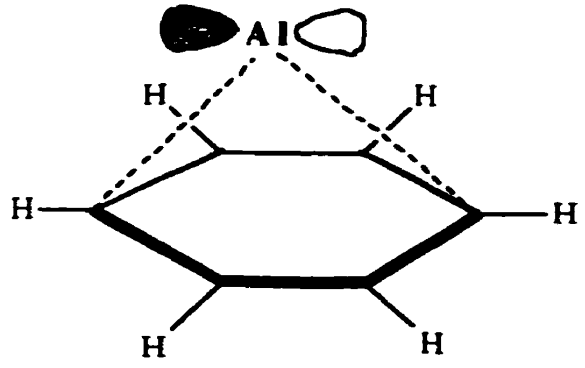

Figure 1.11. Structure of the σ Al-benzene complex.

Ab initio studies of the aluminum-benzene complex support the formation of a 1,4-addition complex as the most stable bonding for the Al-benzene complex.[46] The spin density on aluminum was calculated to be 0.04[46] or 0.18[47], which indicates a substantial transfer of spin density. However, Mitchell et al.[35] using time-resolved resonance fluorescence spectroscopy have measured a binding energy 49 kJ $mole^{-1}$ for $Al(C_6H_6)$ in the gas phase and have argued on thermodynamical grounds that a π–complex is more feasible than aluminocyclohexadienyl.

(d) Methane reactions:

In 1983, Klabunde and Tanaka reported[48] ground-state insertion of aluminum atoms into the C-H bond of methane at 10 K. In 1985, Parnis and Ozin have investigated[49] the reactivity of Al with CH_4. The reaction involved photoactivation of Al from ground state, $Al(^2P)$ to the excited state, $Al(^2S)$ generating energy. The electronic and vibrational energy generated in the photoactivation of Al is transferred to CH_4. The reaction was found to be reversible, equation 1.15.

$$Al + CH_4 \rightleftharpoons CH_3AlH \qquad 1.15$$

(e) Ether reactions:

In 1990, Chenier et al.[50] and Howard et al.[51] studied the reaction of ground-state Al atoms with symmetric cyclic and acyclic ethers at 77 K by ESR spectroscopy. The study showed that Al atoms react with the ethers to form novel C-C, C-O and C-H insertion products. In addition, a carbon-centered radical was always formed by loss of a hydrogen atom from the carbon adjacent to the alkoxyl group. In contrast to acyclic ethers, the cyclic ethers are resistant to alumino hydride formation and in most cases a carbon radical resulting from ring opening at the C-O bond is formed. Mono- and di-ligand

complexes, Al[ether] and Al[ether]$_2$, were tentatively identified and were thought to be the primary intermediates for all the reactions that occurred.

(f) Methyl bromide reactions:

Klabunde et al.[52] studied the reaction of ground-state Al atoms with methyl bromide (CH_3Br) under matrix isolation conditions (12 K in argon and 77 K in pure CH_3Br) by IR spectroscopy. The results showed a remarkable reactivity between Al atoms and CH_3Br at low temperatures. The high reactivity is due to the low ionization potential of Al (ca. 578.9 kJ mol^{-1}) and the high diatomic bond energy of Al-Br (444 ± 8 kJ mol^{-1}).[53] The low ionization potential leads to the formation of a more ionic Al-Br bond, equation 1.16.[52]

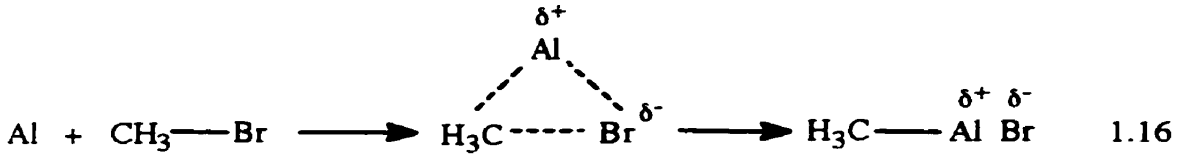

1.16

1.1.5.1.2 Aluminum-atom reactions with inorganic compounds:

(a) Carbonyl reactions:

In 1984, Kasai and Jones[54] studied the interaction of Al atoms with CO in solid argon at 4 K. The ESR spectral data showed a paramagnetic carbonyl compound was formed containing one aluminum atom and two carbon monoxide ligands, i.e., $Al(CO)_2$, Figure 1.12. Chenier et al.[55] have prepared $Al(CO)_2$ in inert hydrocarbon matrices from Al atoms and CO and examined its ESR spectrum. The data were consistent with a bent planar π radical of C_{2v} symmetry having the unpaired electron in a molecular orbital perpendicular to the molecular plane and constructed from the Al $3p_x$ and carbon monoxide 2 π^* orbitals while the Al "lone-pair" electrons reside in a sp^2 orbital directed along the C_2

axis, Figure 1.12. In 1985, Howard et al.[56,57] and Hampson et al.[58] repeated the experiments using isotopically labelled CO. Not only did ^{13}CO and $C^{17}O$ unequivocally give the stoichiometry of the reaction but also the results of the ESR study could also be used to establish the sign of the aluminum and carbon anisotropic hyperfine interactions.

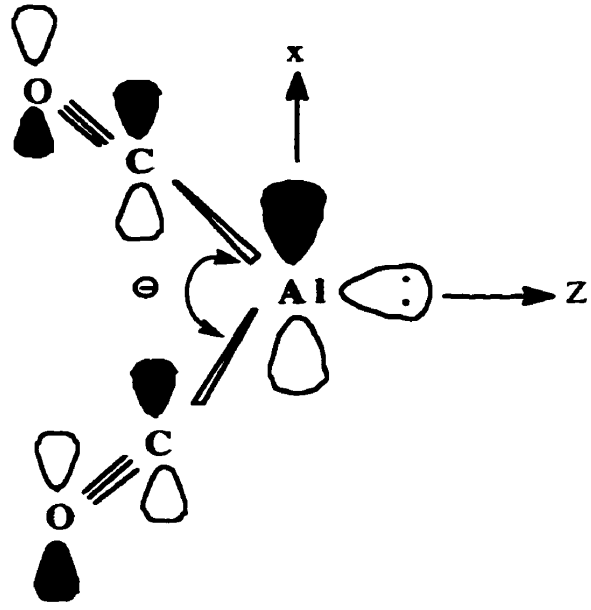

Figure 1.12. Proposed structure for $Al(CO)_2$.

(b) Ammonia reactions:

In 1991, Howard et al.[59] studied the reaction of ground-state Al atoms with NH_3 in adamantane at 77 K on a rotating cryostat by ESR spectroscopy. The results show the formation of three paramagnetic mononuclear Al complexes; $Al(NH_3)_4$, $HAlNH_2$ and $Al(NH_3)_2$.

(c) Trivalent phosphorus reactions:

In 1989, Histed et al.[60] examined the products of the reaction between Al atoms and $P(CH_3)_3$ and $P(OCH_3)_3$ on a rotating cryostat in hydrocarbon matrices at 77 K by ESR spectroscopy. The data reveal the presence of the seven-electron binary complexes $Al[P(CH_3)_3]_2$ and $Al[P(OCH_3)_3]_2$. The magnetic parameters of these complexes are consistent with π radicals of C_{2v} symmetry. The unpaired electron is located in a molecular orbital perpendicular to the P-Al-P plane which is constituted largely from the Al atomic $3p_x$ orbital with a contribution from P $3p_x$ and/or $3d_{xz}$, $3d_{xy}$ atomic orbitals.

1.1.5.2 Gallium-atom reactions:

1.1.5.2.1 Gallium-atom reactions with organic compounds:

The mode of interaction of gallium atoms with methane[61] and ethylene[62,63] is similar to that of Al atoms[34,36,64,65], but ESR experiments indicate otherwise for interaction with butadiene[43] and benzene.[12,44,45]

(a) Alkene reactions:

The reaction of Ga atoms with ethylene[62,63] has been studied by ESR spectroscopy. The dominant species formed in an argon matrix at 4 K or an adamantane matrix at 77 K is a π-complex where the unpaired electron is in an orbital on the metal parallel to the π bond.[63] The binding energy of Ga-ethylene[62] is estimated to be about 42 kJ mol^{-1}, which can be compared to about 75 kJ mol^{-1} for the Al-ethylene complex.[35] A second ethylene can add to the π-complex to form a cyclic σ-bonded complex, gallacyclopentane (GaC_4H_8), estimated to be 13 kJ mol^{-1} more stable than Ga-ethylene (42 kJ mol^{-1}).[63] Recent experimental and theoretical work suggests that gallium and aluminum have interact in a similar fashion with the compounds C_5H_5 and C_5Me_5, respectively.[66,67]

(b) Butadiene reactions:

ESR studies of the interaction of Ga atoms with buta-1,3-diene suggests the formation of 1-substituted allyl, $GaCH_2CHCHCH_2^{\bullet}$. Gallium atoms did not undergo a 1,4-cheleotropic addition to buta-1,3-diene to give gallacyclopentene as in the case of the reaction of Al atoms with buta-1,3-diene, Figure 1.9(**b**).[43]

An ab initio study of the interaction of gallium atoms with 1,3-butadiene was carried out by McKee.[68] The ab initio calculations predict that the σ-complex, gallacyclopentene, GaC_4H_6 is weak which is consistent with ESR results. According to the calculations gallacyclopentene adopts an envelope conformation where the C-C and C=C bonds only differ by 0.079 Å (1.475 and 1.396 Å) and the Ga-C σ-interactions are 2.148 and 2.444 Å.

(c) Benzene reactions:

ESR studies of the interaction of Ga atoms with benzene[44] in an adamantane matrix at 77 K suggest that the mode of interaction is different from that observed for Al atoms under identical conditions. Gallium was found to interact with benzene with a transfer of only 0.2 unpaired electrons which suggested formation of a weak Ga-benzene complex with the degeneracy of the Ga p orbitals lifted by interaction with the benzene matrix.

An ab initio study of the interaction of Ga atoms with benzene was carried out by McKee.[68] The calculations predict two modes of interaction of similar strength; one is dominated by dispersion forces, Figure 1.13, and the other by electrostatics, Figure 1.14. The aluminum-benzene reaction is thought to be dominated by the charge transfer/electrostatic interaction whereas the Ga-benzene reaction is thought to be dominated by an interaction arising from dispersion forces due to the greater polarizability of Ga. The charge transfer/electrostatic interaction is less significant for the Ga-benzene complex due to

the small electrostatic attraction between the Ga atom and the benzene ring (long Ga-benzene bond). Experimental ESR results are in agreement with the dispersion interaction.

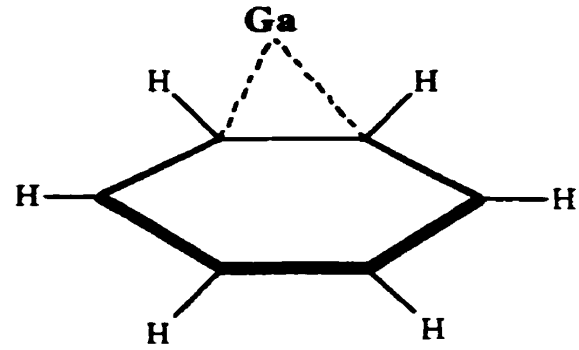

Figure 1.13. Structure of the π Ga-benzene complex.

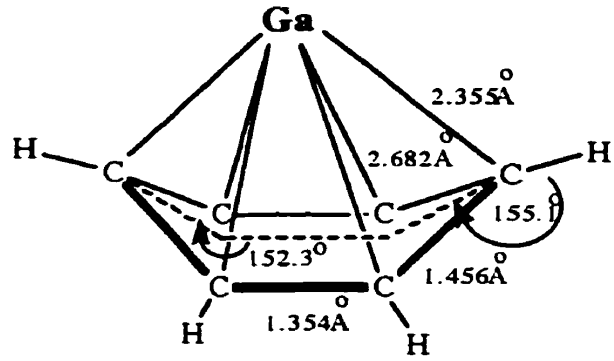

Figure 1.14. Structure of the σ Ga-benzene complex.

(d) Methane reactions:

Ground state gallium atoms (^2P),[61] like Al atoms,[64] do not react with methane. However, atoms in the excited state (^2S) will react to form the insertion product $HGaCH_3$.

The insertion of Ga into a C-H bond of methane produces a compound which is endothermic by 22 kJ mol^{-1}.[68]

(e) Methyl bromide (CH_3Br) reactions:

Klabunde et al.[52] studied the reactivity of Ga atoms with CH_3Br under matrix isolation conditions (12 K in argon and 77 K in pure CH_3Br) by IR spectroscopy. The results show the formation of a CH_3GaBr complex. The high reactivity of Ga atoms with CH_3Br was attributed to the low ionization potential of Ga (ca. 578.9 kJ mol^{-1}) and strong bond energy of Ga-Br (444 ± 17 kJ mol^{-1}).[53] The reactivity trend of group 13 atoms with CH_3Br was determined to be Al > Ga > In >> Tl.

1.1.5.2.2 Gallium-atom reactions with inorganic compounds:

(a) Carbonyl reactions:

ESR and IR studies of the interaction of Ga atoms with CO have been carried out by Howard et al.[69] The ESR and IR spectra indicate the formation of a bent molecule with C_{2v} symmetry. The magnetic data are consistent with a bent planar π radical having the unpaired electron in a $^2B_1$ orbital constructed from the $4p_x$ and carbon monoxide $2\pi^*$ orbitals. The IR spectrum of $Ga(CO)_2$ in adamantane has a symmetric CO stretching mode at 2009 cm^{-1} and an antisymmetric CO stretching mode at 1929.9 cm^{-1}, consistent with a bent dicarbonyl.

1.1.5.3 Indium and thallium atom reactions:

Indium and thallium atom chemistry has not received much attention in the past years. There are two studies where In atom reactions were carried out. The first reported study was by Jeong and Klabunde[70] where In was evaporated, in a matrix isolation reaction chamber, by laser ablation and deposited onto a target containing methane gas. Infrared and UV-VIS studies of the reaction mixture indicated no interaction between In and CH_4 occurred. The second study was carried out by Klabunde et al.[52] where In and Tl

atoms were reacted with CH_3Br under matrix isolation conditions (12 K in argon and 77 K in pure CH_3Br). The IR results showed that In atoms reacted completely with CH_3Br to form the CH_3InBr complex whereas the reaction of Tl atoms with CH_3Br did not take place.

1.2 Ab Initio Molecular Orbital Calculations:

There are three primary computational chemistry tools, two (molecular mechanics and semiempirical molecular orbital theory) rely on experimental data, while the third (ab initio quantum chemistry) is capable of reproducing experimental results without additional data. Ab initio theory is used for cases where little experimental information is available (e.g. in a new area of chemistry) or when experiments are not feasible. However, the ab initio approach finds itself at a disadvantage relative to other methods with respect to computational speed.[71]

The three primary computational chemistry methodologies are capable of predicting the structure of molecules and all three provide relative conformational energies. This does not mean that they behave identically. For example, molecular mechanics can often give bond lengths to an accuracy of ±0.004Å in molecules similar to those used in parametrizing the force field. In contrast, Hartree-Fock ab initio methods require significantly more computer resources to achieve results that may be an order of magnitude less accurate. More accurate ab initio calculations (i.e., post-Hartree-Fock methods) can match the accuracy of molecular mechanics, but at an increased cost in computer time. On the other hand, ab initio methods can be applied to situations where no empirical parametrization is possible.

Their combination of generality and flexibility makes ab initio methods a powerful complement to experimental measurements, as well as to other computational techniques,

for small to intermediate size systems. Ab initio methods can be applied to study the ground- or excited-state potential energy surfaces. With better computer programs and resources, the quality of the wave function can be improved, in contrast to molecular force-field or semiempirical methods that are difficult to improve systematically.

Even though molecular mechanics and semiempirical methods are capable of describing many molecular properties, certain properties are beyond the scope of either approach. In such cases ab initio methods may offer the only theoretical approach to the problem. For example, semiempirical methods cannot accurately treat the manifold of valence and Rydberg excited states of linear polyenes, nor can they handle the hyperfine spin properties of first or second row elements. Similarly, molecular mechanics and semiempirical methods are not adequate for many properties of molecules containing transition metal atoms.[73]

1.2.1 Principles of Ab Initio Hartree-Fock Calculations:

The Hartee-Fock approximation, like the molecular orbital approximation, is central to theoretical chemistry. It is a starting point for more accurate methodologies which include the effects of electron correlation.[71, 72]

One of the major concerns of quantum chemists, since the birth of quantum mechanics, has been finding and describing approximate solutions to the electronic Schrödinger equation. The Hartee-Fock approximation usually constitutes the first step at solving such an equation. In what follows, it is assumed that, the Born-Oppenheimer approximation for the electron-nuclei separability is valid.[71]

The simplest antisymmetric wave function, which can be used to describe the ground state of an N-electron system, is a single Slater determinant. Such a function is conventionally denoted as:

$$| \psi_o \rangle = | \chi_1 \chi_2 \cdots \chi_N \rangle \qquad 1.17$$

where $| \psi_o \rangle$ is the electronic wave function and $\{\chi_i\}$ a set of still undetermined, molecular spin-orbital functions. The optimum wave function will give the lowest possible electronic energy,

$$E_o = \langle \psi_o | H | \psi_o \rangle \qquad 1.18$$

where H is the full electronic Hamiltonian, subject to normalization:

$$\langle \psi_o | \psi_o \rangle = 1 \qquad 1.19$$

By minimizing E_o with respect to the choice of spin orbitals, the Hartree-Fock equation is derived which determines the optimal spin orbitals $\{\chi_j\}$:

$$f_{(i)} \chi_j(x_i) = \xi_j \chi_j(x_i) \qquad 1.20a$$

$$f_{(i)} = -\frac{1}{2} \nabla_i^2 - \sum_{a=1}^{N} \frac{Z_a}{r_{ia}} + v_{(i)}^{HF} \qquad 1.20b$$

where $f_{(i)}$ is the Fock operator, $v_{(i)}^{HF}$ is the average potential experienced by the i-th electron due to the presence of other electrons, x_i is a coordinate representing spin and spatial position, r_{ia} is the distance between the i-th electron and a-th nucleus, ∇_i^2 is the Laplacian operator and ξ_j is the j-th orbital energy. The charge of the a-th nucleus is Z_a and the sum in equation 1.20b runs over all nuclei. The Hartree-Fock equation, equations 1.20, is nonlinear and must be solved iteratively. The procedure for solving the Hartree-Fock equation is called the Self-Consistent-Field (SCF) method.

The SCF method makes an initial guess at the spin orbitals, so one can calculate the average field (v^{HF}) seen by each electron and then solve the eigenvalue equation 1.20a for a new set of spin orbitals. Using these new spin orbitals, one can obtain new fields and repeat the procedure until self-consistency is reached.

1.2.2 The SCF Procedure:

The computational procedure for obtaining the unrestricted Hartree-Fock wave function is described in this section for a system with a different number of α ("up") and β ("down") spins. The procedure is similar to that for restricted closed shell Hartree-Fock wave functions. The main steps in the procedure, omitting the technical details of their actual implementation[71, 72] are:

(1) Specify a molecule (a set of nuclear coordinates (R_A), atomic number (Z_A), and number of electrons (N)) and a basis set.

(2) Calculate all required molecular integrals.

(3) Provide an initial guess for the two density matrices ρ^α and ρ^β. An obvious choice is to set these matrices to unity and use H^{core} as an initial guess to both Fock matrices, F^α and F^β. The first iteration produces identical orbitals for α and β spin, i.e., a restricted solution. If $N^\alpha \neq N^\beta$ then all subsequent iterations will have different density matrices ($\rho^\alpha \neq \rho^\beta$), and an unrestricted solution results.

(4) Obtain the Fock matrix $F = H^{core} + G$, where G is the two-electron part of the Fock matrix.

Given approximations for ρ^α and ρ^β at each step of the iteration, F^α and F^β can be formed and the two generalized matrix eigenvalue problems can be solved for the expansion coefficients C^α and C^β:

$$F^{\alpha} C^{\alpha} = S C^{\alpha} E^{\alpha} \qquad 1.21$$

$$F^{\beta} C^{\beta} = S C^{\beta} E^{\beta} \qquad 1.22$$

where E^{α} and E^{β} are diagonal matrices of orbital energies and S is the overlap matrix for spin-orbitals. This leads to the formation of new approximations to ρ^{α} and ρ^{β}.

(5) Determine whether the procedure has converged by examining if the density matrix of the last step is very close to the previous density matrix. If the procedure has not converged, return to step (4) with the new density matrix.

(6) If the procedure has converged then use the resulting solution represented by C, ρ, F etc. to calculate expectations values (such as energy, dipole moment etc.) and other quantities of interest (such as the charge density and other properties derived from a population analysis).

1.2.3 Polyatomic Basis Sets:

After choosing a set of nuclear coordinates, the calculation of the wave function is completely specified by the set of basis functions. The choice of a proper basis set is partly an art. There are two main considerations in selecting a basis set. First is the desire to use the most efficient and accurate functions possible to represent the molecular orbitals. The second consideration is the speed of two-electron integral evaluation. Only Slater- and Gaussian-type functions are currently in common use. Slater-type functions provide a somewhat superior description of electronic properties, but they lead to more difficult computations. Factors to consider are the ability of the basis set to span the Hilbert vector space in which wave functions are defined, and the time required to evaluate molecular integrals. Most polyatomic calculations now use Gaussian orbitals because of the speed

with which integrals can be evaluated.[71] Computer facilities and budget also may limit the choice to a small basis set of functions.

1.2.3.1 Minimal basis sets: STO-3G:

Minimal basis sets such as STO-3G are computationally inexpensive and can be used for rather large molecules. The STO-3G basis set is termed "minimal" because it includes the least number of functions per atom. For example, one usually considers 1s, 2s and 2p, i.e., five functions, to form a minimal basis set for Li and Be. In a hydrogenic model, the 2p orbital would not be occupied in these atoms. In a proper quantum mechanical approach, however, this is not the case and the 2sp (2s and 2p), 3sp, 4sp, 3d, etc. shells must also be considered. The minimal basis set consists of one function for H and He, five functions for Li to Ne, nine functions for Na to Ar, thirteen functions for K and Ca, eighteen functions for Sc to Kr, ..., etc. Because the minimal basis set is so small, it does not lead to quantitatively accurate results. It does, however, contain the essentials to describe simple chemical bonds and other qualitative properties.[71, 72]

1.2.3.2 Double zeta basis sets: 4-31G:

A double zeta basis set uses two functions for each orbital, whereas the minimal basis set has one. The best orbital exponents of the two functions are slightly above and slightly below the optimal exponent of the minimal basis function. This feature allows the electron density represented by these basis functions to be flexible enough to accommodate expansion or contraction as required in a given environment.

The 4-31G basis set is not exactly a double zeta basis since only the valence functions are doubled and a single function is still used for each inner shell orbital. It is called a "split valence (shell)" basis set. The inner shells contribute little to most chemical properties. By not splitting the inner shell functions, the total energy is somewhat affected,

but little effect is observed on dipole moments, valence ionization potentials, charge density, dissociation energies, and most other calculated quantities of chemical interest. The 4-31G basis set consists of two functions for H and He, nine functions for Li to Ne, thirteen functions for Na to Ar, etc.[71]

1.2.3.3 Polarized basis sets: 6-31G* and 6-31G**:

In the previous section double zeta basis sets were mentioned; the next step in improving the basis set will be triple zeta, quadruple zeta, etc. If the minimal basis set is enlarged rather than adding functions of higher angular momentum quantum number, the basis set would not be well balanced. Therefore, a better strategy is to add polarization functions, i.e., d-type functions to the first row atoms Li to F and p-type functions to H. The reason for the term "polarization function" is as follows. Consider the hydrogen atom (which has a 1s orbital occupied in the ground state) placed in a uniform electric field. The electron cloud is attracted to the positive direction of the electric field causing asymmetric charge distribution about the nucleus. It is polarized. An approximate solution to this problem is a mixture of the original 1s orbital and a p-type function along the direction of the field. If the H atom is in a molecule, it will experience a nonuniform electric field arising from its nonspherical environment. To accommodate this effect, polarization functions and p-type functions are added to a basis set. In a similar way, d-type functions, which are unoccupied in first row atoms, play the role of polarization functions for the atoms Li to F. The 6-31G* and 6-31G** basis sets resemble the 4-31G basis set with d-type basis functions added to only the heavy atoms (*), or d-type functions for heavy atoms and p-type functions for hydrogen (**).

The 6-31G* and 6-31G** basis sets are formed by adding polarization functions to the split-valence 6-31G basis set. Calculations at the 6-31G* and 6-31G** level provide normally quantitative results considerably superior to the STO-3G and 4-31G levels.

However, these basis sets are not perfect and they can be improved by going to triple zeta, by adding f-type functions to heavy atoms and d-type functions to hydrogen, by improving the description of the inner shell electrons, or by including orbitals not centred in the nuclei (diffuse functions). As technology improves, it will be possible to use more and more accurate basis sets.[71]

1.2.4 Hartree-Fock Calculations:

In this section some of the important properties that can be derived from an SCF calculation are discussed.[71]

1.2.4.1 Total energies:

This is defined as:

$$E_{tot} = E_o + \sum_{A} \sum_{B>A} \frac{Z_A Z_B}{R_{AB}} \qquad 1.23$$

where E_o is the electronic Hartree-Fock energy and the second term represents the internuclear repulsion (Z_A and Z_B are the atomic numbers of nuclei A and B, R_{AB} is the distance between the A-th nucleus and the B-th nucleus). In ab initio calculations, the total potential energy hypersurface, E_{tot}, is the main quantity for chemical structure determination, since the predicted equilibrium geometry of a molecule occurs when E_{tot} is a minimum. The electronic energy is dependent on the basis set. The better the basis set, the lower the total energy. The energetics of a chemical reaction can then be determined from the energy differences between nuclear configurations. The SCF approximation often gives valid qualitative results for an energy change and the energy involved in a chemical reaction. As well, reaction paths and mechanisms can be elucidated from the curvature properties of the potential energy hypersurface.

1.2.4.2 Population analysis:

Population analysis gives information about the electron density around each atom. Ab initio SCF calculations produce a one-electron charge density, $\rho(\bar{r})$, describing the probability of finding an electron in an element of volume $d\bar{r}$ centered at point $\bar{r}$. In terms of the atomic basis set $\{\phi'_\nu(\bar{r})\}$, the electron density is given by:

$$\rho(\bar{r}) = \sum_{\mu} \sum_{\nu} P'_{\mu\nu}\, \phi'^{*}_{\mu}(\bar{r})\, \phi'_{\nu}(\bar{r}) \qquad 1.24$$

where $P'_{\mu\nu}$ is the density matrix and $\phi'_\nu(\bar{r})$ is the v-th atomic orbital at point $\bar{r}$ and $\phi'_\mu(\bar{r})$ is the μ-th atomic orbital at point $\bar{r}$. The indices v and μ can refer to the same or to different atoms. This density function, $\rho(\bar{r})$, is commonly plotted as contour maps for visual interpretation of the charge density and to define the molecular shape. A population analysis is a useful tool for interpreting the electron density in terms of "chemical concepts" such as atomic charges and bond orders.

1.2.4.3 Atomic charges:

For a pair of chosen atoms p and q, Mulliken defined net atom ($n(p)$) and bond ($n(p,q)$) populations by:[72]

$$n(p) = \sum_{\alpha \text{ on } p} P_{\alpha\alpha} \qquad 1.25$$

$$n(p,q) = \sum_{\beta \text{ on } q}^{\alpha \text{ on } p} 2\, P_{\alpha\beta}\, S_{\alpha\beta} \qquad 1.26$$

where positive and negative values of $n(p,q)$ are taken to indicate a bonding or antibonding situation between the two atoms. The indices "α" and "β" in equation 1.26 run over the atomic orbitals centred over the nuclei p and q, respectively. In the case of charge accumulation between atoms p and q we expect $n(p,q) > 0$.

Atomic charges are defined by subtracting the gross atom population, $n(p)$, from the number of electrons provided by the neutral atom, $N_o(p)$:

$$Q(p) = N_o(p) - n(p) \qquad 1.28$$

where $Q(p)$ is the electron contribution to the net atomic charge.[73]

1.2.4.4 Spin densities:

The charge density contributed by electrons of α spin is:

$$\rho^{\alpha}(\bar{r}) = \sum_{a}^{N^{\alpha}} \left|\psi_a^{\alpha}(\bar{r})\right|^2 \qquad 1.29$$

in terms of the occupied molecular orbitals $\psi_a^{\alpha}(\bar{r})$ within the unrestricted Hartree-Fock approach. The charge density contributed by electrons of β spin is:

$$\rho^{\beta}(\bar{r}) = \sum_{a}^{N^{\beta}} \left|\psi_a^{\beta}(\bar{r})\right|^2 \qquad 1.30$$

where N^{α} and N^{β} is the number of α and β electrons, respectively.

In an unrestricted wave function, electrons of α and β spin have different spatial distributions ($\rho^{\alpha} \neq \rho^{\beta}$), and it is convenient to define a spin density $\rho^{s}(\bar{r})$ by

$$\rho^{s}(\bar{r}) = \left|\rho^{\alpha}(\bar{r}) - \rho^{\beta}(\bar{r})\right| \qquad 1.31$$

From this equation, it is clear that in regions of space where there is a higher probability of finding an electron of α spin than there is of finding an electron of β spin, the spin density is positive. The spin density is negative where electrons of β spin are most common. The individual densities ρ^{α} and ρ^{β} are positive everywhere. The spin density describes the

distribution of unpaired electrons in a system. One expects nonzero contributions to $\rho^s(\bar{r})$ in radical species.

1.2.4.5 Equilibrium geometries:

The equilibrium geometry of molecules can be predicted by electronic structure calculations. The problem of finding an equilibrium geometry is equivalent to a mathematical problem of nonlinear unconstrained minimization. One of the methods used for such minimization is called the line search. The minima is obtained by increasing or decreasing each variable (for example the C-C bond distance) until a minimum energy for the system is obtained. One cycles through all the variables a number of times, varying each one in sequence, until the optimum values no longer change. If there is a large coupling between variables, this procedure will converge very slowly. Other procedures depend on knowing the first derivatives and, possibly, the second derivatives of the energy with respect to the nuclear coordinates. These are much better procedures but require the evaluation of a number of derivatives. In the past, these derivatives have been calculated numerically, but there are now a number of programs that can perform these calculations by efficient analytical procedures.

In the Born-Oppenheimer approximation, the total energy defines the potential surface as a function of the coordinates of the nuclei. The motion of the nuclei on this surface determines the possible chemical reactions, the molecular vibrations, etc. The points on the potential surface of most interest are the stationary points. The type-1 saddle points define the standard transition structures ("states"), and the minima define equilibrium geometries. The details of the potential surface are difficult to know, because the number of degrees of freedom increases rapidly with the molecular size. For medium-sized molecules, it may still be possible to find the potential surface global minimum, that is, the most stable chemical structure.[71]

2. PLAN OF RESEARCH

The interaction between an Al atom and various small organic molecules has attracted a significant amount of theoretical and experimental interest. Spectroscopic investigations of the interaction between Al atoms and benzene, by two separate research groups, have suggested the formation of an Al-benzene molecular complex. However, there is some controversy as to the nature of the bond formed between the Al atom and the benzene moiety.

In the first study, Kasai and McLeod[14] recorded the ESR spectrum for the product resulting from the cocondensation of Al atoms and benzene in a neon matrix at 4 K. A good computer simulation of the ESR spectrum was obtained assuming an interaction between the ground-state Al atom ($3s^23p^1$) and only two of the six protons of the benzene ring. Based on these observations, Kasai and McLeod concluded that the Al-benzene molecular complex is a π complex similar to AlC_2H_4. The complex forms when the Al atom interacts through one C-C unit of the ring by dative bonding of the semioccupied Al $3p_x$ orbital and two antibonding p_π orbitals on two adjacent carbon atoms, as was the case with ethylene.

In a subsequent investigation, Chenier et al.[43] studied the reaction of Al atoms and benzene in hydrocarbon matrices at 77 K. The isolation of the AlC_6H_6 complex in adamantane allowed the ESR spectrum to be recorded from 4 K to room temperature. At 4 K the ESR spectrum showed the resolvable hyperfine interaction of one Al atom with two equivalent hydrogen nuclei similar to that found by Kasai and McLeod. However, the spectrum changed as the temperature was raised. The ESR spectrum recorded at 220 K

suggested that the Al atom interacts with six equivalent hydrogen nuclei. The spectrum was highly dependent on temperature and the original spectrum was observed by lowering the temperature of the sample from 220 to 4 K in the cavity of the spectrometer. Based on these observations, Chenier et al. proposed a η^2 complex in which the Al bridges two para C atoms with hyperfine interaction to the two para protons. This structure is similar to the 1,4-cheleotropic cyclization product of Al and buta-1,3-diene at 77 K in hydrocarbon matrices. At higher temperatures the Al atom, acting as a rotor, overcomes the barrier to rotation and all six hydrogen nuclei become equivalent. It is interesting to note that other metals form complexes with benzene. For instance, in an infrared study of the interaction between Li atoms and benzene in solid argon,[73] reported by Manceron and Andrews, Li atoms reacted with benzene spontaneously to form mono- and diligand-complexes (LiC_6H_6, $Li(C_6H_6)_2$). The Li isotopic shift for the Li-ring stretching mode indicated to the authors that the metal was situated in an axial position. Mitchell et al.[35] have measured a binding energy of 49 kJ mol^{-1} in the gas phase for the $Al(C_6H_6)$ complex by using time-resolved resonance fluorescence spectroscopy. They have argued on thermodynamic grounds that a π complex similar to that suggested by Kasai and McLeod is more feasible than the complex proposed by Chenier et al. Therefore an alternate interpretation of the ESR results reported by Howard and coworkers would be the migration of the Al atom from one C-C unit to the next, Figure 2.1, at a rate whereby the hydrogen nuclei in the complex appear to be equivalent experimentally.

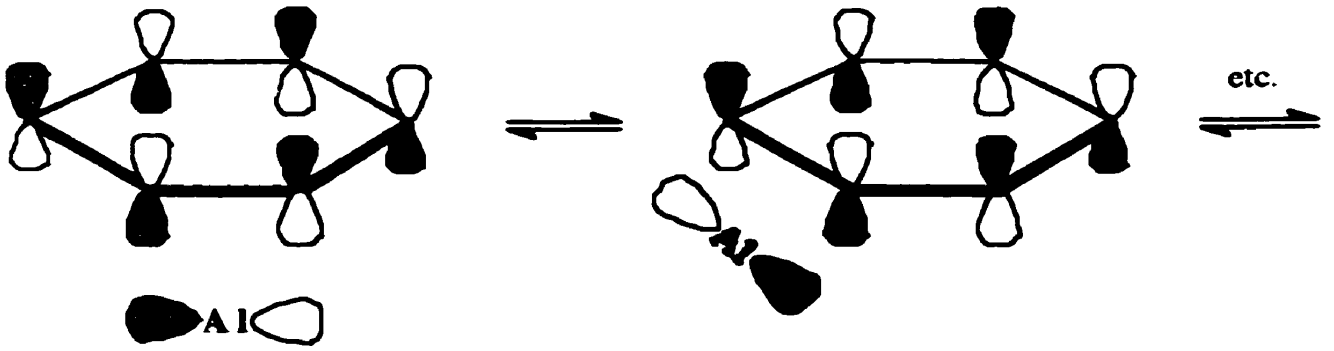

Figure 2.1. Aluminum bonding with individual C-C units.

Due to the unusual bonding of Al atoms with alkenes and arenes and the controversy developed over the bonding in the Al-benzene complex, we have decided to investigate the hydrolysis products of the intermediates formed in the reaction of Al atoms with benzene at 77 K by using the GC-MS technique. Concurrently an ab initio quantum chemical study of the Al-benzene complex was planned to provide a theoretical basis for the type of bonding formed between Al and benzene.

Another Group 13 element which has received a considerable amount of attention is gallium. Gallium atoms[44,61,62,63] like aluminum atoms are known to interact with hydrocarbons such as methane, ethylene, and benzene. Recent experimental and theoretical work suggests that gallium and aluminum react in a similar fashion with C_5H_5 and C_5Me_5, respectively.[45,66] In many cases the reactivity of gallium atoms toward hydrocarbons is similar to that of aluminum atoms, but there are exceptions. For example, when Ga atoms are reacted with benzene[44] at 77K a paramagnetic species is generated with magnetic parameters consistent with a trapped atom or a weak Ga-benzene complex that has had the degeneracy of the Ga p orbitals lifted by interaction with the benzene matrix. In addition, a

well-resolved spectrum of cyclohexadienyl developed when samples of Ga atoms in C_6H_6 were annealed in the cavity of the spectrometer. In contrast, the reaction of Al atoms with benzene gave a mononuclear monoligand complex, $Al[C_6H_6]$ with relatively strong bonding between the metal atom and the ligand. More specifically, Ga was found to have a 4p spin population of 0.8 whereas the 3p spin population of Al was determined to be 0.3.

To shed more light on the chemistry and bonding of organogallium compounds with respect to the aluminum analogues, the study of the hydrolysis products of the organogallium compounds produced in the reaction of gallium atoms with benzene, toluene, and trifluorotoluene was proposed.

The metal atom reactions of the remaining group 13 elements, In and Tl have not been extensively studied. For the sake of completeness we planned to identify the hydrolysis products of the organoindium and organothallium compounds produced in the reaction of In and Tl atoms with arenes and to compare them with those generated by the organoaluminum and organogallium compounds.

3. EXPERIMENTAL

3.1 Synthesis and Reactions of Organo Group 13 Compounds:

3.1.1 Preparation of the Reactants Used in the Synthesis of the Organo Group 13 Compounds:

The materials required to synthesize the organo group 13 compounds are the group 13 metals, the aromatic substrate and in some cases an inert matrix. The source and preparation of the materials used for synthesis of the organo group 13 compounds are outlined below.

3.1.1.1 Group 13 metals:

Aluminum wire (99.94%, Fisher), gallium nuggets (99.99%, Fisher), indium and thallium rod (99.999%, BDH) were used to produce the desired metal vapour. The metals were preheated to their melting point under vacuum, prior to cooling the cryostat, to remove any surface impurities.

3.1.1.2 Aromatic substrates:

The aromatic substrates used in the study to prepare the organo group 13 compounds were: benzene (Caledon), toluene (BDH), trifluorotoluene (99+%, Aldrich), *p*-bromotoluene (98%, Aldrich) and chlorobenzene* (BDH). Benzene and toluene were purified by distillation and dried over molecular sieves (3A) prior to being degassed for use

---

* The reaction involving chlorobenzene and Al atoms was carried out at the rotating cryostat facility at the National Research Council (NRC) in Ottawa. The hydrolysis products of this reaction were analyzed at Laurentian University.

in the metal atom reactor. The general procedure for degassing the substrates is described in section 3.1.1.5.

3.1.1.3 Inert matrix:

On occasion adamantane (99+%, Aldrich) was used as a matrix to isolate the organo Group 13 compounds. The adamantane was degassed by the freeze-thaw method described in section 3.1.1.5 prior to being used in the metal atom reactor.

3.1.1.4 Reactants:

The reactants used to study the reactivity of the Al-C bond were: water (triple distilled), deuterium oxide (99.9%, Norell) and methyl iodide (Baker). The reactants were used (without further purification) after thorough degassing.

3.1.1.5 General procedures used to degas the substrates, matrix and reactants:

A 10 mL capacity bulb, Figure 3.1, fitted with a teflon rotoflow stopcock and a B10 male adapter was half filled with the substrate, matrix or reactant. The bulb was connected to a vacuum line and the roughing pump was activated. The contents of the bulb were frozen using a liquid N_2 bath. The rotoflow stopcock was slowly opened and the Edwards Pirani vacuum gauge was monitored. Once the needle on the vacuum gauge had settled to ca. $5x10^{-2}$ Torr, the stopcock of the bulb was closed. The bulb was warmed up to room temperature by replacing the liquid nitrogen bath with a methanol-liquid nitrogen slurry* bath, then a methanol bath to prevent the cracking of the sample flask due to rapid heating. The freeze-thaw cycle described above was repeated until deflection of the needle of the vacuum gauge could no longer be detected upon opening the stopcock. The above procedure was next repeated using the diffusion pump (pressure ca. 10^{-5} Torr). The

* The slurry was made by slowly adding liquid nitrogen to methanol until solid methanol coexisted with the liquid. The temperature of this bath was approximately -96°C.

Edwards Penning vacuum gauge was monitored and the procedure was considered complete when deflection of the gauge needle could no longer be detected.

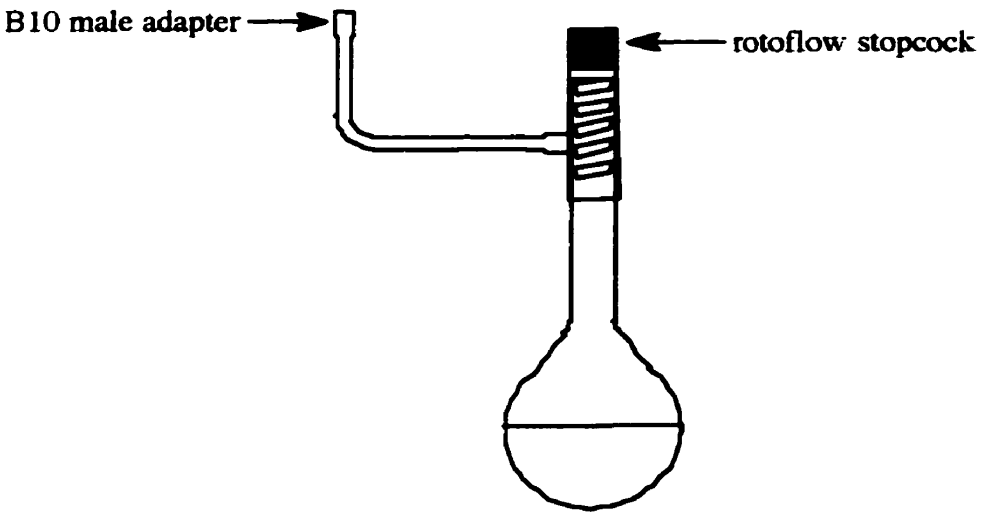

Figure 3.1. Bulb.

3.1.2 Metal Atom Reactor:

The metal atom reactor, known as a "rotating cryostat", was used to deposit the metal atoms onto frozen layers of the organic reactants at 77 K. The description of the rotating cryostat has been divided into three sections: (a) the reaction vessel, (b) the diffusion pump and (c) the roughing pump.

(a) The reaction vessel.

The general arrangement of the reaction vessel is shown in Figures 3.2 and 3.3. The stainless steel reaction vessel housed a hollow stainless drum. The shaft of the drum

consisted of two concentric tubes welded together at the top. The inner tube supported the drum and had a thin wall to reduce heat conduction to the drum, while the outer tube which carried the driving pulley and the rotating seal was much thicker.

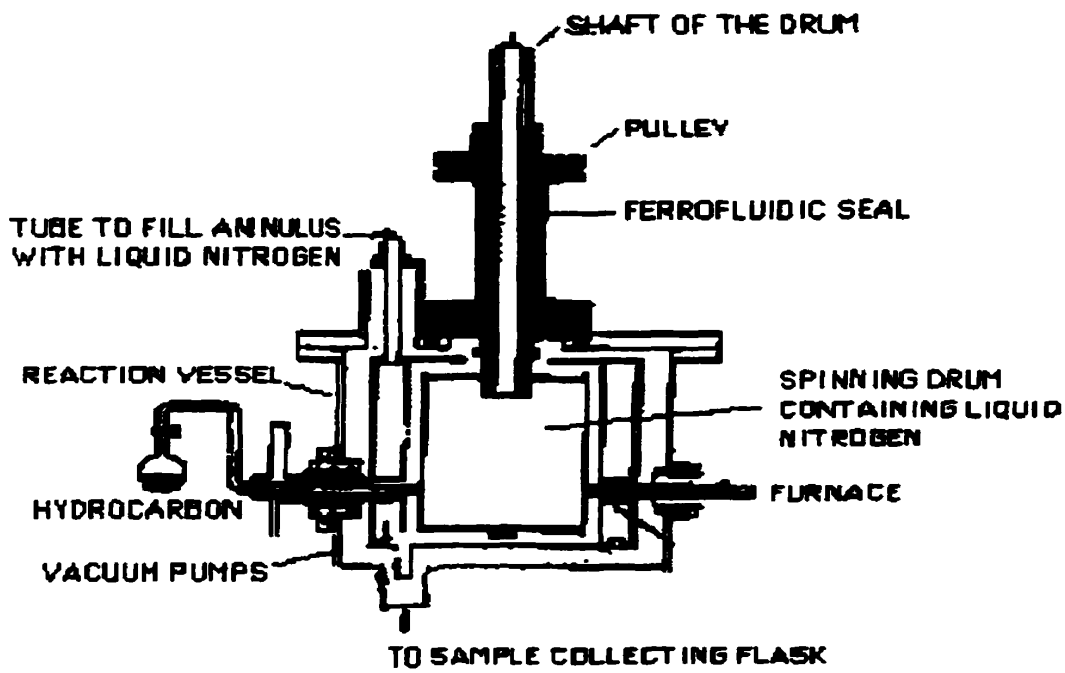

Figure 3.2. General arrangement of cryostat.[27]

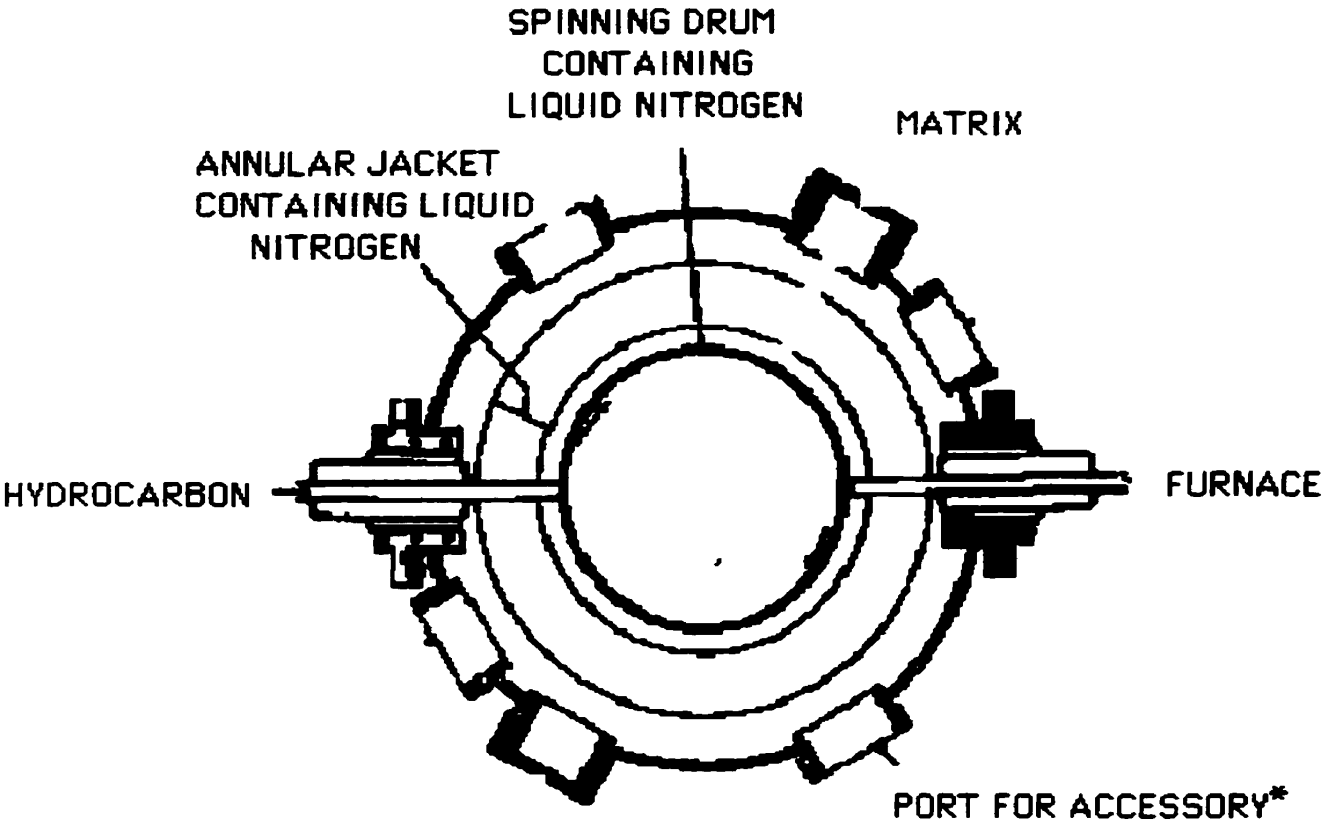

Figure 3.3. Cross-sectional view of the cryostat.[27]

* Note that there are a number of extra portholes which can be used to introduce extra reactants and or furnaces.

The heart of the apparatus was the ferrofluidic seal, which allowed the drum to rotate at high speed (ca 2400 r.p.m.) and yet provided an effective vacuum seal for the shaft so that pressures of $<10^{-5}$ Torr could be maintained in the cryostat.

An outer stationary container called an "annulus", filled with liquid nitrogen, surrounded the drum and acted as a radiation shield. This reservoir was also used to cool the ancillary equipment, namely the knife, which was used for removing the deposits from the drum for examination by gas chromatography-mass spectrometry (GC-MS).

The solid or liquid reactants used in the present study were placed in glass bulbs and were carefully degassed before use. The bulb was attached to a jet in the side of the reaction vessel and was held at a constant temperature throughout a run so that the vapor pressure behind the jet gave the required rate of deposition of the material. The inlet jet was kept at a temperature slightly above that of the bulb to prevent condensation of the material in the slit situated at the end of the jet.

The metal atoms were produced by a resistively heated furnace assembly shown in Figure 3.4. The plug which was fitted into the outer housing of the cryostat was machined of brass. The furnace components, subjected to extreme heat, were made of molybdenum rod and sheet. One of the molybdenum electrodes was directly attached to the brass plug. The other electrode was isolated from the brass plug by a glass sheath. The brass plug was hollowed and a hose inlet and outlet attached to allow for water cooling of the electrodes. The metal to be evaporated was placed in a tungsten basket (V-shaped) clamped between the molybdenum electrodes. The baskets were designed to direct the metal vapor onto the cold surface of the rotating drum which was situated about 4 mm away. The furnace could tolerate temperatures of up to 2300°C.

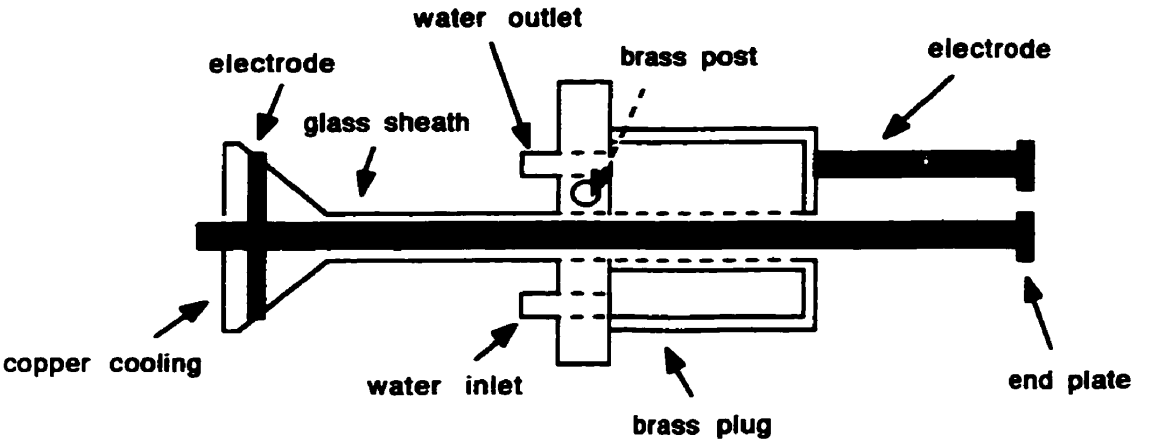

Figure 3.4. Cryostat furnace.

The pressure in the evacuated chamber was kept low (10^{-5}-10^{-7} Torr) allowing the atoms to move freely without undergoing collisions with other atoms during their travel from the hot surface (furnace) to the cold surface (drum).

(b) The diffusion pump:

The diffusion pump used in this study was made by Edwards High Vacuum (Model No. 160). The pump heater operated at 1350 watts and 210 V respectively. The diffusion pump was used to provide a pressure between 10^{-5} and 10^{-7} Torr.

(c) The roughing pump:

The roughing pump used in the study was a Duo Seal Vacuum Pump (Model No. 1402) made by Welch Scientific Company. The roughing pump was used for pumping the system from atmospheric pressure to 10^{-2} Torr.

3.1.2.1 Preparation of the furnace:

The molybdenum electrodes and endplates of the furnace were polished with fine emory paper and rinsed with petroleum ether. A tungsten basket (Ernest F. Fullam, Inc., No. 12070) was suspended between the two electrodes of the furnace by slipping the ends of the tungsten wire beneath the front plates of the electrodes. The molybdenum screws on the front electrode plates were tightened to ensure good contact between the electrode and the basket. Anywhere between 18-73 mg of metal were placed in the basket. The furnace assembly was at this point inserted into the appropriate porthole of the cryostat. The glass flange and sleeve were cooled by circulating cold tap water through a copper coil fixed to the electrode mounting plate (see Figure 3.4, *vide supra*). The electrical connection was made by clamping the electrical leads of a step-down transformer to the furnace. One of the leads was attached to the molybdenum electrode protruding from the glass sheath. The second lead was clamped onto the brass post fixed onto the outer casing of the plug. The step-down transformer was connected to a rheostat to adjust the current to the desired level and the rheostat was in turn plugged into the mains. An ammeter (Hidki) was placed around one of the electrical leads of the step-down transformer to measure the current passing through to the furnace.

3.1.2.2 Preparation of the reaction vessel:

Access to the inside of the reaction vessel for purpose of cleaning the reaction surface was accomplished by removing the large window fixed to the reaction vessel with Allen screws. The surface of the stainless steel drum (located in the centre of the reaction vessel) was cleaned with a kimwipe soaked in petroleum ether. On occasion it was necessary to first wipe the surface of the drum with dilute HCl to remove excess metal from the previous experiment. This was followed by wiping the surface of the drum with distilled water. The copper funnel situated under the drum and used to direct the sample

into the collection tube was also cleaned at this point. Next the bulbs containing the degassed substrate, matrix and water, deuterium oxide or methyl iodide were fitted into the appropriate port holes. Finally the furnace used to evaporate the metal was placed in a porthole. The configuration of the bulbs containing the compounds and the furnace needed for the reaction is shown in Figure 3.5. The window was replaced and the Allen screws tightened to make sure that the O-ring was depressed evenly. It should be noted that the furnace and bulb assemblies formed a seal when inserted into the openings of the reaction vessel with the aid of O-rings lightly lubricated with Apiezon N grease. Finally the sample collection tube fitted with a rotoflow stopcock and B10 female quick fit joint was slipped onto the B10 male joint situated under the reaction vessel.

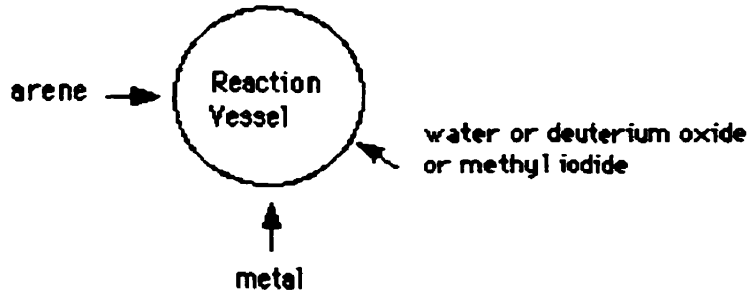

Figure 3.5. Configuration of the reactant bulbs and furnace in the reaction vessel.

3.1.2.3 Evacuation of the reaction vessel:

The roughing pump (Welch, model No. 1402) was connected with the aid of vacuum tubing to a clean, dry, liquid nitrogen trap fitted with a gauge head. The trap was in turn connected to a three way valve which could be switched between the diffusion pump, the reaction vessel and the roughing pump. With the valve closed to the diffusion

pump and the reaction vessel, the roughing pump was started. The trap was lowered into a Dewar filled with liquid nitrogen. Once a pressure of $4x10^{-2}$ Torr was obtained on the Edwards Pirani vacuum gauge (model No. 502), the valve lever was switched to the position marked "roughing" causing the evacuation of the reaction vessel. Generally, pressures of ca. $2.4x10^{-2}$ Torr were ultimately reached with the aid of the roughing pump.

3.1.2.4 Preparation of the diffusion pump (Edwards, model No. 160):

The water cooling system for the diffusion pump oil was turned on. The valve lever was turned from "roughing" to "backing". In this mode the roughing pump was pumping on the diffusion pump removing air or volatile material which may have been trapped in the diffusion pump oil. The system was allowed to pump until a pressure of $5x10^{-2}$ Torr was registered on the vacuum gauge (Edwards Pirani, model No. 502). The diffusion pump oil heater was connected to the mains and the oil allowed to heat for approximately 1/2 hour. During this time the reaction chamber was subjected to evacuation. In other words, the valve lever was placed in the position labelled "roughing". The liquid nitrogen reservoir attached to the diffusion pump was filled at this point. When the reaction chamber reached a pressure of $2.4x10^{-2}$ Torr, the valve was switched from "roughing" to "backing" and the butterfly valve of the diffusion pump was opened. The pressure inside the reaction vessel was monitored with the aid of the Edwards Penning gauge head and vacuum gauge controller (model No. 505). Once a pressure of 10^{-5}-10^{-7} Torr was attained the cryostat was ready for operation.

3.1.2.5 Operation of the cryostat:

Once a pressure of 10^{-5}-10^{-7} Torr had been attained in the reaction chamber, the drum and annulus (the outer casing of the reaction vessel) were filled with liquid nitrogen. The drum was rotated at this point by slowly turning the MultiDrive DC Motor Speed Controller (mounted on the cryostat stand) to the position between 65-70%. It was

essential that the amperage output of the motor not exceed 7.5 A. Typically, the inert matrix (adamantane) or reactant (H_2O, D_2O or CH_3I) was allowed to condense on the surface of the drum for a period of a ca. 2 min. This facilitated removal of the reaction mixture from the drum. The amount of the matrix and reactants introduced into the system was controlled by the vapour pressure of the substance. The vapour pressure was controlled by an appropriate cold temperature bath. The selection of the cold temperature bath will be discussed in section 3.1.2.8.

The matrix or reactant was next covered by a layer of the hydrocarbon (i.e., benzene, toluene, bromotoluene or trifluorotoluene) needed to form the organo Group 13 compounds. This measure was taken to prevent the reaction of the metal atoms with H_2O, D_2O or CH_3I. After depositing the hydrocarbon onto the drum for approximately 2 min, current was passed through the tungsten basket of the furnace to produce the metal vapour. The current required to produce the metal vapour was dependent upon the type of metal, the amount of metal and the efficiency of the contact made with the electrode. A summary of the current used to produce the various metal vapours is presented at the end of this section along with the corresponding experimental conditions used for each synthesis (see Table 3.1). The metal vapour and hydrocarbon were cocondensed for approximately 8 minutes. The current passing through the basket was reduced to zero and deposition of the hydrocarbon was maintained for an additional 2 minutes. In order to obtain sufficient material for analysis the procedure outlined above was repeated at least 1 more time. Deposition times ranged from 28 to 63 minutes.

At the end of the deposition time, the rotation of the drum was stopped. The material on the surface of the drum was scraped off into the sample collector (maintained at 77 K with liquid nitrogen) situated under the reaction vessel. A knife edge mounted in the reaction vessel housing was swiveled so that it leaned against the deposit and the drum was

rotated manually. The material was directed into the sample collector with the aid of a copper funnel mounted inside the reaction vessel directly beneath the drum. The rotoflow stopcock on the sample collector was closed. The work up of the reaction mixture is discussed in section 3.1.2.7.

3.1.2.6 Summary of the experimental parameters used to prepare the group 13 organometallic compounds:

The experimental parameters used to prepare the Group 13 organometallic compounds are presented in Table 3.1. More specifically, the weight of the metal used, the current used to vapourize the metal, the vapour pressure of the matrix, hydrocarbon and reactant maintained during the run, the operating pressure inside the reaction vessel and the reaction time are presented for all the individual experiments carried out in the study. Details of the actual preparation of the organo Group 13 compounds are presented in sections 3.1.2.6.1-16. The exact deposition sequence for the individual runs can be found in Appendix 1.

3.1.2.6.1 Aluminum, benzene and water reaction:

Aluminum metal vapour was produced by passing 10 to 32 A of current through a tungsten basket containing 20 to 64 mg of aluminum wire (Fisher). The metal vapours were condensed on a liquid N_2 cooled surface along with benzene vapours. The vapour pressure of the benzene was maintained throughout the run at ca. 1 Torr (with the aid of a bath consisting of an anisole-liquid nitrogen slurry) with the exception of one run where the vapour pressure of the benzene was 0.05 Torr. Water which was used to promote the hydrolysis of the organometallic compound was deposited intermittently during the run at ca. 1 Torr (ice-water bath). The sequence and deposition times of the various components of the runs were: 2 min water, 2 min benzene, 8 min benzene and aluminum metal vapour,

Table 3.1. Summary of the Experimental Conditions for the Preparation and Reaction of Group 13 Organometallic Compounds.

Metal	weight (mg)	current (A)	Matrix	vapour pressure (Torr)	Hydrocarbon	vapour pressure (Torr)	Reactant	vapour pressure (Torr)	Vessel Pressure (Torr)	Reaction Time (min)
Al	63.6	17-25	benzene	1	benzene	1	H_2O	1	$6\text{-}8\times10^{-5}$	32
Al	48.7	50	benzene	1	benzene	1	H_2O	1	9.8×10^{-7}	32
Al	63.3	11	benzene	1	benzene	1	H_2O	1	8×10^{-7}	32
Al	63.0	12-14	benzene	1	benzene	1	H_2O	1	6×10^{-5}	32
Al	25.3	10-16	benzene	0.05	benzene	0.05	H_2O	1	9.95×10^{-7}	32
Al	26	20-32	benzene	1	benzene	1	D2O	1	1.8×10^{-6}	36
Al	23.5	9-10	benzene	0.05	benzene	0.05	D2O	1	1×10^{-6}	36
Al	21	16	benzene	0.05	benzene	0.05	D2O	1	2×10^{-6}	36
Al	16	12-20	adamantane	1	benzene	1-1.2	H2O	1	5×10^{-6}	36
Al	13	10	adamantane	1	benzene	1	H2O	1	1×10^{-5}	36
Al	24.2	10	adamantane	1	benzene	0.1	H2O	1	1×10^{-6}	36
Al	43	14	benzene	1	benzene	1	CH_3I	1	1×10^{-6}	32
Al	40.5	12-38	benzene	1	benzene	1	CH_3I	1	$10^{-5}\text{-}8\times10^{-7}$	32
Al	18.3	10-14	adamantane	1	benzene	0.1	CH_3I	1	2×10^{-6}	32
Al	28	10-12	toluene	1	toluene	1	H_2O	1	4×10^{-7}	36
Al	25	10-12	toluene	0.5	toluene	0.5	H_2O	1	8×10^{-7}	36
Al	28	10-12	toluene	1	toluene	1	H_2O	1	4×10^{-6}	36
Al	23.3	9-10	toluene	1	toluene	1	H_2O	1	5×10^{-7}	36
Al	22	8-10	adamantane	1	toluene	0.5	H_2O	1	5×10^{-6}	39

Table 3.1. continued

Metal	weight (mg)	current (A)	Matrix	vapour pressure (Torr)	Hydrocarbon	vapour pressure (Torr)	Reactant	vapour pressure (Torr)	Vessel Pressure (Torr)	Reaction Time (min)
Al	67.43	10-24	p-Br-toluene	1.5	p-Br-toluene	1.5	H_2O	1	$1x10^{-6}$	36
Al	62.4	15-17	p-Br-toluene	1	p-Br-toluene	1	H_2O	1	$1x10^{-6}$	36
Al[a]	10[a]	12[a]	adamantane[a]	1[a]	p-Br-toluene[a]	0.1[a]	H_2O[a]	1[a]	N/A[a]	N/A[a]
Al[a]	10[a]	12[a]	p-Brtoluene[a]	1[a]	p-Br-toluene[a]	0.1[a]	D_2O[a]	1[a]	N/A[a]	N/A[a]
Al[a]	10[a]	12[a]	Cl-benzene[a]	1[a]	Cl-benzene[a]	0.1[a]	D_2O[a]	1[a]	N/A[a]	N/A[a]
Al	27	8-10	CF_3-benzene	0.01	CF_3-benzene	0.01	H_2O	1	$1x10^{-6}$	38
Al	29.1	14-17	CF_3-benzene	0.01	CF_3-benzene	0.01	H_2O	1	$1.9x10^{-6}$	38
Al	19.27	8-10	CF_3-benzene	0.01	CF_3-benzene	0.01	H_2O	1	$2x10^{-5}$	38
Ga	72.8	11	benzene	1	benzene	1	H_2O	1	$1x10^{-6}$	44
Ga	40.5	6-9	benzene	1	benzene	1	H_2O	1	$3x10^{-6}$	44
Ga	63	8-10	toluene	1	toluene	1	H_2O	1	$5x10^{-6}$	41.5
Ga	40	4-8	CF_3-benzene	0.01	CF_3-benzene	0.01	H_2O	1	$1x10^{-7}$	48
Ga	36.2	6-8	CF_3-benzene	0.01	CF_3-benzene	0.01	H_2O	1	$2.5x10^{-7}$	48
Ga	32.4	5-7	CF_3-benzene	0.01	CF_3-benzene	0.01	H_2O	1	$9.1x10^{-6}$	48
In	24.9	8-9	CF_3-benzene	0.01	CF_3-benzene	0.01	H_2O	1	$1x10^{-7}$	48
In	35.7	12-14	CF_3-benzene	0.01	CF_3-benzene	0.01	H_2O	1	$3x10^{-5}$	48
In	36.5	10	CF_3-benzene	0.01	CF_3-benzene	0.01	D_2O	1	$4x10^{-5}$	48
In	24.47	10	CF_3-benzene	0.01	CF_3-benzene	0.01	H_2O	1	$1x10^{-5}$	48
Tl	43.92	8-9	CF_3-benzene	0.01	CF_3-benzene	0.01	H_2O	1	$1.5x10^{-5}$	44
Tl	66	7-9	CF_3-benzene	0.01	CF_3-benzene	0.01	H_2O	1	$1x10^{-5}$	44

[a] Samples which were prepared at NRC in Ottawa

2 min benzene, 3 min water, 2 min benzene, 8 min benzene and aluminum metal vapour, 2 min benzene and 3 min water.

3.1.2.6.2 Aluminum, benzene and deuterium oxide reaction:

Aluminum metal vapour was produced by passing 9 to 32 A of current through a tungsten basket containing 21 to 26 mg of aluminum wire (Fisher). The metal vapours were condensed on a liquid N_2 cooled surface along with benzene vapours. The vapour pressure of the benzene was maintained throughout the run at ca. 1 Torr (with the aid of a bath consisting of an anisole-liquid nitrogen slurry) with the exception of runs 2 and 3 where the vapour pressure of the benzene was 0.05 Torr (by using a *p*- cymene-liquid nitrogen slurry bath). Deuterium oxide, used to promote the deuterolysis of the organometallic compound, was deposited intermittently during the run at ca. 1 Torr (ice-water bath). The sequence and deposition times of the various components of the runs were: 2 min deuterium oxide, 2 min benzene, 10 min benzene and aluminum metal vapour, 2 min benzene, 3 min deuterium oxide, 2 min benzene, 10 min benzene and aluminum metal vapour, 2 min benzene and 3 min deuterium oxide.

3.1.2.6.3 Aluminum, benzene, adamantane and water reaction:

Aluminum metal vapour was produced by passing 10 to 20 A of current through a tungsten basket containing 13 to 24 mg of aluminum wire (Fisher). The metal vapours were condensed on a liquid N_2 cooled surface along with benzene vapours. The vapour pressure of the benzene was maintained throughout the run at ca. 1.2 Torr (with the aid of a bath consisting of a bromobenzene-liquid nitrogen slurry) with the exception of one run where the vapour pressure of the benzene was 0.1 Torr. The vapour pressure of adamantane (matrix) during the run was approximately 1 Torr (water bath at ca. 80°C). Water, used to promote the hydrolysis of the organometallic compound, was deposited

intermittently during the run at ca. 1 Torr (ice-water bath). The sequence and deposition times of the various components of the runs were: 2 min adamantane, 2 min benzene, 10 min benzene and aluminum metal vapour, 2 min adamantane, 3 min water, 2 min adamantane, 10 min benzene and aluminum metal vapour, 2 min benzene and 3 min water.

3.1.2.6.4 Aluminum, benzene and methyl iodide reaction:

Aluminum metal vapour was produced by passing 10 to 38 A of current through a tungsten basket containing 18 to 43 mg of aluminum wire (Fisher). The metal vapours were condensed on a liquid N_2 cooled surface along with benzene vapours. The vapour pressure of the benzene was maintained throughout the run at ca. 1 Torr (with the aid of a bath consisting of an anisole-liquid nitrogen slurry) with the exception of one run where the vapour pressure of the benzene was 0.1 Torr and an inert matrix (adamantane) was used. Methyl iodide which was used to promote alkylation of the organometallic compound was deposited intermittently during the run at ca. 1 Torr (chloroform-liquid nitrogen slurry bath). In runs 1 and 2, the CH_3I was added directly onto the drum whereas in run 3 the CH_3I was added to the sample collector tube. The usual sequence and deposition times of the various components of run 1 and 2 were: 2 min methyl iodide, 2 min benzene, 10 min benzene and aluminum metal vapour, 2 min benzene, 10 min benzene and aluminum metal vapour, 2 min benzene and 4 min methyl iodide. The sequence and deposition times followed for run 3 were: 2 min adamantane, 2 min benzene, 10 min benzene and aluminum metal vapour, 2 min benzene, 10 min benzene and aluminum metal vapour, 2 min benzene and 3 min adamantane.

3.1.2.6.5 Aluminum, toluene and water reaction:

Aluminum metal vapour was produced by passing 9 to 12 A of current through a tungsten basket containing 23 to 28 mg of aluminum wire (Fisher). The metal vapours were condensed on a liquid N_2 cooled surface along with toluene vapours. The vapour

pressure of the toluene was maintained throughout the experiment at ca. 1 Torr (with the aid of a bath consisting of a bromobenzene-liquid nitrogen slurry) with the exception of one run where the vapour pressure of the toluene was 0.5 Torr. Water, used to promote the hydrolysis of the organometallic compound, was deposited intermittently during the run at ca. 1 Torr (ice-water bath). The sequence and deposition times of the various components of the runs were: 2 min water, 2 min toluene, 10 min toluene and aluminum metal vapour, 2 min toluene, 3 min water, 2min toluene, 10 min toluene and aluminum metal vapour, 2 min toluene and 3 min water.

3.1.2.6.6 Aluminum, toluene, adamantane and water reaction:

Aluminum metal vapour was produced by passing 8 to 10 A of current through a tungsten basket containing 22 mg of aluminum wire (Fisher). The metal vapours were condensed on a liquid N_2 cooled surface along with toluene vapours. The vapour pressure of the toluene was maintained throughout the run at ca. 0.5 Torr (with the aid of a bath consisting of an anisole-liquid nitrogen slurry). The vapour pressure of adamantane (matrix) during the run was approximately 1 Torr (water bath ca. 80°C). Water, used to promote the hydrolysis of the organometallic compound, was deposited intermittently during the run at ca. 1 Torr (ice-water bath). The sequence and deposition times of the various components of the run were: 2 min water, 2 min adamantane, 8 min toluene and aluminum metal vapour, 2 min adamantane, 3 min water, 2 min adamantane, 15 min toluene and aluminum metal vapour, 2 min adamantane and 3 min water.

3.1.2.6.7 Aluminum, *p*- bromotoluene and water reaction:

Aluminum metal vapour was produced by passing 10 to 24 A of current through a tungsten basket containing 67 mg of aluminum wire (Fisher). The metal vapours were condensed on a liquid N_2 cooled surface along with *p*- bromotoluene vapours. The vapour pressure of the *p*- bromotoluene was maintained throughout the first run at ca. 1.5 Torr

(with the aid of a distilled water-ice bath). In the second run 62 mg of Al wire was used and the vapour pressure of *p*- bromotoluene was reduced to 1 Torr (with the aid of a bath consisting of an anisole-liquid nitrogen slurry). Water, used to promote the hydrolysis of the organometallic compound, was deposited intermittently during the run at ca. 1 Torr (ice-water bath). The sequence and deposition times of the various components of the runs were: 2 min water, 2 min *p*- bromotoluene, 10 min *p*- bromotoluene and aluminum metal vapour, 2 min *p*- bromotoluene, 3 min water, 2 min *p*- bromotoluene, 10 min *p*- bromotoluene and aluminum metal vapour, 2 min *p*- bromotoluene and 3 min water.

3.1.2.6.8 Aluminum, *p*- bromotoluene and water reaction:

This reaction was prepared at the NRC in Ottawa by the method described in section 3.1.2.5.

3.1.2.6.9 Aluminum, *p*- bromotoluene and deuterium oxide reaction:

This reaction was prepared at the NRC in Ottawa by the method described in section 3.1.2.5.

3.1.2.6.10 Aluminum, chlorobenzene and deuterium oxide reaction:

This reaction was carried out at the NRC in Ottawa by the method described in section 3.1.2.5.

3.1.2.6.11 Aluminum, trifluorotoluene and water reaction:

Aluminum metal vapour was produced by passing 8 to 17 A of current through a tungsten basket containing 19 to 29 mg of aluminum wire (Fisher). The metal vapours were condensed on a liquid N_2 cooled surface along with trifluorotoluene vapours. The vapour pressure of the trifluorotoluene was maintained at ca. 0.01 Torr throughout the run with the aid of a bath consisting of a *p*- cymene-liquid nitrogen slurry. Water, used to promote the hydrolysis of the organometallic compound, was deposited at ca. 1 Torr (ice-

water bath) intermittently during the run. The sequence and deposition times of the various components of the runs were: 2 min water, 2 min trifluorotoluene, 10 min trifluorotoluene and aluminum metal vapour, 2 min trifluorotoluene, 3 min water, 2 min trifluorotoluene, 12 min trifluorotoluene and aluminum metal vapour, 2 min trifluorotoluene and 3 min water.

3.1.2.6.12 Gallium, benzene and water reaction:

Gallium metal vapour was produced by passing 6 to 11 A of current through a tungsten basket containing 41 to 73 mg of gallium metal (Fisher, BDH). The metal vapours were condensed on a liquid N_2 cooled surface along with benzene vapours. The vapour pressure of the benzene was maintained throughout the run at ca. 1 Torr with the aid of a bath consisting of an anisole-liquid nitrogen slurry. Water, used to promote the hydrolysis of the organometallic compound, was deposited intermittently during the run at ca. 1 Torr (ice-water bath). The sequence and deposition times of the various components of the runs were: 2 min water, 2 min benzene, 13 min benzene and gallium metal vapour, 2 min benzene, 3 min water, 2 min benzene, 13 min benzene and gallium metal vapour, 2 min benzene and 5 min water.

3.1.2.6.13 Gallium, toluene and water reaction:

Gallium metal vapour was produced by passing 8 to 10 A of current through a tungsten basket containing 63 mg of gallium metal (Fisher, BDH). The metal vapours were condensed on a liquid N_2 cooled surface along with toluene vapours. The vapour pressure of the toluene was maintained throughout the run at ca. 1 Torr with the aid of a bath consisting of a bromobenzene-liquid nitrogen slurry. Water, used to promote the hydrolysis of the organometallic compound, was deposited intermittently during the run at ca. 1 Torr (ice-water bath). The sequence and deposition times of the various components of the runs were: 2 min water, 2 min toluene, 10.5 min toluene and gallium metal vapour, 2

min toluene, 3 min water, 2 min toluene, 15 min toluene and gallium metal vapour, 2 min toluene and 3 min water.

3.1.2.6.14 Gallium, trifluorotoluene and water reaction:

Gallium metal vapour was produced by passing 4 to 8 A of current through a tungsten basket containing between 32 to 40 mg of gallium metal (Fisher, BDH). The metal vapours were condensed on a liquid N_2 cooled surface along with trifluorotoluene vapours. The vapour pressure of the trifluorotoluene was maintained throughout the run at ca. 0.01 Torr with the aid of a bath consisting of a *p*- cymene-liquid nitrogen slurry. Water, used to promote the hydrolysis of the organometallic compound, was deposited intermittently during the run at ca. 1 Torr (ice-water bath). The sequence and deposition times of the various components of the runs were: 2 min water, 2 min trifluorotoluene, 15 min trifluorotoluene and gallium metal vapour, 2 min trifluorotoluene, 3 min water, 2 min trifluorotoluene, 15 min trifluorotoluene and gallium metal vapour, 2 min trifluorotoluene and 5 min water.

3.1.2.6.15 Indium, trifluorotoluene and water reaction:

Indium metal vapour was produced by passing 8 to 14 A of current through a tungsten basket containing between 24 to 37 mg of indium metal (Fisher). The metal vapours were condensed on a liquid N_2 cooled surface along with trifluorotoluene vapours. The vapour pressure of the trifluorotoluene was maintained throughout the run at ca. 0.01 Torr with the aid of a bath consisting of a *p*- cymene-liquid nitrogen slurry. Water, used to promote the hydrolysis of the organometallic compound, was deposited intermittently during the run at ca. 1 Torr (ice-water bath). The sequence and deposition times of the various components of the run were: 2 min water, 2 min trifluorotoluene, 15 min trifluorotoluene and indium metal vapour, 2 min trifluorotoluene, 3 min water, 2 min

trifluorotoluene, 15 min trifluorotoluene and indium metal vapour, 2 min trifluorotoluene and 5 min water.

3.1.2.6.16 Thallium, trifluorotoluene and water reaction:

Thallium metal vapour was produced by passing 8 to 9 A of current through a tungsten basket containing 44 to 66 mg of thallium metal (BDH). The metal vapours were condensed on a liquid N_2 cooled surface along with trifluorotoluene vapours. The vapour pressure of the trifluorotoluene was maintained throughout the run at ca. 0.01 Torr with the aid of a bath consisting of a *p*- cymene-liquid nitrogen slurry. The water used to promote the hydrolysis of the organometallic compound, was deposited at ca. 1 Torr (ice-water bath) intermittently during the run. The sequence and deposition times of the various components of the run were: 2 min water, 2 min trifluorotoluene, 13 min trifluorotoluene and thallium metal vapour, 2 min trifluorotoluene, 3 min water, 2 min trifluorotoluene, 13 min trifluorotoluene and thallium metal vapour, 2 min trifluorotoluene and 5 min water.

3.1.2.7 Sample warm up:

The sample was collected at liquid nitrogen temperature (-196°C), and slowly warmed up to room temperature (20-25°C) with the aid of a number of baths of varying temperatures. The sample was warmed up slowly to prevent cracking of the sample flask and catalyzing new reactions as a result of the rapid heating. The baths used were: an acetone-liquid nitrogen slurry (-95.4°C), a chlorobenzene-liquid nitrogen slurry (-45.6°C) and an ice-water bath (0°C). The sample was left in each bath for approximately 30 min except for the ice-water bath where it was left overnight.

3.1.2.8 Selection of the cold temperature baths for the hydrocarbon, matrix and reactant.

The vapour pressure of the compounds used in the preparation of the Group 13 organometallic compounds was controlled with baths of varying temperatures. The

absolute vapour pressure (P in mm of Hg) is related to the absolute temperature (T in K) by the following expression:

$$\log_{10}P = (-0.05223\ a)/(T) + b \qquad 3.1$$

where a and b are constants characteristic of the substance of interest. The constants a and b for a number of compounds were available in the Handbook of Chemistry and Physics (70^{th} edition)[53] and those pertinent to the present study are listed in Table 3.2. In addition, temperatures required to produce a pressure of 1 Torr for common substances like benzene, toluene etc. were also available.[53]

Table 3.2. Values of the constants a and b, for the compounds used in the present study.

Compound	a	b
Benzene	42,904	9.556
Toluene	39,198	8.330

Baths with temperatures required to produce the desired vapour pressure were prepared. Table 3.3 summarizes the temperatures and the baths used to produce the vapour pressures of the compounds used in the present study.

Table 3.3. Summary of the bath temperatures needed to produce the various vapour pressures of the compounds used in the present study.

Substance	Role	Vapour Pressure Needed (Torr)	Bath Temperature (°C)	Bath
Adamantane	Matrix	1	80	water
Water	Reactant	1	0	Ice-Water
Deuterium Oxide	Reactant	1	0	Ice-Water
Methyl Iodide	Reactant	1	-63	Chloroform*
Benzene	Reactant	1	-37	Anisole*
		0.1	-57	Methyl Aniline*
		0.05	-67.9	*p*- Cymene*
Toluene	Reactant	1	-30.6	Bromobenzene*
		0.5	-37	Anisole*
Trifluorotoluene	Reactant	0.01	-67.9	*p*- Cymene*
p- Bromotoluene	Reactant	1.5	0	Ice-Water

* Slurries were made by adding, with mixing, liquid nitrogen to the solvent until the temperature was such that solid was maintained by the solution.

3.2 Analysis of the Reaction Mixtures Resulting from the Reaction of Organo Group 13 Compounds with H_2O, D_2O and CH_3I:

3.2.1 Standards:

The GC-MS standards, 1,3-cyclohexadiene, 1-methyl-1,4-cyclohexadiene and 1,4-cyclohexadiene were purchased from Aldrich Chemical Company. The synthesis of the deuterated benzene follows.

3.2.1.1 Synthesis of deuterated benzene (C_6H_5-D):

Deuterated benzene was synthesized by a Grignard reaction. Therefore, the first step was to clean and subsequently dry all the glassware in an oven for approximately 1 h. The equipment was assembled hot. Magnesium turnings (1.3 g, 0.053 mol) were added to a 250 mL three-necked round bottom flask. The three-necked flask was equipped with a condenser, a dropping funnel, a glass stopper and a magnetic stirring bar. Also the dropping funnel and the condenser were fitted with drying tubes containing calcium chloride. A mixture of 9.5 g (0.060 mol) of bromobenzene and 60 mL of anhydrous ether was added to the dropping funnel. Approximately 1 mL of the bromobenzene was added to the reaction flask to initiate the reaction. The ether-bromobenzene mixture was added dropwise and the reaction mixture well stirred. Upon completing the addition of the ether-bromobenzene mixture, the contents of the flask were refluxed for about 1/2 hour. Deuterium oxide (58 mL) was added to the reaction in two, 29 mL portions and the contents stirred for 10 min. Hydrochloric acid (6 M) was added with stirring until the white precipitate, present in the reaction flask, dissolved. The solution was transferred to a separatory funnel and the organic layer was separated from the aqueous layer. The aqueous layer was extracted with three 25 mL portions of ether. The ether layers were combined and added to the original organic layer. Magnesium sulfate was added to the

flask containing the organic phase. Finally, the diethyl ether was removed on a rotoevaporator and the product analyzed by GC-MS. Deuterated benzene (C_6H_5-D) has a similar fragmentation pattern to that of benzene (C_6H_6).[74] The molecular ion, $C_6H_5D^+$ (m/e=79) loses H, D, C_2H_2 or C_2HD to form $C_6H_4D^+$ (m/e=78), $C_6H_5^+$ (m/e=77), $C_4H_3D^+$ (m/e=53) and $C_4H_4^+$ (m/e=52), respectively. The ion $C_6H_4D^+$ loses D or C_2HD to form $C_6H_4^+$ (m/e=76) and $C_4H_3^+$ (m/e=51), respectively. The ion $C_6H_5^+$ loses H$^\bullet$ or C_2H_2 to form $C_6H_4^+$ (m/e=76) and $C_4H_3^+$ (m/e=51), respectively. The ion $C_4H_3D^+$ loses D to form $C_4H_3^+$ (m/e=51). The molecular ion, $C_6H_5D^+$, can also lose C_3H_2D to form $C_3H_3^+$ (m/e=39), Figure 3.6.

3.2.2 Preparation of Samples for Analysis by GC-MS:

The samples, prepared on the rotating cryostat, were treated by one of two procedures. In the first procedure, 1 mL of dichloromethane was transferred with the aid of a 1 mL syringe, (Hamilton Series RN1001), to the flask containing the reaction mixture. The sample was transferred with the aid of a 1 mL syringe to a glass vial containing 3A molecular sieves.* One μL of the solution was transferred with the aid of 10 μL GC syringe, (Hamilton Series 701N), into another vial containing 1 mL of dichloromethane (1000-fold dilution) and 3A molecular sieves. The resulting solution was diluted 1000-fold, 100-fold and 10-fold by transferring 1, 10 and 100 μL of the solution respectively, to separate vials containing 1 mL of dichloromethane. The solutions were subjected to analysis by GC-MS in order of increasing concentration. It should be noted that if an acceptable chromatogram** was obtained with the most dilute sample, it was not necessary to analyze the more concentrated solutions.

---

* Molecular sieves were activated by heating at 300°C for 3 h in an oven.

** A chromatogram with good baseline resolution; the ideal peak symmetry (symmetry=B/A where A=distance from peak front to peak maximum and B=distance from peak maximum to peak end) is 1.0.[75]

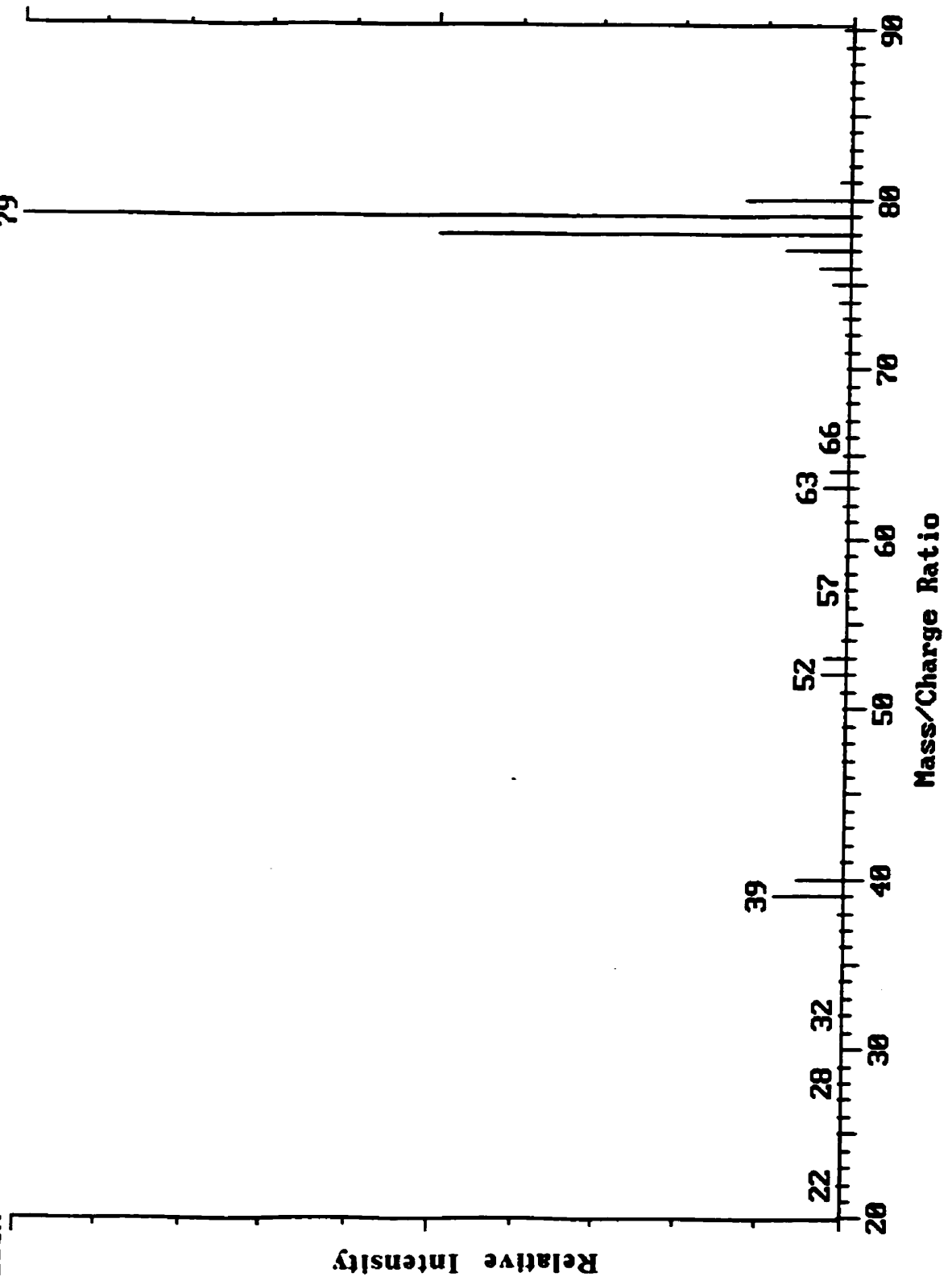

Figure 3.6. Mass spectrum of deuterated benzene resulting from the Grignard reaction.

In the second procedure, 1 mL of HCl (6 M) was added to the flask containing the sample prepared on the rotating cryostat. This mixture was subsequently transferred to a separatory funnel and washed with three 1 mL portions of dichloromethane. The organic layers were combined in a flask and dichloromethane was removed with the aid of a rotary evaporator. One mL of dichloromethane was added to the residue in the flask and transferred to a glass vial containing 3A molecular sieves. The resulting sample was diluted as outlined in the first procedure.

3.2.3 Instrumentation:

The samples generated in this study were analyzed using a Varian Saturn II gas chromatograph-mass spectrometer. This instrument consisted of a Varian Model 3400 gas chromatograph equipped with a septum programmable injection (SPI) port coupled to an ion trap mass spectrometer operating in the electron impact ionization mode at 70 eV.

All analyses were carried out using two nonpolar fused silica columns, (PTE, 30 m x 0.25 mm, 0.25 μm film thickness) or (PTE, 60 m x 0.25 mm, 0.25 μm film thickness), supplied by Supelco.

3.2.4 Operating Parameters for the GC-MS:

The GC-MS operating parameters for the analysis of the products formed in the reactions involving benzene and water, benzene and deuterium oxide, benzene and methyl iodide and toluene and water are listed in Tables 3.4 and 3.6. For the *p*- bromotoluene and water, chlorobenzene and water and trifluorotoluene and water reactions the same parameters listed in Tables 3.5 and 3.6 were used except for a mass spectrometer parameter known as the filament delay. The filament delay was dependent upon the nature of the solvent and reactants in the reaction mixture The filament delay was adjusted from one run to another to protect the filament and the instrument from high concentrations of ions

produced by the reactants and solvents. In general, each reaction mixture was analyzed using two different filament delays. In the first analysis, the filament was not activated until the solvent had eluted out of the column and the chromatographic run was aborted approximately 10 seconds prior to the elution of the reactants (i.e. chlorobenzene or *p*-bromotoluene). This ensured the detection of new products eluting at retention times between that of the solvent and the reactants. In the second analysis, the filament remained off until chlorobenzene or *p*- bromotoluene were eluted from the column. This ensured the detection of products with retention greater than that of the reactants. The adjustment of the filament delay was dependent on the concentrations of the compounds analyzed.

Table 3.4. GC program for the reactions involving benzene and water, benzene and deuterium oxide, benzene and methyl iodide and toluene and water.

Segment	Temperature (°C)	Rate (°C min^{-1})	Time (min)	Total (min)
1	33-40	0.2	35.00	35.00
2	40-50	1.0	10.00	45.00
3	50-80	5.0	6.00	51.00
4	80-250	20.0	8.50	59.50

Table 3.5. GC program for the reactions involving *p*- bromotoluene and water, chlorobenzene and water and trifluorotoluene and water.

Segment	Temperature (°C)	Rate (°C min^{-1})	Time (min)	Total (min)
1	35-37	0.2	10.00	10.00
2	37-50	1.0	13.00	23.00
3	50-80	5.0	6.00	29.00
4	80-250	20.0	8.50	37.50

Table 3.6. **MS method for the reactions involving benzene and water, benzene and deuterium oxide, benzene and methyl iodide, toluene and water, chlorobenzene and water, *p*- bromotoluene and water, and trifluorotoluene and water.**

Parameter	Set value
Flow rate	6 psi
Multiplier voltage	1750 volts
Manifold set temperature	220°C
Emission set current	20 microamps
A/M amplitude set voltage	4.0 volts
Target value	40000
Low mass	20 amu
High mass	250 amu
Scan rate	500 milliseconds
Segment acquire time	59 minutes
Filament delay	230 seconds
Mass defect	50 millimass/100 amu
Background mass	19 amu

4. RESULTS AND DISCUSSION

4.1 Interaction of Group 13 Atoms with Hydrocarbons:

Group 13 metal atoms (Al, Ga, In and or Tl) were reacted with a number of hydrocarbons, namely, benzene, toluene, trifluorotoluene, *p*- bromotoluene and chlorobenzene. Metal atoms, produced by resistively heating metal wire or pellets, and the hydrocarbon vapour were introduced through portholes into the metal atom reactor maintained at ca. 10^{-5} Torr. The reactants condensed on the surface of the rotating, liquid nitrogen-filled drum located in the centre of the reactor and a metal-hydrocarbon intermediate was thought to form at the metal-hydrocarbon interface.

The metal-hydrocarbon intermediates were reacted with water, deuterium oxide or methyl iodide. This was done by depositing a layer of water, deuterium oxide or methyl iodide onto the surface of the reaction mixture. Next, the mixture was scraped under vacuum and at 77 K into a sample tube. The contents of the tube were then slowly warmed to room temperature with the aid of a series of cold temperature baths.

The hydrolysis, deuterolysis or alkylation products were analyzed by GC-MS. The results are presented in sections 4.1.1-4.1.5.

4.1.1 Reactions of Group 13 Atoms with Benzene:

4.1.1.1 Reaction of Al atoms with benzene:

4.1.1.1.1 Hydrolysis of the intermediate formed in the reaction of Al atoms and benzene:

Aluminum atoms were reacted with benzene under a number of experimental conditions. More specifically, the weight of the Al wire used to produce the aluminum

atoms was varied from 20 to 64 mg and the amount of benzene was changed by adjusting the vapour pressure of benzene to 0.05 or 1 Torr. A typical total ion current (TIC) chromatogram of the hydrolysis products is presented in Figure 4.1. The peak of interest is labelled 1 and has been assigned to 1,4-cyclohexadiene. Confirmation of this assignment was obtained by comparison of the retention times and mass spectral data, Figure 4.2, with those for authentic samples of benzene, 1,3-cyclohexadiene and 1,4-cyclohexadiene. The data for the example corresponding to Figure 4.1 are presented in Table 4.1. It is worth noting that the mass spectral data for 1,3-cyclohexadiene and 1,4-cyclohexadiene are very similar, Figure 4.3, and one could only distinguish between the two by the use of retention times.

The reactions were repeated several times. The amount of 1,4-cyclohexadiene in the mixture ranged from 0.06% to 0.20%.* The small conversion is not surprising considering how the reactions were carried out, i.e., generally only 6 mg of Al were vaporized during a run and the concentration of substrate added to the reaction was approximately 1000 times greater than that of the metal.

It is worth mentioning that adamantane, an inert matrix, was used in a few instances so that smaller amounts of benzene could be used in the reaction. The objective was to try to increase the Al atom-benzene ratio. The mass chromatogram of the hydrolysis products of this reaction mixture showed the presence of two compounds, namely, benzene and adamantane. The fact that 1,4-cyclohexadiene was not detected under these experimental conditions suggests that adamantane interfered in some way in the reaction. It is possible that the water was unable to penetrate the adamantane making hydrolysis of the Al-benzene intermediate impossible.

---

* The percentage was calculated by dividing the area counts determined electronically for 1,4-cyclohexadiene by the sum of the area counts of benzene and 1,4-cyclohexadiene and multiplying this ratio by 100.

Figure 4.1. Total ion current chromatogram of the products resulting from hydrolysis of the organometallic compound formed in the reaction of Al atoms and benzene. (The compound labelled * is due to contamination, see text).

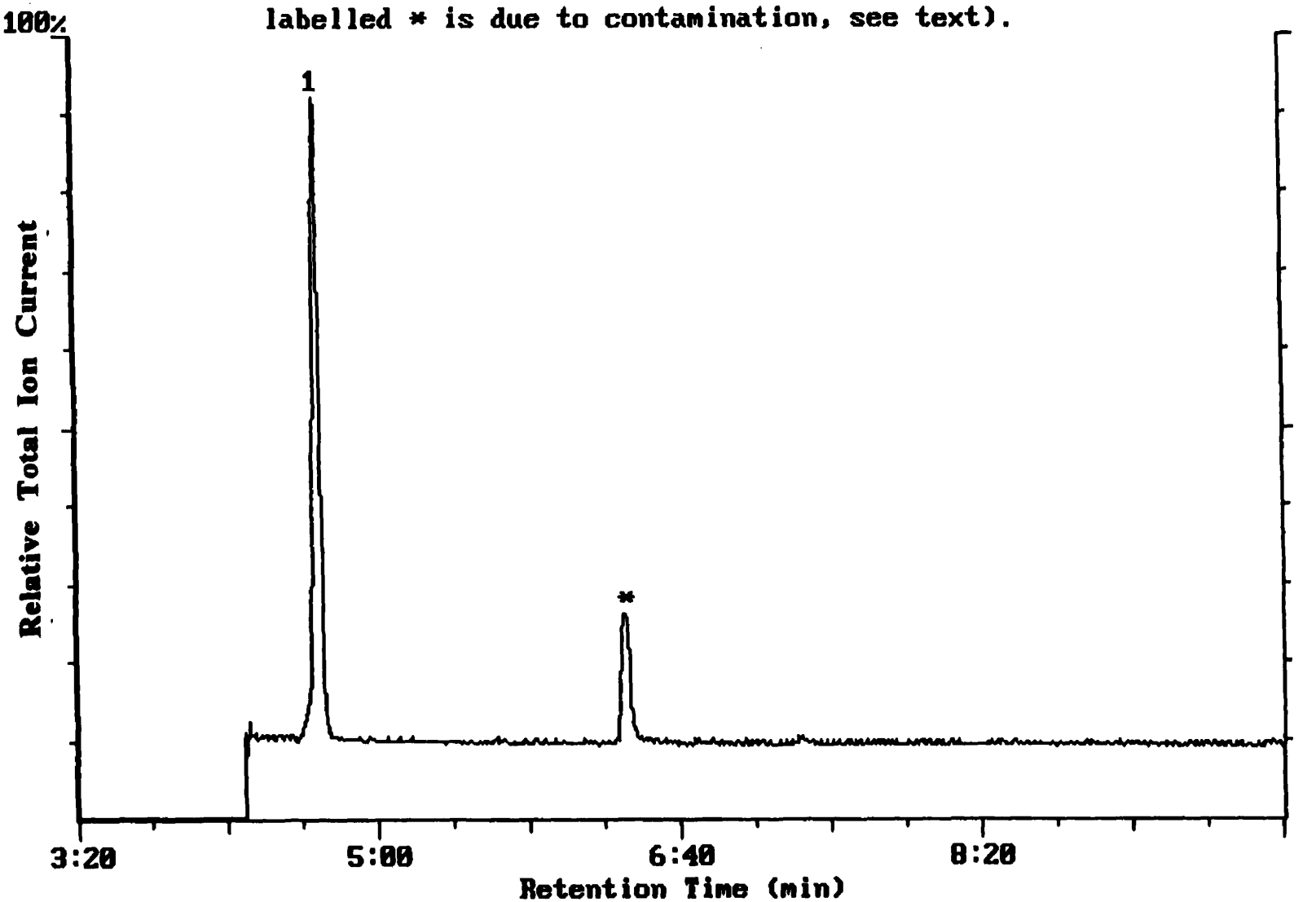

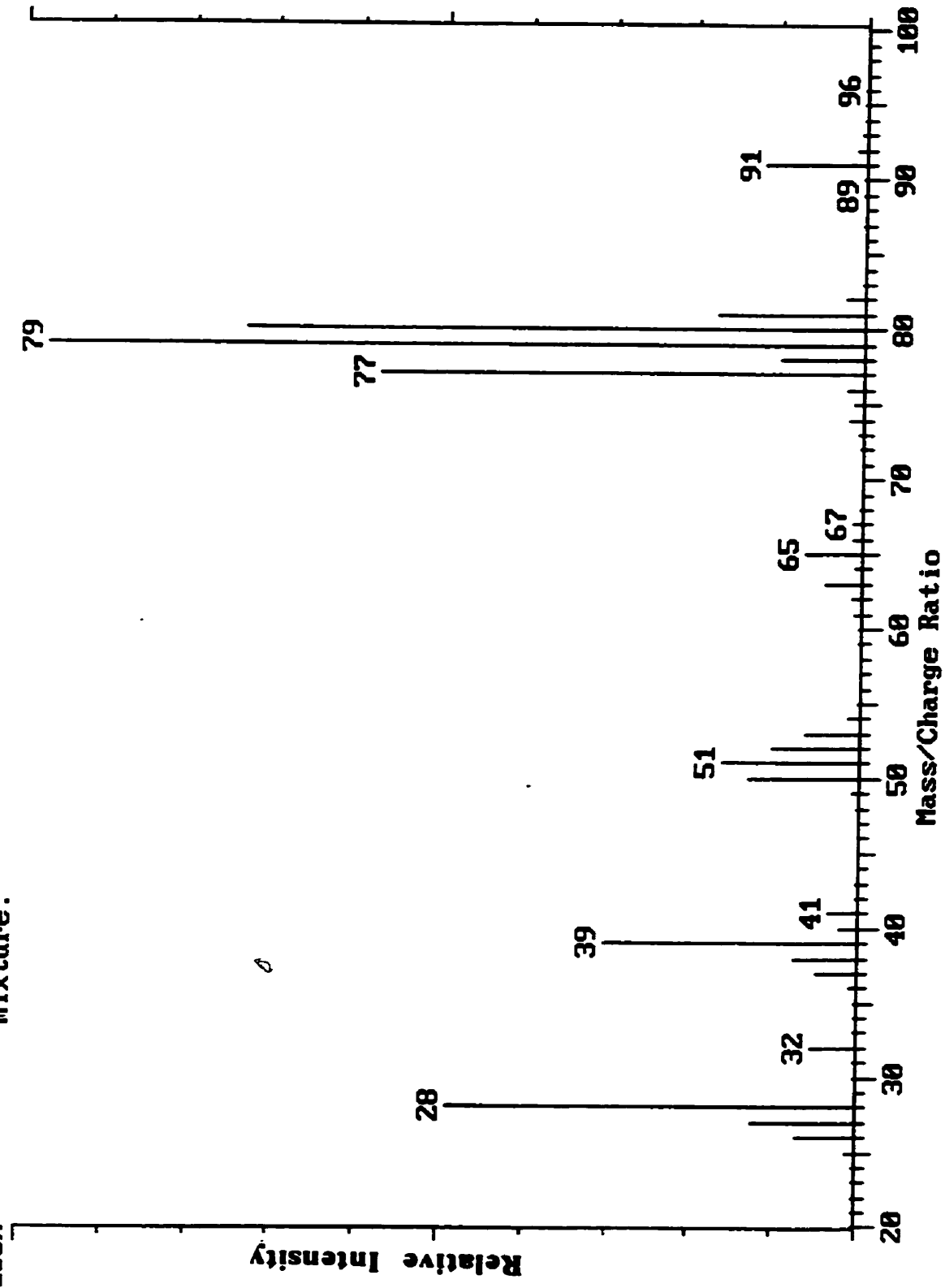

Figure 4.2. Mass spectrum of the hydrolysis product (peak 1, Figure 4.1) resulting from the hydrolysis of the Al atom–benzene reaction mixture.

In another attempt to increase the yield of 1,4-cyclohexadiene, the concentration of the benzene in the system was altered from 1 to 0.05 Torr. In fact, the yield increased to 0.6% when the vapour pressure of the benzene was decreased to 0.05 Torr.

Table 4.1. Retention times and mass spectral data for hydrolysis products resulting from the reaction of Al atoms and benzene.

Peak No.	Retention Time (min)	m/e for main fragments*
1	4:41	28(43.3) 38(6.6) 39(29.4) 40(3.0) 50(11.3) 51(15.2) 52(9.3) 53(6.0) 54(1.1) 63(4.1) 65(6.2) 77(51.7) 78(9.3) 79 (100) 80(74.7) 81(20.0)
Benzene	3:37	28(43.3) 38(4.9) 39(14.4) 40(0.7) 50(13.4) 51(18.5) 52(16.1) 53(0.9) 63(4.7) 65(0.6) 77(22.1) 78(100) 79 (10.1)
1,3-cyclohexadiene	3:46	28(25.7) 38(5.2) 39(24.2) 40(1.9) 50(13.1) 51(15.5) 52(7.1) 53(4.4) 54(0.8) 63(3.4) 65(2.6) 77(31.6) 78(7.0) 79 (100) 80(70.7) 81(25.4)
1,4-cyclohexadiene	4:39	28(32.1) 38(6.5) 39(28.3) 40(2.4) 50(11.0) 51(15.8) 52(7.9) 53(5.3) 54(1.1) 63(3.7) 65(5.3) 77(45.7) 78(7.4) 79 (100) 80(71.7) 81(22.0)

*. The number in brackets represents the percentage of the base peak.

Figure 4.3. Total ion current chromatogram of a mixture containing benzene, 1,3-cyclohexadiene and 1,4-cyclohexadiene. The mass spectra of the compounds have been inlaid. (The y-axis of the mass spectra represents the relative intensity of the ions).

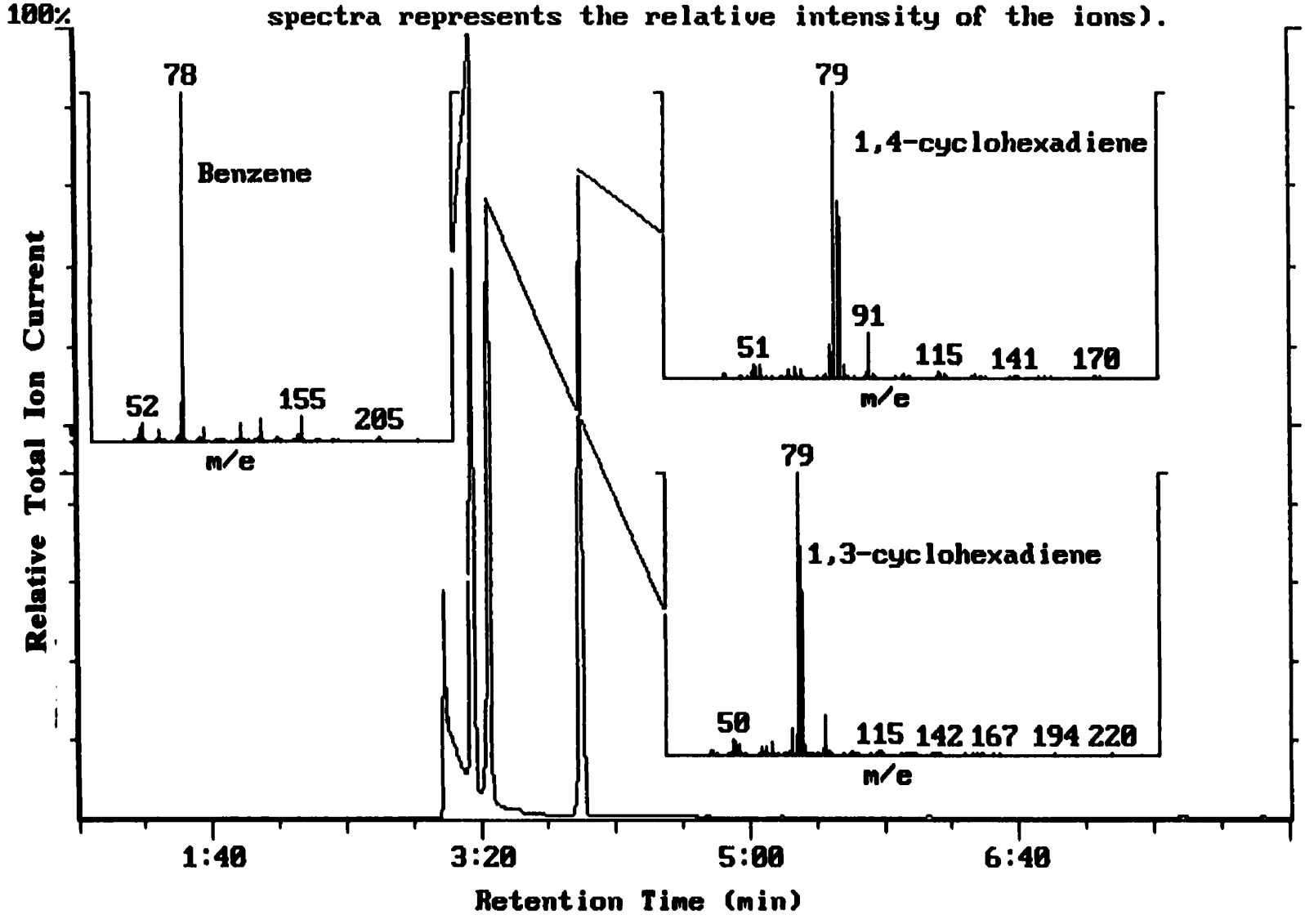

In a few instances, water was replaced by deuterium oxide. The reason for using deuterium oxide (D_2O) instead of water (H_2O) was to find out more information on how the reaction takes place, i.e. to find out what role in terms of hydrogen donation the water plays. It is known that Al-C bonds in organoaluminum adducts are replaced with deuterium atoms when treated with D_2O. Therefore incorporation of deuterium into the molecule would indicate the number and location of the Al-C bonds. Figure 4.4 shows the total ion current (TIC) chromatogram of the deuterolysis product. The peak of interest (labelled-1 in Figure 4.4) has been assigned to 1,4-cyclohexadiene-3,6-d_2 ($C_6H_6D_2$). The retention time of the compound is identical to that of 1,4-cyclohexadiene within experimental error. The mass spectral data of the product formed is shown in Figure 4.5. The fragment with an m/e ratio of 82 is consistent with the incorporation of 2 deuterium atoms into the 1,4-cyclohexadiene molecule. Confirmation of this assignment was obtained by comparing the mass spectral data to that obtained for 1,4-cyclohexadiene, taking into account the isotopic substitution.

Franklin and Carroll[76] proposed that undeuterated 1,4-cyclohexadiene fragmented as shown in scheme 4.1. The molecular ion, $C_6H_8^+$ loses H, to form the benzenium ion $C_6H_7^+$ (m/e=79) which in turn loses either C_2H_2 or two H yielding $C_4H_5^+$ (m/e=53) and $C_6H_5^+$ (m/e=77), respectively. The subsequent loss of C_2H_2 from $C_6H_5^+$ results in the formation of $C_4H_3^+$ (m/e=51). Alternatively, the molecular ion can lose two H to form $C_6H_6^+$ (m/e=78). Fragmentation of $C_6H_6^+$ gives $C_4H_3^+$ (m/e=51), $C_4H_4^+$ (m/e=52), $C_6H_4^+$ (m/e=76) and $C_3H_3^+$ (m/e=39), respectively. The $C_4H_2^+$ ion (m/e=50) forms when $C_6H_4^+$ loses C_2H_2 or $C_4H_4^+$ loses two H. When the molecular ion loses C_2H_2, $C_4H_6^+$ (m/e=54) is formed which undergoes further fragmentation yielding $C_3H_3^+$ (m/e=39).

Figure 4.4. Total ion current chromatogram of the products resulting from deuterolysis of the organometallic compound formed in the reaction of Al atoms and benzene. (The compound labelled * is due to contamination, see text).

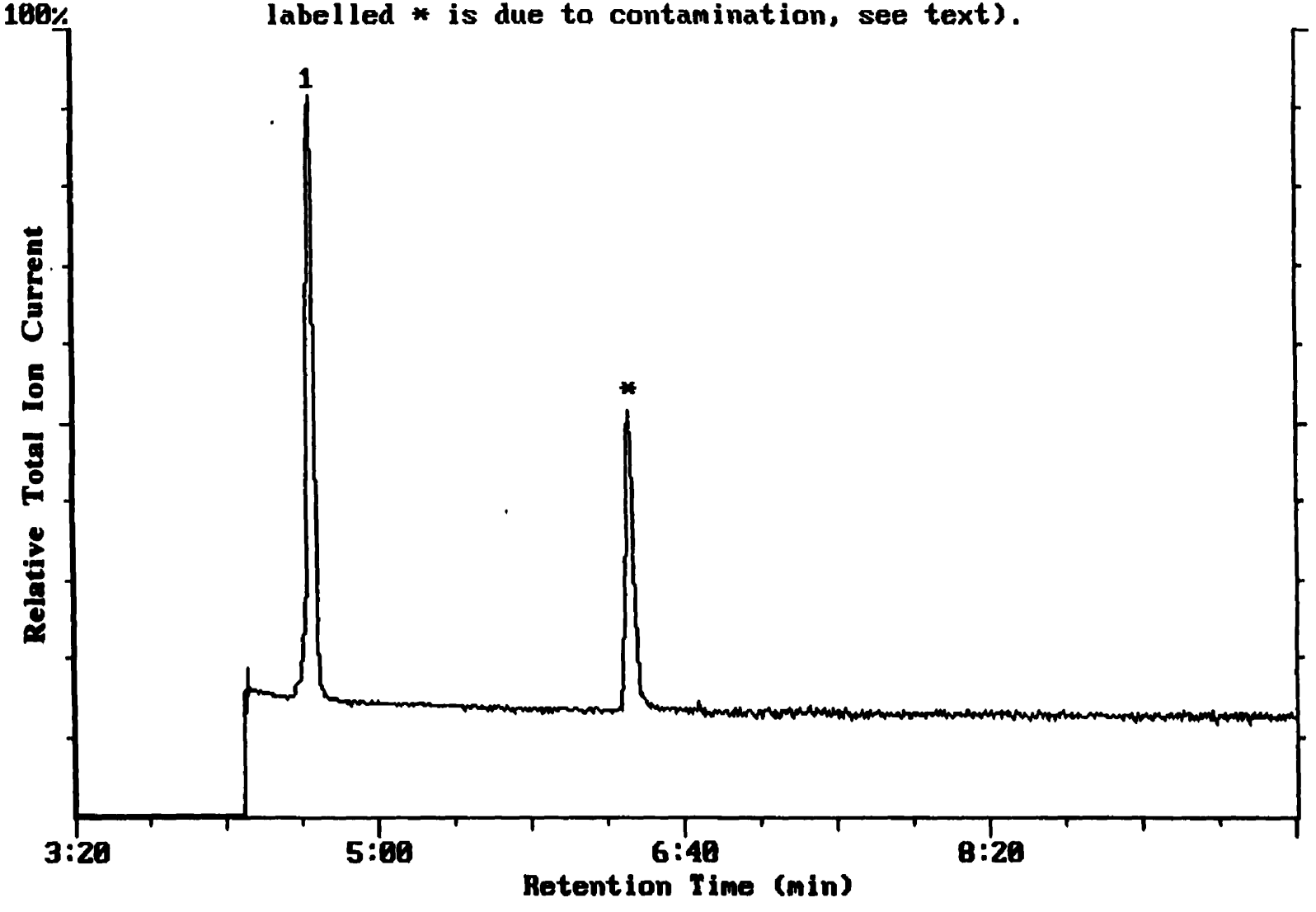

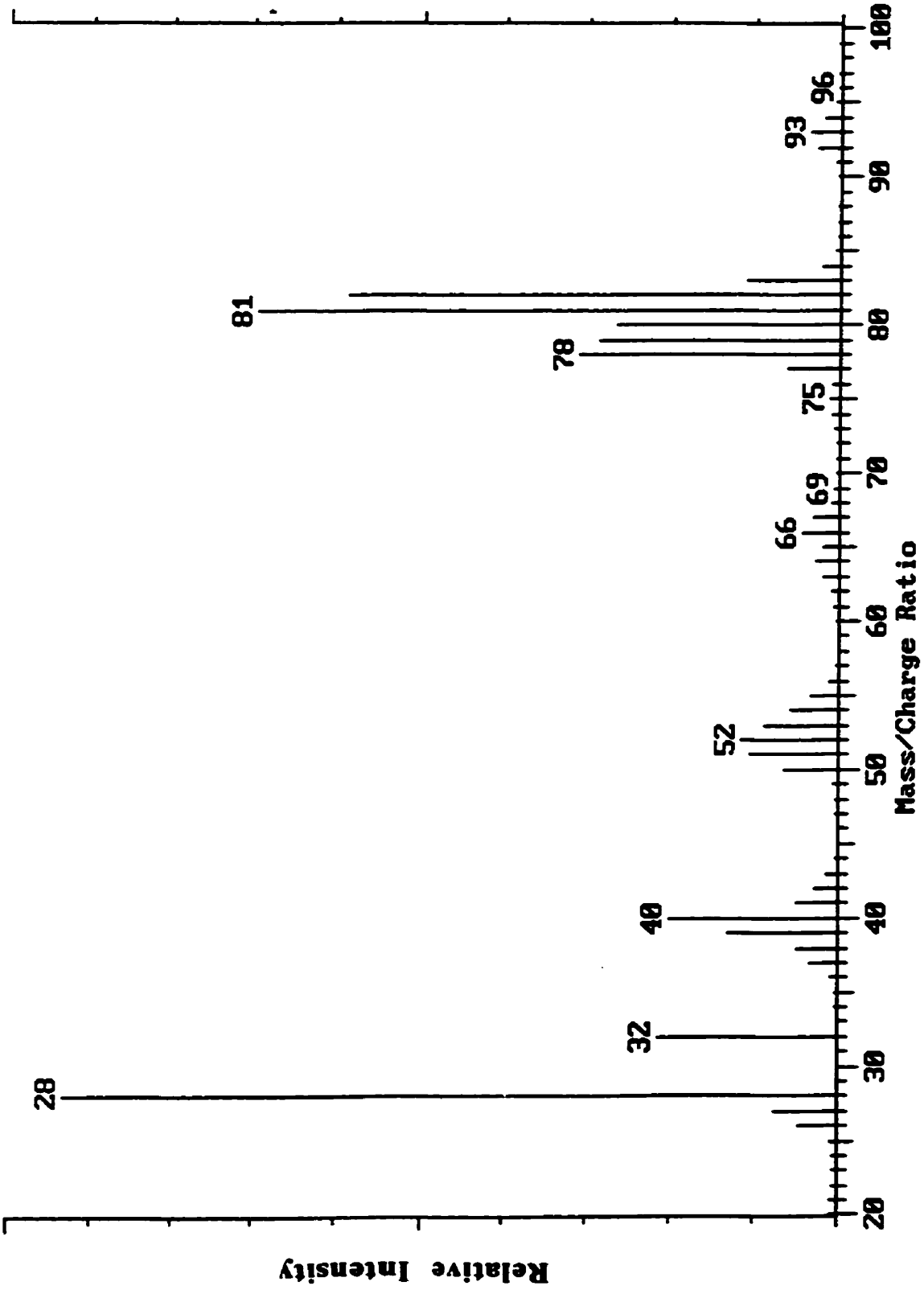

Figure 4.5. Mass spectrum of the deuterolysis product (peak 1, Figure 4.4) resulting from the deuterolysis of the Al atom-benzene reaction mixture.

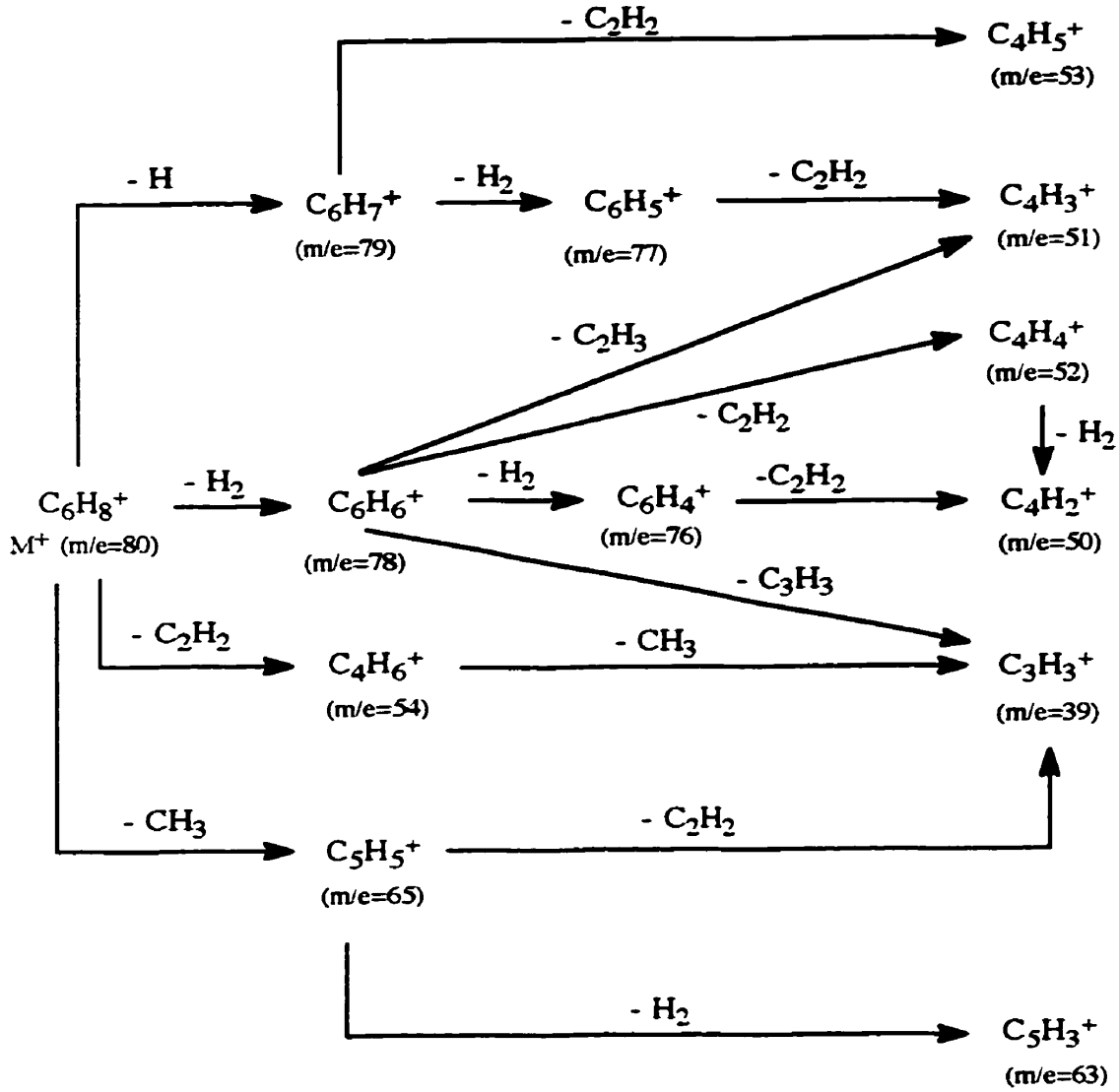

Scheme 4.1. Fragmentation scheme for 1,4-cyclohexadiene.[76]

Finally, $C_5H_5^+$ (m/e=65) results from the loss of CH_3 from the molecular ion. The $C_5H_5^+$ ion fragments to give $C_3H_3^+$ (m/e=39) and $C_5H_3^+$ (m/e=63), respectively.

For the case of 1,4-cyclohexadiene-3,6-*d* $_2$ a similar fragmentation scheme can be prepared, scheme 4.2. However, in addition to the loss of H, 2H, C_2H_2 and CH_3, the molecular ion can also lose D, HD, C_2HD, CH_2D and CD_2H. From the primary fragmentation one would expect the formation of clusters of ions with an m/e ranging from 79-82, 65-67 and 55-56. The primary ions would undergo further fragmentation in a similar fashion to that suggested for 1,4-cyclohexadiene. The secondary fragmentation would produce clusters of ions with an m/e ranging from 76-79, 63-65, 50-55 and 39-41. The proposed fragmentation pattern is consistent with the experimental mass spectral data obtained for the compound which is thought to be 1,4-cyclohexadiene-3,6-*d* $_2$.

The fact that 1,4-cyclohexadiene is formed when the Al-benzene reaction mixture is hydrolyzed suggests that Al atoms mediate the reduction of benzene. The incorporation of deuterium at C-1 and C-4 suggests that an Al atom was attached to these carbon atoms prior to the deuterolysis. Based on an ESR spectroscopic study of the reaction of Al atoms with benzene at 77 K, Howard et al.[36] proposed that an Al atom cheleotropically added to C-1 and C-4 of benzene. The monobenzene aluminum(0) intermediate was found by these workers to be stable between 4-278 K. Deuterolysis of this intermediate (1) would indeed yield 1,4-cyclohexadiene-3,6-*d* $_2$, equation 4.1.

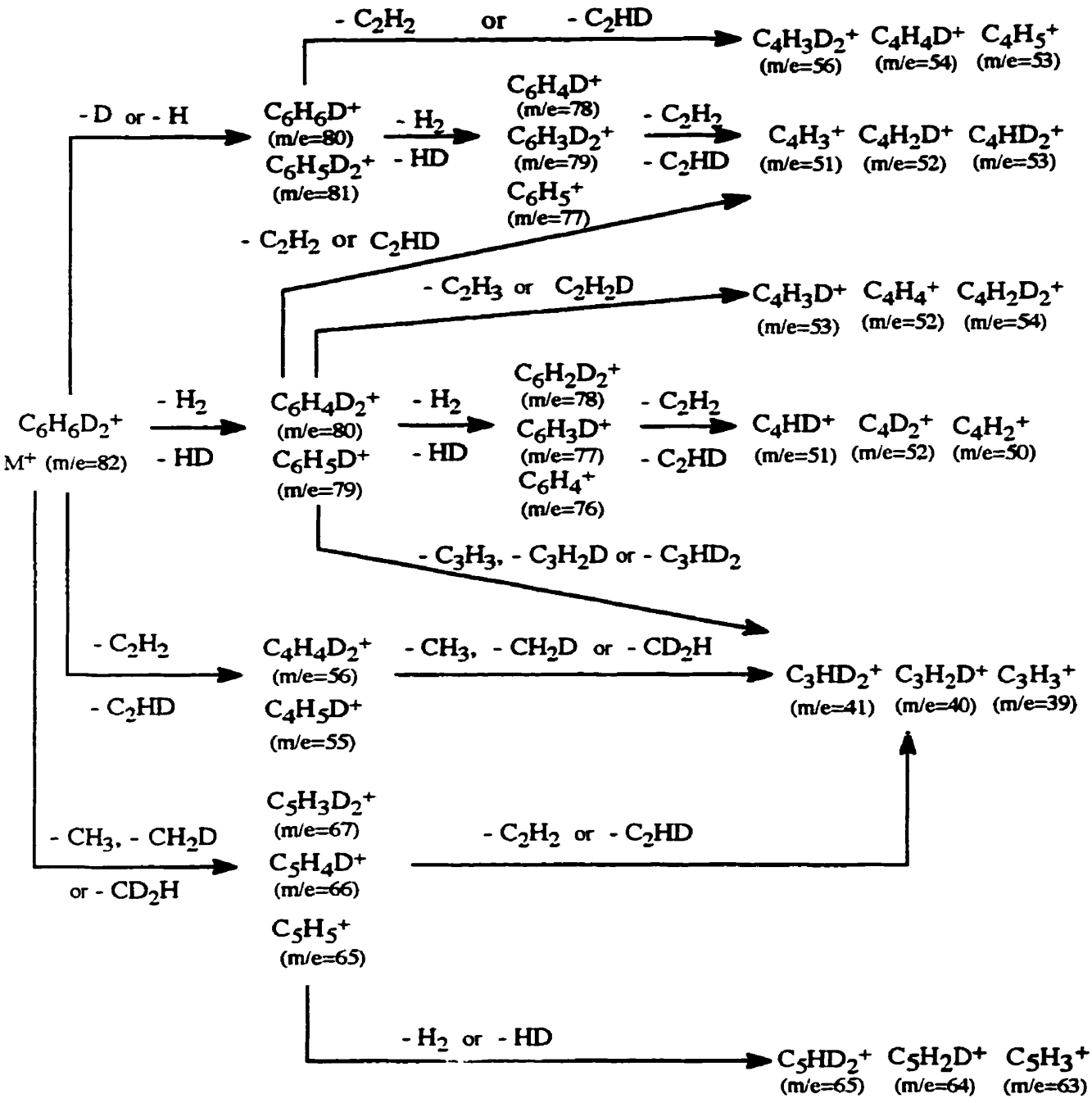

Scheme 4.2. Fragmentation scheme for 1,4-cyclohexadiene-3,6-*d* 2.

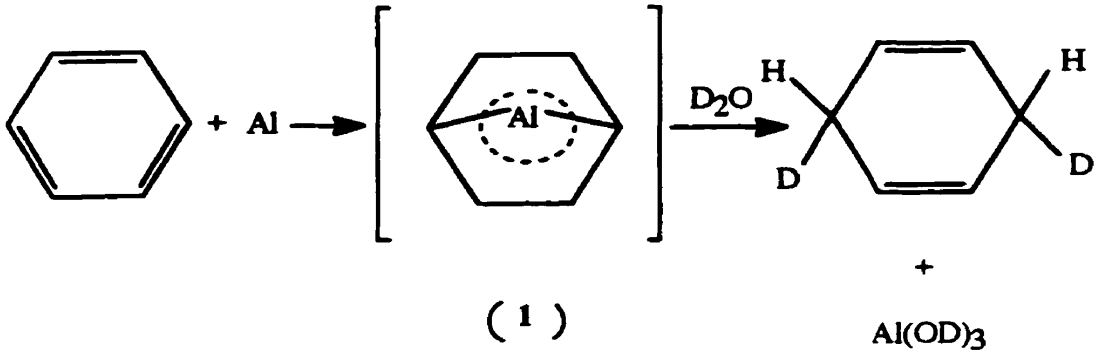

4.1

(1)

As previously stated, Kasai and McLeod[14] also studied the Al atom reaction with benzene. These workers suggested that the ESR spectroscopic data was most consistent with the formation of a monobenzene aluminum(0) species where the Al atom interacts with only two of the six protons of benzene by forming a π bond with only one of the C=C units. Deuterolysis of a π-bonded intermediate would result in the regeneration of benzene and $Al(OD)_3$ and deuterium would not be incorporated into the molecule. Benzene was detected in the hydrolysis reaction mixture. However this may be excess starting material. Kasai and McLeod[12] have noted that the transfer of spin density from Al to the C=C unit of benzene is considerably greater than that observed for ethylene. Therefore, should the bonding between Al and an isolated C=C unit of benzene have considerable σ character (**2**), deuterolysis of the intermediate would result in the formation of 1,3-cyclohexadiene-5,6-*d* $_2$, equation 4.2.

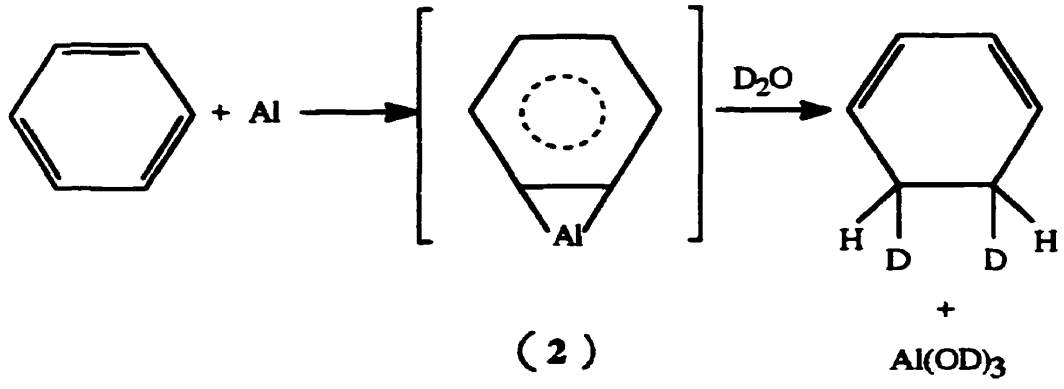

4.2

(2)

As there is no evidence for the formation of 1,3-cyclohexadiene in the hydrolysis of the Al-benzene reaction mixture, formation of intermediate (**2**) can be eliminated.

Because only one species is identified in the ESR study and 1,4-cyclohexadiene-3,6-d_2 results when the intermediate is subjected to deuterolysis it can be concluded that intermediate (**1**) forms when Al atoms are reacted with benzene under cryogenic conditions.

Aromatic compounds can be reduced using the Birch reduction. In the Birch reduction of benzene[77], benzene is treated with lithium metal in liquid ammonia in the presence of a weak acid, such as t-butyl alcohol (t-BuOH), resulting in the formation of 1,4-cyclohexadiene. The reaction is believed to occur in four steps, of which the first is the transfer of one electron from the lithium atom to the π system of benzene, generating the benzene radical anion. Reaction of the highly basic radical anion with the weakly acidic alcohol generates a conjugate acid of the radical anion that can accept a second electron from Li and a second proton from t-BuOH in two subsequent steps to form the 1,4-cyclohexadiene, scheme 4.3.

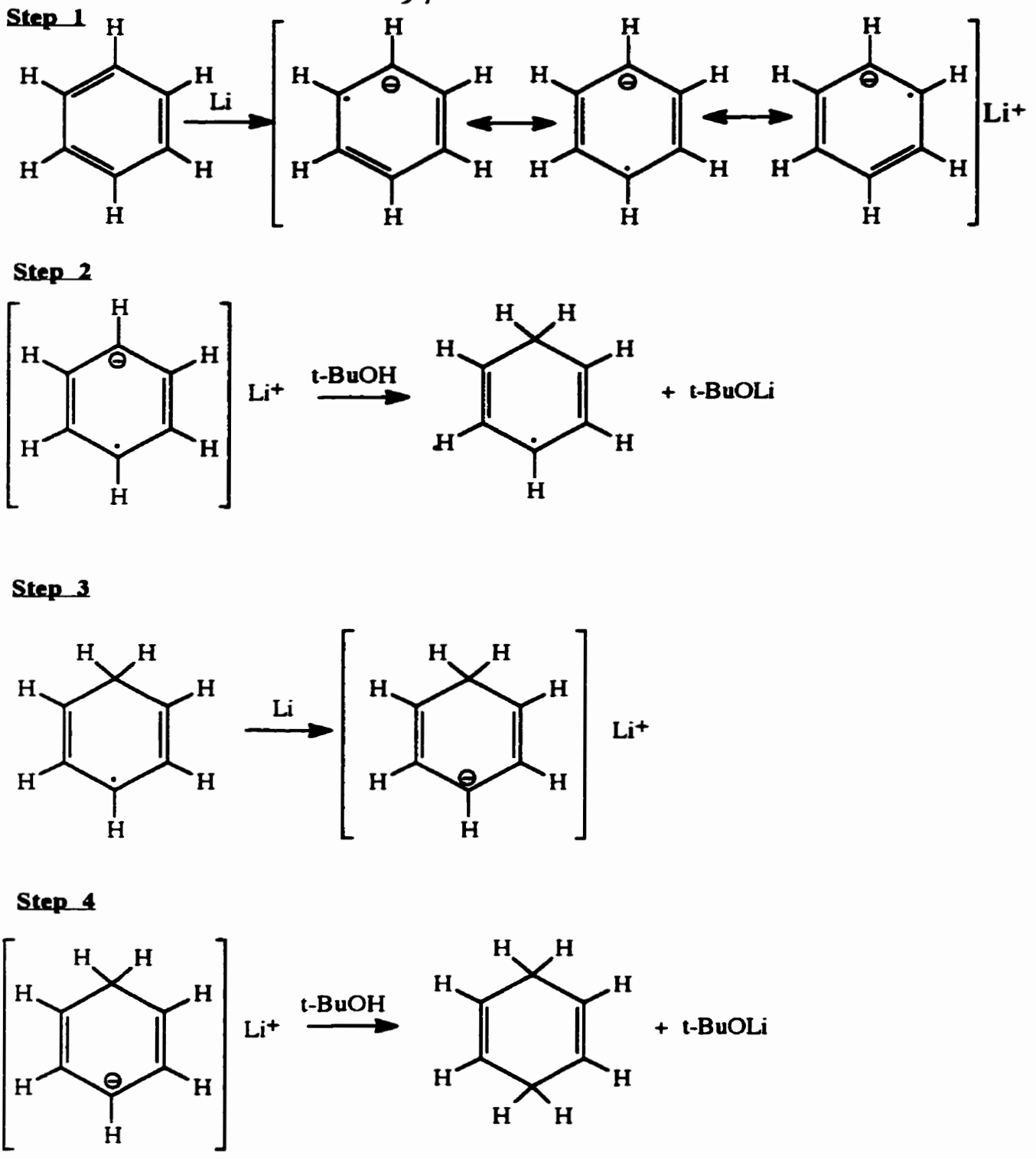

Scheme 4.3. Mechanism for the Birch reduction of benzene.[77]

ESR spectroscopy has been used to study the interaction which exists between alkali metal atoms and aromatic hydrocarbons. More specifically, it has been used to characterize the radical anion formed when the metal transfers an electron to the aromatic moiety. Depending on the metal, hydrocarbon, temperature and solvent used, the cation-radical anion can exist as free ions, solvent-separated ion pairs, or as contact ion pairs. If the metal centre retains some of the unpaired spin density, as would be the case in an ion pair, hyperfine coupling of the alkali metal is observed in the ESR spectrum. The magnitude of the coupling constant is thought to be an indication of the tightness of the ion pair. An increase in the coupling constant as experimental conditions are changed (i.e., temperature) has been assumed to indicate that the ions in the ion pair are closer.[78] The hyperfine coupling constants for alkali metal aromatic radical ions have been summarized by Catterall et al.[79] and Symons.[80] In general, the coupling constants for these systems are small, ranging from 0 - 3 G.[81,82] An estimate of the spin densities is obtained when the experimental hyperfine coupling constant is divided by the one electron parameter calculated for the s orbital of the alkali metal atom. The spin densities calculated for the alkali metal aromatic radicals lie between 0 and 2.5%, suggesting that anywhere from 100 - 97.5% of the unpaired spin density resides on the benzene ring.

In the case of the Al-benzene intermediate, analysis of the Al hyperfine coupling constants[44,45] indicated that the unpaired spin populations of the 3s and 3p orbitals of Al were 0.0024 and 0.34, respectively. The remaining spin population of 0.7 was thought to reside on the benzene ring. Detection of the coupling confirms that the Al atom is bonded to the benzene moiety. When one compares the values of the unpaired populations on Al with that of the alkali metal systems one can conclude that Al is more tightly associated to benzene. Howard et al.[44,45] found this intermediate to be stable to at least 232 K.

We therefore propose that under our experimental conditions Al atoms react to form the Al-benzene intermediate characterized using ESR spectroscopy by Howard et al.[44,45] When the Al-benzene intermediate is annealed in the presence of deuterium oxide, deuterolysis of the C-Al bonds occur and 1,4-cyclohexadiene-3,6-d_2 is formed. We are not able to comment on the nature of the deuterolysis. We have no way of knowing at this point, whether the reduction is a stepwise process, as is the case for the Birch reduction, or whether the deuterolysis is concerted. However, in our case it is believed that the transfer of electrons from the metal to the benzene moiety is made prior to protonation (deuteration) because the proton source is not present until after the Al-benzene complex is formed. Therefore, our results do not support the formation of a radical anion as an intermediate.

4.1.1.1.2 Addition of methyl iodide to the intermediate formed in the reaction of Al atoms with benzene:

It was anticipated that the Al-benzene intermediate, formed in the reaction between Al atoms and benzene, would undergo reductive alkylation. This was based on the fact that the Al-benzene intermediate could be reduced to 1,4-cyclohexadiene in the presence of a proton donor. Therefore Al atoms were reacted with benzene, as described in section 4.1.1.1.1, with the exception that methyl iodide was added to the reaction mixture instead of deuterium oxide. Al wire (42 mg) was heated while benzene (vapour pressure of 1 Torr) was being condensed onto the liquid nitrogen filled rotating drum of the cryostat. After approximately 10 minutes, metal atom and benzene deposition were stopped and methyl iodide (vapour pressure of 1 Torr) was deposited onto the reaction mixture for 4 minutes. After repeating this procedure twice, the reaction mixture was collected and slowly warmed up to room temperature with the aid of a number of cold temperature baths. The experiment was carried out twice.

The total ion current (TIC) chromatograms of the alkylation products resulting from the two experiments are presented in Figures 4.6a and 4.6b. There are four compounds common to both reaction mixtures. The compounds with retention times of 4:18 (peak labelled 2) and 5:24 (peak labelled 3) were also detected in the GC-MS spectrum of a standard solution of the methyl iodide. Therefore it was concluded that these compounds are impurities and are not formed in the alkylation reaction of the Al-benzene intermediate. The peaks labelled * in Figures 4.6a and 4.6b were also found when 1 μL of the CH_2Cl_2 was analyzed under the same experimental conditions as that for the reaction mixture, therefore it was concluded that these compounds are not formed in the reaction between Al atoms, benzene and methyl iodide. The mass spectral data corresponding to the peaks labelled 1 and 4 are presented in Table 4.2. Peaks 1 and 4 have been assigned to benzene and toluene, respectively. Confirmation of this assignment was obtained by comparison of the retention times and mass spectral data with those for authentic samples of benzene and toluene. The mass fragmentation pattern of toluene proposed by Beynon et al.[76] is shown in scheme 4.4. The molecular ion of toluene $C_7H_8^+$ loses one H or two H to form $C_7H_7^+$ (m/e=91) and $C_7H_6^+$ (m/e=90), respectively. The $C_7H_7^+$ ion loses two H or C_2H_2 to form $C_7H_5^+$ (m/e=89) and $C_5H_5^+$ (m/e=65), respectively. The $C_7H_5^+$ ion loses one H or two C to form $C_7H_4^+$ (m/e=88) and $C_5H_2^+$ (m/e=62), respectively. The molecular ion can also lose the CH_3 group to form $C_6H_5^+$ (m/e=77) which in turn loses one C to form $C_5H_5^+$ (m/e=65). The $C_5H_5^+$ ion loses C_2H_2 to form the $C_3H_3^+$ ion (m/e=39).[74]

Figure 4.6a. Total ion current chromatogram of the products resulting from hydrolysis of the organometallic compounds formed in the reaction of Al atoms, benzene and methyl iodide, first run. (The compounds labelled * are due to contamination, see text).

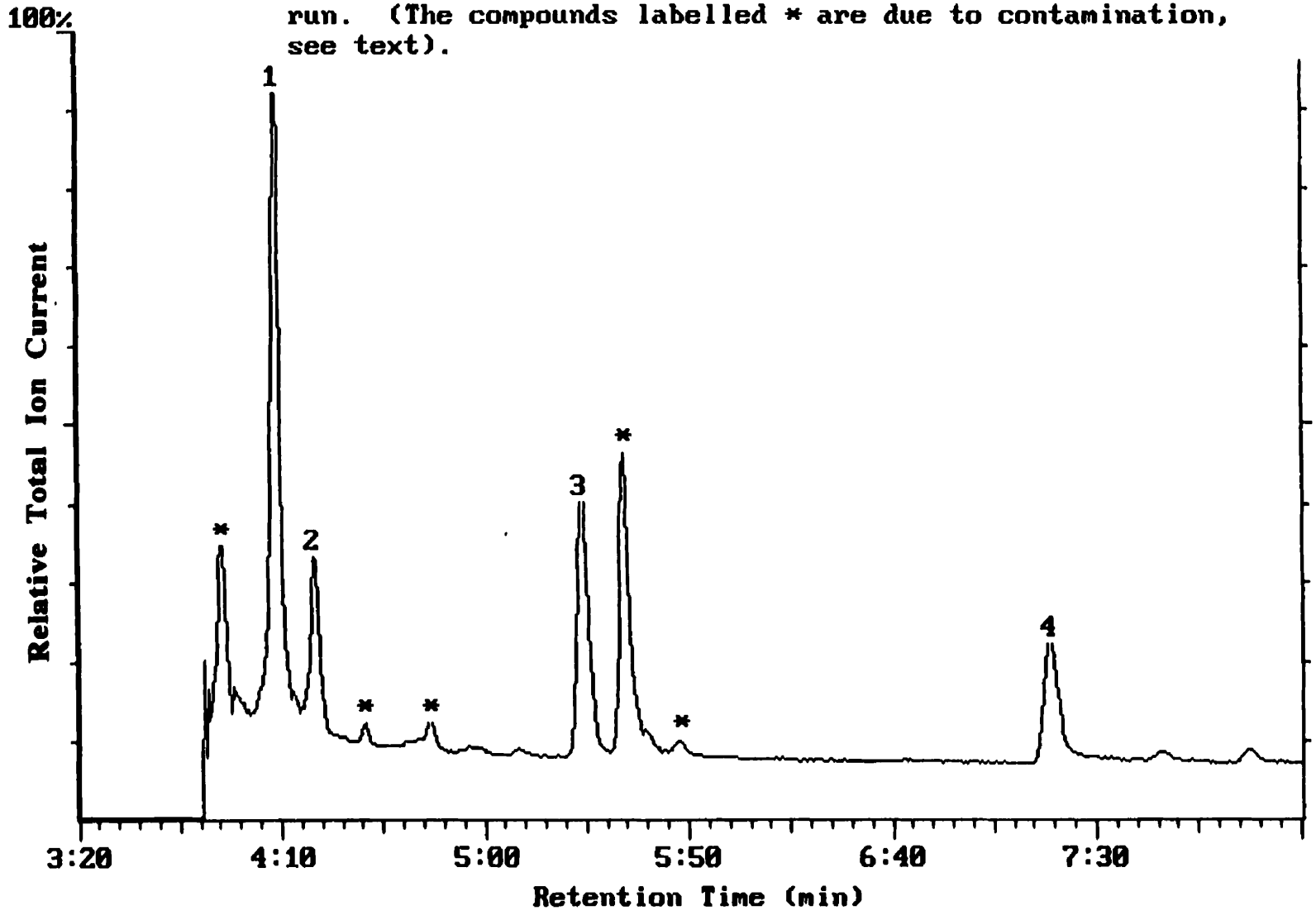

Figure 4.6b. Total ion current chromatogram of the products resulting from hydrolysis of the organometallic compounds formed in the reaction of Al atoms, benzene and methyl iodide, second run. (The compounds labelled * are due to contamination, see text).

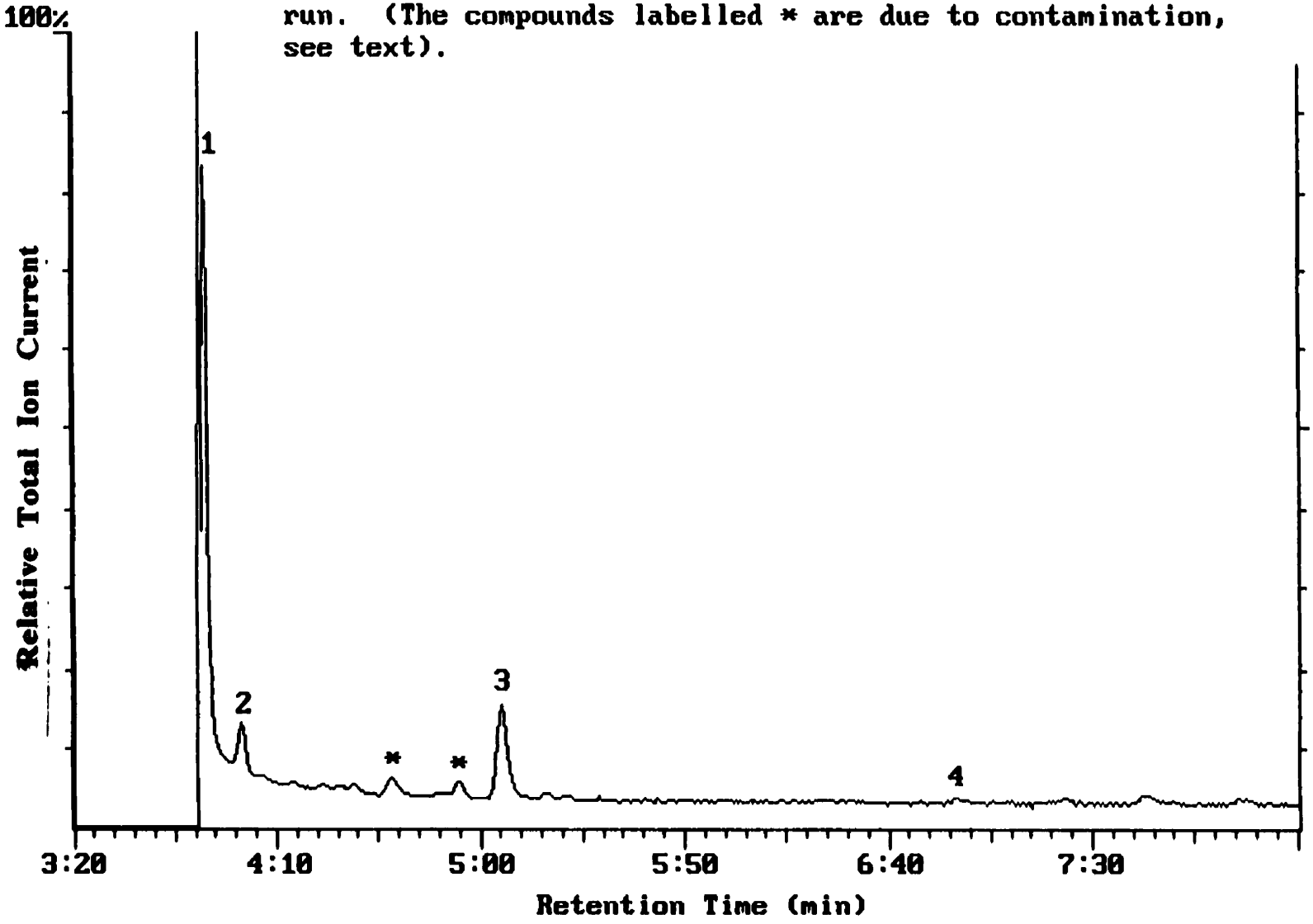

Table 4.2. **Retention times and mass spectral data for products resulting from the addition of methyl iodide to the Al-benzene reaction mixture.**

Peak No.	Retention Time (min)	m/e for main fragments*
1	4:09	39(11.8) 51(8.8) 52(10.7) 76(3.6) 77(16.3) 78(100) 79(9.8)
4	7:19	39(18.9) 62(4.5) 65(12.1) 77(1.1) 85(0.4) 86(0.7) 90(1.9) 91(100) 92(49.4)
Benzene	4:10	39(27) 51(44.7) 52(24.9) 76(5.6) 77(27.5) 78(100) 79(8.2)
Toluene	7:26	39(15.4) 62(1.4) 65(11.4) 77(1.4) 85(0.2) 86(0.2) 90(2.1) 91(100) 92(54.8)

* The number in brackets represents the relative abundance of the fragment.

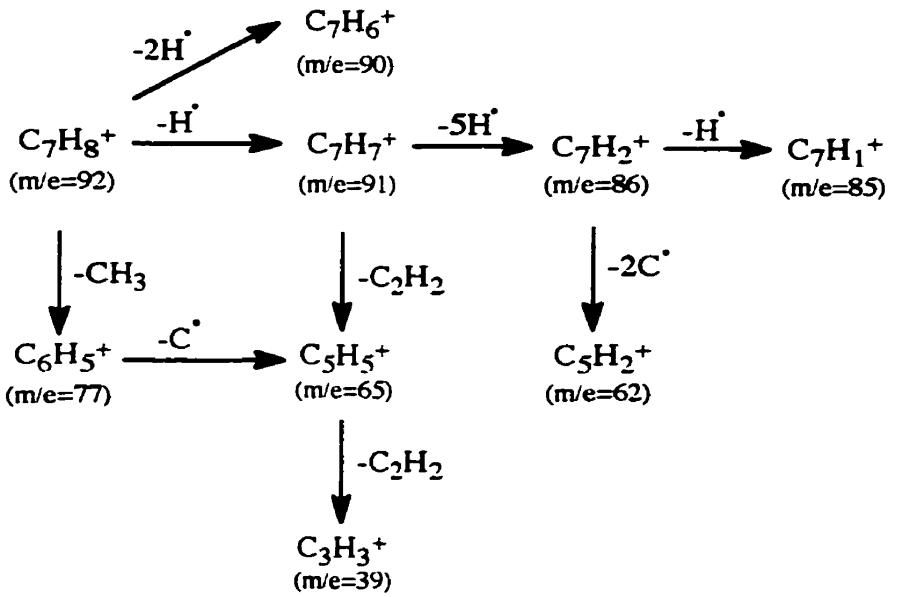

Scheme 4.4. The fragmentation scheme of toluene.[74]

The experiment was repeated with a modification in the deposition procedure. The Al metal vapour was condensed on the surface of the drum along with benzene (0.1 Torr) and adamantane (1.0 Torr). The methyl iodide (5 mL) was added directly to the sample collecting tube prior to the start of the run. Reaction of the methyl iodide with the Al-benzene intermediate occurred when the deposit was scraped off the drum into the sample collecting tube. The procedure was modified to rule out the possibility that the Al atoms react with the methyl iodide to form a reactive intermediate which subsequently attacks benzene. In the modified procedure we should in fact observe the reaction between methyl iodide and the Al-benzene intermediate.

The total ion current (TIC) chromatogram of the reaction mixture resulting from the addition of methyl iodide to the Al atom-benzene-adamantane deposit is presented in Figure 4.7. The peaks labelled * in Figure 4.7 were also found when 1 μL of the CH_2Cl_2 was analyzed under the same experimental conditions as that for the reaction mixture, therefore it was concluded that these compounds are not formed in the reaction between Al atoms, benzene, adamantane and methyl iodide. The compounds of interest were labelled 1 (retention time = 4:39) and 2 (retention time = 5:05), respectively. These compounds were found to be methylcyclohexane and toluene, respectively, based on a comparison of the mass spectral data to those for authentic samples, Table 4.3.

The mass fragmentation pattern of toluene[74] is shown in scheme 4.4 and has been explained in detail above. The mass fragmentation of methylcyclohexane is shown in scheme 4.5. The molecular ion of methylcyclohexane, $C_7H_{14}^+$, loses CH_3 to form the cyclohexane ion $C_6H_{11}^+$ (m/e=83). Fragmentation of the cyclohexane ion was proposed by Abramson and Futrell.[81] The cyclohexane ion, $C_6H_{11}^+$, loses one H, CH_2, C_2H_3 or C_2H_4 to form the ions $C_6H_{10}^+$ (m/e=82), $C_5H_9^+$ (m/e=69), $C_4H_8^+$ (m/e=56) and $C_4H_7^+$

(m/e=55), respectively . The $C_4H_7^+$ ion loses CH or CH_2 yielding $C_3H_6^+$ (m/e=42) and $C_3H_5^+$ (m/e=41), respectively. The $C_3H_3^+$ (m/e=39) ion is produced by the loss of two H• from the $C_3H_5^+$ ion.[81] The mass spectrum of the cyclohexane part of the compound labelled 1 in Figure 4.7, is consistent with the one reported by Abramson and Futrell.[81]

Table 4.3. Retention times and mass spectral data of products formed by adding methyl iodide to the Al-benzene-adamantane reaction mixture.

Peak No.	Retention Time (min)	m/e for main fragments*
1	4:39	39(77.6) 41(84.6) 42(29.0) 55(89.1) 56(32.1) 69(24.1) 82(28.0) 83(100) 98(19.6)
2	5:05	39(12.7) 62(1.3) 65(11.5) 77(1.6) 85(0.2) 86(0.2) 90(1.2) 91(100) 92(66.3)
Methylcyclohexane	3:55	39(56.1) 41(65.1) 42(19.9) 55(82.2) 56(22.4) 69(19.5) 82(25.7) 83(100) 98(17.8)
Toluene	4:23	39(14.3) 62(1.4) 65(8.4) 77(0.68) 85(0.2) 86(0.2) 90(2.4) 91(100) 92(54.7)

* The number in brackets represents the relative abundance of the fragment.

The retention times of the authentic samples are slightly different than those of the reaction mixture because the authentic samples were run at a much later date. With repeated usage and routine maintenance of the GC column, the material and length of the column change causing small deviations in the retention time. The difference in the retention times of compounds 1 and 2, i.e., 5:05-4:39 or 26 sec. and the difference in the retention times of methylcyclohexane and toluene (4:23-3:55 or 28 sec.) are identical within experimental error.

Figure 4.7. Total ion current chromatogram of the products resulting from hydrolysis of the organometallic compounds formed in the reaction of Al atoms, benzene, adamantane and methyl iodide. (The compounds labelled * are due to contamination, see text).

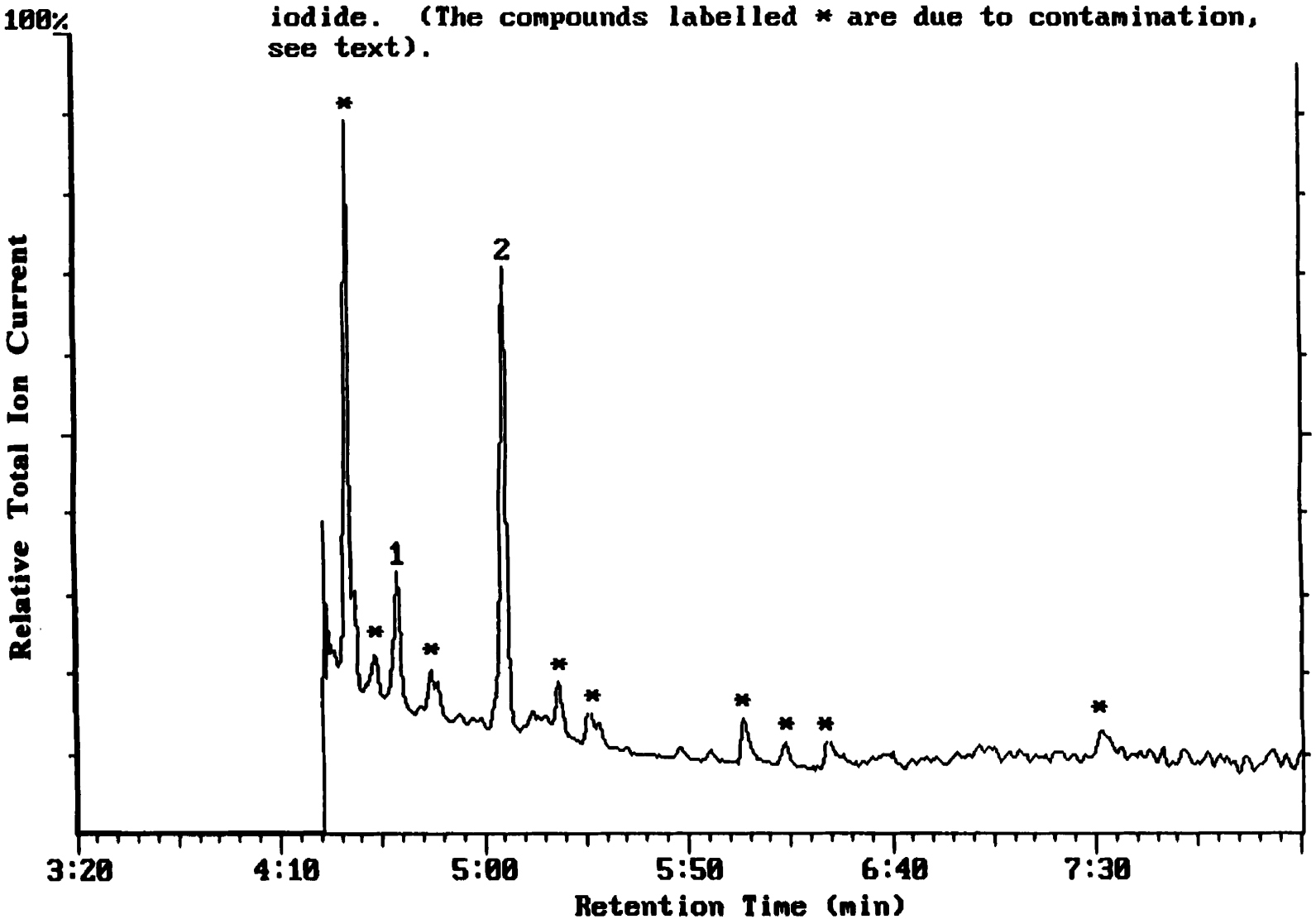

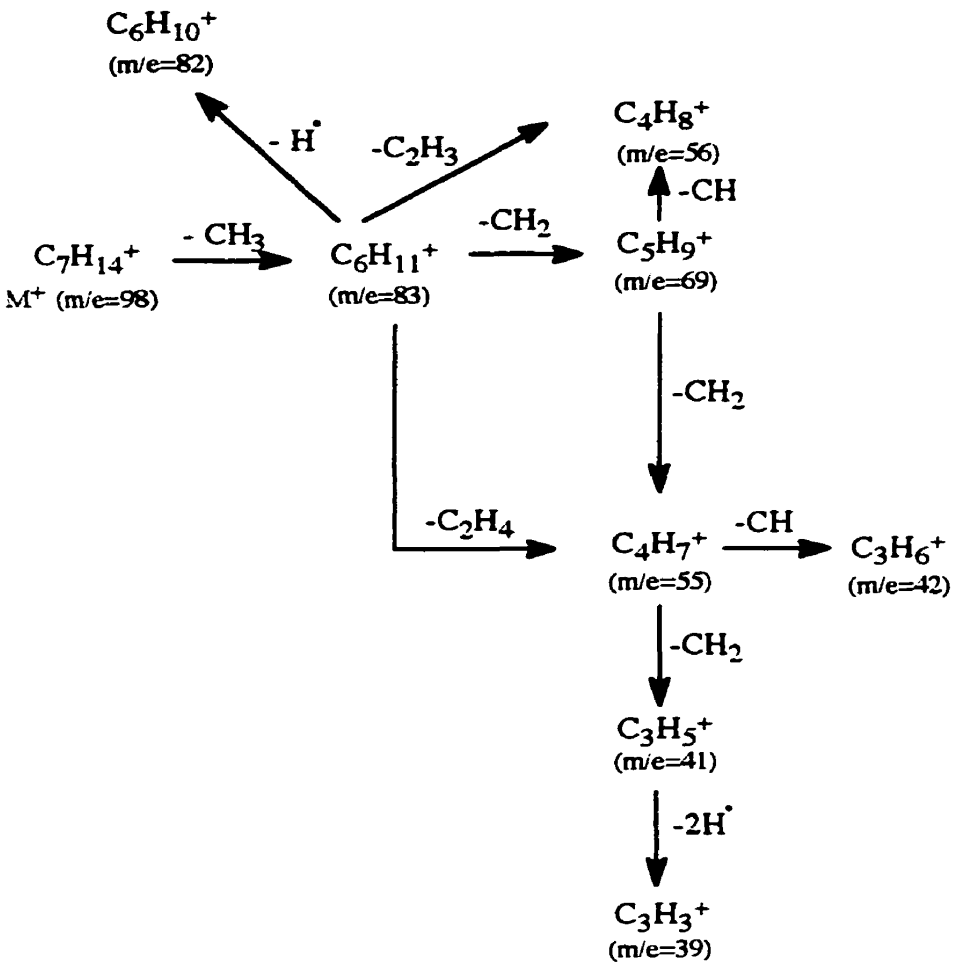

Scheme 4.5. Proposed fragmentation of methylcyclohexane.

The amount of toluene in the reaction mixture of the trials 1, 2 and 3 varied from 18.5% to 3.5% to 35.0%. It is not surprising that the greatest amount of toluene was formed in trial 3 as the ratio of [benzene] : [Al] is smaller when adamantane is used as an inert matrix. Methylcyclohexane was only observed in trial 3 (16.0%).

As indicated previously methyl iodide was added to the Al-benzene reaction to see if the Al-benzene intermediate would undergo methylation. We expected, based on the

protonation reaction of the Al-benzene intermediate, that dimethylcyclohexadiene and or methylcyclohexadiene would form if the methylation reaction was successful. We used the boiling points of 1,4-dimethyl-1,3-cyclohexadiene (135-8°C)[82] and the several methylcyclohexadienes (102-115°C)[82] to help predict the retention times of the expected products relative to toluene. In addition we searched the mass spectral data for compounds with fragments with an m/e ratios of 108 and 94 i.e., the m/e ratios expected for dimethylcyclohexadiene and methylcyclohexadiene respectively. We were unable to find any evidence for the reductive alkylation of the Al-benzene intermediate.

Instead, the methyl iodide interacts with Al atoms and benzene to form toluene or methylcyclohexane. A study carried out by Klabunde and coworkers[52] showed that Al atoms insert into the C-Br bond of methyl bromide to form CH_3AlBr when Al atoms are reacted with methyl bromide in an argon matrice at 12 K. It is possible that in our case Al metal activated the methyl iodide to give CH_3AlI which upon dissociation gives methyl radicals.[77] These methyl radicals could subsequently react with benzene to form toluene. The formation of toluene in the experiment where the Al-benzene reaction mixture is scraped into a sample collecting tube containing methyl iodide indicates that the methyl iodide reaction with Al is faster than the reaction with the Al-benzene intermediate.

The presence of methylcyclohexane is more difficult to explain because somehow both alkylation and complete reduction of the benzene ring occur. There are at least two possible explanations. Firstly toluene, formed by reaction of methyl radicals with benzene, could be reduced by Al metal present in the reaction mixture. Such a process is not unprecedented as the Birch reduction of toluene[80] (Li in liquid ammonia), scheme 4.6, yields methylcyclohexane. Alternatively, the reduction of methylcyclohexadiene, formed by the addition of methyl iodide to the Al-benzene intermediate would also yield methylcyclohexane.

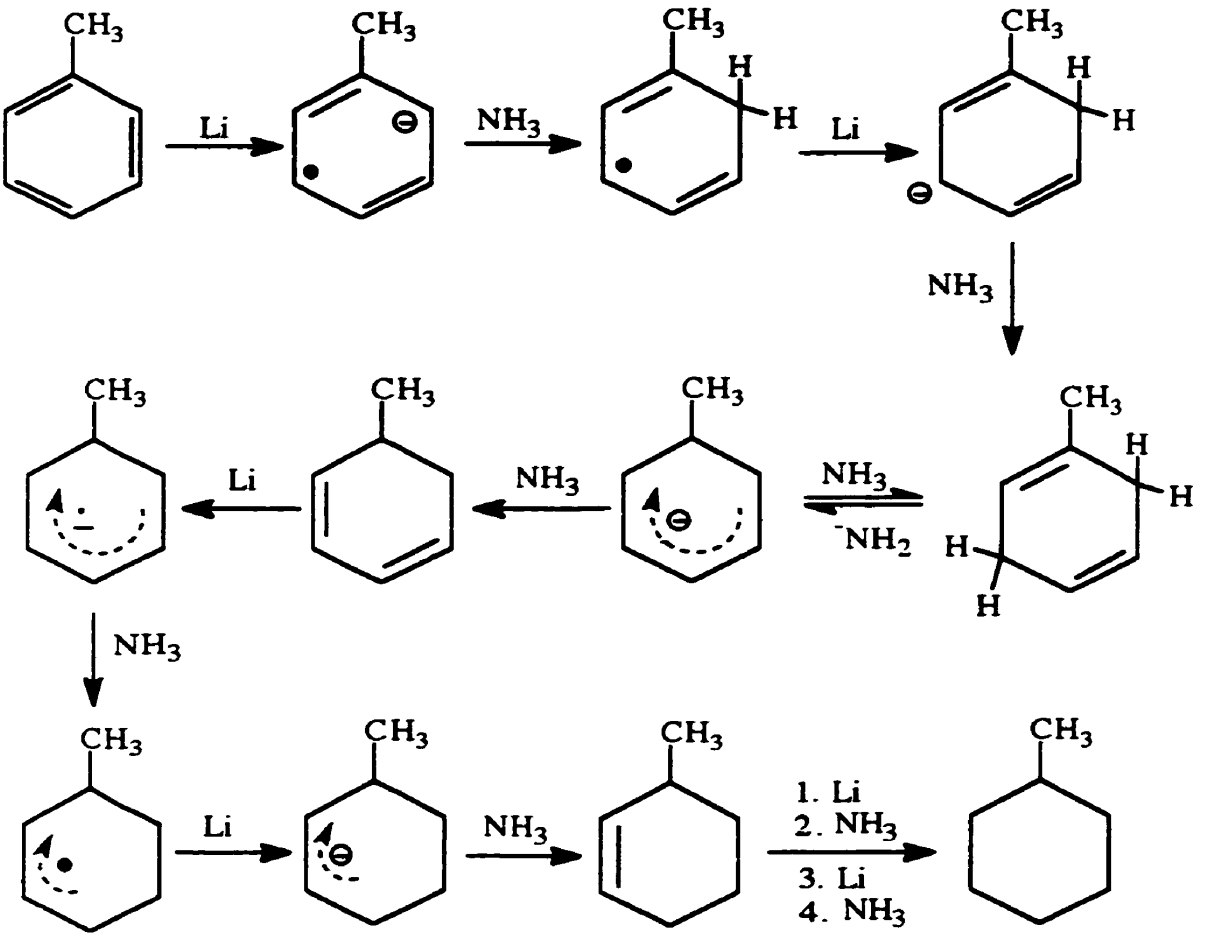

Scheme 4.6. Mechanism for Birch reduction of toluene.[83]

These findings motivated the study of the reaction of Al atoms with toluene which is presented in section 4.1.2.1 of the thesis.

4.1.1.2 Reaction of Ga atoms with benzene:

4.1.1.2.1 Hydrolysis of the intermediate formed in the reaction of Ga atoms and benzene:

As previously stated, the EPR study of Ga atoms and benzene indicated that a weak Ga-benzene intermediate forms. The exact nature of the intermediate could not be determined. However, analysis of the magnetic parameters suggested that the complex was very loose in comparison to that found for Al-benzene. In addition, Howard et al.[86] detected the presence of cyclohexadienyl when the sample was warmed up in the cavity of the EPR spectrometer. We therefore decided to study the hydrolysis products of the reaction mixture of Ga and benzene to see if we could shed light on the types of intermediates formed.

Gallium atoms were reacted with benzene under two different experimental conditions (the weight of the Ga pellets used to produce the gallium atoms was changed from 40 to 73 mg and the amount of benzene was kept constant at a vapour pressure of 1.0 Torr). A typical total ion current (TIC) chromatogram of the hydrolysis products is presented in Figure 4.8. The peak of interest is labelled 1 and has been assigned to 1,4-cyclohexadiene. Confirmation of this assignment was obtained by comparison of the retention times and mass spectral data, Figure 4.9, with that for an authentic sample of 1,4-cyclohexadiene. The data extracted from the chromatogram in Figure 4.8 are presented in Table 4.4.

Figure 4.8. Total ion current chromatogram of the product resulting from hydrolysis of the organometallic compound formed in the reaction of Ga atoms and benzene. (The compounds labelled * are due to contamination, see text).

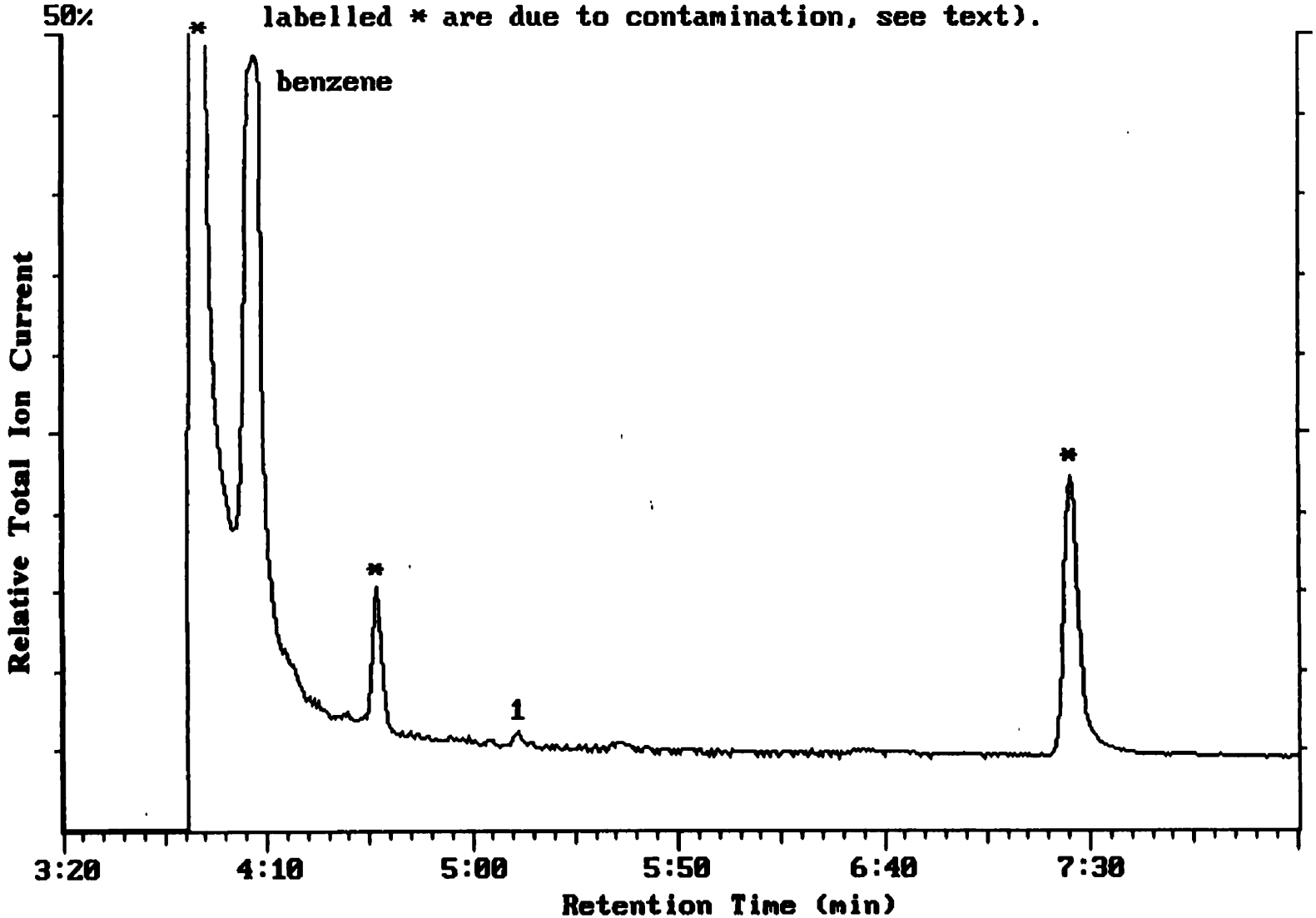

Figure 4.9. Mass spectrum of the hydrolysis product (peak 1, Figure 4.7) resulting from the hydrolysis of the Ga atom-benzene reaction mixture.

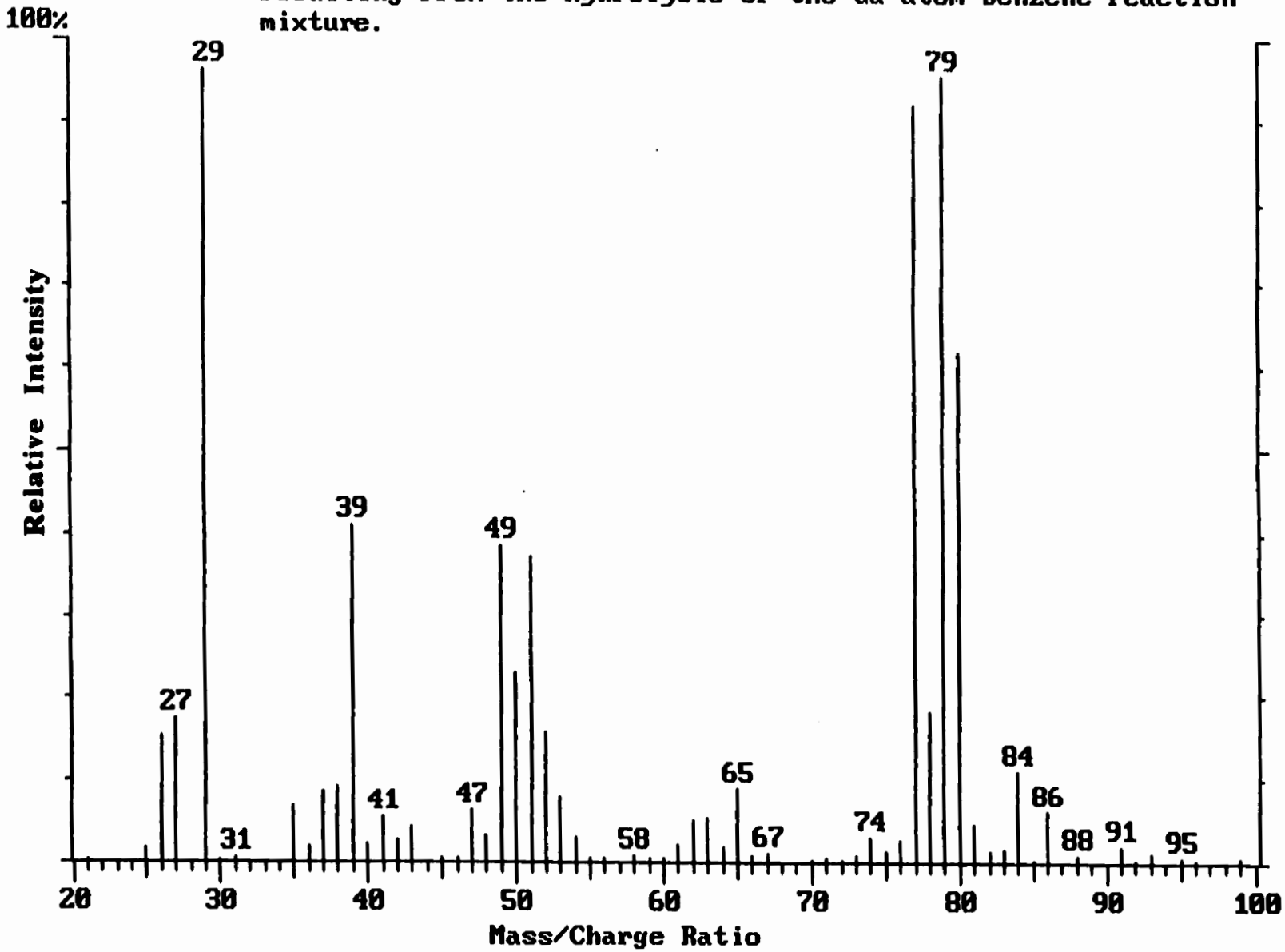

Table 4.4. Retention times and mass spectral data for hydrolysis products resulting from the reaction of Ga atoms and benzene.

Peak No.	Retention Time (min)	m/e for main fragments*
1	5:11	38(9.6) 39(42.9) 40(2.0) 50(24.0) 51(39.2) 52(16.6) 53(8.1) 54(2.8) 63(5.4) 65(9.3) 77(96.3) 78(19.1) 79 (100) 80(64.8) 81(4.5)
Benzene	4:07	28(43.3) 38(4.9) 39(14.4) 40(0.7) 50(13.4) 51(18.5) 52(16.1) 53(0.9) 63(4.7) 65(0.6) 77(22.1) 78(100) 79 (10.1)
1,3-cyclohexadiene	4:17	28(25.7) 38(5.2) 39(24.2) 40(1.9) 50(13.1) 51(15.5) 52(7.1) 53(4.4) 54(0.8) 63(3.4) 65(2.6) 77(31.6) 78(7.0) 79 (100) 80(70.7) 81(25.4)
1,4-cyclohexadiene	5:12	28(32.1) 38(6.5) 39(28.3) 40(2.4) 50(11.0) 51(15.8) 52(7.9) 53(5.3) 54(1.1) 63(3.7) 65(5.3) 77(45.7) 78(7.4) 79 (100) 80(71.7) 81(22.0)

*. The number in brackets represents the percentage of the base peak.

As in the case of the reaction of Al atoms and benzene, hydrolysis of the Ga-benzene reaction mixture resulted in the formation of 1,4-cyclohexadiene. For the Ga-benzene reaction this result is not surprising considering that cyclohexadienyl was observed in the EPR spectrum of the Ga-benzene reaction mixture.

Howard et al.[84] were puzzled by the formation of cyclohexadienyl. Addition of a hydrogen atom to benzene is necessary for the formation of cyclohexadienyl. They attempted to determine the origin of this hydrogen atom. The use of deuterated adamantane ruled out the possibility that the matrix was furnishing the hydrogen atom because no deuterium was incorporated into the cyclohexadienyl radical. This led the authors to suggest that extraneous water must provide the hydrogen atoms. The Ga atoms must react with water to give HGaOH which provides the hydrogen atom needed to react with the benzene. It is interesting that HGaOH has never been observed in adamantane by EPR spectroscopy at 77 K unlike HAlOH. This may mean that HGaOH is not as stable as HAlOH and decomposes readily. Alternatively the Ga atoms may transfer an electron to the benzene ring producing a radical anion. The radical anion can abstract a proton from the extraneous water forming cyclohexadienyl. In both cases the amount of product formed would be limited by the concentration of extraneous water present.

If the formation of cyclohexadienyl is indeed dependent on extraneous water, this may contribute to the low conversion of benzene to 1,4-cyclohexadiene observed (0.02 - 0.05 %). We can not compare the yields directly with those obtained in the Al-mediated reactions because it is not possible to precisely control the concentration of metal evaporated.

A third possible explanation for the formation of cyclohexadienyl involves a metal hydride. It is possible that gallium atoms could insert into a C-H bond of benzene to form a metal hydride and that hydrogen is transferred from the hydride to a second benzene molecule to form cyclohexadienyl. It is evident that further studies involving the reaction between Ga, benzene and deuterium oxide and Ga, benzene-d_6 and water will have to be carried out before we can start differentiating between the mechanisms proposed above.

4.1.2 Reaction of Group 13 Atoms with toluene:

4.1.2.1 Reaction of Al atoms with toluene:

Previously we showed that, Al and Ga atoms mediate the reduction of the benzene ring and upon hydrolysis, 1,4-cyclohexadiene is formed. Toluene was next selected to determine how substituents such as CH_3 influence the reduction of the benzene ring. In the Birch reduction, toluene is reduced by Na in the presence of C_2H_5OH to produce 1-methyl-1,4-cyclohexadiene. We were interested to see if Al atom reduction would give similar results. Secondly a study of the reduction of toluene by Al atoms could help shed light on why and how methylcyclohexane formed upon alkylation of the Al-benzene intermediate discussed in section 4.1.1.1.2.

4.1.2.1.1 Hydrolysis of the intermediate formed in the reaction of Al atoms and toluene:

Aluminum atoms were reacted with toluene under a number of experimental conditions. The weight of the Al wire used to produce the aluminum atoms was varied from 22 to 28 mg and the amount of toluene was changed by adjusting the vapour pressure of toluene to 0.5 or 1 Torr. A typical total ion current (TIC) chromatogram of the hydrolysis products is presented in Figure 4.10. The two peaks of interest are labelled 1 and 2 and have been assigned to toluene and 1-methyl-1,4-cyclohexadiene respectively. Confirmation of this assignment was obtained by comparison of the retention times and mass spectral data with those for authentic samples of toluene and 1-methyl-1,4-cyclohexadiene, Figure 4.10, 4.11 and 4.12. The data corresponding to Figure 4.10 are presented in Table 4.5.

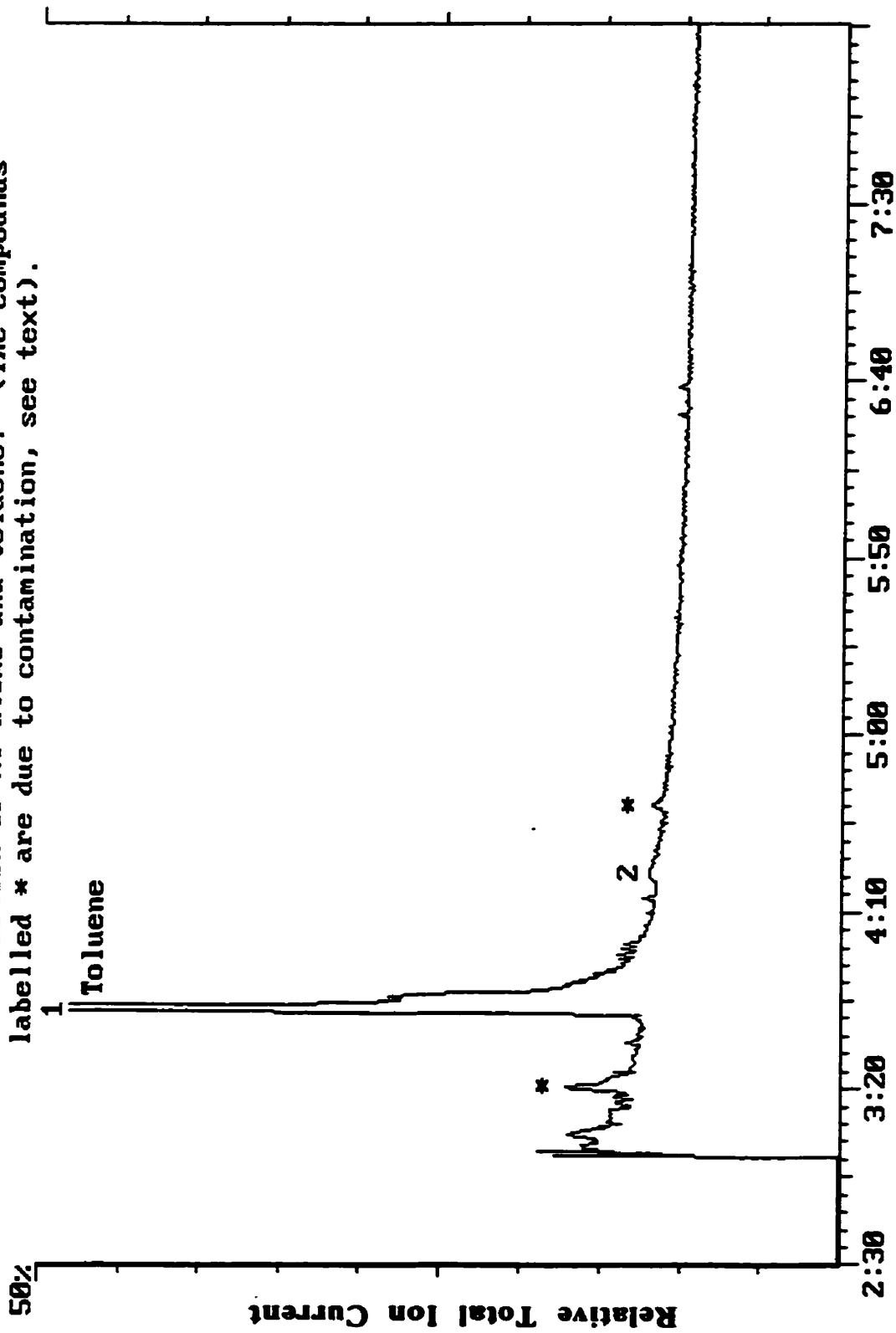

Figure 4.10. Total ion current chromatogram of the products resulting from hydrolysis of the organometallic compounds formed in the reaction of Al atoms and toluene. (The compounds labelled * are due to contamination, see text).

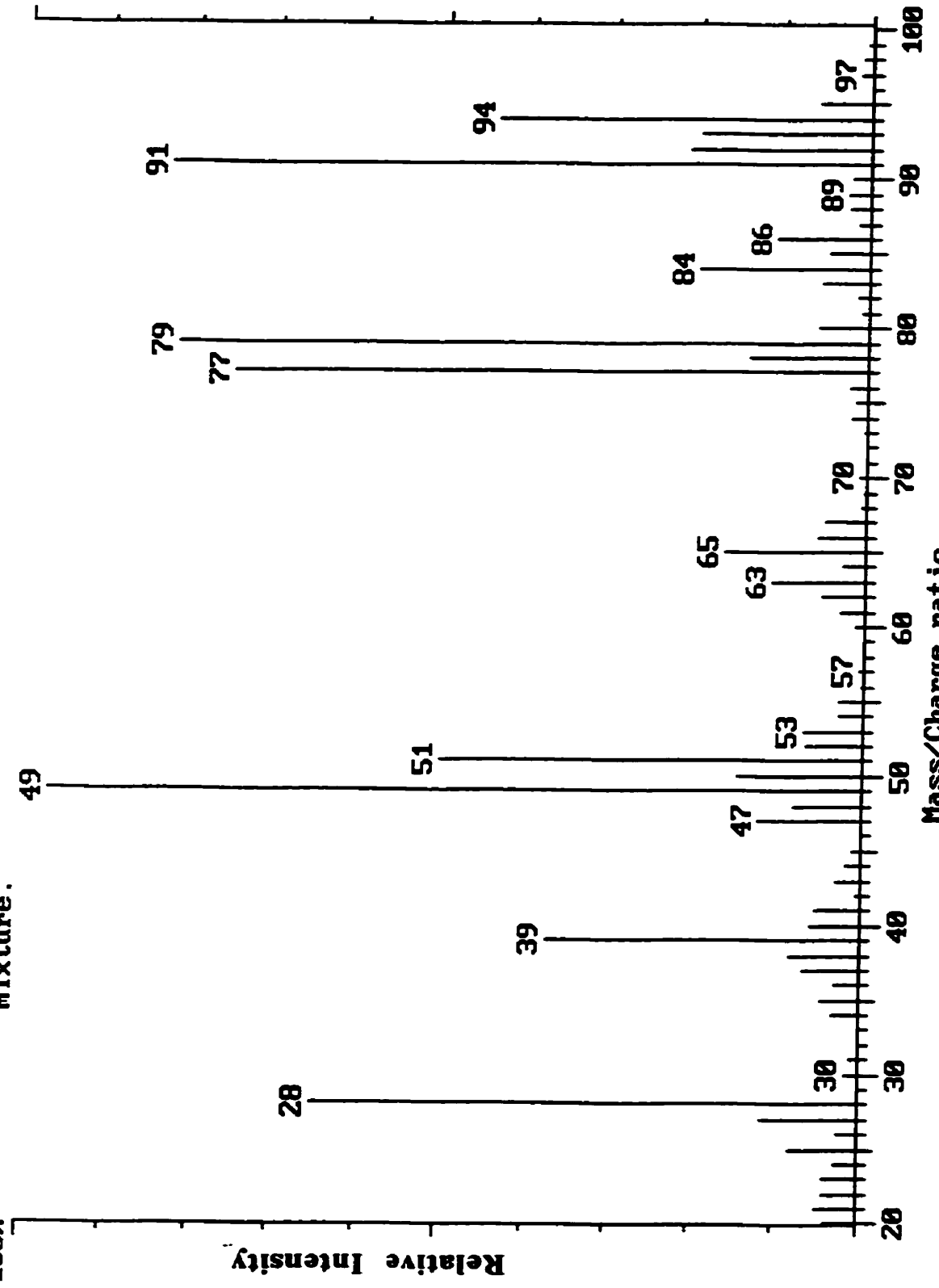

Figure 4.11. Mass spectrum of the hydrolysis product (peak 2, Figure 4.10) resulting from the hydrolysis of the Al atom–toluene reaction mixture.

Figure 4.12. Total ion current chromatogram of a mixture containing toluene and 1-methyl-1,4-cyclohexadiene. The mass spectra of the compounds have been inlaid. (The y-axis of the mass spectra represents the relative intensity of the ions).

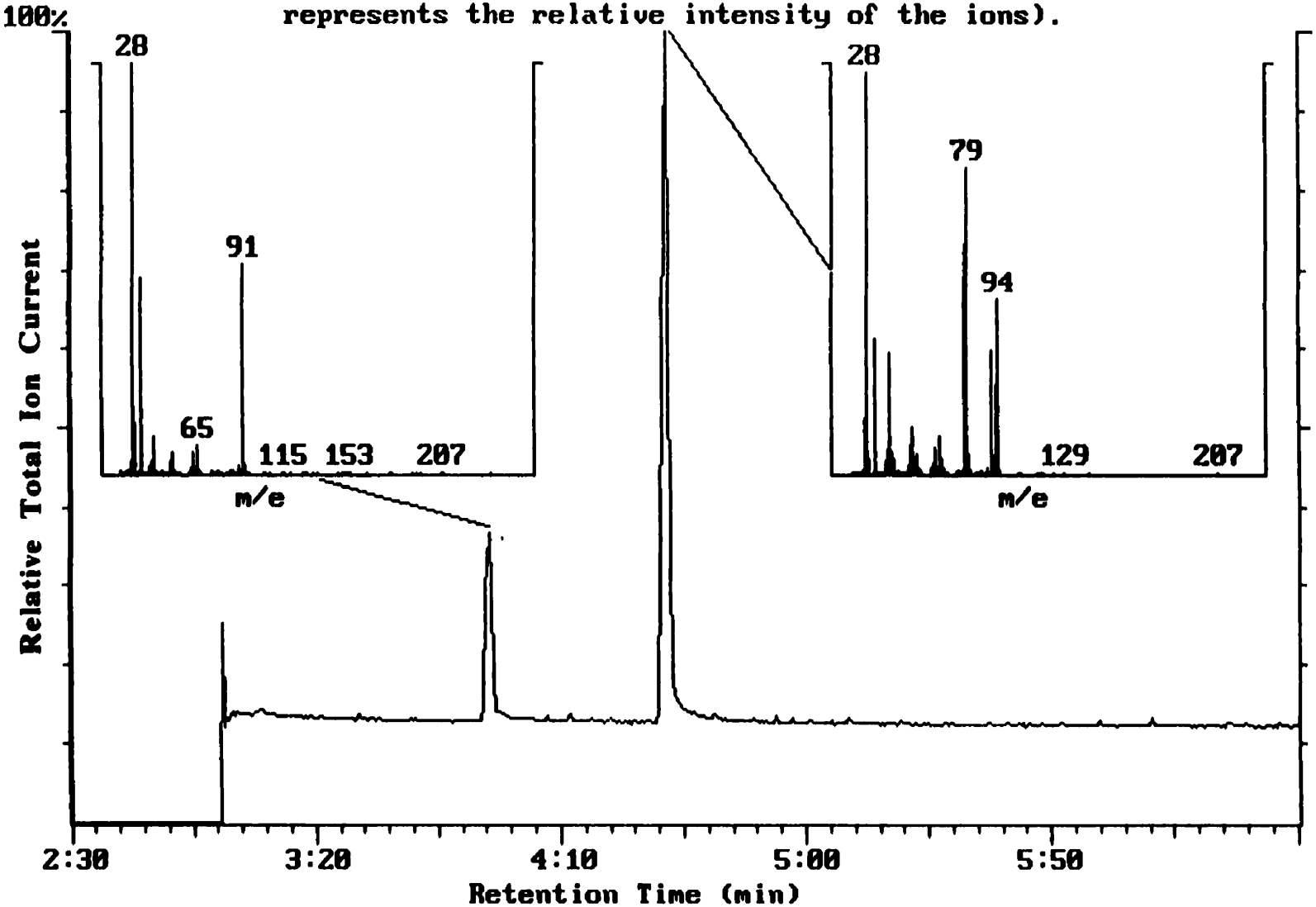

Table 4.5. Retention times and mass spectral data for hydrolysis products resulting from the reaction of Al atoms and Toluene.

Peak No.	Retention Time (min)	m/e for main fragments*
1	3:43	39(14.1) 62(2.3) 65(10.4) 77 (1.4) 85(0.5) 86(0.6) 90(1.8) 91(100) 92(52.5)
2	4:21	39(37.3) 50(14.81) 51(50.12) 52(6.42) 53(6.7) 63(10.9) 65(16.5) 77(75.3) 78(13.8) 79(82.0) 91(83.2) 92(21.2) 93(20.0) 94(44.2)
Toluene	3:56	39(22.2) 62(1.4) 65(15.3) 77 (1.9) 85(0.2) 86(0.2) 90(0.9) 91(100) 92(28.7)
1-Methyl-1,4-cyclohexadiene	4:31	39(39.5) 50(9.3) 51(15.1) 52(4.8) 53(6.1) 63(8.5) 65(11.9) 77(75.9) 78(12.8) 79(100) 91(40.7) 92(5.6) 93(29.1) 94(57.5)

* The number in brackets represents the percentage of the base peak.

A proposed fragmentation pattern of 1-methyl-1,4-cyclohexadiene is presented in scheme 4.8. The molecular ion, $C_7H_{10}^+$ loses H, 2H or 3H, to form $C_7H_9^+$ (m/e=93), $C_7H_8^+$ (m/e=92) and $C_7H_7^+$ (m/e=91) respectively. The molecular ion, $C_7H_{10}^+$ loses CH_3, to form the benzenium ion $C_6H_7^+$ (m/e=79) which in turn loses either C_2H_2 or two H yielding $C_4H_5^+$ (m/e=53) and $C_6H_5^+$ (m/e=77) respectively. The formation of the remaining fragments can be rationalized using the 1,4-cyclohexadiene fragmentation scheme, scheme 4.1, section 4.1.1.1.1. Loss of C_2H_2 from $C_6H_5^+$ results in the formation of $C_4H_3^+$ (m/e=51). Alternatively, the benzenium ion $C_6H_7^+$ can lose a H to form $C_6H_6^+$ (m/e=78). Fragmentation of $C_6H_6^+$ gives $C_4H_3^+$ (m/e=51), $C_4H_4^+$ (m/e=52)

and $C_3H_3^+$ (m/e=39), respectively. The $C_4H_2^+$ ion (m/e=50) forms when $C_4H_4^+$ loses two H. The $C_5H_5^+$ ion (m/e=65) results from the loss of CH_2 from the benzenium ion $C_6H_7^+$. Finally, $C_5H_5^+$ fragments to give $C_3H_3^+$ (m/e=39) and $C_5H_3^+$ (m/e=63), respectively.

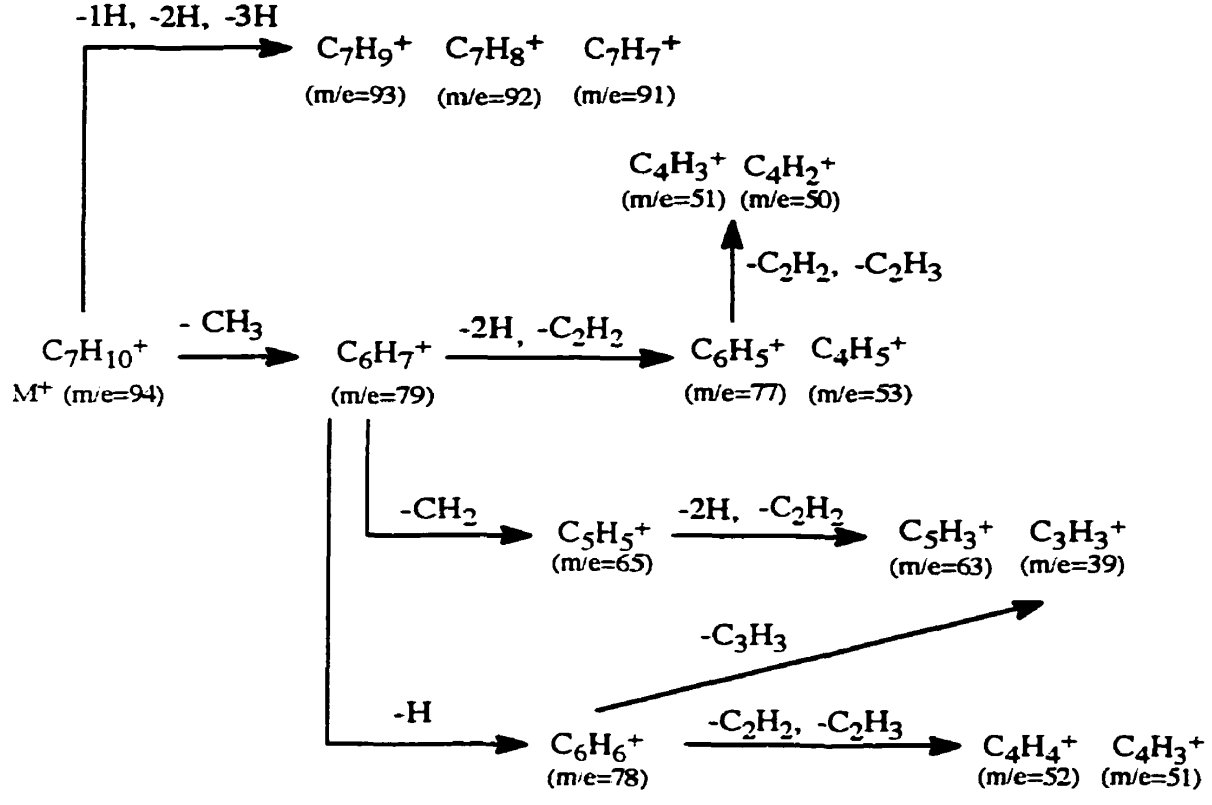

Scheme 4.7. Fragmentation scheme for 1-methyl-1,4-cyclohexadiene.

The reactions were repeated three times. The amount of 1-methyl-1,4-cyclohexadiene in the mixture ranges from 1.8% to 10.7 %. The small conversion is due to the high concentration of substrate (0.5-1.0 Torr) compared to the small amount of metal vaporized (ca. 6 mg).

As stated earlier one of the reasons for using toluene was to study the effect of an electron-donating group, such as the methyl group, on the Al-atom-mediated reduction of the benzene ring, i.e. to find out where the Al atom attacks the toluene ring. It is known that Al interacts with benzene at the 1,4 position. Hydrolysis of the Al-benzene intermediate results in the formation of 1,4-cyclohexadiene. Considering that 1-methyl-1,4-cyclohexadiene is formed when the Al atom-toluene reaction mixture is hydrolyzed suggests that the Al atom cheleotropically adds to position 2 (6) and 5 (3) of the toluene ring.

It is interesting to note that the Birch reduction of toluene also results in the formation of 1-methyl-1,4-cyclohexadiene. As outlined in scheme 4.8, the Birch reduction requires the transfer of an electron from sodium to the toluene ring to form the radical anion. The radical anion is protonated by the solvent to give a radical which is in turn reduced by another sodium atom to give a carbanion. The carbanion accepts a proton from the solvent and 1-methyl-1,4-cyclohexadiene results. Electron-donating groups such as methyl decrease the rate of reaction.

In our case the proton donor (water) is not easily accessible. The reaction mixture and the water are separated by a frozen layer of toluene. It is difficult to imagine that the water could diffuse through the toluene layer at 77 K to protonate the toluene radical anion. In an unpublished EPR study[85] no evidence was found for the formation of methylcyclohexadienyl. Instead a strong broad unresolved central feature was observed when Al atoms were reacted with toluene in adamantane. The lack of Al hyperfine

interaction rendered identification of the species impossible. In addition, carbanion formation should result in highly coloured reaction mixtures which was not the case. This information is consistent with reaction of the Al atoms with the toluene rather than transfer of electrons to form radical anions and carbanions as is the case in the Birch reduction.

It is interesting to note that toluene is reduced to give 1-methyl-1,4-cyclohexadiene and that no other products such as methylcyclohexene or methylcyclohexane were detected. The amount of 1-methyl-1,4-cyclohexadiene formed in the reaction is relatively small. From these results it is highly unlikely that methylcyclohexane formed in the reaction between Al, benzene and methyl iodide in the presence of adamantane originates from the reduction of toluene which is also present in the reaction mixture (see section 4.1.1.1.2).

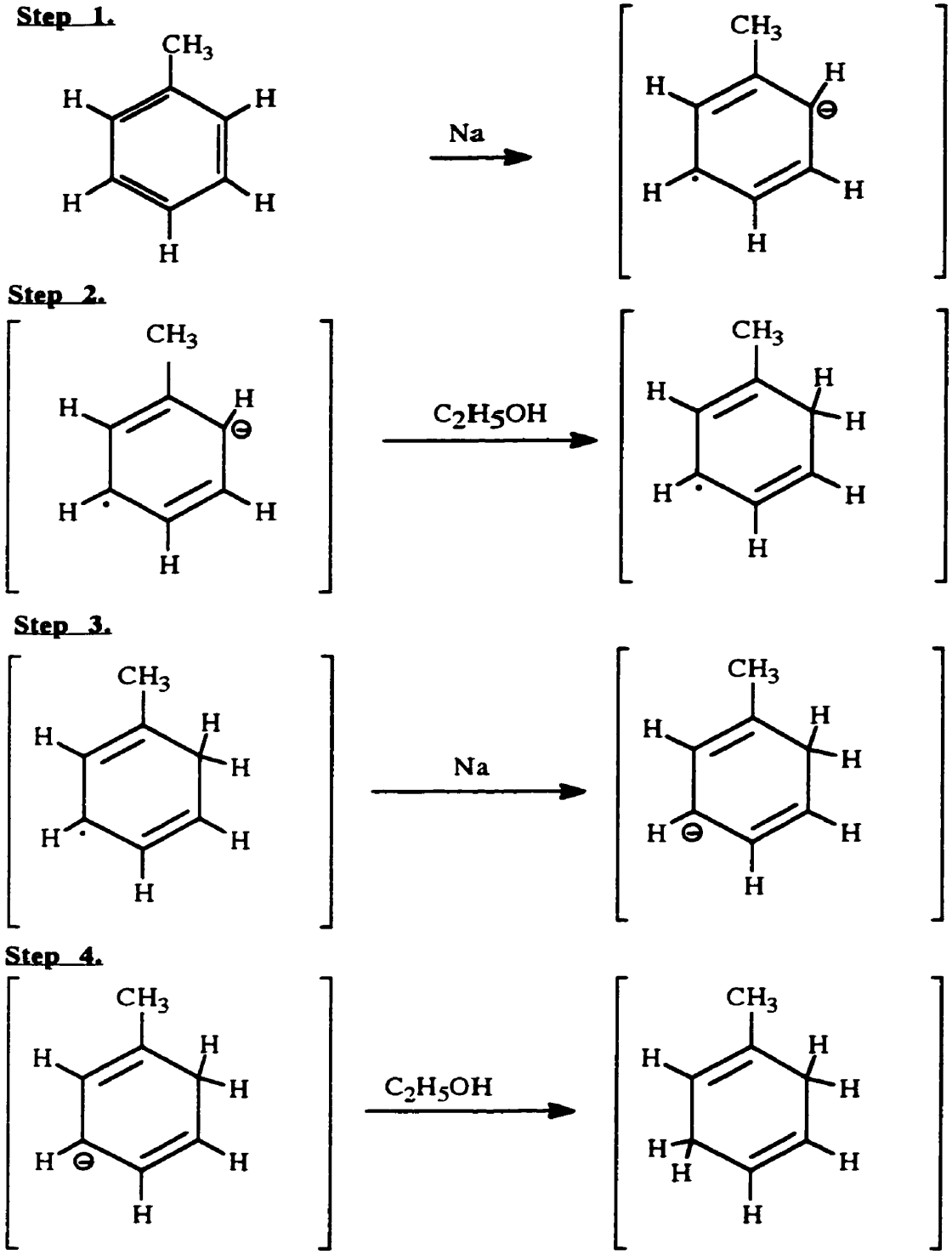

Scheme 4.8. Mechanism for the formation of 1-methyl-1,4-cyclohexadiene by the Birch reduction.

4.1.2.2 Reaction of Ga Atoms with Toluene:

4.1.2.2.1 Hydrolysis of the intermediate formed in the reaction of Ga atoms and toluene:

Gallium atoms were reacted with toluene under the same experimental conditions as those used for the reaction of Ga atoms with benzene, section 4.1.1.2. A typical total ion current (TIC) chromatogram of the hydrolysis products is presented in Figure 4.13. The peaks labelled * in Figure 4.13 were also found when 1 μL of the CH_2Cl_2 was analyzed under the same experimental conditions as that for the reaction mixture, therefore it was concluded that these compounds are not formed in the reaction between Ga atoms, toluene and water. The peaks of interest are labelled 1 and 2 and have been assigned to toluene and 1-methyl-1,4-cyclohexadiene, respectively. Confirmation of this assignment was obtained by comparison of the retention times and mass spectral data with those for authentic sample of toluene and 1-methyl-1,4-cyclohexadiene. The data for the example corresponding to Figure 4.13 are presented in Table 4.6. The mass spectrum of the product formed is shown in Figure 4.14. The fragmentation of 1-methyl-1,4-cyclohexadiene has been previously described in section 4.1.2.1.1.

Figure 4.13. Total ion current chromatogram of the products resulting from hydrolysis of the organometallic compounds formed in the reaction of Ga atoms and toluene. (The compounds labelled * are due to contamination, see text).

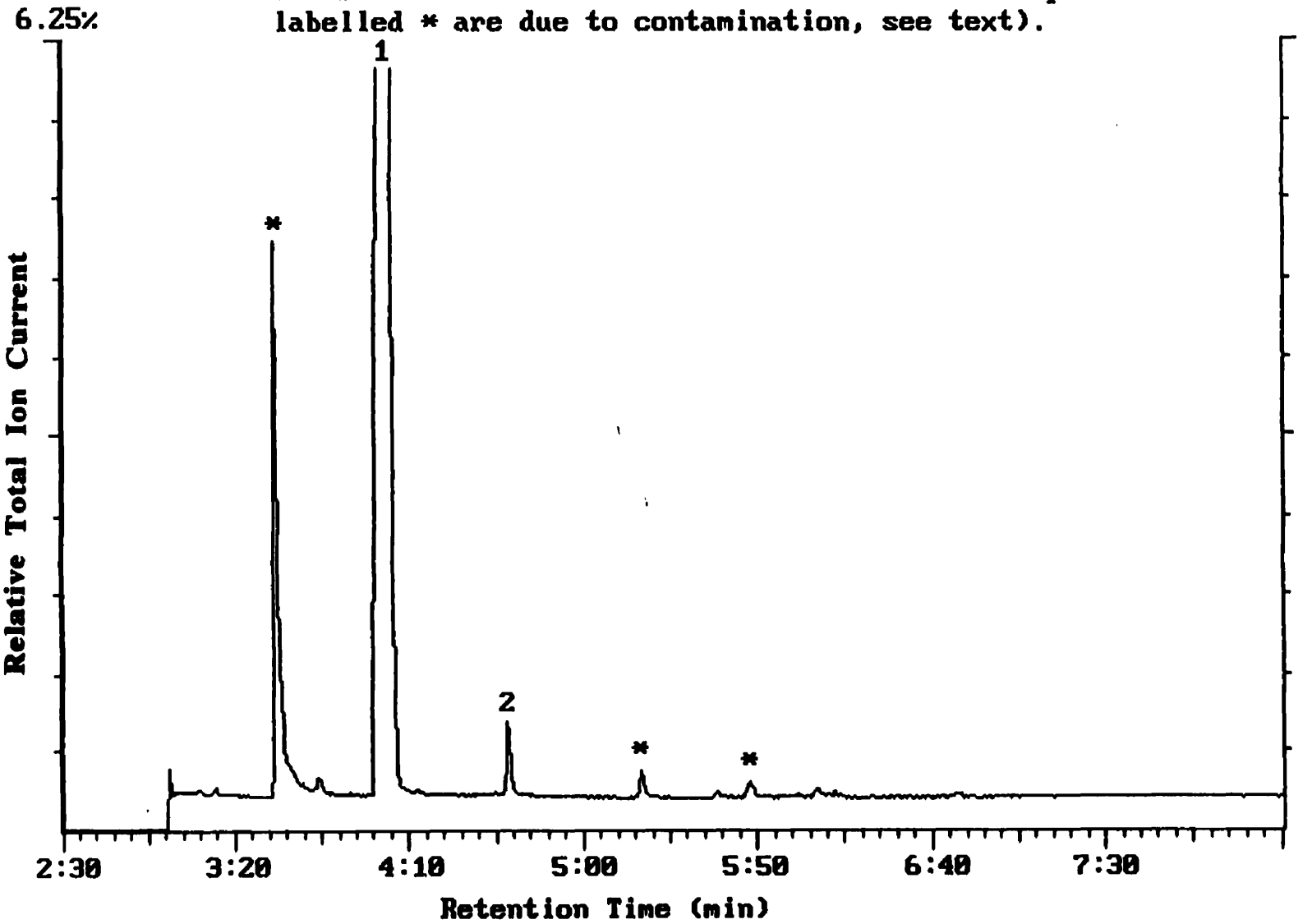

Figure 4.14. Mass spectrum of the hydrolysis product (peak 2, Figure 4.13) resulting from the hydrolysis of the Ga atom-toluene reaction mixture.

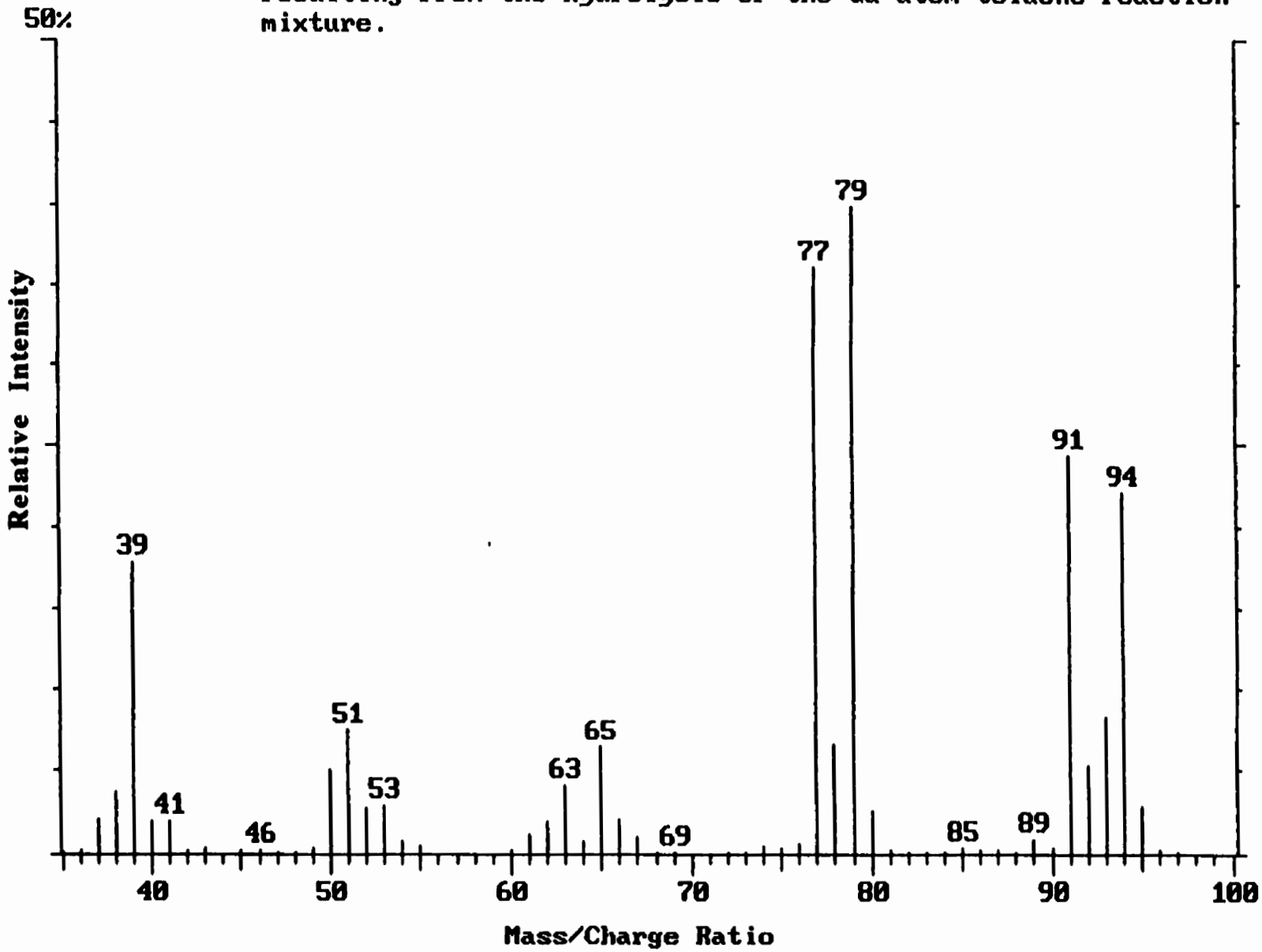

Table 4.6. Retention times and mass spectral data for hydrolysis products resulting from the reaction of Ga atoms and Toluene.

Peak No.	Retention Time (min)	m/e for main fragments*
1	4:05	39(11.83) 62(1.1) 65(3.29) 77 (0.22) 85(0.8) 86(1.3) 90(11.6) 91(100) 92(47.5)
2	4:38	39(45.0) 50(12.4) 51(20.4) 52(7.6) 53(7.2) 63(9.8) 65(15.4) 77(89.9) 78(18.1) 79(100) 91(53.8) 92(10.3) 93(21.5) 94(55.4)
Toluene	3:56	39(22.2) 62(1.4) 65(15.3) 77 (1.9) 85(0.2) 86(0.2) 90(0.9) 91(100) 92(28.7)
1-Methyl-1,4-cyclohexadiene	4:31	39(39.5) 50(9.3) 51(15.1) 52(4.8) 53(6.1) 63(8.5) 65(11.9) 77(75.9) 78(12.8) 79(100) 91(40.7) 92(5.6) 93(29.1) 94(57.5)

* The number in brackets represents the percentage of the base peak.

The reactions were repeated three times. The amount of 1-methyl-1,4-cyclohexadiene in the reaction mixtures ranged from 0.05% to 1.0%. The small conversion is due to the small amount of Ga atoms vaporized (Ga metal < 5 mg) compared to the high concentration of substrate (1000 times greater than that of the metal).

The reactions of Ga atoms with toluene have produced the same product (1-methyl-1,4-cyclohexadiene) as that of Al atoms with toluene. The percentage yield of the product was found to be smaller for Ga-toluene reactions than Al-toluene reactions. This difference could be due to the small amount of Ga (< 5 mg) vaporized during the reaction compared to that of Al (6 mg or more). From the hydrolysis study we can conclude that gallium and aluminum react with toluene in a similar fashion. We would like

to point out that caution must be exercised in drawing conclusions based on product studies as there can be more than one reaction pathway which can lead to any given compound.

4.1.3 Reaction of Group 13 Atoms with Trifluorotoluene:

4.1.3.1 Reaction of Al atoms with trifluorotoluene:

We next reacted Al atoms with trifluorotoluene. The objective was to determine the reactivity of Al atoms towards different competitive sites in one compound. From the study on benzene we determined that Al atoms reduce the aromatic ring to give 1,4-cyclohexadiene. When toluene was reacted with Al atoms, reduction of the aromatic ring resulted in the formation of 1-methyl-1,4-cyclohexadiene. Trifluorotoluene offers many competitive sites for Al atoms to attack, namely the three C-F bonds and the aromatic ring. In addition, it was of some interest to study the effect of introducing an electron withdrawing group on the product formed in the Al atom reaction.

4.1.3.1.1 Hydrolysis of the intermediate formed in the reaction of Al atoms and trifluorotoluene:

Aluminum atoms were reacted with trifluorotoluene under a number of experimental conditions. More specifically, the weight of the Al wire used to produce the aluminum atoms was varied from 19.3 to 29.1 mg and the amount of trifluorotoluene was controlled by setting the vapour pressure of trifluorotoluene to 0.01 Torr. A typical total ion current (TIC) chromatogram of the hydrolysis products is presented in Figure 4.15. The hydrolysis mixture is fairly complex. There are at least ten compounds formed. The mass spectral data for these compounds are summarized in Table 4.7. The run was repeated

Figure 4.15. Total ion current chromatogram of the products resulting from hydrolysis of the organometallic compounds formed in the reaction of Al atoms and trifluorotoluene. (The compounds labelled * are due to contamination, see text).

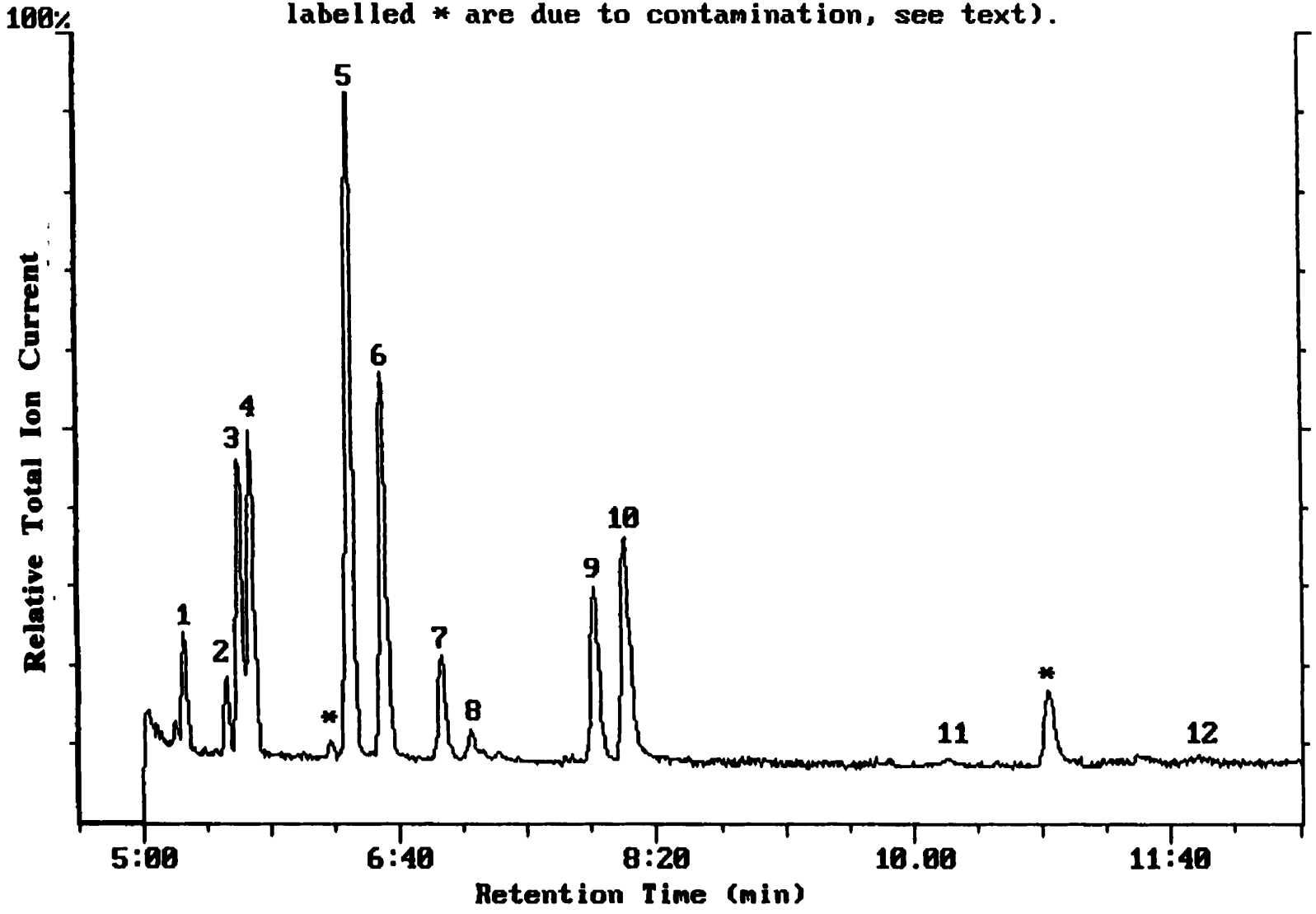

using deuterium oxide instead of water and the mass spectral data for the compounds detected in the deuterolysis mixture are presented in Table 4.8.

Table 4.7. Retention times and mass spectral data for hydrolysis products resulting from the reaction of Al atoms and trifluorotoluene.

Peak No.	Retention Time (min)	m/e for main fragments*
1	5:16	28(100) 32(25.2) 39(8.4) 50(10.1) 51(13.5) 69(10.7) 77(37.8) 79(60.1) 109(4.31) 127(22.4) 148(18.7)
2	5:33	28(100) 32(23.9) 39(30.2) 41(24.9) 54(14.1) 69(13.2) 79(20.2) 81(37.9) 115(10.0) 135(5.30) 150(13.2)
3	5:38	28(78.4) 32(11.3) 39(16.8) 50(14.1) 51(20.5) 69(16.0) 77(54.4) 79(100) 109(7.3) 127(36.8) 129(11.0) 148(32.1)
4	5:42	28(63.6) 39(14.7) 50(14.0) 51(21.4) 69(17.8) 77(65.3) 79(100) 109(18.0) 127(20.0) 148(22.1)
5	6:21	28(12.8) 39(16.2) 50(5.2) 51(6.3) 63(9.7) 65(13.7) 77(1.2) 89(4.2) 90(1.7) 91(100) 92(55.9)
6	6:33	28(51.4) 39(13.4) 50 (12.4) 51(19.4) 69(13.8) 77(53.5) 79(100) 109(7.5) 127(40.8) 129(11.2) 148(25.7)
7	6:57	32(35.2) 39(22.6) 50(24.5) 51(30.0) 75(14.6) 77(45.3) 78(40.7) 79(19.7) 101(9.24) 109(12.5) 115(14.4) 127(100) 128(46.1) 130(14.8)
8	7:08	39(41.3) 50(22.4) 51(34.0) 52(8.8) 53(8.5) 65(13.1) 77(43.8) 78(9.2) 79(85.5) 80(10.9) 91(8.6) 109(47.7) 115(100) 127(15.1) 129(9.9) 130(64.9)

* The number in brackets represents the percentage of the base peak.

Table 4.7. continued

Peak No.	Retention Time (min)	m/e for main fragments*
9**	7:56	28(85.2) 39(10.4) 50(19.1) 51(21.9) 63(4.4) 77(31.8) 78(34.7) 101(7.4) 127(100) 128(45.7)
10**	8:08	28(72.3) 39(8.2) 50(15.8) 51(35.2) 63(5.3) 77(15.0) 78(32.0) 109(21.8) 127(100) 128(48.6)
11**	10:13	39(13.2) 50(10.6) 51(13.2) 59(10.2) 63(12.2) 77(9.13) 83(21.1) 91(28.9) 109(100) 110(35.1)
12**	11:55	39(13.7) 50(10.5) 51(14.0) 57(8.87) 63(10.8) 83(39.2) 91(52.2) 109(100) 110(43.1)

* The number in brackets represents the percentage of the base peak.

** The peaks labelled 9, 10, 11, and 12 are thought to arise from peak splitting due to the unorthodox injector and column programs. See text.

Table 4.8. Retention times and mass spectral data for the deuterolysis products resulting from the reaction of Al atoms and trifluorotoluene.

Peak No.	Retention Time (min)	m/e for main fragments*
3	4:21	69(14.5) 78(29.4) 79(30.7) 80(39.5) 81(100) 93(6.38) 102(7.28) 110(8.03) 111(15.5) 127(8.53) 128(35.7) 129(31.4) 130(7.09) 131(13.8) 149(16.7) 150(37.3)
4	4:23	69(6.61) 78(20.7) 79(29.0) 80(24.9) 81(100) 93(6.14) 110(8.27) 111(26.7) 128(18.2) 129(17.2) 149(8.43) 150(21.0)
5	4:51	66(8.73) 67(12.2) 92(9.54) 93(70.4) 94(100) 95(48.4)
6	4:56	69(7.28) 78(26.2) 79(28.8) 80(23.6) 81(100) 93(7.0) 110(4.69) 111(10.8) 128(32.8) 129(36.4) 131(16.0) 150(21.9)
7	5:09	99(41.1) 110(12.1) 111(29.2) 112(15.5) 116(40.8) 117(55.7) 118(16.1) 128(13.9) 129(11.9) 132(30.2) 133(29.9)
8	5:17	76(19.9) 78(27.8) 79(42.6) 81(49.5) 82(49.9) 93(15.4) 94(19.1) 95(14.5) 96(29.8) 97(27.0) 102(13.3) 110(13.9) 111(37.2) 112(25.0) 115(13.8) 116(66.1) 117(100) 118(24.3) 129(16.8) 131(9.51) 132(34.5) 133(51.9)
9**	5:49	78(22.6) 79(22.9) 127(25.4) 128(100) 129(35.6)
10**	5:57	77(6.08) 78(7.0) 79(21.3) 110(20.1) 127(46.5) 128(100) 129(40.3)

* The number in brackets represents the percentage of the base peak.

** The peaks labelled 9 and 10 are thought to arise from peak splitting due to the unorthodox injector and column programs. See Table 3.5.

The major product, with a retention time of 6:21, was shown to be toluene by comparing the retention time and mass spectral data to those of an authentic sample (*cf.* data for toluene in Table 4.2 to that for entry 2 in Table 4.7). The mass spectral data for the deuterolysis product eluting at 4:51 is consistent with $C_6H_5CD_3$. The M^+ with an m/e ratio of 95 as well as the fragmentation pattern is what one would expect for $C_6H_5CD_3$.

There are several hydrolysis products that have an M^+ with an m/e ratio of 148, i.e., the compounds with retention times of 5:16, 5:38, 5:42 and 6:33, respectively. Deuterolysis of the reaction mixture generated products with an M^+ of 150, i.e., the compounds with the retention times of 4:21, 4:23 and 4:56, respectively. These are thought to be deuterated analogues of the hydrolysis products eluting at 5:38, 5:42 and 6:33. Comparison of the m/e ratios of the molecular ions (148 vs. 150) suggests that two deuterium atoms were incorporated into the product. Considering that the starting material is trifluorotoluene and that aluminum atoms have been shown to mediate the reduction of the aromatic ring, five possible compounds come to mind, namely, 6-trifluoromethyl-1,4-cyclohexadiene (**1**), 1-trifluoromethyl-1,4-cyclohexadiene (**2**), 1-trifluoromethyl-1,3-cyclohexadiene (**3**), 2-trifluoromethyl-1,3-cyclohexadiene (**4**) and 5-trifluoromethyl-1,3-cyclohexadiene (**5**).

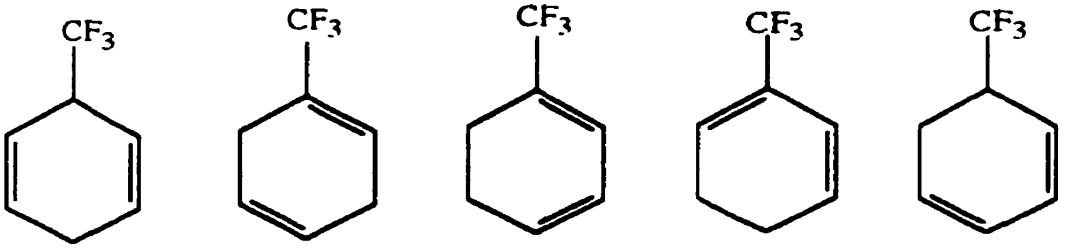

1 **2** **3** **4** **5**

In all five cases one would expect the parent compound to lose one F to form the ion, $C_7H_7F_2^+$ with an m/e ratio of 129, scheme 4.10.

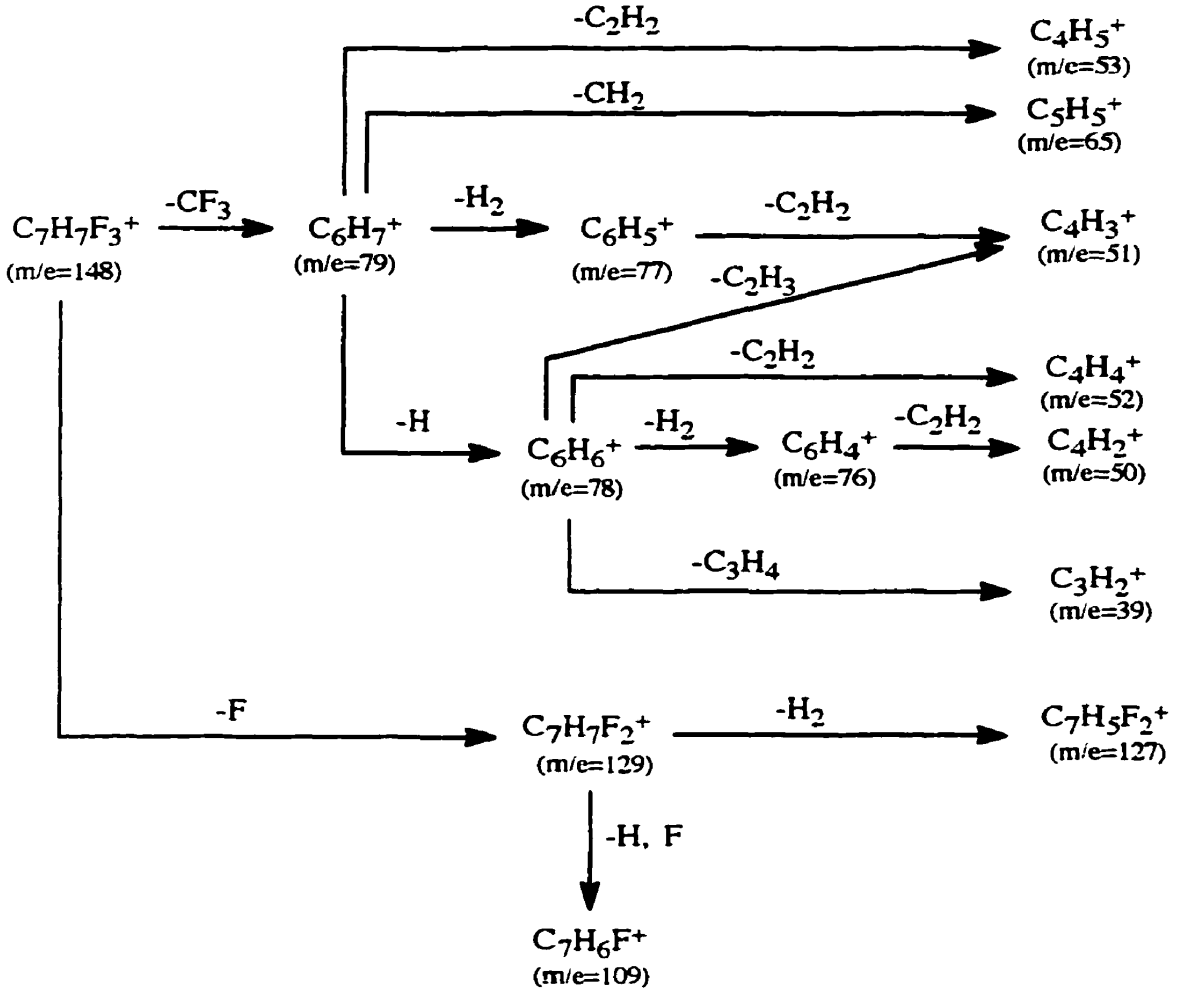

Scheme 4.9. Fragmentation scheme for trifluoromethylcyclohexadiene.

In the case of the deuterated analogues, loss of F produces $C_7H_5D_2F_2^+$ with an m/e ratio of 131. Should the parent compound lose two H and one F, the ion $C_7H_5F_2^+$ (**6**) would form, characterized by an m/e ratio of 127.

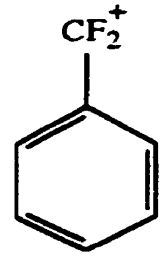

6

In the case of the deuterated analogues, clustering around an m/e ratio of 127 would occur because theoretically it would be possible to lose two H, two D or one H and one D. Therefore fragments with an m/e ratio of 129, 127 and 128 would be expected. This was indeed observed for the compounds with retention times of 4:21, 4:23 and 4:56.

The formation of fluorinated benzenium ion would also result in the fragmentation of methyl-substituted cyclohexadienes. This would occur from a loss of F from the parent ion followed by a loss of HF. The fragmentation for 6-trifluoromethyl-1,4-cyclohexadiene is shown in equation 4.3.

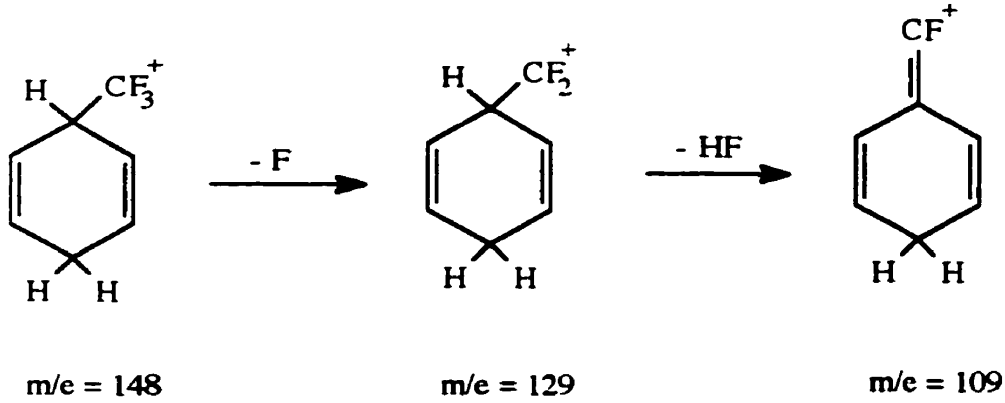

m/e = 148 m/e = 129 m/e = 109

4.3

For the deuterated analogues, loss of HF or DF are possible resulting in $C_7H_4D_2F^+$ or $C_7H_5DF^+$ with an m/e ratio of 111 and 110, respectively. Again, this is the case for the deuterolysis products with retention times of 4:21, 4:23 and 4:56.

Loss of CF_3 from the parent ion results in a fragment with an m/e ratio of 79 corresponding to $C_6H_7^+$. The deuterated trifluoromethylcyclohexadienes would fragment to give $C_6H_5D_2^+$ with an m/e ratio of 81. In fact, the hydrolysis products with retention times of 5:38, 5:42 and 6:33 and the deuterolysis products which elute at 4:21, 4:23 and 4:56 have base peaks of 79 and 81, respectively.

Finally, one would expect that fragmentation of the cyclohexadiene ring itself would closely resemble that presented by Franklin and Carroll[76] for 1,4-cyclohexadiene, i.e., clusters of ions ranging from 37-41, 50-55, 65-69 and 77-79 should be observed. The positioning of the double bonds within the cyclohexadiene ring would not alter the mass spectral data significantly. This was shown previously with 1,4-cyclohexadiene and 1,3-cyclohexadiene. We had to use retention times to assign the chromatographic peaks because the mass spectral data were virtually identical. Unfortunately, authentic samples of the trifluoromethyl-1,3- and 1,4-cyclohexadienes are not readily available to confirm the assignments. From our study of the unsubstituted cyclohexadienes we would predict that the trifluoromethyl-1,3-cyclohexadienes would elute before the trifluoromethyl-1,4-cyclohexadienes.

The two hydrolysis products with retention times of 6:57 and 7:08 respectively have very similar mass spectral data. The m/e ratio of the M^+ is 130 for both compounds. The corresponding deuterated analogues have retention times of 5:09 and 5:17 respectively and the m/e ratio of the M^+ is 133. A difference of 146 - 130 or 16 exists between the molecular weight of the starting material, trifluorotoluene, and the hydrolysis products. The difference in the m/e ratio of the M^+ for the hydrolysis and deuterolysis products is

133 - 130 or 3. This would suggest the incorporation of 3 deuterium atoms upon deuterolysis. A number of substituted 1,3-cyclohexadienes (**7**) and 1,4-cyclohexadienes (**8**) are consistent with these observations.

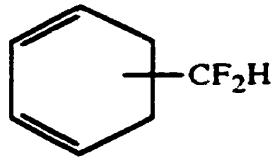

7

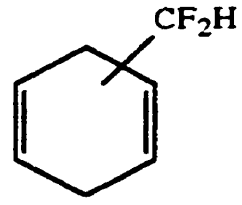

8

Analysis of the mass spectral data (scheme 4.11) supports this assignment. The parent compound loses one H to form the ion $C_7H_7F_2^+$ with an m/e ratio of 129 which in turn loses two H to form the ion $C_7H_5F_2^+$ with an m/e ratio of 127. The parent compound loses one F to form the fragment with an m/e ratio of 111. This fragment has been attributed to $C_7H_8F^+$. The fragment with an m/e ratio of 109 has been attributed to $C_7H_6F^+$ and forms upon loss of two H to form the ion $C_7H_8F^+$. The fragment with an m/e ratio of 91 has been attributed to $C_7H_7^+$ and forms upon loss of one F followed by loss of HF from the parent compound. The parent compound loses the difluoromethyl group to form the cyclohexadiene fragment with an m/e ratio of 79, $C_6H_7^+$. Fragmentation of the cyclohexadiene ring closely resembles that presented by Franklin and Carroll[76] for 1,4-cyclohexadiene. Therefore the clusters of ions ranging from 37 - 41, 50 - 55, 65 - 69 and 77 - 79 are a result of the fragmentation of the cyclohexadiene ring.

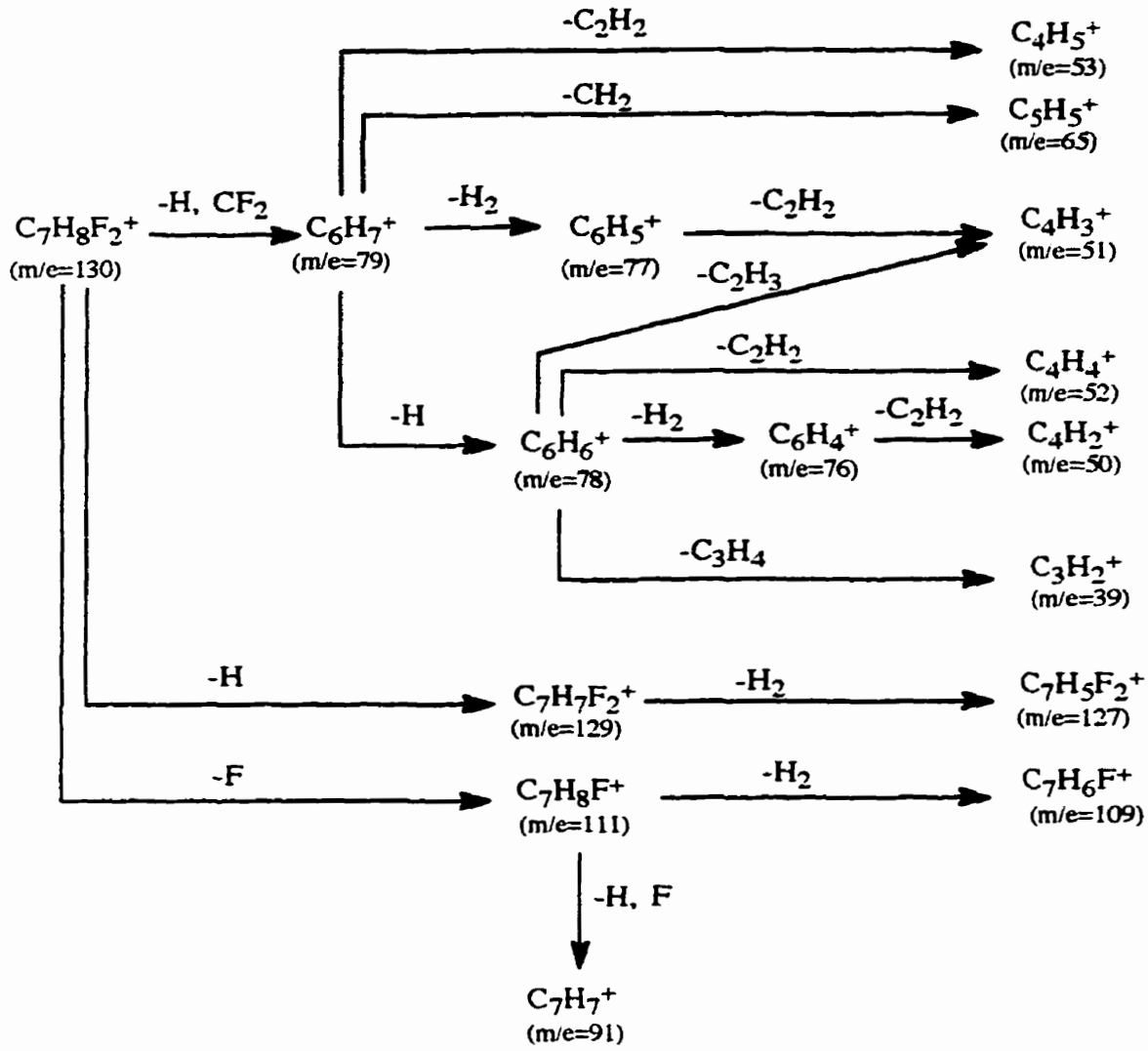

Scheme 4.10. Fragmentation scheme for difluoromethylcyclohexadiene

Two hydrolysis products (with retention times of 7:56 and 8:08, respectively) have an M^+ with an m/e ratio of 128. Difluorotoluene, which can be formed from the starting material, trifluorotoluene, by substitution of F by H, has a molecular weight of 128. The deuterolysis experiment supports the hypothesis that difluorotoluene forms because the m/e

ratio of the M^+ for the compounds corresponding to the above mentioned hydrolysis products is 129, which is indicative of the formation of $CDF_2C_6H_5$. It is believed that the two hydrolysis products are in fact the same compound and that peak splitting occurred due to the unorthodox injector and column programs used in the analysis of the sample. The analysis is unorthodox because the column was not maintained at a fixed temperature (*cf.* 35 - 37°C at a rate of 0.2°/min) while the sample was transferred from the septum programmable injector. The sample was analyzed using a more traditional approach, i.e., the column was maintained at 37°C for 2 min to allow for loading of the sample from the injector to the column. Only the M^+ of one compound had a m/e ratio of 128 under these conditions. We chose to present the data using the unorthodox program because the quality of the chromatography and the mass spectral data were superior under these conditions.

The mass spectral data matches with that for difluorotoluene (NIST Registry No. 4306). As in the case of toluene, difluorotoluene (difluoromethylbenzene) easily loses H forming the $(M-1)^+$ ion with a high relative abundance, i.e., the relative abundance of the ion at an m/e ratio of 127 (M-1) is 100%. The fragment with an m/e ratio of 109 has been attributed to $C_7H_6F^+$ and forms upon the loss of one F from the parent compound. The loss of CHF_2 results in the formation of an ion with an m/e ratio of 77 consistent with the formation of $C_6H_5^+$. Analysis of the spectral data for the deuterated analogue is also consistent with this assignment.

The mass spectral data for the hydrolysis products with retention times of 10:13 and 11:55 are similar to those for monofluorotoluene (monofluoromethylbenzene, NIST Registry No. 2071). As discussed above, the two hydrolysis products are thought to be the same compound, the two chromatographic peaks arising from peak splitting due to the unorthodox injector and column programs used in the analysis of the sample. The

fragmentation of monofluorotoluene is characterized by the M^+ with an m/e ratio of 110, an $(M-1)^+$ ion and an $(M-19)^+$ from the loss of F. It is interesting to note that the monofluorotoluene is a minor product in comparison to all the other products mentioned. In fact, in the deuterolysis study we were unable to detect the presence of $CD_2FC_6H_5$.

By comparing the peak heights of the compounds identified in the hydrolysis study a rough estimate of the relative amount of the hydrolysis products was obtained, Table 4.9. The major product formed was toluene (~25%). Four different trifluoromethylcyclohexadienes, two difluoromethylcyclohexadienes, one difluorotoluene and one monofluorotoluene formed, accounting for ~48%, ~8%, ~16% and ~4% of the reaction mixture, respectively.

Table 4.9. Relative amounts of the hydrolysis products found for the reaction between Al and trifluorotoluene.

Compound	Retention Time	Relative Proportion*	
		Run #1	Run #2
Trifluoromethylcyclohexadiene	5:16	6.2	5.6
Trifluoromethylcyclohexadiene	5:38	15.0	16.5
Trifluoromethylcyclohexadiene	5:42	12.0	12.3
Toluene	6:21	25.1	23.7
Trifluoromethylcyclohexadiene	6:33	13.9	14.1
Difluoromethylcyclohexadiene	6:57	5.4	4.9
Difluoromethylcyclohexadiene	7:08	2.8	2.9
Difluorotoluene	7:56, 8:08	15.9	16.3
Monofluorotoluene	10:13, 11:55	3.7	4.1

* Based on the $AC_i/\Sigma AC_j \times 100$ where AC_j is the area counts for product i, obtained from the electronic integration of the peaks in the total ion chromatogram.

From the hydrolysis and deuterolysis of the aluminum atom-trifluorotlouene reaction mixture, we can conclude that aluminum atoms: a) readily insert into C-F bonds and b) as in the case of benzene, mediate the reduction of the aromatic ring.

The formation of toluene, difluorotoluene and monofluorotoluene is evidence for aluminum atom insertion into the C-F bond, scheme 4.11. Insertion of aluminum atoms into C-halogen bonds has been previously reported by Klabunde and coworkers.[52] More specifically, they reported the insertion of aluminum atoms into the C-Br bond of methyl bromide to form CH_3AlBr. It would appear that, in our case, the aluminum atom can insert into one, two or all three of the C-F bonds of trifluorotoluene.

It is also interesting that only a 4% of the monofluorotoluene was detected whereas relatively large quantities of difluorotoluene and toluene were present in the reaction mixture. This observation suggests that the dialuminum adduct reacts rapidly to form the trialuminum adduct, i.e., insertion of the second aluminum atom facilitates addition of the third aluminum atom.

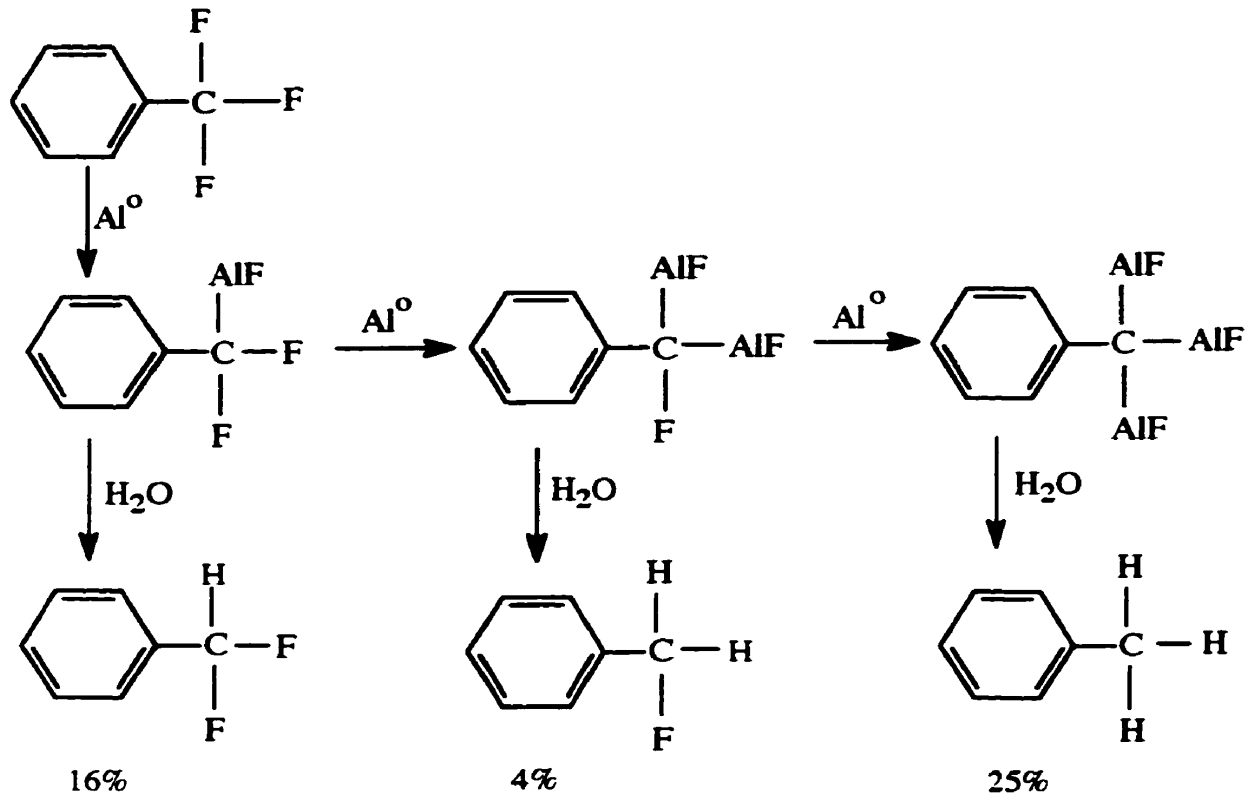

Scheme 4.11. The proposed reaction pathways for formation of difluorotoluene, monofluorotoluene and toluene from Al atoms and trifluorotoluene.

The formation of the four trifluoromethylcyclohexadienes is evidence that the Al also mediates the reduction of the aromatic ring. In the case of benzene and toluene, Al adds across the 1,4 positions of the aromatic ring. Hydrolysis of the aluminum adduct results in the formation of a 1,4-cyclohexadiene. However, for trifluorotoluene, the large number of trifluoromethylcyclohexadienes formed upon hydrolysis of the reaction mixture can only be explained if aluminum atoms add across the 1,2 position of the aromatic ring as well as the 1,4 positions to form the adducts shown in scheme 4.12.

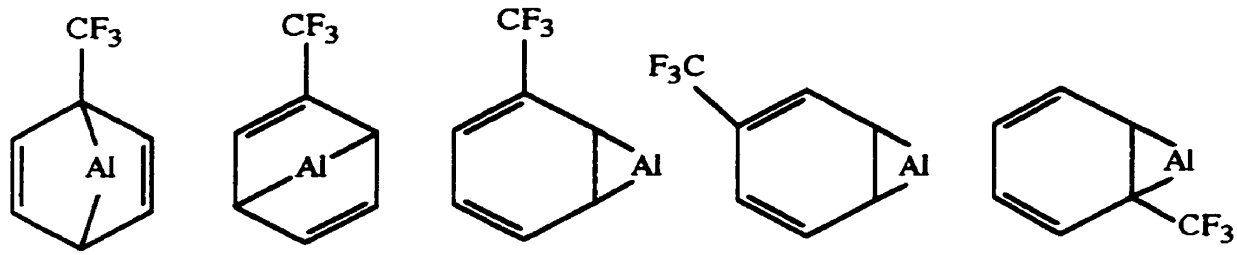

9 10 11 12 13

Scheme 4.12. The structure of possible aluminum adducts formed in the reaction between aluminum atoms and trifluorotoluene.

The difluoromethylcyclohexadienes are the hydrolysis products of dialuminum adducts, i.e., adducts where an aluminum atom has inserted into one of the C-F bonds and a second aluminum atom has added either to a 1,2 position or a 1,4 position of the aromatic ring. We were unable to determine exactly how addition to the aromatic ring occurred because authentic samples of difluoromethyl-1,3 and 1,4-cyclohexadienes are not readily available for direct comparison of retention times and mass spectral data. A few examples of the aluminum adducts leading to the formation of difluoromethylcyclohexadienes is shown in scheme 4.13. The difluoromethylcyclohexadienes are present in relatively small quantities compared to toluene for instance. This would seem to indicate that Al atom insertion into the second C-F bond and subsequently the third C-F bond is easier than reduction of the aromatic ring.

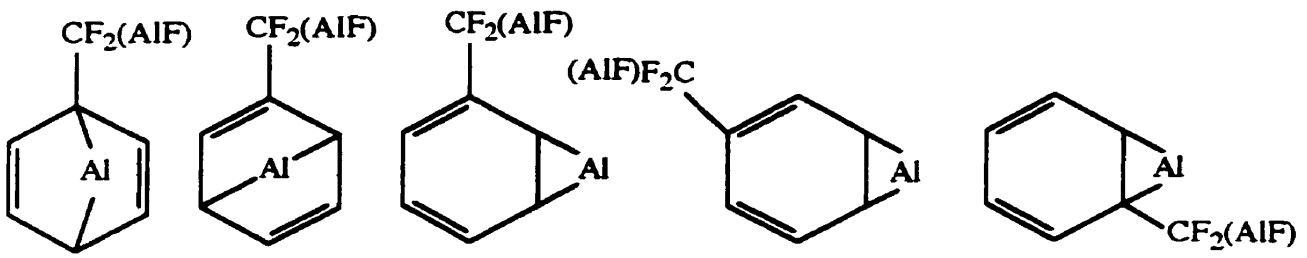

14 **15** **16** **17** **18**

Scheme 4.13. Possible aluminum adducts leading to the formation of difluoromethylcyclohexadienes.

4.1.3.2 Reaction of Ga atoms with trifluorotoluene:

4.1.3.2.1 Hydrolysis of the intermediate formed in the reaction of Ga atoms and trifluorotoluene:

Gallium atoms were reacted with trifluorotoluene under a number of experimental conditions. More specifically, the weight of the Ga metal used to produce the gallium atoms was varied from 32.4 to 40 mg and the amount of trifluorotoluene was controlled by setting the vapour pressure of trifluorotoluene to 0.01 Torr. A typical total ion current (TIC) chromatogram of the hydrolysis products is presented in Figure 4.16. The mass spectra corresponding to the compounds labelled 1-10 are summarized in Table 4.10.

As in the case of the reaction of Al atoms and trifluorotoluene, hydrolysis of the Ga-trifluorotoluene reaction mixture resulted in the formation of ten different compounds. These compounds are identical to those produced in the Al atom-trifluorotoluene reaction as is evidenced by the retention times and the mass spectral data (*cf.* Tables 4.7 and 4.10).

Figure 4.16. Total ion current chromatogram of the products resulting from hydrolysis of the organometallic compounds formed in the reaction of Ga atoms and trifluorotoluene. (The compounds labelled * are due to contamination, see text).

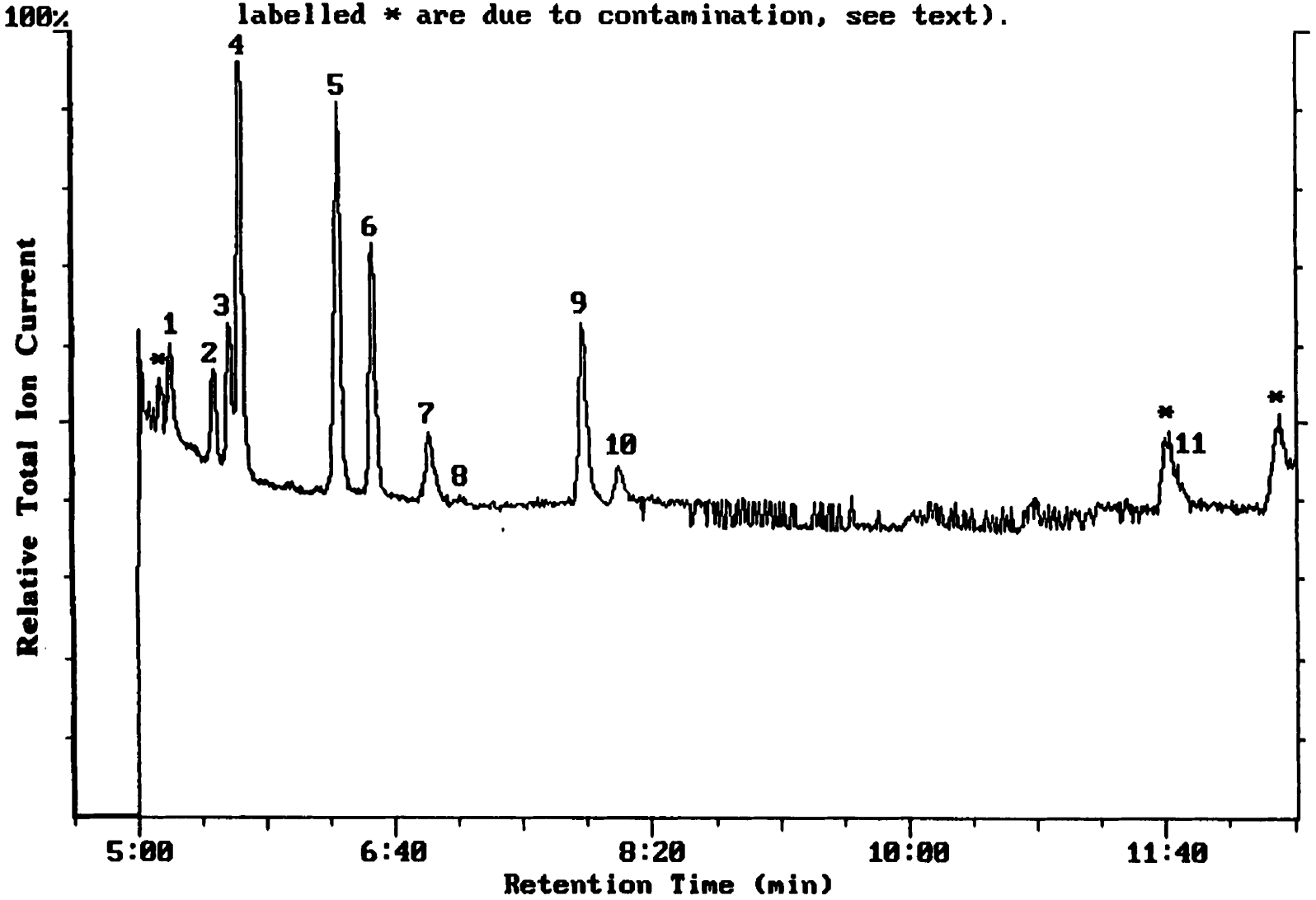

Table 4.10. **Retention times and mass spectral data for the hydrolysis products resulting from the reaction of Ga atoms and trifluorotoluene.**

Compound	Retention Time (min)	m/e for main fragments*
1	5:13	28(100) 32(79.8) 39(3.5) 49(15.4) 50(5.82) 51(11.5) 69(4.60) 77(12.1) 79(15.4) 127(13.3) 148(4.81)
2	5:30	39(76.5) 41(61.5) 50(14.1) 51(24.8) 53(26.9) 54(37.8) 67(11.8) 69(32.0) 77(27.1) 79(51.0) 81(100.0) 109(12.0) 115(25.7) 135(14.9) 150(34.3)
3	5:36	39(20.6) 50(18.6) 51(24.6) 69(20.3) 77(63.9) 79(100) 109(9.16) 127(44.3) 129(14.3) 148(30.5)
4	5:40	28(60.6) 32(15.8) 39(14.2) 50(16.6) 51(22.9) 69(19.6) 77(75.4) 79(100) 109(21.2) 127(23.0) 148(21.8)
5	6:18	28(30.2) 39(18.1) 50 (7.96) 51(7.77) 63(10.5) 65(13.9) 77(2.30) 89(4.09) 90(1.37) 91(100) 92(58.3)
6	6:32	28(20.5) 39(13.9) 50(21.4) 69(15.6) 77(64.0) 79(100) 109(8.76) 127(45.1) 129(13.5) 148(24.4)
7	6:54	39(36.0) 50(27.7) 51(41.5) 75(17.9) 77(58.5) 78(40.4) 79(42.4) 101(10.4) 109(25.1) 115(29.6) 127(100) 128(38.9) 130(31.7)
8	7:05	39(49.1) 50(34.6) 51(72.7) 52(10.9) 53(11.8) 65(10.9) 77(61.8) 78(10.9) 79(100) 80(13.6) 91(9.09) 109(50.9) 115(97.3) 127(54.6) 129(18.2) 130(64.6)
9**	7:54	39(10.2) 50(18.1) 51(21.3) 63(4.15) 77(33.5) 78(38.1) 101(7.17) 127(100) 128(46.3)
10**	8:07	39(6.35) 50(14.5) 51(32.2) 63(5.3) 77(12.2) 78(28.1) 109(24.5) 127(100) 128(46.0)
11	11:45	39(13.4) 50(8.76) 51(14.6) 57(3.08) 63(8.22) 83(13.8) 91(100) 109(33.6) 110(14.6)

*The number in brackets represents the percentage of the base peak.

**The peaks labelled 9 and 10 are thought to arise from peak splitting due to the unorthodox injector and column programs. See Table 3.5.

The compounds with a retention time of 5:13, 5:36, 5:40 and 6:32, respectively, have an M^+ with an m/e ratio of 148 and are a series of trifluoromethyl-1,4 and 1,3-cyclohexadienes. The possible structures of these compounds are **1**, **2**, **3**, **4** or **5** shown in section 4.1.3.1, page 133. These results show that Ga atoms mediate the reduction of the aromatic ring. Ga atoms add either across the 1,4 positions of trifluorotoluene or to the 1,2 positions of the trifluorotoluene. Hydrolysis of the gallium adducts results in the formation of a trifluoromethyl-1,4-cyclohexadiene or a trifluoromethyl-1,3-cyclohexadiene. The structure of possible gallium adducts formed in the reaction between gallium atoms and trifluorotoluene are presented in scheme 4.14.

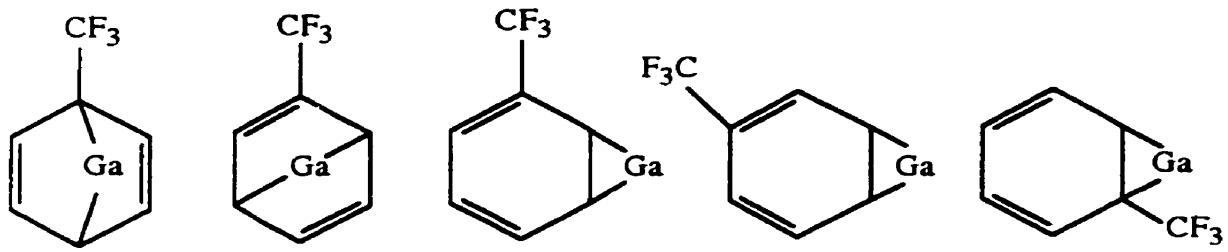

Scheme 4.14. The structure of possible gallium adducts formed in the reaction between Ga atoms and trifluorotoluene.

The compounds with retention times of 6:18, 7:54* and 11:45 were assigned to toluene, difluorotoluene and monofluorotoluene, respectively. These occur upon hydrolysis of gallium adducts produced upon insertion of Ga atoms into one, two or three C-F bonds, scheme 4.15.

---

* As explained in section 4.1.3.1.1, the compounds eluting at 7:54 and 8:07 are believed to be the same compound. Peak splitting due to unorthodox injector and column programs is the reason for observing two chromatographic peaks.

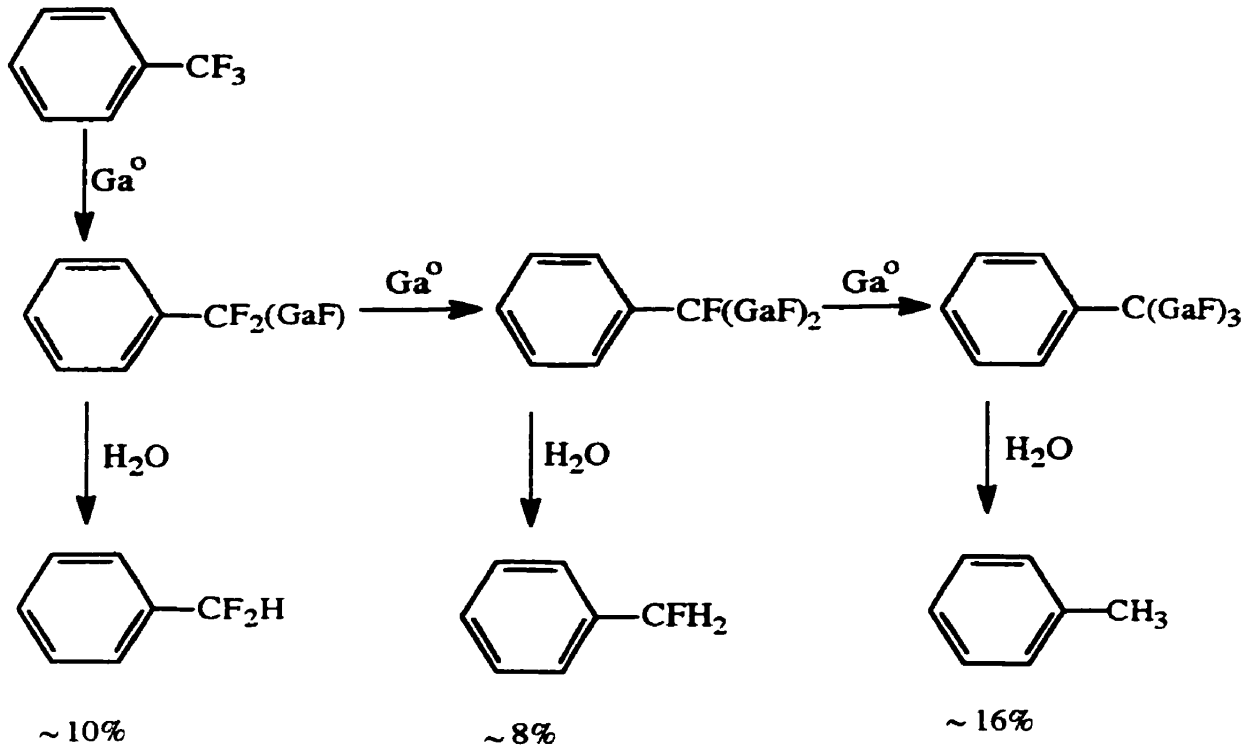

Scheme 4.15. The proposed reaction pathway for formation of difluorotoluene, monofluorotoluene and toluene from Ga atoms and trifluorotoluene.

The compounds with a retention time of 6:54 and 7:05, respectively, have very similar mass spectral data. The M^+ with an m/e ratio of 130 suggests that these compounds are difluoromethylcyclohexadienes. The difluoromethylcyclohexadienes are the hydrolysis products of digallium adducts, i.e., adducts where a gallium atom has inserted into one of the C-F bonds and a second Ga atom has added across a 1,2 or a 1,4 position of the aromatic ring. Possible structures for these gallium adducts are presented in scheme 4.16.

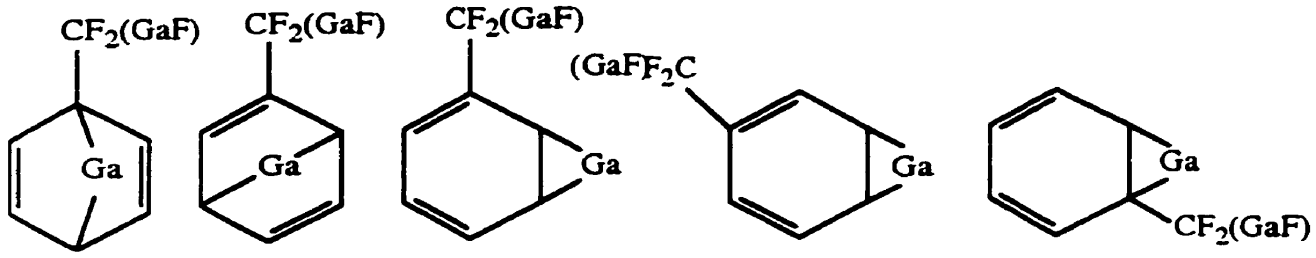

Scheme 4.16. The structure of possible gallium adducts formed in the reaction between Ga atoms and trifluorotoluene.

A comparison of the peak heights of the hydrolysis products gives a rough estimate of the relative amount of each compound present in the reaction mixture, Table 4.11.

Table 4.11. Relative amounts of the hydrolysis products found for the reaction between Ga atoms and trifluorotoluene.

Compound	Retention Time	Relative Proportion*	
		Run #1	Run #2
Trifluoromethylcyclohexadiene	5:13	10.1	10.9
Trifluoromethylcyclohexadiene	5:36	11.6	10.6
Trifluoromethylcyclohexadiene	5:40	15.9	17.3
Toluene	6:18	16.0	15.8
Trifluoromethylcyclohexadiene	6:32	13.3	12.1
Difluoromethylcyclohexadiene	6:54	8.6	8.4
Difluoromethylcyclohexadiene	7:05	7.5	6.7
Difluorotoluene	7:54, 8:09	9.0	10.6
Monofluorotoluene	11:45	8.4	7.1

* Based on the $AC_i/\Sigma AC_i$ x 100 where AC_i is the area counts for product i, obtained from the electronic integration of the peaks in the total ion chromatogram.

The reactions of Ga atoms with trifluorotoluene yields a number of trifluoromethylcyclohexadienes (51%), toluene (16%), two difluoromethylcyclohexadienes (16%), difluorotoluene (10%) and monofluorotoluene (8%). The relative proportion of the different products vary slightly for the Ga- and Al-trifluorotoluene reactions (cf. Tables 4.9 and 4.11). Toluene (25%) was the major product formed in the Al-trifluorotoluene reaction whereas in the Ga-trifluorotoluene reaction the trifluoromethylcyclohexadiene eluting at 5:40 is formed in the same relative proportion as toluene, i.e., 17% and 16% respectively. In both the Al- and Ga-trifluorotoluene reactions monofluorotoluene is the minor product. In general terms we have found that Σ[trifluorocyclohexadienes] > [difluorocyclohexadienes] ~ [toluene] > [difluorotoluene] > [monofluorotoluene] for the reaction of Ga atoms with trifluorotoluene. For the Al atom-trifluorotoluene reaction Σ[trifluorocyclohexadienes] > [toluene] > [difluorotoluene] > Σ[difluorocyclohexadienes] > [monofluorotoluene]. The Ga atoms appear to favour reduction of the aromatic ring as 67% of the products formed (compared to 57% for Al atoms) are derivatives of cyclohexadiene.

4.1.3.3 Reaction of In atoms with trifluorotoluene:

4.1.3.3.1 Hydrolysis of the intermediate formed in the reaction of In atoms and trifluorotoluene:

Indium atoms were reacted with trifluorotoluene under a number of experimental conditions. More specifically, the weight of the In metal used to produce the indium atoms was varied from 24.5 to 36.5 mg and the amount of trifluorotoluene was controlled by setting the vapour pressure of trifluorotoluene to 0.01 Torr. A typical total ion current (TIC) chromatogram of the hydrolysis products is presented in Figure 4.17. The mass spectral data corresponding to the compounds labelled 1-3 are summarized in Table 4.12.

Figure 4.17. Total ion current chromatogram of the products resulting from hydrolysis of the organometallic compounds formed in the reaction of In atoms and trifluorotoluene. (The compounds labelled * are due to contamination, see text).

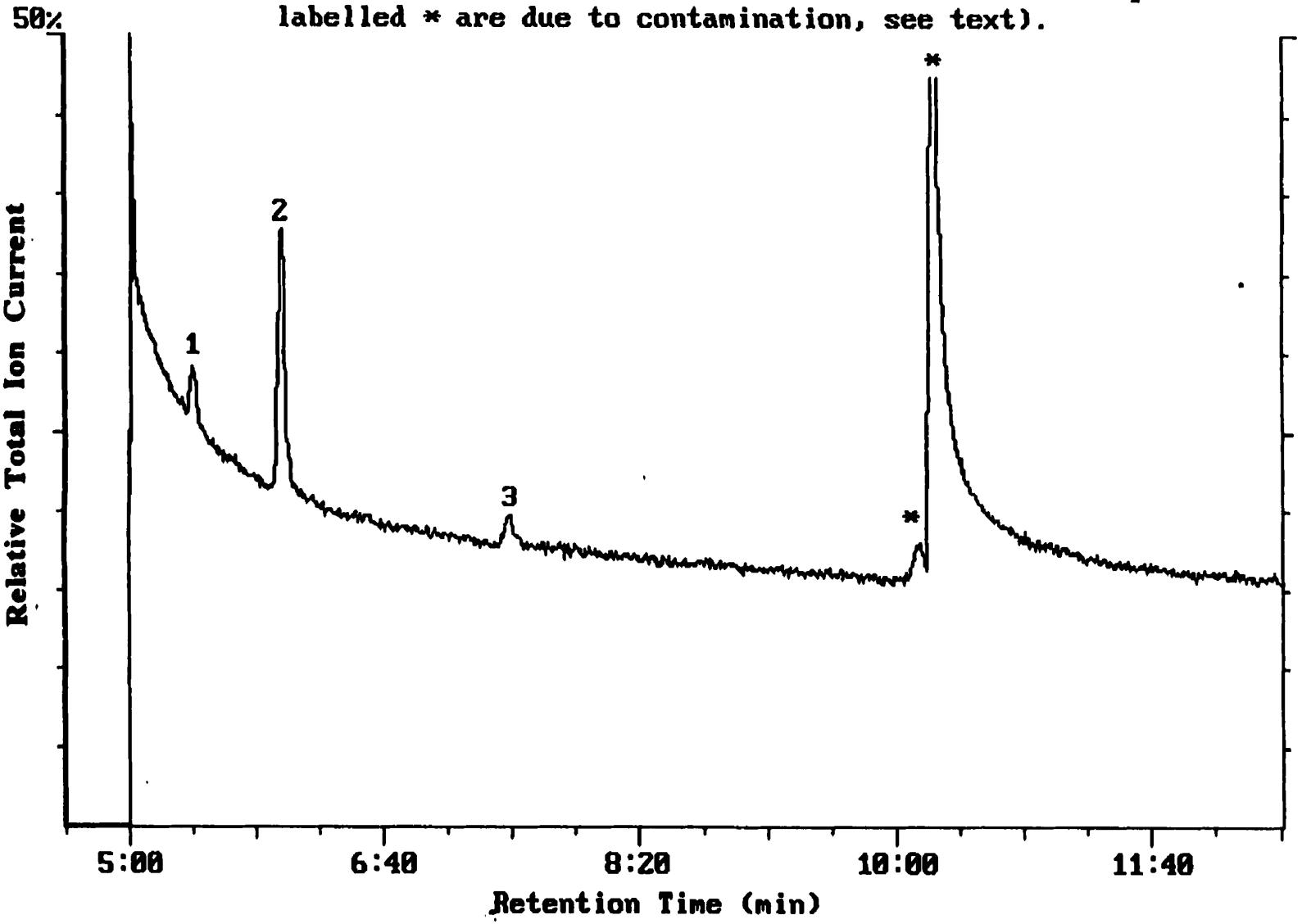

Hydrolysis of the In atom reaction with trifluorotoluene resulted in the formation of three different compounds. These compounds are identified to be trifluoromethylcyclohexadiene (retention time of 5:26), toluene (retention time of 6:00) and difluorotoluene (retention time of 7:29) compounds. These compounds are similar to the ones formed in the Al- and Ga-trifluorotoluene reaction mixtures as is evidenced by the retention times and the mass spectral data (*cf.* Tables 4.7, 4.10 and 4.12).

The compound with a retention time of 5:26, and an M^+ with an m/e ratio of 148 is a trifluoromethyl-1,4 or 1,3-cyclohexadiene. The possible structures of this compound are **1**, **2**, **3**, **4** or **5** shown in section 4.1.3.1, page 133. The results show that In atoms mediate the reduction of the aromatic ring. Indium atoms add either across the 1,4 positions or to the 1,2 positions of the trifluorotoluene. Hydrolysis of the indium adducts results in the formation of a trifluoromethyl-1,4-cyclohexadiene or a trifluoromethyl-1,3-cyclohexadiene. The structure of possible indium adducts formed in the reaction between indium atoms and trifluorotoluene is presented in scheme 4.17.

Table 4.12. Retention times and mass spectral data for the hydrolysis products resulting from the reaction of In atoms and trifluorotoluene.

Compound	Retention Time (min)	m/e for main fragments*
1	5:26	39(18.1) 50(36.0) 51(42.9) 69(32.5) 77(79.3) 79(100) 109(16.5) 127(56.6) 129(0.35) 148(22.0)
2	6:00	28(7.3) 39(19.8) 50 (10.2) 51(10.1) 63(12.2) 65(15.5) 77(1.3) 89(4.3) 90(1.6) 91(100) 92(52.2)
3	7:29	39(11.3) 50(22.8) 51(28.1) 63(4.96) 77(32.5) 78(33.6) 101(7.2) 127(100) 128(40.2)

*The number in brackets represents the percentage of the base peak.

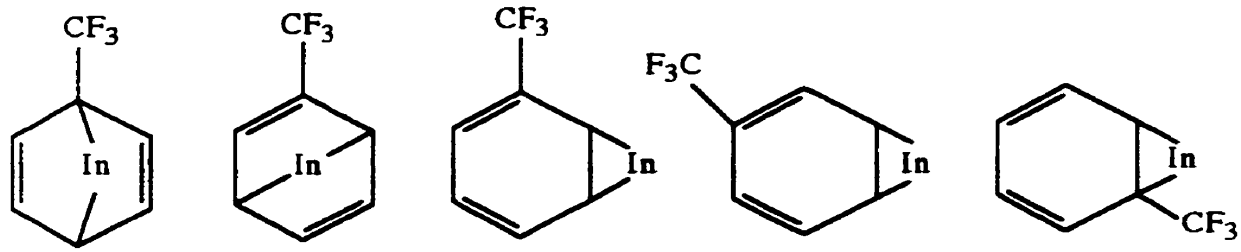

Scheme 4.17. The structure of possible indium adducts formed in the reaction between In atoms and trifluorotoluene.

The compounds with retention times of 6:00 and 7:29 were assigned to toluene and difluorotoluene, respectively. These occur upon hydrolysis of indium adducts produced upon insertion of In atoms into one, or three C-F bonds, scheme 4.18.

A comparison of the peak heights of the hydrolysis products gives a rough estimate of the relative amount of each compound present in the reaction mixture, Table 4.13.

Table 4.13. Relative amounts of the hydrolysis products found for the reaction between In atoms and trifluorotoluene.

Compound	Retention Time	Relative Proportion*
Trifluoromethylcyclohexadiene	5:26	33.6
Toluene	6:00	43.7
Difluorotoluene	7:29	22.7

* Based on the $AC_i/\Sigma AC_i \times 100$ where AC_i is the area counts for product i, obtained from the electronic integration of the peaks in the total ion chromatogram.

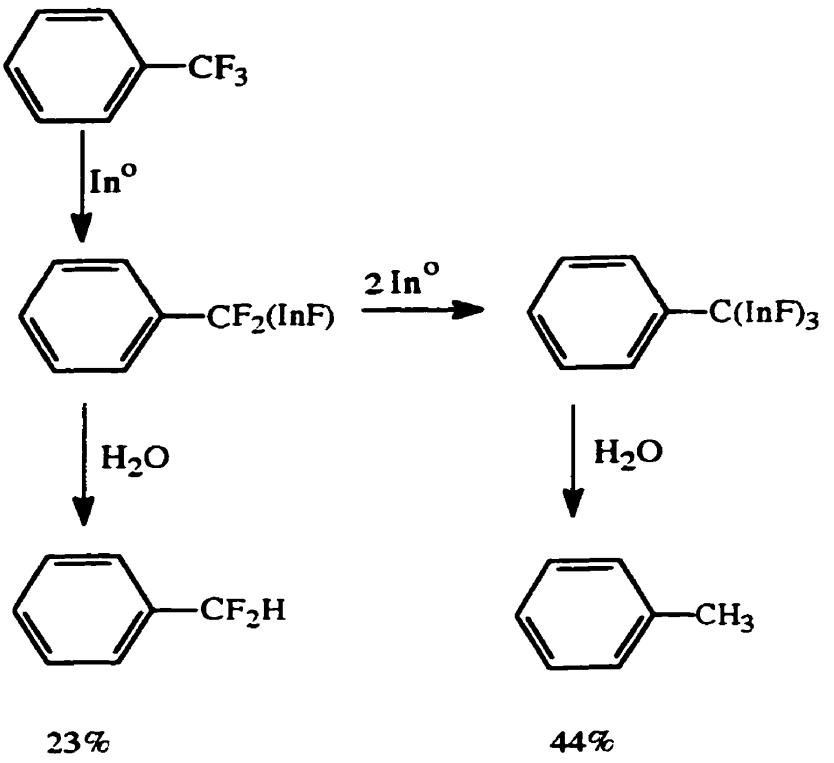

Scheme 4.18. The proposed reaction pathway for formation of difluorotoluene, and toluene from In atoms and trifluorotoluene.

The reactions of In atoms with trifluorotoluene have produced only three products (trifluoromethylcyclohexadiene, toluene, and difluorotoluene) in comparison to five products for Al and Ga atoms with trifluorotoluene. The In-trifluorotoluene reaction produced 34%, 43% and 23% of trifluoromethylcyclohexadiene, toluene, and difluorotoluene, respectively. It is interesting to note that whereas four isomers of trifluoromethylcyclohexadiene are formed in relatively equal proportions in the reaction of Al atoms and Ga atoms with trifluorotoluene, only one trifluoromethylcyclohexadiene isomer is detected in the reaction of In atoms with trifluorotoluene. Indium atoms seem to

favour insertion into the C-F bonds of trifluorotoluene rather than reduction of the aromatic ring.

4.1.3.4 Reaction of Tl atoms with trifluorotoluene:

4.1.3.4.1 Hydrolysis of the intermediate formed in the reaction of Tl atoms and trifluorotoluene:

Thallium atoms were reacted with trifluorotoluene under a number of experimental conditions. More specifically, the weight of the Tl metal used to produce the Tl atoms was varied from 43.92 to 66 mg and the amount of trifluorotoluene was controlled by setting the vapour pressure of trifluorotoluene to > 0.01 Torr. The total ion current (TIC) chromatogram showed no products formed when Tl was reacted with trifluorotoluene.

Thallium and indium atoms are not very reactive towards trifluorotoluene. Klabunde at al.[52] and Joly et al.[86] found the reactivity order of group 13 metal atoms/clusters for the reaction with methyl bromide and aromatic alkenes, respectively, to be Al > Ga > In > Tl. They concluded that the reactivity of the atoms is greatly influenced by the heats of vaporization which are also in the order Al > Ga > In > Tl.

4.1.4 Reaction of Al Atoms with Chlorobenzene:

The reason for carrying out chlorobenzene reactions was to examine the reactivity of Al atoms with different competitive sites in the same compound. Chlorobenzene offers two different competitive sites for Al atoms to attack, the C-Cl bond and the C=C bonds of the benzene ring.

4.1.4.1 Deuterolysis of the intermediate formed in the reaction of Al atoms and chlorobenzene:

This reaction was carried out at the National Research Council (NRC) in Ottawa and analyzed in our laboratory at Laurentian University. Aluminum atoms were reacted with chlorobenzene by the same method described in section 3.1.2.5. In this reaction, water (H_2O) was replaced by deuterium oxide (D_2O). The reason for using D_2O instead of H_2O was to find out more information on how the reaction takes place, i.e. to find out what role, in terms of hydrogen donation, the water plays. It is known that Al-C bonds in organoaluminum adducts are replaced with deuterium atoms when treated with D_2O. Therefore incorporation of deuterium into the molecule would indicate the number and location of the Al-C bonds.

A typical total ion current (TIC) chromatogram is presented in two segments. Figures 4.18a is the chromatogram of segment 1 and Figure 4.18b is the chromatogram of segment 2. The peaks of interest are labelled 1 (Figure 4.18a) and 2 (Figure 4.18b). The other peaks labelled * have been excluded from the discussion because they were also found when 1 μL of the CH_2Cl_2 was analyzed under the same experimental conditions as that for the reaction mixture, therefore it was concluded that these compounds are not formed in the reaction between Al atoms, chlorobenzene and D_2O. The mass spectral data of the compounds corresponding to peaks 1 and 2 are shown in Figures 4.19 and 4.20, respectively. A comparison of the mass spectral data and retention times (Table 4.14) with those for authentic samples led us to assign 1 to deuterated benzene (C_6H_5D) and 2 to 1,1'-biphenyl ($C_{12}H_{10}$).

The reactions were repeated twice. The amount of deuterated benzene and 1,1'-biphenyl in the mixture ranged from 30% to 50% and 50% to 60%, respectively.

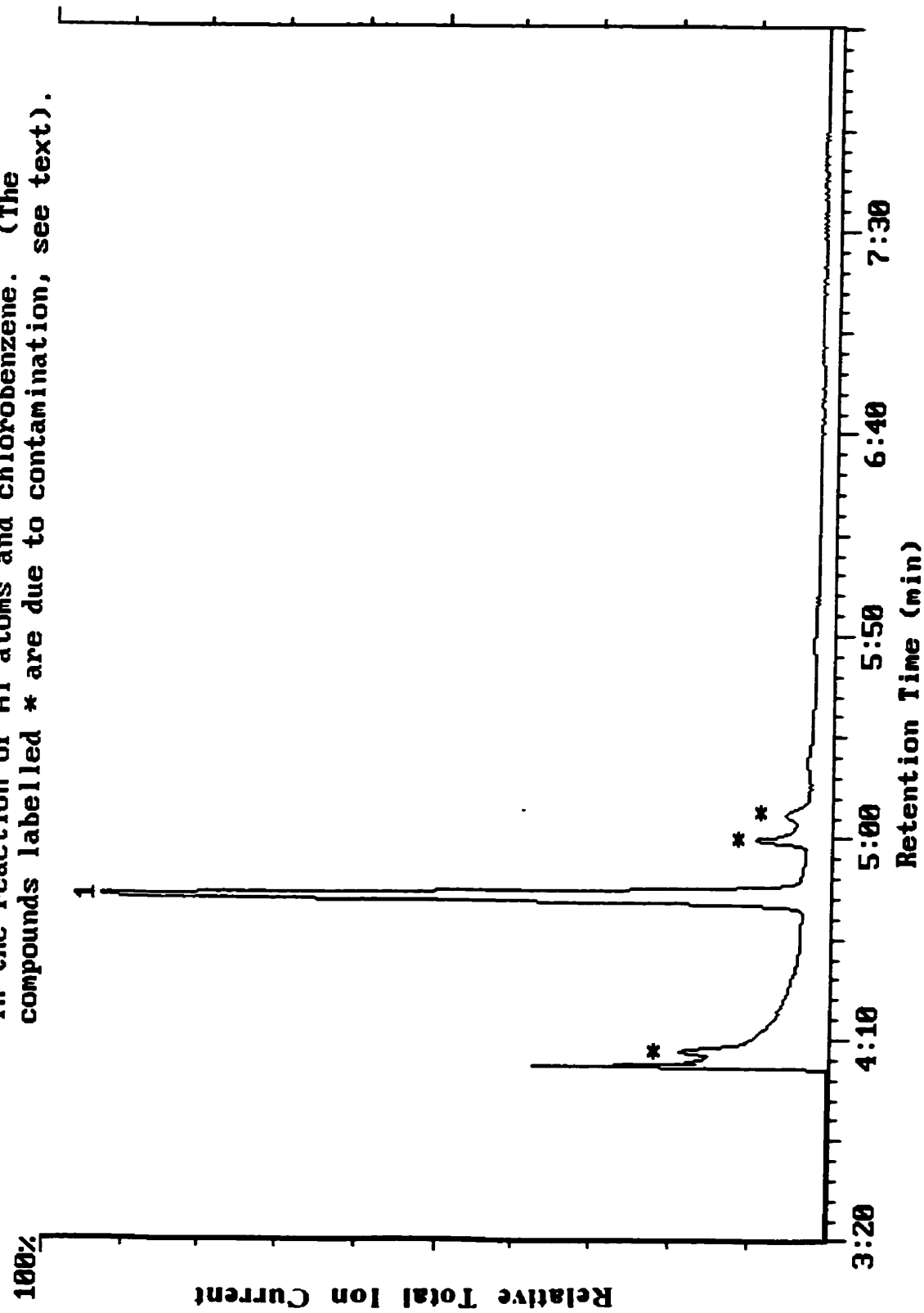

Figure 4.18a. Total ion current chromatogram of the product resulting from deuterolysis of the organometallic compound formed in the reaction of Al atoms and chlorobenzene. (The compounds labelled * are due to contamination, see text).

Figure 4.18b. Total ion current chromatogram of the product resulting from deuterolysis of the organometallic compound formed the reaction of Al atoms and chlorobenzene. (The compounds labelled * are due to contamination, see text).

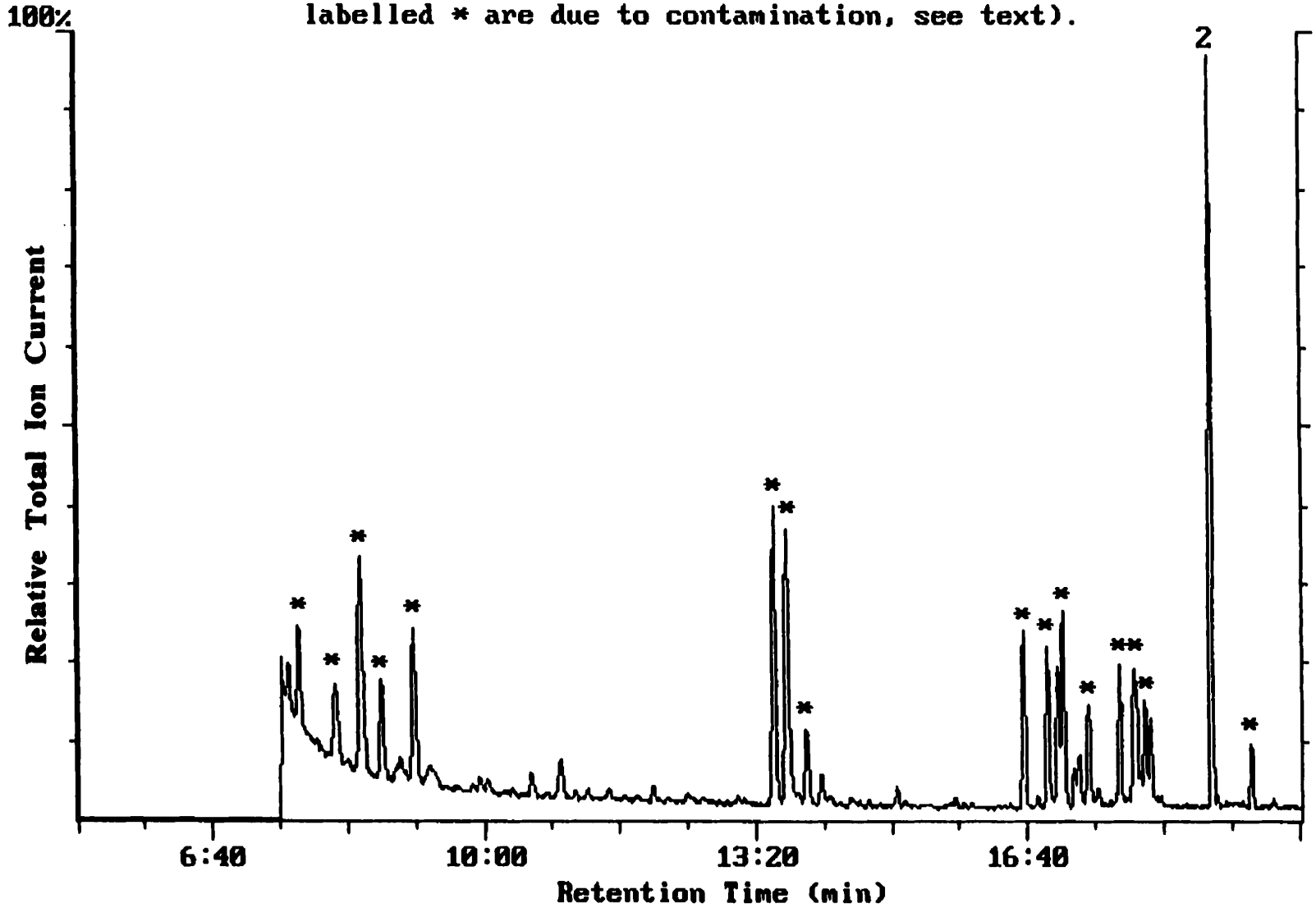

Figure 4.19. Mass spectrum of the deuterolysis product (peak 1, Figure 4.18a) resulting from the deuterolysis of the Al atom-chlorobenzene reaction mixture.

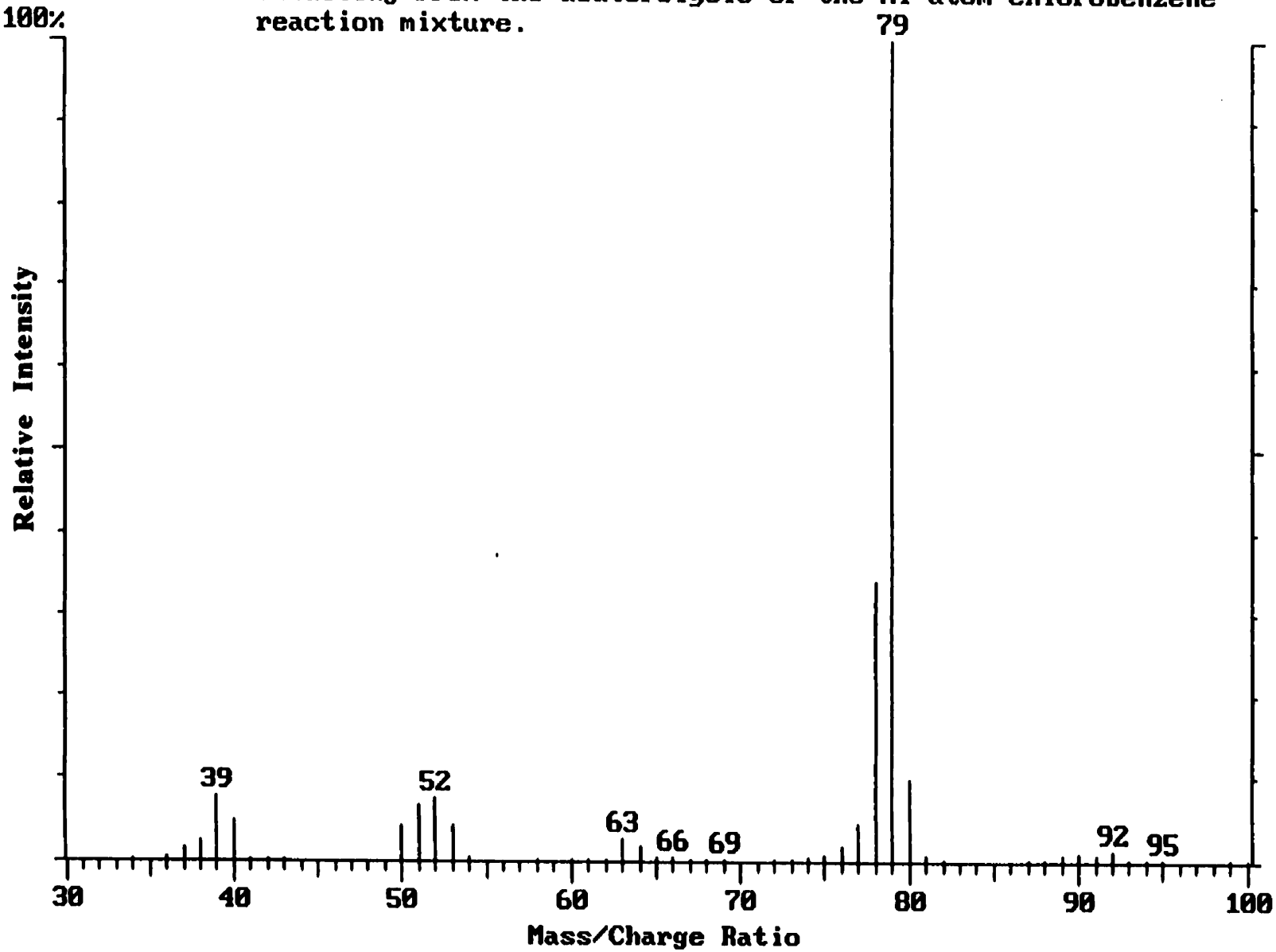

Figure 4.20. Mass spectrum of the deuterolysis product (peak 2, Figure 4.18b) resulting from the deuterolysis of the Al atom-chlorobenzene reaction mixture.

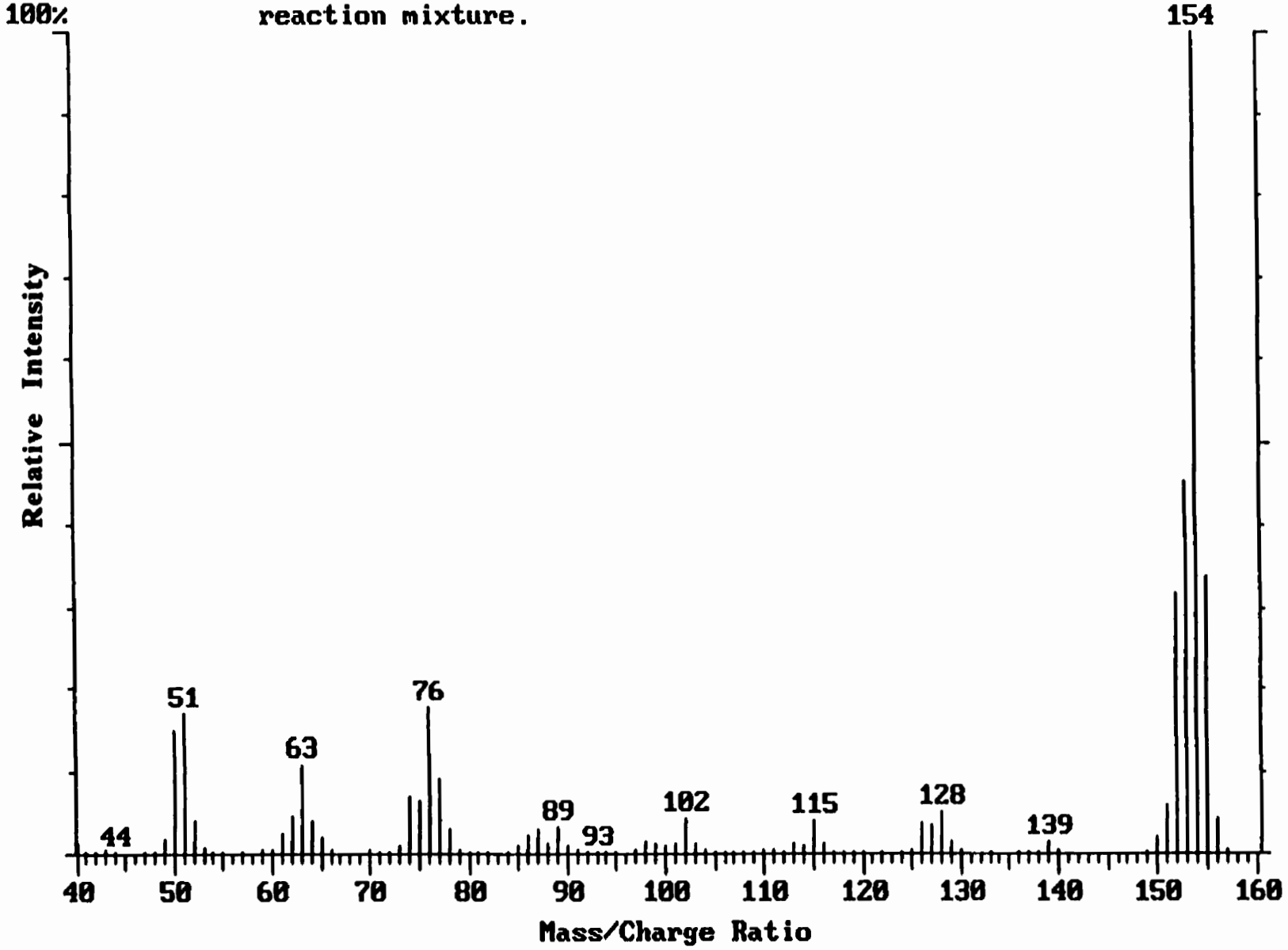

Table 4.14. Retention times and mass spectral data for deuterolysis products resulting from the reaction of Al atoms and chlorobenzene.

Peak No.	Retention Time (min)	m/e for main fragments*
1	3:34	39(6.7) 51(5.0) 63(2.4) 77(3.6) 78(30.5) 79(100) 80(47.9)
2	18:53	40(1.6) 50(14.0) 51(16.7) 63(10.4) 74(7.0) 75(6.7) 76(17.6) 77(9.2) 78(2.7) 89(3.5) 102(4.1) 115(4.1) 128(5.5) 139(1.7) 152(32.9) 153(44.2) 154(100) 155(34.9)
Deuterated benzene	3:32	39(14.2) 51(19.2) 63(3.5) 77(10.3) 78(45.2) 79(100) 80(52.9)
1,1'-Biphenyl	18:55	40(4.1) 50(11.0) 51(26.3) 63(10.3) 74(3.2) 75(4.0) 76(23.2) 77(11.3) 78(4.2) 89(5.0) 102(6.6) 115(4.5) 128(5.1) 139(1.0) 152(43.2) 153(44.0) 154(100) 155(36.1)

* The number in brackets represents the percentage of the base peak.

The fact that deuterated benzene and 1,1'-biphenyl are formed when the Al-chlorobenzene reaction mixture undergoes deuterolysis suggests that the Al atom inserts into the C-Cl bond, forming a weak complex. Deuterolysis of the insertion product yields deuterated benzene. Dissociation of the insertion product results in the formation of the benzene radical and •AlCl. Two benzene radicals can react together to form 1,1'-biphenyl. The results also show that 1,1'-biphenyl was present in larger quantities than deuterated

benzene (ratio 3:1) suggesting that radical-radical reaction is more favorable than radical-deuterium reaction, scheme 4.19.

In previous reactions, Al atoms mediated the reduction of the benzene ring and upon hydrolysis a cyclohexadiene compound was formed. In this reaction, Al atoms did not reduce the benzene ring. They inserted into the C-Cl bond.

There have been no previous studies reported for the Al-chlorobenzene reaction by any group. This compound was mainly studied to investigate the reactivity of Al atoms with a compound (chlorobenzene) with different competitive sites (C=C and C-Cl).

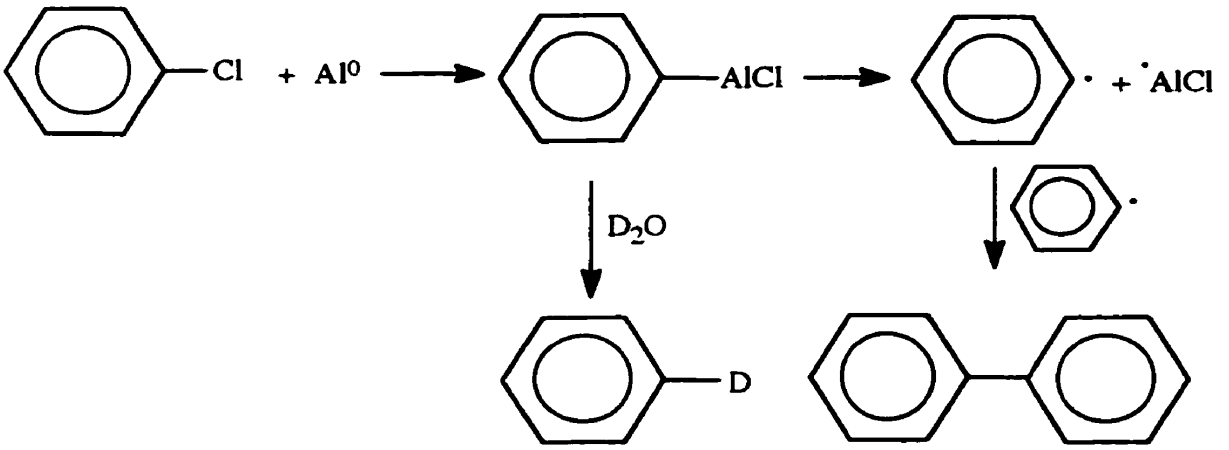

Scheme 4.19. Proposed mechanism for the Al atom, chlorobenzene and deuterium oxide reaction.

4.1.5 Reaction of Al Atoms with *p*- Bromotoluene:

We next reacted Al atoms with *p*- bromotoluene. The objective was to determine the reactivity of Al atoms towards several functional groups. From the study on benzene we determined that Al atoms reduce the aromatic ring to give 1,4-cyclohexadiene. When toluene was reacted with Al atoms, reduction of the aromatic ring resulted in the formation of 1-methyl-1,4-cyclohexadiene. Al atoms were also shown to insert into C-halogen bonds in the reactions involving trifluorotoluene and chlorobenzene. These results would suggest that the aromatic ring and C-Br bond of *p*- bromotoluene are both potential reactive sites for reaction with Al atoms.

4.1.5.1 Hydrolysis of the intermediate formed in the reaction of Al atoms and *p*- bromotoluene:

This reaction was carried out at the National Research Council (NRC) in Ottawa and analyzed in our laboratory at Laurentian University. Aluminum atoms were reacted with *p*- bromotoluene by the same method described in section 3.1.2.5. A typical total ion current (TIC) chromatogram of the hydrolysis products is presented in Figure 4.21. The peaks of interest are labelled 1, 2 and 3 and have been assigned to toluene, bromobenzene and *p*- bromotoluene respectively based on a comparison of the retention times and mass spectral data with those of authentic samples. The mass spectral data of the compounds identified as 1 and 2 in Figure 4.21 are presented in Table 4.15 and Figures 4.22 and 4.23.

The amount of toluene and bromobenzene in the mixture was 4.3% and 5.2%, respectively.

Figure 4.21. Total ion current chromatogram of the products resulting from hydrolysis of the organometallic compounds formed in the reaction of Al atoms and p-bromotoluene. (The compounds labelled * are due to contamination, see text).

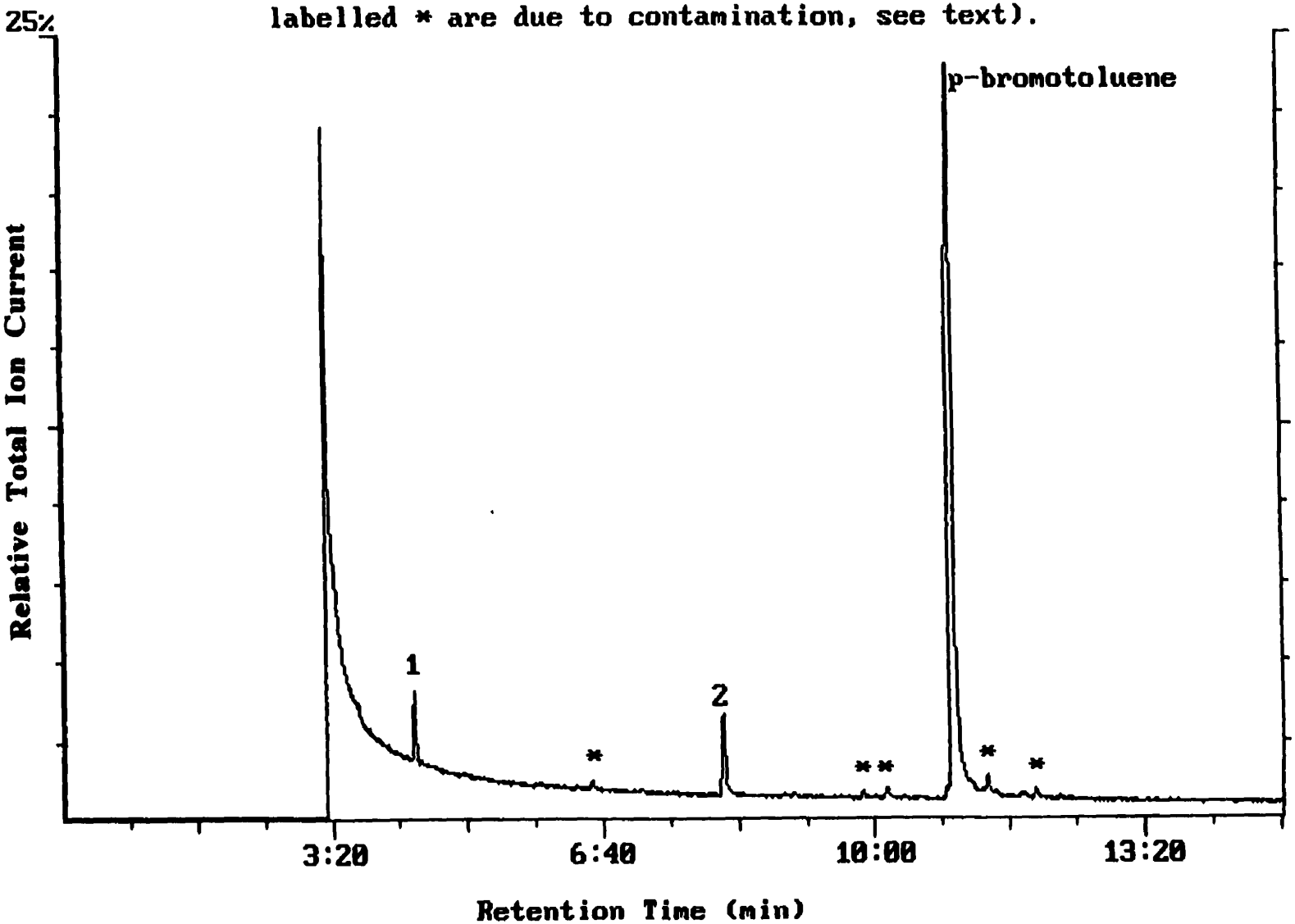

Figure 4.22. Mass spectrum of the hydrolysis product (peak 1, Figure 4.21) resulting from the hydrolysis of the Al atom-p-bromotoluene reaction mixture.

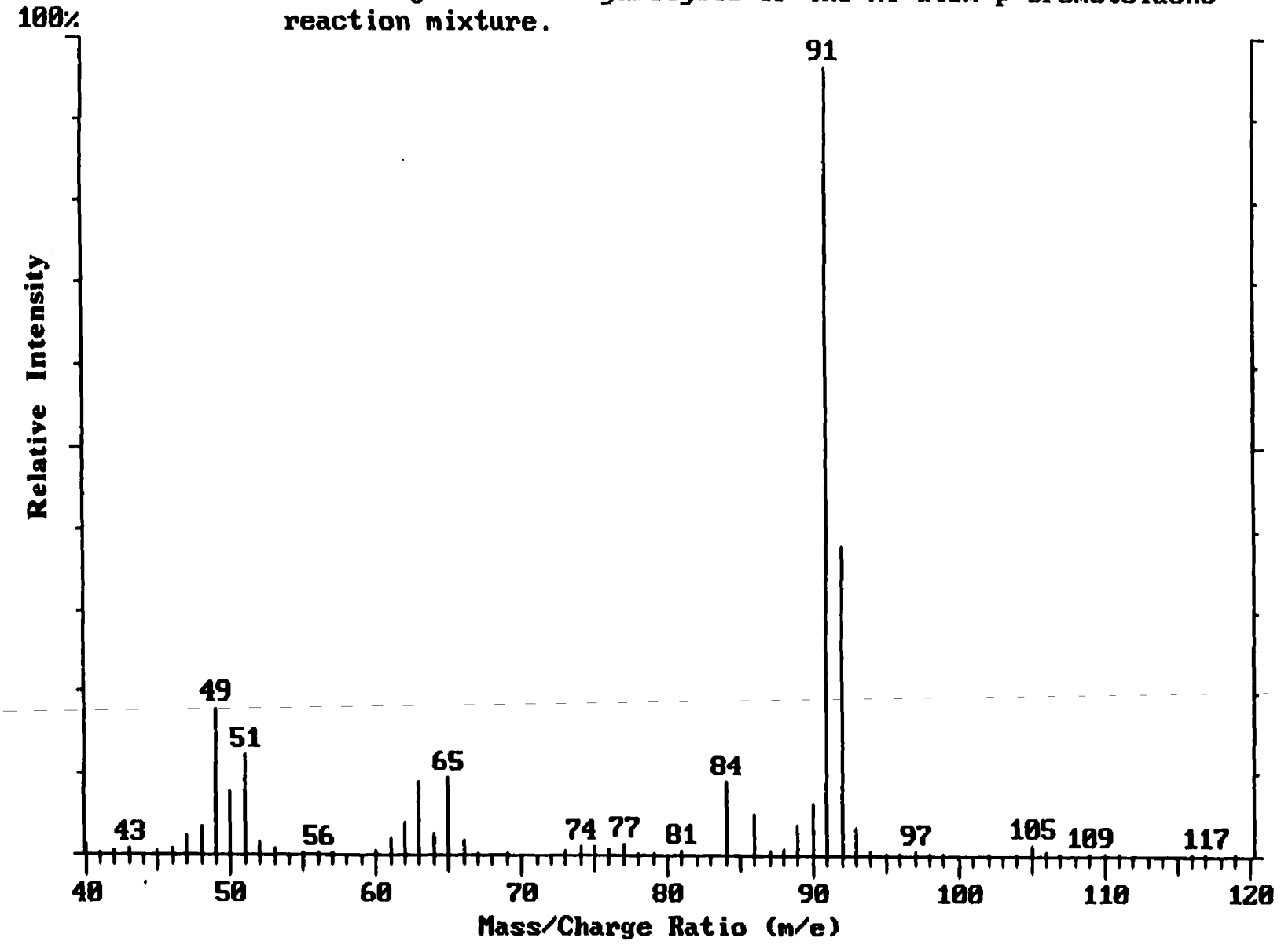

Figure 4.23. Mass spectrum of the hydrolysis product (peak 2, Figure 4.21) resulting from the hydrolysis of the Al atom-*p*-bromotoluene reaction mixture.

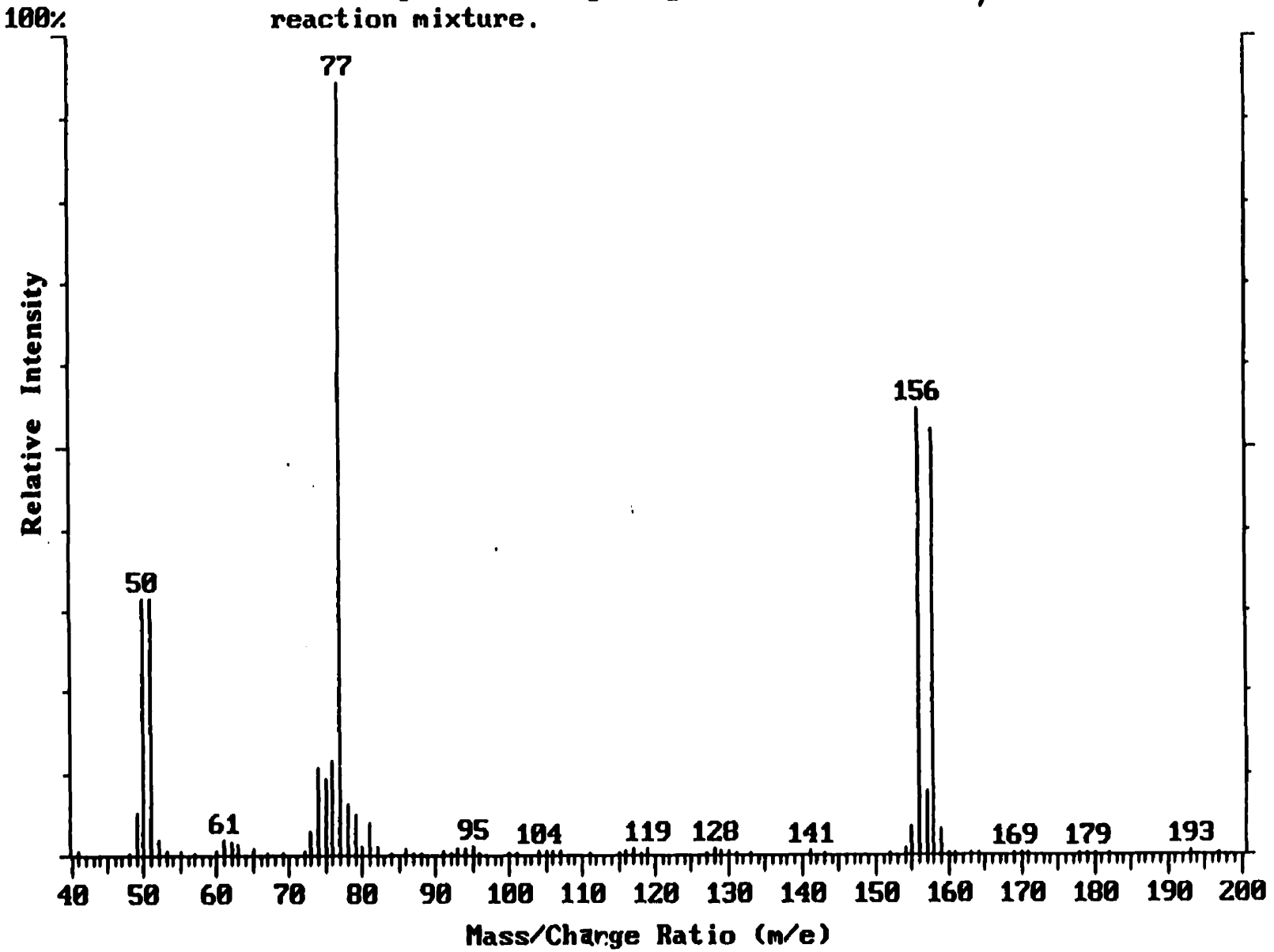

Table 4.15. Retention times and mass spectral data for hydrolysis products resulting from the reaction of Al atoms and *p*- bromotoluene.

Peak No.	Retention Time (min)	m/e for main fragments*
1	4:21	39(22.2) 62(0.04) 65(9.1) 77 (1.8) 85(0.1) 86(0.1) 90(6.0) 91(100) 92(35.4)
2	8:10	40(24.4) 50(33.2) 51(40.3) 52(2.1) 65(0.7) 76(11.9) 77(100) 130(0.5) 156(57.0) 157(7.2)158(54.8)
Toluene	4:22	39(22.2) 62(1.4) 65(15.3) 77 (1.9) 85(0.2) 86(0.2) 90(0.9) 91(100) 92(28.7)
Bromobenzene	8:10	40(28.3) 50(42.3) 51(51.7) 52(5.6) 65(0.01) 76(14.5) 77(100) 130(0.9) 156(62.1) 157(12.5)158(55.1)

* The number in brackets represents the percentage of the base peak.

A mechanism for the fragmentation of toluene has previously been presented, section 4.1.1.1.2, scheme 4.6.

A mechanism for the fragmentation of the molecular ion, $C_6H_5Br^+$, is proposed as shown in scheme 4.20. The molecular ion, $C_6H_5Br^+$ (m/e=156), loses a Br or HBr to form $C_6H_5^+$ (m/e=77) and $C_6H_4^+$ (m/e=76). The $C_6H_5^+$ and $C_6H_4^+$ ions lose C_2H or C_2H_2 to form $C_4H_4^+$ (m/e=52), $C_4H_3^+$ (m/e=51) and $C_4H_2^+$ (m/e=50) , respectively. The molecular ion can also lose CBr or C_2H_2 to form $C_5H_5^+$ (m/e=65) and $C_4H_3Br^+$ (m/e=130), respectively. Fragmentation of $C_5H_5^+$ yields $C_4H_4^+$ (m/e=52) and $C_3H_3^+$ (m/e=39). The ion $C_4H_3Br^+$ ion fragments to $C_4H_3^+$ (m/e=51) and $C_3H_3^+$ (m/e=39).

Alternatively, the molecular ion can lose one H to form $C_6H_4Br^+$ (m/e=155) which in turn loses C_2HBr yielding $C_4H_3^+$ (m/e=51).

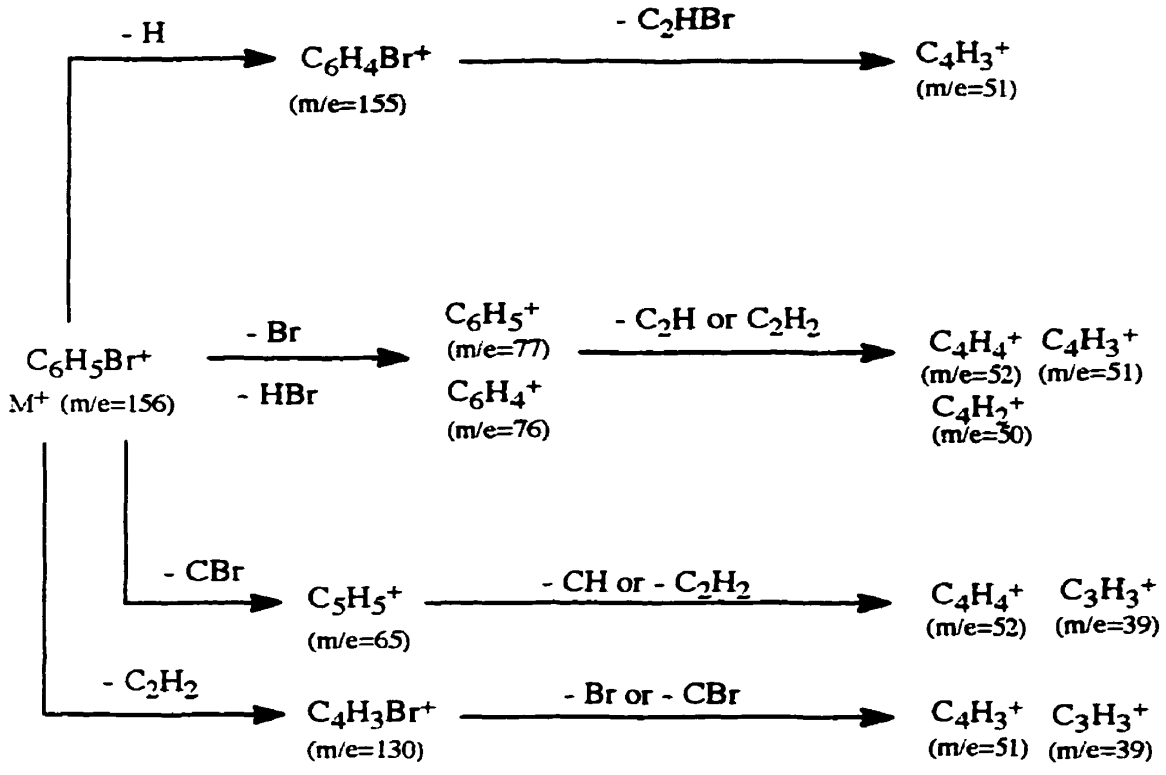

Scheme 4.20. Fragmentation scheme for bromobenzene.

To explain the formation of toluene from bromotoluene we propose that Al atoms insert into the C-Br bond (D = 280 ± 21 kJ/mol)[53] to form $CH_3C_6H_4AlBr$. Hydrolysis of $CH_3C_6H_4AlBr$ yields toluene. In the case of bromobenzene, Al atoms insert into the C-CH_3 bond (D = 607 ± 21 kJ/mol)[53] forming $CH_3AlC_6H_4Br$. Subsequent hydrolysis of the organoaluminum compound leads to the formation of bromobenzene, scheme 4.21.

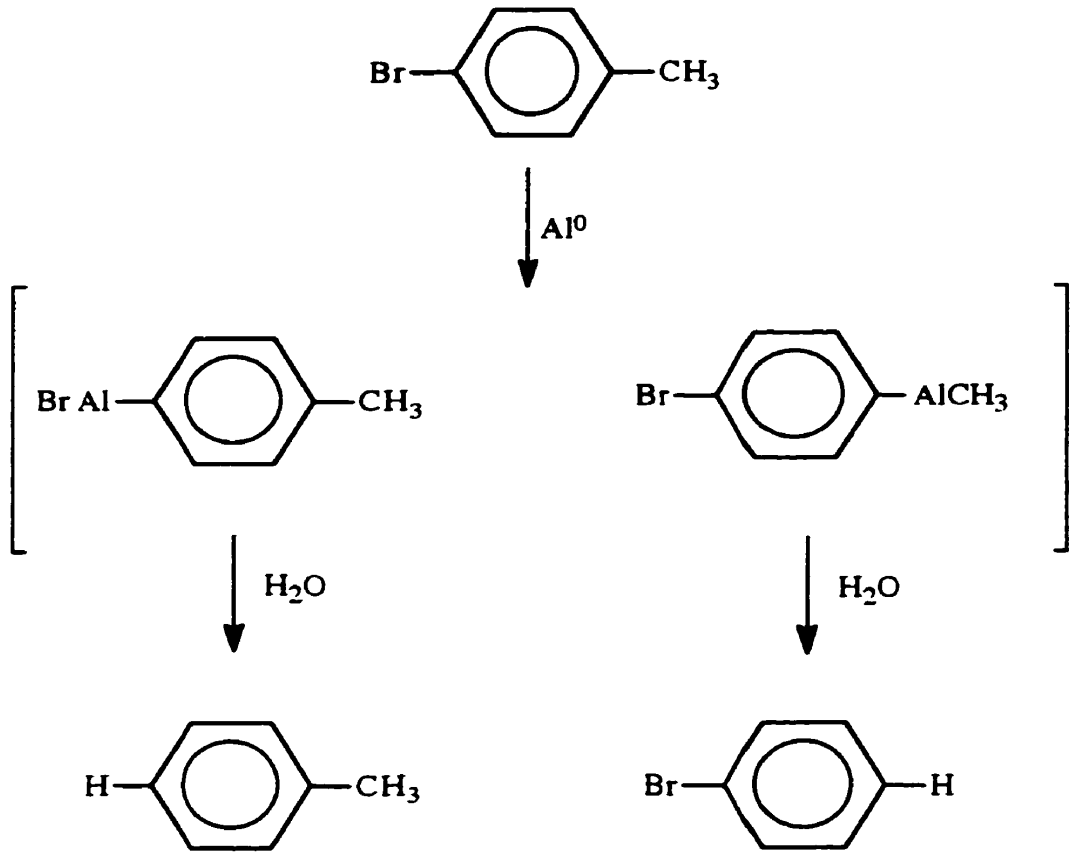

Scheme 4.21. Proposed mechanism for the Al atom, *p*- bromotoluene and water reaction.

4.2. Theoretical Study of The Interaction of Aluminum Atoms with Hydrocarbons:

Aluminum atoms are known to interact with hydrocarbons such as acetylene,[32,33] ethylene[31,34,38,64], butadiene[42], and benzene[36,38,65]. However, there is controversy concerning the structure of the complex with even the simplest hydrocarbon. The interactions between an Al atom and various small organic molecules have recently attracted much theoretical and experimental interest. Organoaluminum σ bonds are typically strong, and their electronic structure can often be qualitatively understood by using Hartree-Fock calculations.

Recent ab initio quantum chemical studies of the chemical bond between the Al atom and organic molecules (C_2H_2, C_2H_4, C_6H_6) have shown that strong coupling between different electronic states of the Al atom is an important factor in the bond formation.[46,47]

McKee[46], Silva and Head[47] studied the Al-benzene complex theoretically. Their results support the formation of a complex similar to the one suggested by Howard et al.[36], where Al interacts with the two para-carbons forming a σ-type complex.

An exploratory study of a substituted benzene derivative (toluene) has been included in the thesis to assess the effect that a side group (methyl) can have on the interaction of Al with such compounds. The presence of a side group can affect the net atomic charge and atomic spin population around the ring producing different sites for electrophilic, nucleophilic, or radical attacks.

All calculations have been made using the Gaussian 92 Program.[87] Geometries have been optimized at the UHF/6-31G* level which includes a set of d-orbitals on the Al atom. Single point calculations were done at the same level of theory. This level of theory has been shown to give reasonable results in several studies of Al-containing species.[46,47]

Ab initio quantum chemical studies of Al with organic molecules are only in the early stages. Thus, only acetylene, ethylene, and butadiene have received great attention recently.[46,47] In an attempt to broaden our understanding of the chemistry of Al, we have examined theoretically the bonding of Al atoms with benzene and toluene.

4.2.1 Reaction of Aluminum Atoms with Hydrocarbons:

4.2.1.1 Reaction of Al atoms with benzene:

McKee carried out his calculations by using the Gaussian 88 program.[46] Geometries were optimized at the UHF/3-21G* levels which include a set of d orbitals on the Al atom. Silva and Head used restricted open shell Hartree-Fock (ROHF) calculations and analytical gradients.[47] Their results were computed using the Dunning-Hay split valence basis for C[9s5p/3s2p], H[4s/2s], and Al[11s7p1d/6s4p1d] where the Al basis has been augmented with a d polarization function (with screening exponent, $\zeta = 0.25$). The theoretical calculations of the Al-benzene complex were restricted to a doublet state (multiplicity = 2).

The ab initio calculations of McKee[46] and Silva[47] on the Al-benzene complex predict that Al interacts with benzene by forming σ-bonds with the two *para* -carbons (boat complex), scheme 4.22.

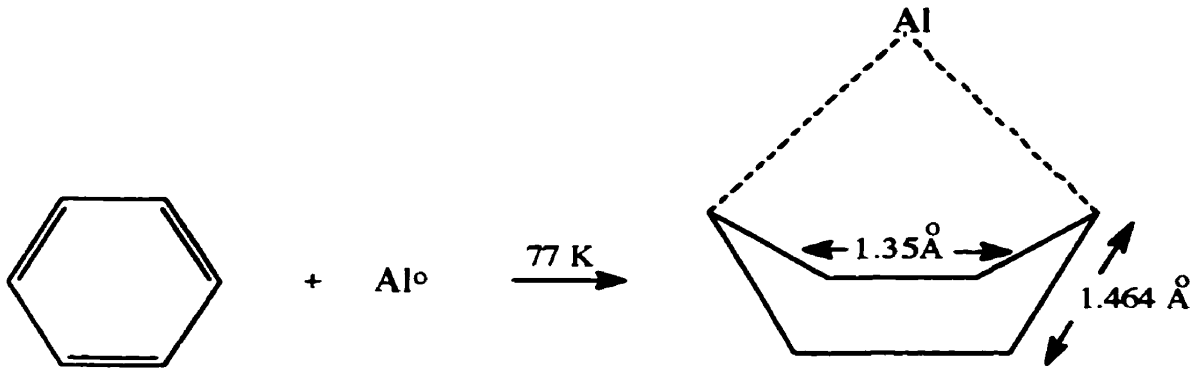

Scheme 4.22. Formation of Al-benzene boat complex.

The boat complex has C_{2v} symmetry. When Al is centred above a planar benzene ring, the symmetry is C_{6v}. The theoretical calculations show that the C_{2v} complex has lower energy than the C_{6v} complex. It was determined that the benzene ring distorts, producing inequivalent C atoms which form a boat structure with the two *para* carbons bent out of the benzene plane by 28°.[46,47] Also the C-C bond length has decreased to 1.35 Å for the two in plane distances and increased to 1.46 Å for the four out of plane distances. The Al-C distance is 2.25 Å which is shorter than that found in the C_{6v} complex (2.56 Å).

We first repeated the work of McKee using the Gaussian 80 program. Geometries were optimized at the UHF/3-21G level. A comparison of the results with those reported in the literature allowed us to assess the validity of our approach.

The first step of our calculations was to study all the possible structures of the Al-benzene complex where benzene is considered as a "frozen", planar structure. Five series of structures were considered with Al approaching the plane of the benzene ring at 0°, 30°, 60°, 90° and centred on top of the ring (C_{6v} symmetry), scheme 4.23.

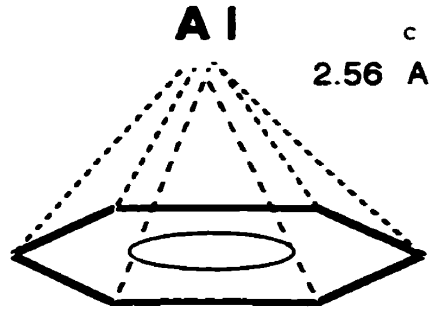

Scheme 4.23. The Al-benzene high symmetry complex (C_{6v}).

The total energy (in hartrees) was measured and plotted against the Al-ring distance (i.e., the distance from Al to the centre of the ring), Figure 4.24. Figure 4.24 shows that the transition structure of the C_{6v} complex has the lowest energy (-469.9728 hartree) at an Al-ring distance of 3.75 Å, and as Al gets closer to the ring, the total energy increases. Because of the relatively long Al-ring bond length (the Al-C will be longer than 3.75 Å), the complex appears to be weakly bound.

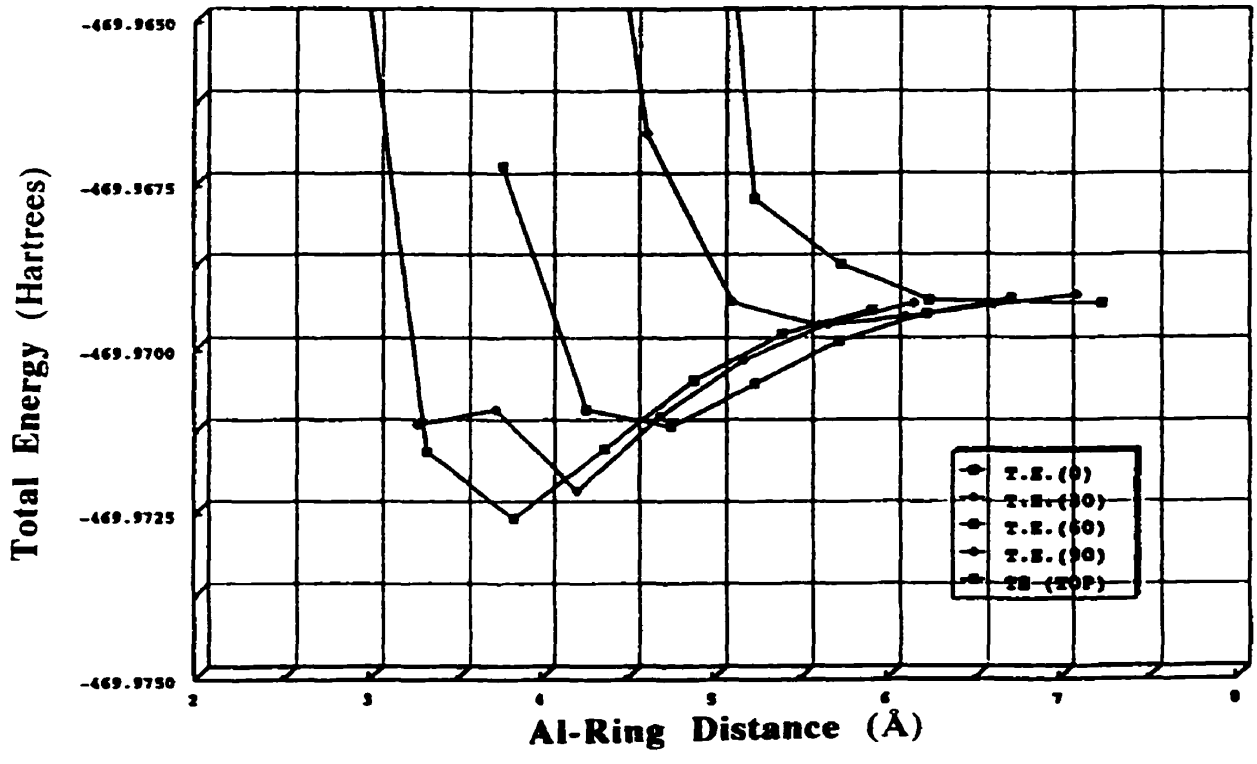

Figure 4.24. Plot of the total energy (in hartrees) of the Al-benzene complex vs. the distance from the Al to the centre of the benzene ring.

Our experimental results show that Al interacts with benzene forming a σ 1,4-complex. The σ 1,4-complex formation suggests that Al approaches the benzene ring from the top and binds with C-1 and C-4 of the benzene ring, forming a C_{2v} complex (boat complex). Therefore, we decided to study a complex with C_{2v} symmetry and to compare the results with that of the C_{6v} complex. For this type of calculation we used the Gaussian 92 program, since it allows a computation for an Al atom with a 6-31G* basis set.

Table 4.16. Total energy calculated at the UHF/6-31G* level for the lowest doublet states of Al-benzene complexes with C_{6v} and C_{2v} symmetry in their equilibrium geometries.

Type of Complex	Total Energy (hartree)	Al-ring Bond Length (Å)
C_{6v}	-472.5333	3.97
C_{2v}	-472.5621	2.21

Table 4.16 shows that the Al-C bond length for the C_{2v} complex is much shorter than that of C_{6v}. This difference suggests that in the C_{2v} complex, Al forms a stronger complex with benzene than in the C_{6v} complex.

Other important quantities of the SCF calculations considered were the total atomic charges and total atomic spin densities. These two quantities can help rationalize and eventually predict the reactive sites of the Al-complexes.

Since the C atoms are equivalent in the C_{6v} complex, we expect each one of its atoms to have the same atomic charge and spin density. In our calculations of this complex, we have observed small differences. We suspect the reason for these differences is the basis set (6-31G*) which adds the six "cartesian" d-type functions ($3d_{xx}$, $3d_{yy}$, $3d_{zz}$, $3d_{xy}$, $3d_{xz}$, and $3d_{yz}$) to the Al atom. These orbitals are positioned over the benzene ring, so only certain carbon atoms are aligned with these orbitals causing different charge

distribution across the benzene ring. When the same procedure is applied to benzene alone, the charge distribution was found to be symmetrical.

We have corrected the atomic charge and spin density values by calculating the average atomic charge and spin density of each equivalent atom, and this will represent the actual charge and spin density of each atom without the effect of the d-type functions of Al (as represented in the basis set 6-31G*), Table 4.17. This problem could be eliminated with better basis sets, but this possibility was beyond our computational capabilities.

Table 4.17. Calculated and corrected Mulliken atomic charges and spin densities for the Al-benzene complex with C_{6v} symmetry. (The values for the hydrogen atoms, with net positive charge are omitted).

Atom	Calculated Values		Corrected Values	
	Atomic Charge	Spin Density	Atomic Charge	Spin Density
Al	-0.0257	0.9993	-0.0257	0.9993
C1	-0.207	0.0018	-0.201	0.0014
C2	-0.198	0.0011	-0.201	0.0014
C3	-0.198	0.0012	-0.201	0.0014
C4	-0.207	0.0018	-0.201	0.0014
C5	-0.198	0.0011	-0.201	0.0014
C6	-0.198	0.0012	-0.201	0.0014

Table 4.18 compares the Mulliken atomic charges and spin densities on Al and carbon atoms for the two complexes (C_{6v} and C_{2v}). For the complex with C_{2v} symmetry, the results show that substantial spin density resides on the benzene ring due to the transfer of about 90% of the Al unpaired electron. Most of the electron density is localized at the 1,4-positions, where we would expect the formation of the boat complex (C_{2v}). For the C_{6v}

symmetry, the results show no electron transfer from Al to the ring, consistent with its characterization as a weak complex. These results, although of only a qualitative nature, can serve for a comparison with the Al-toluene complex results.

Table 4.18. Selected Mulliken atomic charges and spin densities calculated at the UHF/6-31G* level for the Al-benzene complexes C_{6v} and C_{2v}.

Atom	Atomic Charge		Spin Density	
	C_{6v}	C_{2v}	C_{6v}	C_{2v}
Al	0.0257	0.356	0.9993	0.016
C-1	-0.201	-0.466	0.0014	0.449
C-2	-0.201	-0.166	0.0014	0.0156
C-3	-0.201	-0.166	0.0014	0.0156
C-4	-0.201	-0.466	0.0014	0.449
C-5	-0.201	-0.166	0.0014	0.0156
C-6	-0.201	-0.166	0.0014	0.0156

In summary, the theoretical data suggest that when Al atoms react with benzene, scheme 4.24, an Al-benzene complex (**a**) should be formed. Hydrolysis of this complex, would result in the formation of 1,4-cyclohexadiene compound (**b**).

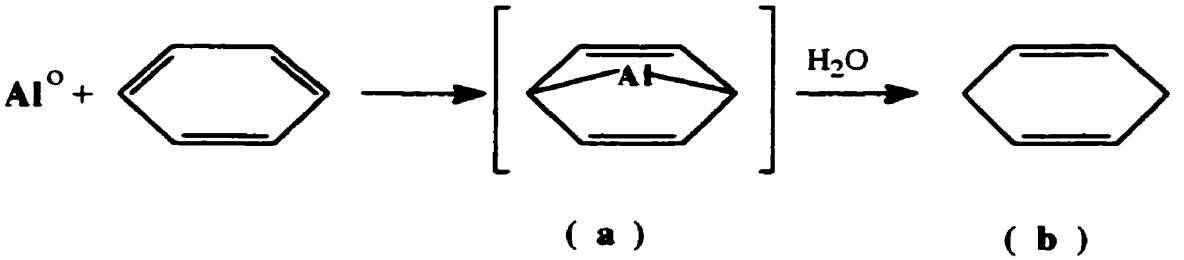

Scheme 4.24. Proposed mechanism for the Al-benzene reaction.

4.2.1.2 Reaction of Al atoms with Toluene:

There are no reported theoretical studies done on this system. To support our experimental results, we have decided to perform exploratory ab initio quantum chemical calculations on the Al-toluene complex and study the effect of the methyl group on the type of interaction between Al and toluene. As before, we have performed UHF calculations on the lowest-lying doublet state, with the largest basis set permitted by the then limited computational facilities at Laurentian University.

The methyl group of toluene, being an electron donor, should affect the atomic charge and spin density around the ring and influence the site of Al-C bond formation.

We approached the study of the equilibrium geometry of this complex in a similar way to that used for the Al-benzene complex. We used the Gaussian 92 computer program with a polarized basis set (6-31G*). The other conditions were the same as described in section 4.2.1.1 of the thesis.

Our experimental results show that when Al was reacted with toluene and water at 77 K and low pressure, 1-methyl 1,4-cyclohexadiene was formed, scheme 4.25.

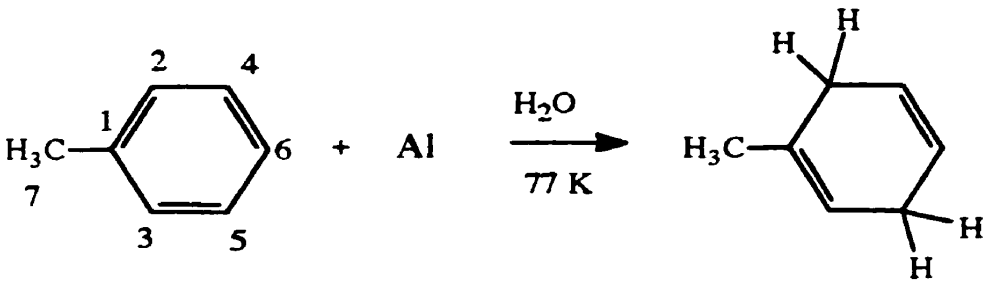

Toluene

1-methyl-1,4-cyclohexadiene

Scheme 4.25. The aluminum-toluene reaction.

The formation of this compound suggests that Al adds to toluene by forming a σ bond across C-2 and C-5. The goal of our theoretical computation was to study whether Al-complexation "activates" these positions in such a way that they are susceptible to attack by a H^+ ion from the water.

The first step of our theoretical study was to determine the effect of two toluene isomers on the Al-C bond, scheme 4.26. The computation was performed at fixed C_s symmetry.

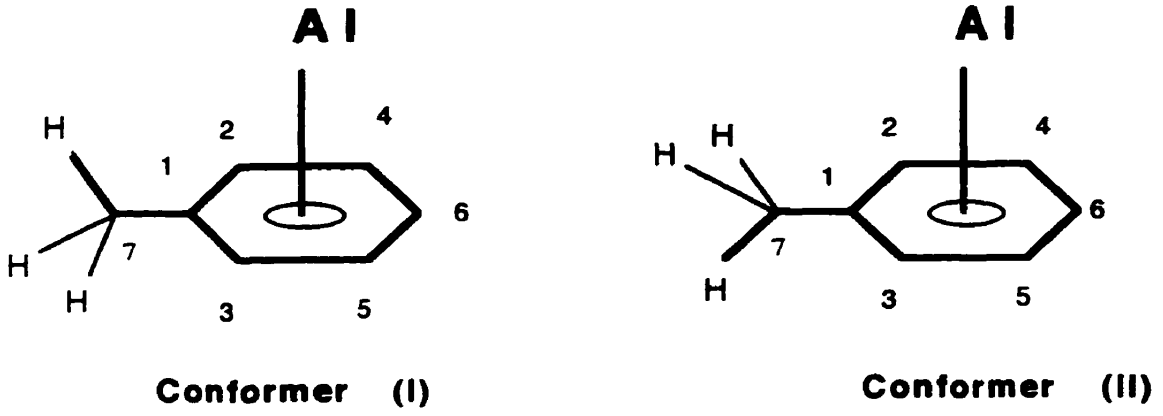

Scheme 4.26. Different conformers of the Al-toluene complex.

Conformer (I) has one of its methyl hydrogens in the symmetry plane containing Al (the one bisecting the benzene ring along the 1-4 position). The other two methyl hydrogens are out of the plane. The reason for carrying out this test was to see if the presence of a hydrogen atom in the same plane with Al would affect the length and position of the bond due to the steric effect. The results of our study are summarized in Table 4.19.

Table 4.19 shows the various Al-C distances of the two conformers of the Al-toluene complex at their equilibrium geometries. The results show that the Al-C6 distance is

shorter in conformer (II), 3.72 Å. In conformer (I) the position of the Al atom has shifted away from the hydrogens of the methyl group towards C6, scheme 4.27, when one of the methyl hydrogens is on the same side of the ring as the Al atom.

Table 4.19. Comparison of the various Al-C distances of the two Al-toluene conformers at their equilibrium geometries.

Bond Type	Al-C Distances (Å)	
	Conformer (I)	Conformer (II)
Al-C1	4.64	4.49
Al-C2	4.44	4.27
Al-C3	4.44	4.27
Al-C4	4.04	3.90
Al-C5	4.04	3.90
Al-C6	3.82	3.72
Al-C7	5.61	5.47

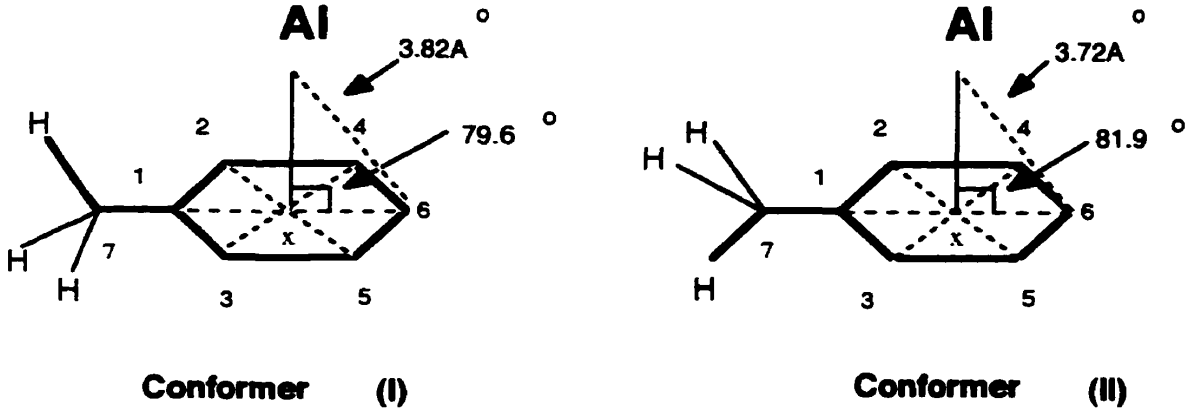

Scheme 4.27. The Al-C6 distances of the two Al-toluene conformers.

In other words, the presence of a methyl hydrogen on the same side of the benzene ring as the Al atom affects the equilibrium geometry of the Al-toluene complex. The Al-X-C6 angle of conformer (I) is smaller than that of conformer (II) due to the repulsion between Al and hydrogen, (X represents the centroid of the toluene ring). This repulsion causes the Al atom to shift away from the methyl hydrogen by 10.4° producing a longer Al-C bond. For conformer (II) where the hydrogen is pointing "down", the Al-C bond is shorter (3.72Å) and the Al-X-C_6 angle is larger due to less steric hindrance. Other quantities have to be considered to understand the relevance of the structural difference between the complexes.

Table 4.20 shows the results of the total energy calculations of the reaction of Al atoms with conformers (I) and (II). Conformer (II) was found to have lower energy than conformer (I) which indicates its greater stability.

Table 4.21 shows the electron density of both conformers to be very similar. From this observation, we conclude that either complex could be used to analyze the reactivity properties of an Al-toluene system.

Table 4.20. Comparison of the total energy of the two Al-toluene conformers.

Conformer	Total Energy (hartree)
Conformer (I)	-511.5974
Conformer (II)	-511.5987

Table 4.21. Comparison of the net atomic charges and spin densities of the two Al-toluene conformers. (Values for the hydrogen atoms are omitted).

Atom	Conformer (I)		Conformer (II)	
	Net Charge	Spin Density	Net Charge	Spin Density
Al	-0.02721	1.0007	-0.03145	1.0003
C-1	0.06323	0.6720	0.06285	0.6740
C-2	-0.2187	0.6800	-0.2184	0.6769
C-3	-0.2187	0.6800	-0.2184	0.6769
C-4	-0.2016	0.6674	-0.2048	0.6637
C-5	-0.2016	0.6674	-0.2048	0.6637
C-6	-0.2112	0.6594	-0.2100	0.6606
C-7	-0.5264	0.0780	-0.5222	0.0785

The final stage of our study was to determine the position on the toluene ring most likely to undergo H^+ ion attack. The source of the H^+ ion is water. Analysis of the net atomic charges and spin densities of conformer (II) in Table 4.21 can help us propose a possible reaction mechanism. The net atomic charges results show that around the toluene ring C2 and C3 are slightly more electron rich (-0.22), scheme 4.28. These positions also exhibit a slightly larger spin density (0.68), scheme 4.29. Both carbons are equivalent and most likely only one would be involved in one step of the reaction.

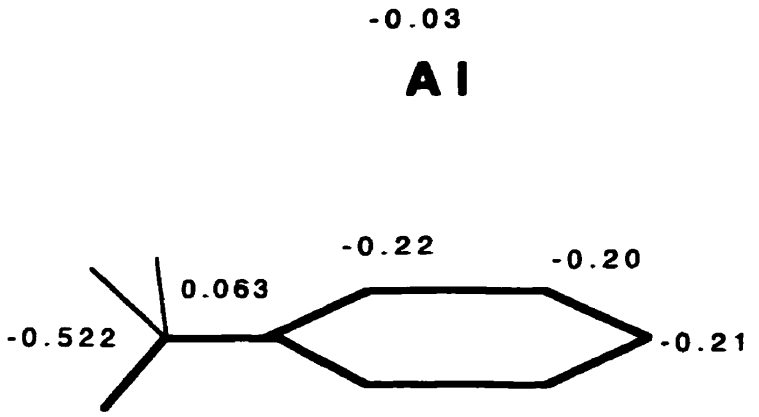

Scheme 4.28. Net atomic charges for the Al-toluene complex

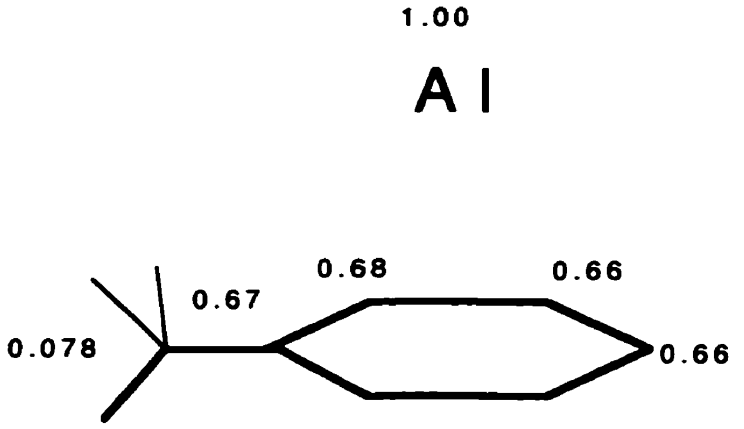

Scheme 4.29. Total atomic spin densities for the Al-toluene complex.

The theoretical results indicate that C2 or C3 is the site more likely to form a bond with the H ion. The other site of attack (C4, C5, C6, and C7) could not be determined from our calculations. This would tend to suggest that the reaction could be a 2 step process. C2 or C3 is attacked by H^+ and a new intermediate is formed. In the second step H^+ attacks C5 to give 1-methyl-1,4-cyclohexadiene. If toluene reacted in a similar fashion as benzene, we would form the Al-toluene complex: (**a**) which upon hydrolysis gives the 1-methyl-1,4-cyclohexadiene compound (**b**), scheme 4.30. However, this is highly unlikely, because the spin densities of C2 and C5 are not equivalent.

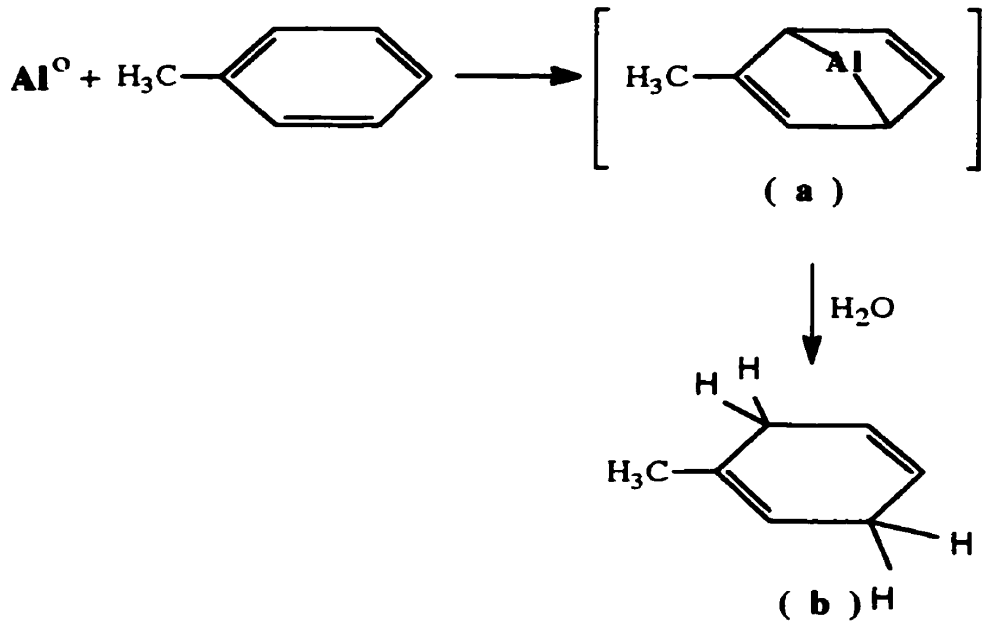

Scheme 4.30. Proposed mechanism for the Al-toluene reaction. (Based on indications from the ab initio computations).

5. CONCLUSION

Group 13 metal atoms (Al, Ga, In and Tl) were reacted with benzene, toluene, trifluorotoluene, bromotoluene and chlorobenzene at 77 K in hydrocarbon matrices on a rotating cryostat. The hydrolysis and deuterolysis products resulting from the reaction mixtures were studied by gas chromatography-mass spectrometry (GC-MS).

The hydrolysis and deuterolysis products of Al- and Ga-benzene reactions indicate the formation of 1,4-cyclohexadiene and 1,4-cyclohexadiene-d_2 , respectively. Ionization and fragmentation schemes were constructed for 1,4-cyclohexadiene and 1,4-cyclohexadiene-d_2 through the use of mass spectral data.

1-Methyl-1,4-cyclohexadiene is the only hydrolysis product formed in the Al- and Ga-toluene reactions. Ionization and fragmentation schemes were constructed for 1-methyl-1,4-cyclohexadiene through the use of its mass spectral data.

In the reactions of Al and Ga atom with trifluorotoluene, the Al and Ga atoms insert into one, two or all three C-F bonds to form difluorotoluene, monofluorotoluene and toluene, respectively. Aluminum and gallium atoms also mediate the reduction of the aromatic ring to form four trifluoromethylcyclohexadiene isomers and two difluoromethylcyclohexadiene isomers. The trifluoromethylcyclohexadiene isomers were formed by addition of Al or Ga atom across the 1,2 position or 1,4 position of the aromatic ring. The difluoromethylcyclohexadiene isomers are the hydrolysis products of dialuminum and digallium adducts where an Al or Ga atom has inserted into one of the C-F bonds and a second Al or Ga atom has added either to the 1,2 position or the 1,4 position of the aromatic ring. In the case of the In atom reactions with trifluorotoluene, only three

major products were formed. Insertion of In atoms into one and three C-F bonds produced difluorotoluene and toluene, respectively. Indium atom also mediated the reduction of the aromatic ring to produce one trifluoromethylcyclohexadiene isomer. Thallium atoms did not react with trifluorotoluene. The reactivity order of the metal atom-trifluorotoluene reaction was found to be Al, Ga > In >> Tl.

Reaction of Al atoms with chlorobenzene and deuterium oxide formed two products, deuterated benzene and 1,1'-biphenyl. Aluminum atoms react with chlorobenzene by forming a σ-complex. Deuterolysis of the σ-complex resulted in the formation of deuterated benzene. Dissociation of the C-AlCl bond of the σ-complex results in a benzene radical which can further react to form 1,1'-biphenyl. Ionization and fragmentation schemes were constructed for deuterated benzene and 1,1'-biphenyl through the use of its mass spectral data.

Reaction of Al atoms with *p*- bromotoluene and water resulted in the formation of toluene and bromobenzene. Toluene and bromobenzene were formed by hydrolysis of the C-AlBr and C-$AlCH_3$ bonds respectively. Aluminum did not reduce the bromotoluene ring as in the case of toluene and benzene.

Theoretical methods were used to study the complexes formed between a neutral aluminum atom and the hydrocarbons, benzene and toluene. Six optimal structures for the aluminum-benzene complex have been studied theoretically with Al approaching the plane of the benzene ring at : (a) 0°, (b) 30°, (c) 60°, (d) 90°, (e) centered on top of the ring (C_{6v} symmetry) and (f) centered on top of the ring (C_{2v} symmetry). Structures (e) and (f) are most likely the forms of the complex observed in low-temperature ESR and GC-MS experiments. The C_{2v} complex involves a boat distortion of benzene and Al σ bond with the benzene out-of-plane *para* C atoms. We find little evidence for a stable Al π complex.

In agreement with experiment, the 1,4-complex (C_{2v}) is found to be lowest in energy at (-472.5621 hartree) the UHF/6-31G* level.

Two conformers (I and II) of the aluminum-toluene complex have been studied theoretically where Al approaches the plane of the toluene ring from the top. Conformer (I) has Al and one of its methyl hydrogens on the same side of the ring and in the same plane, while conformer (II) has one of its hydrogens on the other side of the ring from the Al and in the same plane. Conformer (II) was found to have lower energy (-511.5987 hartree) than conformer (I) (-511.5974). These results indicate that conformer (I) is less stable due to the steric effect caused by the H on the same side of the ring as Al. Analysis of the net atomic charges and spin densities of conformer (II) showed that C2 and C3 are slightly more electron rich and have larger spin densities than the other carbons making them the most probable site for H^+ attack. It is suggested that the Al-toluene reaction follows a 2-step mechanism. The first step could involve the attack at position C2 or C3 by H^+ ion, then the molecule would rearrange itself to give a new structure. The second step involves a H^+ attack at C5 to give the 1-methyl-1,4-cyclohexadiene.

The theoretical results appear to agree with some of the experimental results found for the reactions between Al and benzene and Al and toluene.

Finally, the alkylation reaction of the Al-benzene complex was studied. Reaction of Al atoms with benzene in the presence of CH_3I resulted in the formation of toluene. There was no evidence for the formation of methylcyclohexadiene. Formation of toluene indicates that Al atom reacted with CH_3I to produce the methyl radical. The methyl radical reacts with a benzene molecule yielding toluene.

6. REFERENCES

1. Frankland, E. *J. Chem. Soc.* **1849**, 2, 263.
2. Frankland, E. *Phil. Trans.* **1852**, 142, 417.
3. Walborsky, H.M. *Acc. Chem. Res.* **1990**, 23, 286.
4. Rochow, E.G. *J. Chem. Ed.* **1965**, 42, 41.
5. Ziegler, K. *Angew. Chem.* **1955**, 67, 541.
6. Natta, G. *J. Am. Chem. Soc.* **1955**, 77, 1708.
7. Pauson, P.L. *Nature* **1951**, 68, 1039.
8. Miller, S.A. *J. Chem. Soc.* **1952**, 632.
9. Powell, P. *Principles of Organometallic Chemistry*, 2nd ed.; Chapman and Hall: New York, 1988; pp 1-82.
10. Coates, G.E.; Green, M.L.H.; Powell, P.; Wade, K. *Principles of Organometallic Chemistry* ; Methuen & CO Ltd.: London, 1971; pp 1-24.
11. Elchenbroich, C.H.; Salzer, A. *Organometallics: A concise introduction*, 2nd ed.; VCH : New York, 1992; pp 75-93.
12. Paneth, F.A.; Hofeditz, W.H. *Chem. Ber.* **1929**, 62,1335.
13. Rice, F.D.; Johnston, W.R.; Evering, B.L. *J. Am. Chem. Soc.* **1932**, 3529.
14. Kasai, P.H.; McLeod, D. Jr. *J. Am. Chem. Soc.* **1979**, 101, 5860.
15. Rieke, R.D. *Acc. of Chem. Res.* **1977**, 10, 301.
16. Rieke, R.D. *Science* **1989**, 246, 1260.
17. Skell, P.S.; Westcott, L.D. *J. Am. Chem. Soc.* **1963**, 85, 1023.

18. Timms, P.L. *J. Chem. Ed.* **1972**, 49, 782.

19. Timms, P.L. *Angew. Chem., Int. Ed. Engl.* **1975**, 14, 273.

20. Skell, P.S.; Westcott, L.D.; Goldstein, J.P.; Engel, R.R. *J. Am. Chem. Soc.* **1965**, 87, 2829.

21. Timms, P.L. *Chem. Commun.* **1968**, 1525.

22. Klabunde, K.J. *Angew. Chem., Int. Ed.* **1975**, 14, 287.

23. Klabunde, K.J.; Efner, H. F. *Inorg. Chem.* **1975**, 14, 789.

24. a) Timms, P.L. *Chem. Eng. News* 1974, 52, 23; b) Mackenzie, R.; Timms, P.L. *J. Chem. Soc., Chem. Commun.* **1974**, 650.

25. Benfield, F.W.S.; Green, M.L.H.; Ogden, J.S.; Young, D. *Chem. Commun.* **1973**, 866.

26. Thomas, A.; Bennett, J.E. *Proc. R. Soc. London*, Ser. A **1964**, 280, 123.

27. Bennett, J.E.; Thomas, A.; Mile, B.; Ward, B. *Adv. Phys. Org. Chem.* **1970**, 8, 1.

28. Howard, J.A.; Joly, H.A.; Mile, B.; Histed, M.; Morris, H. *J. Chem. Soc., Faraday Trans. I* **1988**, 84, 3307.

29. Hallwachs, W.; Schafarik, A. *Ann.*, **1859**, 109, 206.

30. Ziegler, K. *Adv. Organomet. Chem.* **1968**, 6, 1.

31. Skell, P.S.; Wolf, L.R. *J. Am. Chem. Soc.* **1972**, 7919.

32. Kasai, P.H.; McLeod, D. Jr. *J. Am. Chem. Soc.* **1975**, 97, 5609.

33. Kasai, P.H.; McLeod, D. Jr.; Watanabe, J. *J. Am. Chem. Soc.* **1977**, 99, 3521.

34. Kasai, P.H. *J. Am. Chem. Soc.* **1982**, 104, 1165.

35. Mitchell, S.A.; Simard, B.; Raynor, D.M.; Hackett, P.A. *J. Phys. Chem.* **1988**, 92, 1655.

36. Howard, J.A.; Mile, B.; Tse, J.S.; Morris, H. *J. Chem. Soc., Faraday Trans. I* **1987**, 83, 3701.

37. Miralles-Sabater, J.; Merchan, M.; Nebot-Gil, I. *Chem. Phys. Lett.* **1987**, 142, 136.

38. Jarrett-Sprague, S.A.; Hillier, I.H. *J. Chem. Soc., Faraday Trans.* **1990**, 86, 1399.

39. Srinivas, R.; Sulzle, D.; Schwarz, H. *J. Am. Chem. Soc.* **1990**, 112, 8334.

40. Tse, J.S. *J. Am. Chem. Soc.* **1990**, 112, 5060.

41. Trenary, M.; Schaefer, H.F. III *J. Chem. Phys.* **1978**, 68, 4047.

42. Trenary, M.; Casida, M.E.; Brooks, B.R., Schaefer, H.F. III *J. Am. Chem. Soc.* **1979**, 101, 1638.

43. Chenier, J.H.B.; Howard, J.A.; Tse, J.S.; Mile, B. *J. Am. Chem. Soc.* **1985**, 107, 7290.

44. Howard, J.A.; Joly, H.A.; Mile, B.; Sutcliffe, R. *J. Phys. Chem.* **1991**, 95, 6819.

45. Howard, J.A.; Joly, H.A.; Mile, B. *J. Am. Chem. Soc.* **1989**, 111, 809.

46. Mckee, M.L. *J. Phys. Chem.* **1991**, 95, 7247.

47. Silva, S.J.; Head, J.D. *J. Am. Chem. Soc.* **1992**, 114, 6479.

48. Klabunde, K.J.; Tanaka, Y. *J. Am. Chem. Soc.* **1983**, 105, 3544.

49. Parnis, J.M.; Ozin, G.A. *J. Am. Chem. Soc.* **1986**, 108, 1699.

50. Chenier, J.H.B; Howard, J.A.; Joly, H.A.; LeDuc, M.; Mile, B. *J. Chem. Soc., Faraday Trans.* **1990**, 86, 3321.

51. Howard, J.A.; Joly, H.A.; Mile, B. *J. Chem. Soc., Faraday Trans.* **1990**, 86, 219.

52. Klabunde, K.J.,;Tanaka, Y.; Davis, S.C. *J. Am. Chem. Soc.* **1982**, 104, 1013.

53. CRC Handbook of Chemistry and Physics, 70th edition, CRC Press Inc.: Boca Raton, Florida, 1989-1990

54. Kasai, P.H.; Jones, P.M. *J. Am. Chem. Soc.* **1984**, 106, 8018.

55. Chenier, J.H.B.; Hampson, C.A.; Howard, J.A.; Mile, B.; Sutcliffe, R.J. *Phys. Chem.* **1986**, 90, 1524.

56. Howard, J.A.; Mile, B.; Morton, J.R.; Preston, K.F.; Sutcliffe, R. *Chem. Phys. Lett.* **1985**, 117, 115.

57. Howard, J.A.; Mile, B.; Morton, J.R.; Preston, K.F., Sutcliffe, R. *J. Phys. Chem.* **1985**, 90, 1033.

58. Hampson, C.A.; Howard, J.A.; Mile, B. *Chem. Commun.* **1985**, 966.

59. Howard, J.A.; Joly, H.A.; Edwards, P.P.; Singer, R.J.; Logan, D.E. *J. Am. Chem. Soc.* **1992**, 114, 474.

60. Histed, M.; Howard, J.A.; Joly, H.A.; Mile, B. *Chem. Phys. Lett.* **1989**, 161, 122.

61. Lefleur, R.D.; Parnis, J.M. *J. Phys. Chem.* **1992**, 96, 2429.

62. Jones, P.M.; Kasai, P.H. *J. Phys. Chem.* **1988**, 92, 1060.

63. Howard, J.A.; Joly, H.A.; Mile, B. *J. Phys. Chem.* **1992**, 96, 1233.

64. Parnis, J.M.; Ozin, G.A. *J. Phys. Chem.* **1989**, 93, 220.

65. Chenier, J.H.B.; Howard, J.A.; Mile, B. *J. Am. Chem. Soc.* **1987**, 109, 4109.

66. Loos, D.; Schnöckel, H.; Gauss, J.; Schneider, U. *Angew. Chem., Int. Ed. Engl.* **1992**, 31, 1362.

67. Gauss, J.; Schneider, U.; Aldrichs, R.; Dohmeir, L.; Schnöckel, H. *J. Am. Chem. Soc.* **1993**, 115, 2402.

68. Mckee, M.L. *J. Am. Chem. Soc.* **1993**, 115, 9608.

69. Howard, J.A.; Sutcliffe, R.; Hampson, C.A.; Mile, B. *J. Phys. Chem.* **1986**, 90, 4268.

70. Jeong, G.; Klabunde, K.J. *J. Am. Chem. Soc.* **1986**, 108, 7103.

71. Richards, W.G.; Horsley, J.A. *Ab Initio Molecular Orbital Calculations for Chemists*; Oxford, 1970; pp 19-62.

72. Szabo, A.; Ostlund, N.S. *Modern Quantum Chemistry: Introduction to Advanced Electronic Structure Theory*; Macmillan Publishing Co., Inc.: New York, 1982; pp 108-203.

73. Manceron, L.; Andrews, L. *J. Phys. Chem.* **1989**, 93, 2964.

74. Beynon, J.H.; Mathias, A.; Williams, A.E. *Org. Mass. Spectrom.* **1971**, 5, 303.

75. Willard, H.H.; Merritt, Jr., L.L.; Dean, J.A.; Settle, Jr., F.A. *Instrumental Methods of Analysis*, Wadsworth Publishing Co.: Belmont, California, 1988; pp 484-485.

76. Franklin, J.L.; Carroll, S.R. *J. Am. Chem. Soc.* **1969**, 91, 6564.

77. Kemp, D.S.; Vellaccio, F. Organic Chemistry, Worth Publishers Inc.: New York, 1984; pp 720-722.

78. Holy, N.L. *Chem. Rev.* **1974**, 74, 243.

79. Catterall, R.; Symons, M.C.R.; Tipping, J.W. *Inorg. Phys. Theor.* **1966**, 1529.

80. Symons, M.C.R. *J. Phys. Chem.* **1967**, 71, 172.

81. Abramson, F.P.; Futrell, J.H.; *J. Phys. Chem.* **1967**, 71, 3791.

82. *Dictionary of organic compounds*, v.4, 5th edition, Chapman and Hall: New York, 1982, p 3795.

83. Carey, F.A.; Sundberg, R.J. *Advanced Organic Chemistry*, Plenum Publishing Co.: New York, 1977, pp 151-152.

84. Howard, J.A.; Tomietto, M.; Tse, J.S.; Joly, H.A. *J. Chem. Soc. Faraday Trans.* **1994**, 20, 3145.

85. Howard, J.A.; Joly, H.A. *Personal Communication*

86. Joly, H.A.; Kepes, M.; Roy, N.; Prpic, J. *Can. J. Chem.* **1998**, 76, 400.

87. Frisch, J.M.; Trucks, G.W.; Head-Gordon, M.; Gill, P.M.W.; Wong, M.W.; Foresman, J.B.; Johnson, B.G.; Schegel, H.B.; Robb, M.A.; Replogle, E.S.; Gomperts R.; Andres, J.L.; Raghavachar, K.; Binkley, J.S.; Gonzalez, C.; Martin, R.L.; Fox, D.J.; Defrees, D.J.; Baker, J.; Stewart, J.J.P.; Pople, J.A.; Gaussian 92, Revision E.2, Gaussian Inc., Pittsburgh PA, **1992**.

Appendix 1

1.1 General deposition procedures for cryostat reactions:

(a) Water or deuterium oxide at 1.0 Torr for 2 min.

(b) Matrix at 1.2 Torr for 2 min.

(c) Reactant and metal (12 amps) for 8 min.

(d) Matrix at 1.2 Torr for 2 min.

(e) Water or deuterium oxide at 1.0 Torr for 3 min.

(f) Matrix at 1.2 Torr for 2 min.

(g) Reactant and metal for 8 min.

(h) Matrix at 1.2 Torr for 2 min.

(i) Water or deuterium oxide at 1.0 Torr for 3 min.

RUN INFORMATION SHEET

TRIAL #1

DATE: Sept. 22, 1993

METAL: Aluminum.

REAGENTS: Benzene, triple distilled water.

MATRIX: Benzene.

PURITY: Benzene was distilled and dried over 3 A molecular sieves.

CRYOSTAT PARAMETERS

. PRESSURE IN REACTION VESSEL:	. 6-8 x 10^{-5} Torr
. SPINNING RATE OF THE DRUM:	. 65%
. FURNACE: . AMOUNT OF METAL	. 63.6 mg
. CURRENT (amps)	. 17-25 A
. REACTION TIME:	. 2 min water, 2 min benzene, 8 min benzene + aluminum, 2 min benzene, 3 min water, 2 min benzene, 8 min benzene + aluminum, 2 min benzene and 3 min water. (total reaction time = 32 min)
. OBSERVATIONS:	. green centre and brown at the edges.

TEMPERATURE BATHS

REAGENT	PRESSURE	TEMPERATURE	BATH
. Benzene	. 1.0 Torr	. -37.5°C	. Anisole
. Water	. 1.0 Torr	. 0°C	. Ice water

FOR PRESSURE UNDER 1.0 TORR, T (K) CAN BE CALCULATED BY:

$$\text{LOG } P_{\text{Torr}} = [-0.05223a/T\ (K)] + b \quad \text{(benzene: } a = 42904,\ b = 9.556)$$

RUN INFORMATION SHEET

TRIAL #1

DATE: June 15, 1994

METAL: Aluminum.

REAGENTS: Benzene, deuterium oxide (D_2O).

MATRIX: Benzene.

PURITY: Distilled benzene.

CRYOSTAT PARAMETERS

. PRESSURE IN REACTION VESSEL:	. 1.8 x 10^{-6} Torr
. SPINNING RATE OF THE DRUM:	. 72%
. FURNACE: . AMOUNT OF METAL	. 26 mg
. CURRENT (amps)	. 20-32 A
. REACTION TIME:	. 2 min D_2O, 2 min benzene, 10 min benzene + aluminum, 2 min benzene, 3 min D_2O, 2 min benzene, 10 min benzene + aluminum, 2 min benzene and 3 min D_2O. (total reaction time = 36 min)
. OBSERVATIONS:	. light green centre with dark brown edges.

TEMPERATURE BATHS

REAGENT	PRESSURE	TEMPERATURE	BATH
. Benzene	. 0.05 Torr	. -67.9°C	. *p*- Cymene
. D_2O	. 1.0 Torr	. 0°C	. Ice water

FOR PRESSURE UNDER 1.0 TORR, T (K) CAN BE CALCULATED BY:

$$\text{LOG } P = [-0.05223a/T\ (K)] + b$$

RUN INFORMATION SHEET

TRIAL #1

DATE: Feb. 3, 1994

METAL: Aluminum.

REAGENTS: Benzene, adamantane, triple distilled water.

MATRIX: Adamantane.

PURITY: Distilled benzene and pure adamantane as received from Aldrich.

CRYOSTAT PARAMETERS

. PRESSURE IN REACTION VESSEL:	. 5-10 x 10^{-6} Torr
. SPINNING RATE OF THE DRUM:	. 70%
. FURNACE: . AMOUNT OF METAL	. ≈16 mg
. CURRENT (amps)	. 12-20 A
. REACTION TIME:	. 2 min adamantane, 2 min benzene, 10 min benzene + Aluminum, 2 min adamantane, 3 min water, 2 min adamantane, 10 min benzene + Aluminum, 2 min benzene and 3 min water. (total reaction time = 36 min)
. OBSERVATIONS:	. very light green centre with brown edges.

TEMPERATURE BATHS

REAGENT	PRESSURE	TEMPERATURE	BATH
. Benzene	. 1.0-1.2 Torr	. -30.6°C	. Bromobenzene
. Adamantane	. 1.0 Torr	. 80°C	. Hot water
. Water	. 1.0 Torr	. 0°C	. Ice Water

FOR PRESSURE UNDER 1.0 TORR, T (K) CAN BE CALCULATED BY:

$$\text{LOG } P = [-0.05223a/T\ (K)] + b$$

RUN INFORMATION SHEET

TRIAL #1

DATE: Jan. 13, 1994

METAL: Aluminum.

REAGENTS: Benzene, methyl iodide (CH_3I).

MATRIX: Benzene.

PURITY: Distilled benzene, pure methyl iodide.

CRYOSTAT PARAMETERS

. PRESSURE IN REACTION VESSEL:	. 1 x 10^{-6} Torr (not stable)
. SPINNING RATE OF THE DRUM:	. 75%
. FURNACE: . AMOUNT OF METAL	. 43 mg
. CURRENT (amps)	. 14 A
. REACTION TIME:	. 2 min CH_3I, 2 min benzene, 10 min benzene + aluminum, 2 min benzene, 10 min benzene + aluminum, 2 min benzene and 4 min CH_3I. (total reaction time = 32 min)
. OBSERVATIONS:	. light green centre and very dark red color on the edges.

TEMPERATURE BATHS

REAGENT	PRESSURE	TEMPERATURE	BATH
. Benzene	. 1.0 Torr	. -37°C	. Anisole
. Methyl Iodide	. 1.0 Torr	. -63°C	. Chloroform

FOR PRESSURE UNDER 1.0 TORR, T (K) CAN BE CALCULATED BY:

$$\text{LOG } P = [-0.05223a/T\ (K)] + b$$

RUN INFORMATION SHEET

TRIAL #1

DATE: April 8, 1994

METAL: Aluminum.

REAGENTS: Toluene, triple distilled water.

MATRIX: Toluene.

PURITY: Pure toluene (tested by GC-MS).

CRYOSTAT PARAMETERS

. PRESSURE IN REACTION VESSEL:	. 10^{-5} - $4x10^{-7}$ Torr (not stable)
. SPINNING RATE OF THE DRUM:	. 75%
. FURNACE: . AMOUNT OF METAL	. 28 mg
. CURRENT (amps)	. 10-12 A
. REACTION TIME:	. 2 min water, 2 min toluene, 10 min toluene + aluminum, 2 min toluene, 3 min water, 2 min toluene, 10 min toluene + aluminum, 2 min toluene and 3 min water. (total reaction time = 36 min)
. OBSERVATIONS:	. green centre and light brown colour on the edges.

TEMPERATURE BATHS

REAGENT	PRESSURE	TEMPERATURE	BATH
. Toluene	. ≈1.0 Torr	. -30.6°C	. Bromobenzene
. Water	. 1.0 Torr	. 0°C	. Ice water

FOR PRESSURE UNDER 1.0 TORR, T (K) CAN BE CALCULATED BY:

$$\text{LOG } P_{\text{Torr}} = [-0.05223a/T\ (K)] + b \qquad \text{(toluene: } a = 39198,\ b = 8.33)$$

RUN INFORMATION SHEET

TRIAL #1

DATE: May 8, 1994

METAL: Aluminum.

REAGENTS: Toluene, adamantane, triple distilled water.

MATRIX: Adamantane

PURITY: Pure toluene and pure adamantane as received from Aldrich.

CRYOSTAT PARAMETERS

. PRESSURE IN REACTION VESSEL:	. 10^{-5} - 10^{-6} Torr
. SPINNING RATE OF THE DRUM:	. 75%
. FURNACE: . AMOUNT OF METAL	. 22 mg
. CURRENT (amps)	. 8 - 10 A
. REACTION TIME:	. 2 min water, 2 min adamantane, 8 min toluene + aluminum, 2 min adamantane, 3 min water, 2 min adamantane, 15 min toluene + aluminum, 2 min adamantane and 3 min water. (total reaction time = 39 min)
. OBSERVATIONS:	. light white centre with dark brown edges.

TEMPERATURE BATHS

REAGENT	PRESSURE	TEMPERATURE	BATH
. Toluene	. 0.5 Torr	. -37°C	. Anisole
. Adamantane	. 1.0 Torr	. 80°C	. Hot water
. Water	. 1.0 Torr	. 0°C	. Ice water

FOR PRESSURE UNDER 1.0 TORR, T (K) CAN BE CALCULATED BY:

$$\text{LOG } P = [-0.05223a/T\ (K)] + b \quad (\text{toluene: } a = 39198 \ \& \ b = 8.330)$$

RUN INFORMATION SHEET

TRIAL #1

DATE: Jan. 10, 1994

METAL: Aluminum.

REAGENTS: *p*- Bromotoluene, triple distilled water.

MATRIX: *p*- Bromotoluene.

PURITY: Pure *p*- Bromotoluene (tested by GC-MS).

CRYOSTAT PARAMETERS

. PRESSURE IN REACTION VESSEL:	. 1 x 10^{-6} Torr
. SPINNING RATE OF THE DRUM:	. 70%
. FURNACE: . AMOUNT OF METAL	. 67.43 mg
. CURRENT (amps)	. 10 - 24 A
. REACTION TIME:	. 2 min water, 2 min Br-toluene, 10 min Br-toluene + aluminum, 2 min Br-toluene, 3 min water, 2 min Br-toluene, 10 min Br-toluene + aluminum, 2 min Br-toluene and 3 min water. (total reaction time = 36 min)
. OBSERVATIONS:	. dark colour covering the drum.

TEMPERATURE BATHS

REAGENT	PRESSURE	TEMPERATURE	BATH
. *p*- Bromotoluene	. >> 1.0 Torr	. 0°C	. Ice Water
. Water	. 1.0 Torr	. 0°C	. Ice water

FOR PRESSURE UNDER 1.0 TORR, T (K) CAN BE CALCULATED BY:

$$\text{LOG } P = [-0.05223a/T\ (K)] + b$$

RUN INFORMATION SHEET

TRIAL #1

DATE: July 15, 1994

METAL: Aluminum.

REAGENTS: Trifluorotoluene, triple distilled water.

MATRIX: Trifluorotoluene.

PURITY: Trifluorotoluene used as received from Aldrich.

CRYOSTAT PARAMETERS

. PRESSURE IN REACTION VESSEL:	. 1 x 10^{-6} Torr
. SPINNING RATE OF THE DRUM:	. 75%
. FURNACE: . AMOUNT OF METAL	. 27 mg
. CURRENT (amps)	. 8 - 10 mg
. REACTION TIME:	. 2 min water, 2 min trifluorotoluene, 10 min trifluorotoluene + aluminum, 2 min trifluorotoluene, 3 min water, 2 min trifluorotoluene, 12 min trifluorotoluene + aluminum, 2 min trifluorotoluene and 3 min water. (total reaction time = 38 min)
. OBSERVATIONS:	. light brown colour covering the drum.

TEMPERATURE BATHS

REAGENT	PRESSURE	TEMPERATURE	BATH
. Trifluorotoluene	. 0.01 Torr	. -67.9°C	. *p*- Cymene
. Water	. 1.0 Torr	. 0°C	. Ice water

FOR PRESSURE UNDER 1.0 TORR, T (K) CAN BE CALCULATED BY:

$$\text{LOG } P_{\text{Torr}} = [-0.05223a/T\ (K)] + b$$

RUN INFORMATION SHEET

TRIAL #1

DATE: Dec. 21, 1993

METAL: Gallium.

REAGENTS: Benzene, triple distilled water.

MATRIX: Benzene.

PURITY: Distilled benzene.

CRYOSTAT PARAMETERS

. PRESSURE IN REACTION VESSEL:	. 1 x 10^{-6} Torr
. SPINNING RATE OF THE DRUM:	. 70%
. FURNACE: . AMOUNT OF METAL	. 72.8 mg
. CURRENT (amps)	. 11 A
. REACTION TIME:	. 2 min water, 2 min benzene, 13 min benzene + gallium, 2 min benzene, 3 min water, 2 min benzene, 13 min benzene + gallium, 2 min benzene and 5 min water. (total reaction time = 44 min)
. OBSERVATIONS:	. dark brown colour covering the drum.

TEMPERATURE BATHS

REAGENT	PRESSURE	TEMPERATURE	BATH
. Benzene	. 1.0 Torr	. -37.5°C	. Anisole
. Water	. 1.0 Torr	. 0°C	. Ice water

FOR PRESSURE UNDER 1.0 TORR, T (K) CAN BE CALCULATED BY:

$$\text{LOG } P = [-0.05223a/T\ (K)] + b$$

RUN INFORMATION SHEET

TRIAL #1

DATE: May 5, 1994

METAL: Gallium.

REAGENTS: Toluene, triple distilled water.

MATRIX: Toluene.

PURITY: Pure toluene.

CRYOSTAT PARAMETERS

. PRESSURE IN REACTION VESSEL:	. 1 x 10^{-6} - 5 x 10^{-6} Torr (not stable)
. SPINNING RATE OF THE DRUM:	. 72%
. FURNACE: . AMOUNT OF METAL	. 6.3 mg
. CURRENT (amps)	. 8 - 10 A
. REACTION TIME:	. 2 min water, 2 min toluene, 10.5 min toluene + gallium, 2 min toluene, 3 min water, 2 min toluene, 15 min toluene + gallium, 2 min toluene and 3 min water. (total reaction time = 41.5 min)
. OBSERVATIONS:	. light brown colour on the drum

TEMPERATURE BATHS

REAGENT	PRESSURE	TEMPERATURE	BATH
. Toluene	. 1.0 Torr	. -30.8°C	. Bromobenzene
. Water	. 1.0 Torr	. 0°C	. Ice water

FOR PRESSURE UNDER 1.0 TORR, T (K) CAN BE CALCULATED BY:

$$\text{LOG } P = [-0.05223a/T\ (K)] + b$$

RUN INFORMATION SHEET

TRIAL #1

DATE: July 26, 1994

METAL: Gallium.

REAGENTS: Trifluorotoluene, triple distilled water.

MATRIX: Trifluorotoluene.

PURITY: Trifluorotoluene used as received from Aldrich.

CRYOSTAT PARAMETERS

. PRESSURE IN REACTION VESSEL:	. 1 x 10^{-7} Torr (too low)
. SPINNING RATE OF THE DRUM:	. 72 %
. FURNACE: . AMOUNT OF METAL	. 40 mg
. CURRENT (amps)	. 4 - 8 A
. REACTION TIME:	. 2 min water, 2 min trifluorotoluene, 15 min trifluorotoluene + gallium, 2 min trifluorotoluene, 3 min water, 2 min trifluorotoluene, 15 min trifluorotoluene + gallium, 2 min trifluorotoluene and 5 min water. (total reaction time = 48 min)
. OBSERVATIONS:	. dark brown colour .

TEMPERATURE BATHS

REAGENT	PRESSURE	TEMPERATURE	BATH
. Trifluorotoluene	. 0.01 Torr	. -67.9°C	. *p*- Cymene
. Water	. 1.0 Torr	. 0°C	. Ice water

FOR PRESSURE UNDER 1.0 TORR, T (K) CAN BE CALCULATED BY:

$$\text{LOG } P = [-0.05223a/T\ (K)] + b$$

RUN INFORMATION SHEET

TRIAL #1

DATE: July 29, 1994

METAL: Indium.

REAGENTS: Trifluorotoluene, triple distilled water.

MATRIX: Trifluorotoluene.

PURITY: Trifluorotoluene used as received from Aldrich.

CRYOSTAT PARAMETERS

. PRESSURE IN REACTION VESSEL:	. 1.0 x 10^{-7} Torr (stable)
. SPINNING RATE OF THE DRUM:	. 72%
. FURNACE: . AMOUNT OF METAL	. 24.9 mg
. CURRENT (amps)	. 8 - 9 A
. REACTION TIME:	. 2 min water, 2 min trifluorotoluene, 15 min trifluorotoluene + indium, 2 min trifluorotoluene, 3 min water, 2 min trifluorotoluene, 15 min trifluorotoluene + indium, 2 min trifluorotoluene and 5 min water. (total reaction time = 48 min)
. OBSERVATIONS:	. light brown colour on the drum.

TEMPERATURE BATHS

REAGENT	PRESSURE	TEMPERATURE	BATH
. Trifluorotoluene	. 0.01 Torr	. -67.9°C	. *p*- Cymene
. Water	. 1.0 Torr	. 0°C	. Ice water

FOR PRESSURE UNDER 1.0 TORR, T (K) CAN BE CALCULATED BY:

$$\text{LOG } P = [-0.05223a/T\ (K)] + b$$

RUN INFORMATION SHEET

TRIAL #1

DATE: October 31, 1994

METAL: Thallium.

REAGENTS: Trifluorotoluene, triple distilled water.

MATRIX: Trifluorotoluene.

PURITY: Trifluorotoluene used as received from Aldrich.

CRYOSTAT PARAMETERS

. PRESSURE IN REACTION VESSEL:	. 1.5 x 10^{-5} Torr
. SPINNING RATE OF THE DRUM:	. 74%
. FURNACE: . AMOUNT OF METAL	. 43.92 mg
. CURRENT (amps)	. 8 - 9 A
. REACTION TIME:	. 2 min water, 2 min trifluorotoluene, 13 min trifluorotoluene + thallium, 2 min trifluorotoluene, 3 min water, 2 min trifluorotoluene, 13 min trifluorotoluene + thallium, 2 min trifluorotoluene and 5 min water. (total reaction time = 44 min)
. OBSERVATIONS:	. dark brown colour ton the drum

TEMPERATURE BATHS

REAGENT	PRESSURE	TEMPERATURE	BATH
. Trifluorotoluene	. >0.01 Torr	. -45°C	. Chlorobenzene
. Water	. 1.0 Torr	. 0°C	. Ice water

FOR PRESSURE UNDER 1.0 TORR, T (K) CAN BE CALCULATED BY:

$$\text{LOG } P = [-0.05223a/T\ (K)] + b$$